GRAPHENE-CA

Coordination Action for Graphene-Driven Revolutions in ICT and Beyond

Coordination and support action

WP3 Defining the Research Agenda

Deliverable 3.1
"Scientific and technological roadmap for graphene in ICT"

Main Author(s):
Francesco Bonaccorso, Andrea Ferrari, Vladimir Falko, Konstantin Novoselov

Nature of deliverable: R = Report
Dissemination level: PU

Due date of deliverable: M12
Actual submission date: M12

Project funded by the European Commission under grant agreement n°284558

LIST OF CONTRIBUTORS

Partner	Acronym	Laboratory Name	Name of the contact
1(coordinator)	CUT	Chalmers tekniska hoegskola	Jari Kinaret
2	UNIMAN	The University of Manchester	Andre Geim
3	UNILAN	Lancaster University	Vladimir Falko
4	UCAM _DENG	The Chancellor, Masters, and Scholars of the University of Cambridge	Andrea Ferrari
5	AMO	Gesellschaft fuer angewandte Mikro- und Optoelektronik mit beschraenkter Haftung AMO GmbH	Daniel Neumaier
6	ICN	Catalan institute of nanotechnology	Stephan Roche
7	CNR	Consiglio nazionale delle ricerche	Vincenzo Palermo
8	NOKIA	Nokia OYJ	Jani Kivioja
9	ESF	Fondation Européenne de la Science	Ana Helman

TABLE OF CONTENTS

Deliverable Summary

The purpose of this document is to present a comprehensive S&T overview of graphene and related two-dimensional materials, targeting a revolution in ICT, with impacts and benefits reaching into most areas of the society. WP3 was coordinated by the University if Cambridge, with the assistance of the Lancaster and Manchester nodes of Graphene-CA.

Information was collected via an open consultation in the Graphene-CA web page, from the main Graphene-CA partners and members of the international advisory board, as well as from workshops organized in Cambridge (3 workshops), Windermere, Lancaster, Madrid and Manchester. The Coordinating nodes also analyzed all key papers in literature, as well as solicited direct input from recognized experts in the various subfields of graphene and related two dimensional materials. They also have organized and/or attended all the main conferences on graphene during the past year held in Europe and worldwide.

This document overviews most aspects of graphene and related two-dimensional materials, ranging from fundamental research challenges to a variety of applications in a large number of sectors. The document will be regularly updated and revised during the voyage of the flagship, in a similar way to the International Technology Roadmap for Semiconductors (ITRS), which is an established guiding document in ICT.

Our mission is to take graphene and related layered materials from a state of raw potential to a point where they can revolutionize multiple industries: from flexible, wearable and transparent electronics to high performance computing and spintronics. This will bring a new dimension to future technology: a faster, thinner, stronger, flexible, and broadband revolution. Our program will put Europe firmly at the heart of the process, with a manifold return on the investment, both in terms of technological innovation and economic exploitation

The graphene flagship will develop novel electronic systems with ultra-high speed of operation, and electronic devices with transparent and flexible form factors. We will advance methods to produce cheap graphene materials, combining structural functions with embedded electronics, in an environmentally sustainable manner. The flagship will extend beyond mainstream ICT to incorporate novel sensor applications, batteries, and composites that take advantage of the extraordinary chemical, biological and mechanical properties of graphene and related two-dimensional materials. This will create societal and technological impacts in a range of fields and address the grand challenges faced by Europe in the coming decades.

The S&T document is topically divided into seven Sections that target, starting from fundamental research, specific areas, such as digital and high-frequency electronics, photonics, energy storage and generation technologies, nanocomposites, and biomedical applications.

List of acronyms

A	Voltage gain
a-C	Amorphous carbon
AFM	Atomic force microscopy
AG	Artificial graphene
Ag	Silver
ALD	Atomic layer deposition
Al_2O_3	Aluminium oxide
APDs	Avalanche photodiodes
Ar	Argon
ARPES	Angle-resolved photoemission spectroscopy
Au	Gold
BC	Block copolymer
BGI	Broken Galilean invariance
$B_3N_3H_6$	Borazine
Bi_2Se_3	Bismuth selenide
Bi2Te3	Bismuth telluride
BLG	Bilayer graphene
BN	Boron nitride
CaC_6	Calcium graphite
C-BN	Carbon- Boron nitride
CdS	Cadmium Sulfide
CdSe	Cadmium Selenide
Cl	Chlorine
C-face	Carbon face
CMG	Chemically modified graphene
CNT	Carbon nanotube
CNWs	Carbon nanowalls
CMOS	Complementary metal oxide semiconductor
Co	Cobalt
Cu	Copper
CVD	Chemical Vapour Deposition
CVFF	Consistent valence force field
D	Raman D peak
DC	Direct current
DDA	Discrete dipole approximation
DFT	Density functional theory
DFPT	Density functional perturbation theory
DGM	Density gradient medium
DGU	Density gradient ultracentrifugation
DNA	Deoxyribonucleic acid
DSSCs	Dye-sensitized solar cells
EELS	Electron energy loss spectroscopy
EDFAs	Erbium-doped fibre amplifiers
EDLC	Electrochemical double layer capacitor
EM	Electromagnetic
EMI	Electromagnetic interference
EPR	Enhanced permeability and retention effect
ET	Electrostatic tactile

FE	Field emission
FET	Field effect transistor
FDTD	Finite-difference time-domain
FIR	Far infrared
FLG	Few-layers graphene
G	Raman G peak
GaAs	Gallium arsenide
GaN	Gallium nitride
GB	Grain boundary
g_d	Output conductance
GFETs	Graphene field-effect transistors
GFNs	Graphene-family nanomaterials
GHz	Giga Hertz
GIC	Graphite intercalation compound
g_m	Transconductance
GO	Graphene oxide
GOTCFs	Graphene oxide transparent conductive films
GPD	Gaphene –based photodetctors
GQDs	Graphene quantum dots
GNR	Graphene nanoribbon
Gr	Graphene
GSA	Graphene saturable absorber
GTCEs	Graphene transparent conductive electrodes
GTCFs	Graphene transparent conductive films
GWC	Graphene-enabled wireless communications
h-BN	Hexagonal Boron nitride
H_2	Hydrogen
HF	High frequency
He	Helium
HEMT	High-electron mobility transistor
HF	Hartree-Fock
HfO_2	Hafnium Oxide
HOMO	Highest occupied molecular orbital
HPC	High Performance Computing
HRTEM	High resolution transmission electron microscope
HSC	Hybrid supercapacitors
K	Potassium
KOH	Potassium hydroxide
ICT	Information communication technology
In	Indium
In_2O_3	Indium oxide
InP	Indium phosphide
InSb	Indium antimonide
IR	Infrared
Ir	Iridium
ITO	Indium Tin Oxide
ITRS	International Technology Roadmap for Semiconductors
LaB_6	Lanthanum hexaboride
LC	Liquid crystal
LEDs	Light emitting diodes

Li	Lithium
LIBs	Lithium ion batteries
LNAs	Low-noise amplifiers
LPE	Liquid Phase Exfoliation
LUMO	Lowest unoccupied molecular orbital
MAC	Medium access control
MBE	Molecular beam epitaxy
MC	Micromechanical cleavage
MD	Molecular dynamics
MgO	Magnesium oxide
MEMS	Micro Electro-Mechanical Systems
MnO_2	Manganese dioxide
MNP	Metallic nanoparticle
MOCVD	Metal-organic Chemical Vapour Deposition
MoS_2	Molybdenum disulfide
$MoSe_2$	Molybdenum disulfide
$MoTe_2$	Molybdenum ditelluride
MOSFET	Metal-oxide-semiconductor field-effect transistor
MRAM	Magnetoresistive random-access memory
MWCVD	Micro wave Chemical Vapour Deposition
NaOH	Sodium hydroxide
$NbSe_2$	Niobium Diselenide
NCs	Colloidal inorganic nanocrystals
NEM	Nano electromechanical
NEMS	Nano electromechanical systems
Ni	Nickel
NIR	Near infrared
$NiTe_2$	Nickel ditelluride
NOEMS	Nano optoelectromechanical systems
NWs	Nanowires
1d	One-dimensional
OLEDs	Organic light-emitting diodes
OT	Optical tweezers
O_2	Oxygen
PAHs	Poly-aromatic hydrocarbons
PbS	Lead sulphide
PC	Photocurrent
PCa	Polycarbonate
PCF	Photonic crustal fiber
PECVD	Plasma enhanced chemical vapour deposition
PEDOT	poly(3,4 ethylenedioxythiophene)
PEG	polyethylene glycole
PEI	Polyethyleneimine
PET	Polyethylene terephthalate
Pd	Palladium
PDLC	Polymer dispersed liquid crystal
PDMS	Polydimethylsiloxane
PHF	Post- Hartree-Fock
PMF	Polarization-maintaing fibers
PMMA	Polymethylmethacrylate

PMTs	Photomultiplier tubes
PRACE	Partnership for advanced computing in Europe
PSS	Polystyrene sulphonate
Pt	Platinum
PV	Photovoltaics
PVA	Polyvinylalcohol
QDs	Quantum dots
QHE	Quantum Hall effect
QMC	Quantum Monte Carlo
QPC	Quantum point contact
RNA	Ribonucleic acid
RPA	Random phase approximation
R&D	Research and Development
RES	Reticuloendothelial system
RIXS	Resonant inelastic x-ray scattering
RGO	Reduced graphene oxide
RF	Radio frequency
ROS	Reactive oxygen species
R2R	Roll to roll
Rs	Sheet resistance
Ru	Ruthenium
SAs	Saturable absorber
SAMs	Self-assembled monolayers
SbF_5	Antimony pentafluoride
SBS	Sedimentation based-separation
SCM	Scanning catalyst microscope
SDC	Sodium Deoxycholate
SESAM	Semiconductor saturable absorber mirror
SERS	Surface enhanced Raman Spectroscopy
SET	Single electron transistors
SiRNA	Small interfering ribonucleic acid
SOI	Si -on-insulator
SPP	Surface plasmon polariton
SPRs	Surface plasmon resonance
s-SNOM	Scattering-type near-field microscopy
S&T	Science and Technology
STEM	Scanning transmission electron microscopy
STM	Scanning tunnelling microscopy
Si	Silicon
SiC	Silicon Carbide
SiO_2	Silicon dioxide
SLG	Single layer graphene
SMMA	Styrene methyl methacrylate
SnO_2	Tin oxide
SQD	Semiconductor quantum dots
STM	Scanning tunnelling microscope
SWIR	Short wavelength infrared
SWNTs	Single Wall Carbon Nanotubes
3d	Three dimensional
T	Trasmittance

$TaSe_2$	Tantalum selenide
TC	Transparent conductor
TCE	Transparent conductor electrode
TCF	Transparent conductor film
TE	Technology enabler
TEM	Transmission electron microscope/microscopy
Ti	Thallium
TiO_2	Titanium dioxide
TDDFT	Time-dependent density functional theory
TLG	Trilayer graphene
TM	Transverse magnetic
TMDs	Transition metal dichalcogenides
TMOs	Transition metal oxides
THz	Tera-Hertz
2d	Two dimensional
2D	Overtone of Raman D peak
2DEG	Two-dimensional electron gas
UHV	Ultra-High vacuum
UV	Ultraviolet
VHs	Van Hove singularities
WDM	Wavelength division multiplexer
WNSN	Wireless nanosensor network
WO_2	Tungsten dioxide
WS	Tungsten sulfide
WS_2	Tungsten disulfide
XMCD	X-ray magnetic circular dichroism
XPS	X-ray photoelectron spectroscopy
ZnO	Zinc oxide
ZnS	Zinc sulfide
ZnSe	Zinc selenide
0d	Zero dimensional

A. Graphene-based disruptive technologies: overview

Technologies, and our economy in general, usually advance either by incremental developments (e.g. scaling the size and number of transistors on a chip) or by quantum leaps (transition from vacuum tubes to semiconductor technologies). Disruptive technologies, which are behind such revolutions, are usually characterised by universal, versatile applications, which change many aspects of our life simultaneously, penetrating every corner of our existence.

In order to become disruptive, a new technology needs to offer not incremental, but dramatic, orders of magnitude improvements. Moreover, the more universal the technology, the better chances it has for broad base success. This can be summarized by the "Lemma of New Technology", proposed by Herbert Kroemer, who won the Nobel Prize in Physics in 2000 for basic work in information and communication technology (ICT): *"The principal applications of any sufficiently new and innovative technology always have been – and will continue to be – applications* ***created*** *by that technology"*[1].

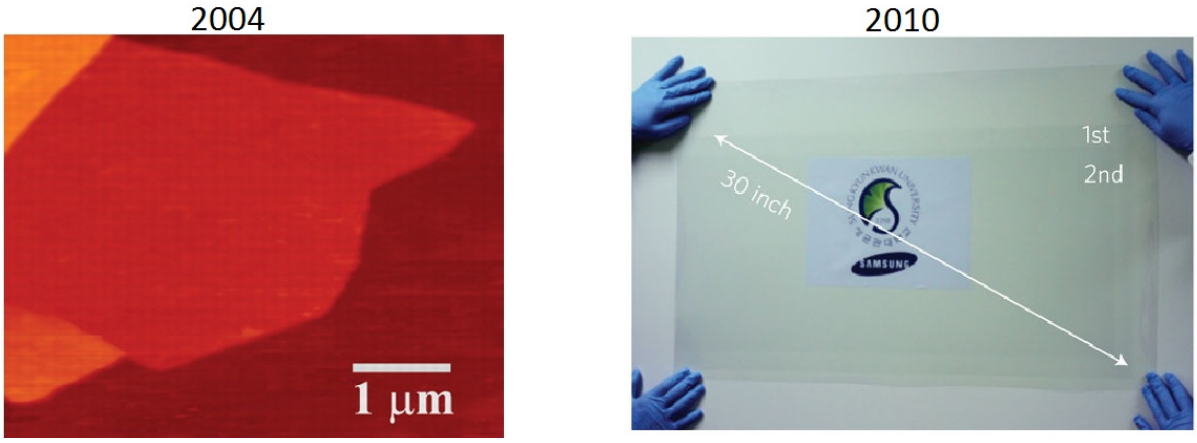

Figure 1: *Rapid evolution of graphene production: from microscale flakes [2] to roll-to-roll processing [4].*

Graphene is no exception to this lemma. Does graphene have a chance to become the next disruptive technology? Can graphene be the material of the 21th century? In terms of its properties it certainly has potential. The 2010 Nobel Prize in Physics already acknowledged the profound novelty of the physical properties that can be observed in graphene: different physics applies to graphene compared with other electronic materials such as common semiconductors. Consequently a plethora of outstanding properties arise from this remarkable material. Many are unique and far superior to those of any other materials. More importantly, such combination of "super" properties cannot be found in any other material. So, it is not a question of if, but a question of how many applications will it be used for, and how pervasive will it become. There are indeed many examples of "wonder" materials that have not yet lived up to expectations, nor delivered the promised revolution, while more "ordinary" ones are now pervasively used. Are the properties of graphene so unique to overshadow the unavoidable inconveniences of switching to a new technology, a process usually accompanied by large R&D and capital investments? The advancing R&D activity on graphene has already shown a phenomenal development aimed at making graphene suitable for industrial applications. The production of graphene is one striking example of the rapid development towards commercialisation, with progress from random generation of microscale graphene flakes in the laboratory [3] to large-scale, roll-to-roll processing of graphene sheets of sizes approaching the metre-scale [4] (Fig. 1).

It is reasonable to expect a rapid clearing of further technological hurdles towards the development of a graphene industry in the coming years.

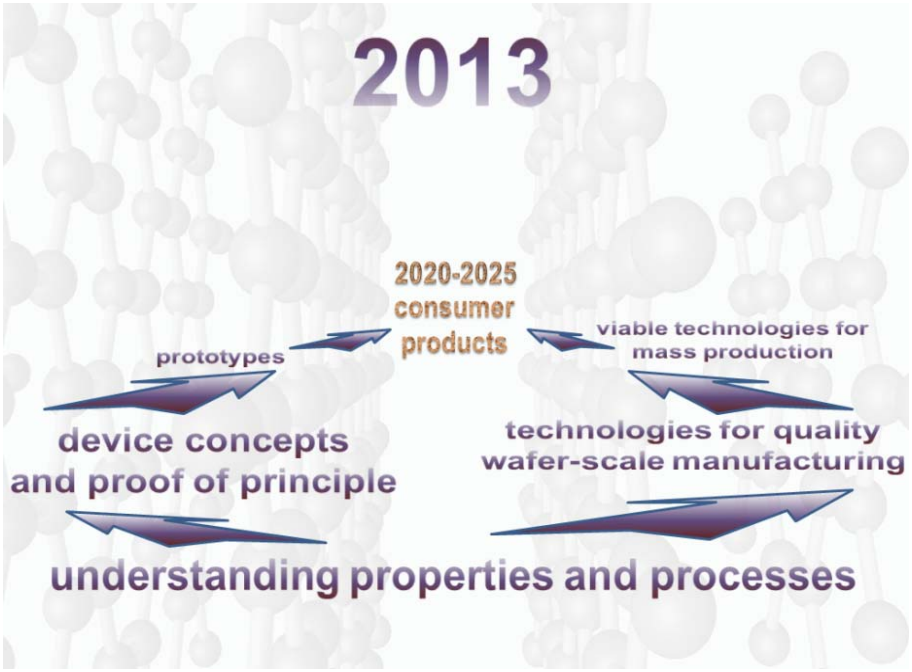

Figure 2: *Towards graphene-based products*

Therefore, in spite of the inherent novelty associated with graphene and the lack of maturity of graphene technology, a meaningful roadmap can be envisaged, including well-defined short-term milestones, and some medium- to long-term targets, intrinsically less detailed, but potentially even more disruptive, see Fig. 2. This should guide the expected transition of the ICT industry towards a technological platform underpinned by graphene, with opportunities in many fields and possible benefits to society as a whole.

A1. Opportunities

A1.1 Power management

To date in Europe nearly the 60% of the energy is electrical (lighting, electronics, telecommunications, motor control). Of the remaining 40%, nearly all is used for transportation. Since in the coming years the transport (of peoples, goods) will transition from wheel to rail (railway high speed, underground, trams), and that on wheel will exploit hybrid or totally electric vehicles, it is envisaged that around 80% of the used energy will be electrical. Power management will be key to allow efficient and safe use of energy. Graphene shows at room temperature many interesting properties for microelectronics. Its high current density and absence of electromigration, and high thermal conductivity, make it ideal for applications and integration in power circuits, as a first level of metallization or heat sink or integrated passives.

A1.2 Hybrid electronics

The introduction of more functions in integrated electronics systems will enable applications in domotics, environment control, and office automation to finally meet the social request for more safety, health and comfort. An increased automation should also consider the average age increase of populations and people at work, and the need of adequate facilities. Sensors or metrological devices based on graphene can further extend

functionalities of hybrid circuits. A 3d integration, easily conceivable considering graphene circuits on silicon, could be the solution for low cost chips with extended functionalities.

A1.3 Flexible electronics

Electronics on plastics or paper is low cost. It will offer the possibility to introduce more information on daily used goods, for example on foods for safety and health, as well as on many other products. Bar codes may not be able to store all the required information. Magnetic or memory supports do not offer the same opportunities as active electronics interacting in a wireless network. The possibility to develop passive components in graphene (resistors, capacitors, antennas) as well as diodes (Schottky) or simple field effect transistor (FET) and the rapid growth of the technology in this direction will enable RF flexible circuits communicating in a wireless environment.

A.1.4 Energy

Graphene is one of the most promising and versatile enabling nanotechnology addressing the "*secure, clean and efficient energy"* Horizon 2020 objective [5]. Graphene will bring disruptive solutions to the current industrial challenges related to energy generation and storage applications, first in nano-enhanced products, then in radically new nano-enabled products. Graphene-based systems for energy production (photovoltaics -PV-, fuel cells), energy storage (supercapacitors, batteries) and hydrogen storage will be developed via relevant proof of concept demonstrators that will progress towards the targeted technology readiness levels required for industrial uptake.

A2. Targets and expected impacts

Graphene is expected to have a strong impact for technological innovations in electronic, optical, and energy sectors, see Table 1.

***Table 1**: Graphene will provide a platform for enabling new technologies and applications (i.e. **radical** [not incremental] advances)*

Graphene features	Enabled applications / technologies
Atomic thinness	Flexible devices; thin and flexible electronic components; modular assembly / distribution of portable thin devices
Foldable material	Engineering new materials by stacking different atomic planes (heterojunctions) or by varying the stacking order of homogeneous atomic planes
All-surface material	Engineering novel 2d materials with tuneable physical/chemical properties by control of the surface chemistry Platform for new chemical /biological sensors
Solution - processable	Novel composite materials with outstanding physical properties (e.g. high thermal conductivity; high Young modulus and tensile strength); Novel functional materials
High carrier mobility	Ultra-high frequency electronic devices
Optical (saturable) absorption; photo-thermoelectric effect	Novel optoelectronic and thermoelectric devices; photodetectors
Field-effect sensitivity	Highly sensitive transducers
High intrinsic capacitance; high specific surface area	Outstanding supercapacitors
Photovoltaic effect, broad-range optical transparency; photocatalytic effects	Energy conversion; energy harvesting; self-powered devices
Theoretically predicted "chiral superconductivity"	Very-high Tc superconductors
Dirac fermions; pseudospin	Valleytronics

Impacts

Graphene technology can provide a spectrum of new forms of devices, thus enabling new concepts of integration and distribution

Graphene technology can enable the realization of new (non-existing so far) materials, which properties could be engineered and customized for new applications

Graphene technology can enable new highly-performing devices available at low cost and large scale, thus allowing major step forwards in many social impact fields (e.g. environmental monitoring, communications, health / medical applications, etc)

Graphene technology can allow significant steps forward in the realization of sustainable devices and green-energy systems

Graphene technology can pave the way to new devices based on yet experimentally unexplored physics

The production of high quality graphene remains one of the greatest challenges, in particular when it comes to maintaining the material properties and performance upon up-scaling, which includes mass production for material/energy-oriented applications and wafer-scale integration for device/ICTs-oriented applications.

Potential electronics applications of graphene include high-frequency devices and RF communications, touch screens, flexible and wearable electronics, as well as ultrasensitive sensors, nano electromechanical systems (NEMS), super-dense data storage, or photonic devices. In the energy field, applications include batteries and supercapacitors to store and transit electrical power, and highly efficient solar cells. However, in the medium term, some of graphene's most appealing potential lies in its ability to transmit light as well as electricity, offering improved performances to light emitting diodes (LEDs), and aid in the production of next-generation devices, such as flexible touch screens, photodetectors, and ultrafast lasers.
Fig. 3 identifies some milestones, which will constitute the main backbone for the expected graphene-driven technological revolution.

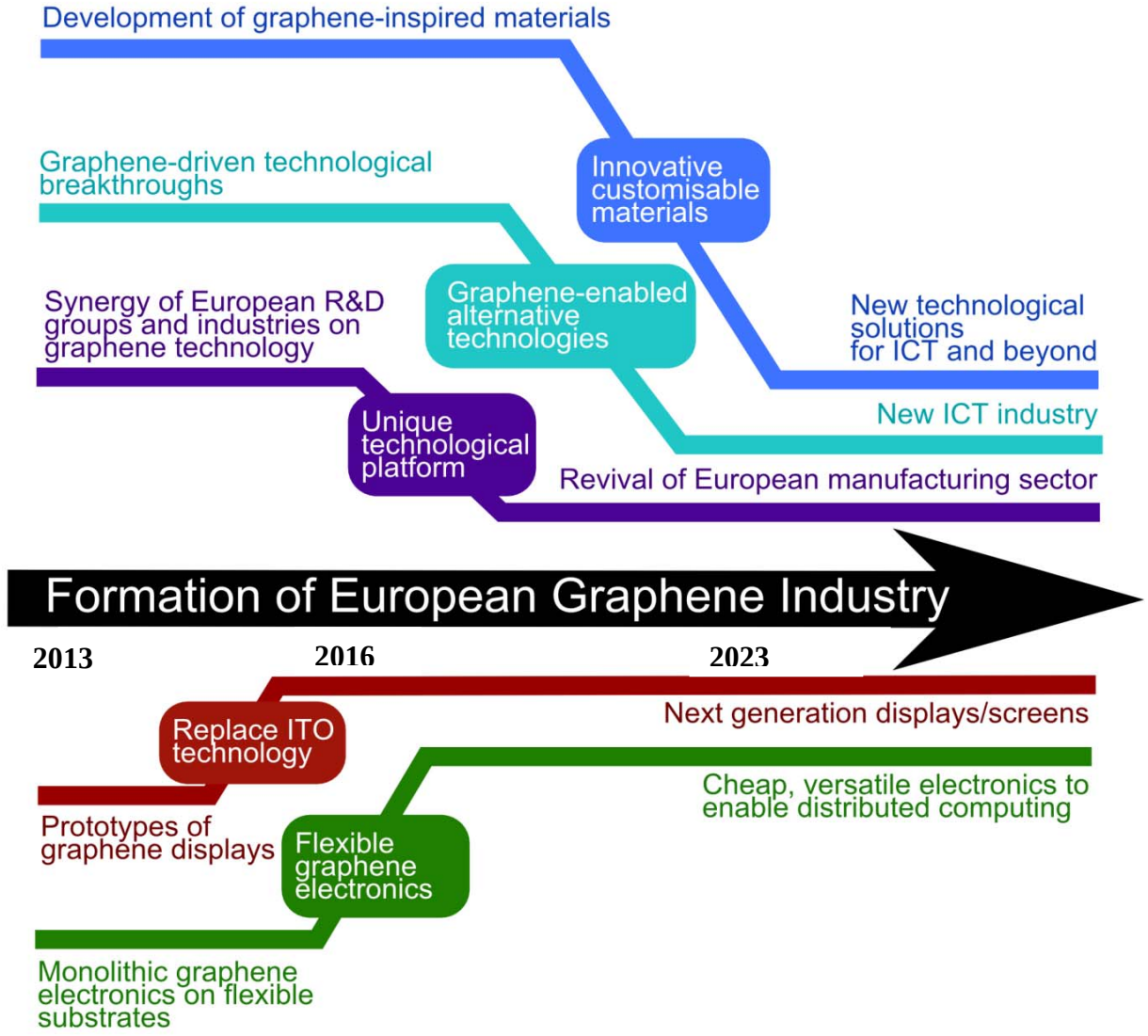

***Figure 3**: Timescale for graphene European industry.*

A2.1 *Transparent conductive films*

Graphene has many record properties, see Fig. 4. It is transparent like (or better than) plastic, but conducts heat and electricity better than any metal, it is an elastic thin film, behaves as an impermeable membrane, and it is chemically inert and stable. Thus it seems the "ideal" for the production of next generation transparent conductors. Indeed, there is a real need to find a substitute for ITO in the manufacturing of various types of displays and touch screens, due to the scarcity of indium and its consequent growing cost. Moreover, the world's largest supply capability of In is overwhelmingly concentrated in China, making alternatives to In-based technologies both economically and politically desirable. It has already been demonstrated that graphene is the best candidate for such a task. Thus, coupled with carbon's abundance, this presents a more sustainable alternative to ITO. Prototypes of graphene-based displays have been produced. Commercial products look near.

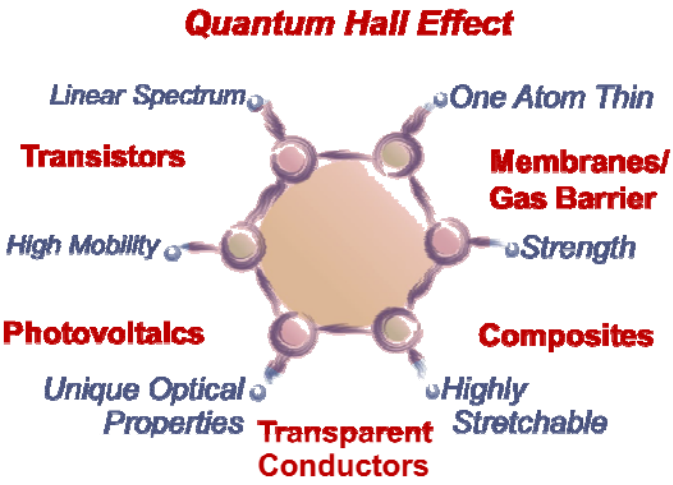

Figure 4*: Graphene properties*

In 2010, collaboration between SKKU and Samsung brought the first roll-to-roll production of 30-inch graphene transparent conductors (TC), with low sheet resistance (Rs) and 90% transmittance (T), already competitive compared to commercial transparent electrodes such as ITO. This demonstrated that graphene electrodes can be efficiently incorporated into a fully functional touch-screen capable of withstanding high strain. Therefore, the integration of graphene-based TCs into devices will probably be the first test-bed for a European alliance. The coordination of industrial and academic partners will help to maximise the exploitation of this new technology. Thus, it is immediate to envision the development of revolutionary flexible, portable and reconfigurable electronics, as pioneered by NOKIA through the MORPH concept (Fig. 5).

Figure 5: *Graphene in NOKIA Morph [6]: the future mobile device will act as a gateway. It will connect users to local environment, as well as the global internet. It is an attentive device that shapes according to the context. It can change its form from rigid to flexible and stretchable [6].*

A2.2 *Graphene electronics*

New horizons have also been opened from the demonstration of high-speed graphene circuits [7] offering high-bandwidth, that will have impact for the next generation of low-cost smart phone and television displays.

Concerning the domain of ICT, Complementary metal oxide semiconductor (CMOS) technology, as currently used in integrated circuits, is rapidly approaching the limits of downsizing transistors, and graphene is considered to be amongst the candidates for post-Si electronics by the ITRS [8]. However, the technology to produce graphene circuits is still in its infancy, and probably at least a decade of additional efforts will be necessary, for example to avoid costly transfer from metal substrates. The device yield rate also needs to be improved, as well as novel architectures, not necessarily based on graphene ribbons.

In 2011 Ref. [7] reported the first wafer-scale graphene circuit (broadband frequency mixer) in which all circuit components, including Graphene field-effect transistors (GFETs) and inductors, were monolithically integrated on a single carbide wafer. The integrated circuit operated as a broadband RF mixer at frequencies up to 10 GHz, with outstanding thermal stability and little reduction in performance (less than one decibel) between 300 and 400K. This paves the way to achieving practical graphene technology with more complex functionality and performance.

A2.3 *Enabling flexible electronics*

Being just one atom thick, graphene immediately appears as the most suitable candidate to eventually realize a new generation of flexible electronics devices. Thin and flexible graphene-based electronic components may be obtained and modularly integrated, and thin portable devices may be easily assembled and distributed. Graphene can withstand dramatic mechanical deformation [9], for instance it can be folded without breaking [9]. On the one hand, such a feature provides a way to tune the electronic properties of the material, through so-called “strain engineering” of the electronic band structure. On the other hand, foldable devices can be imagined as well, together with a wealth of new device form factors, which could enable innovative concepts of integration and distribution within the ICT sector.

By enabling flexible electronics, graphene will allow the exploitation of the existing knowledge base and infrastructures of various companies working on organic electronics (organic light emitting diodes as used in displays, conductive polymers, plastics, printable electronics), providing a unique synergistic framework for collecting and underpinning many distributed technical competences.

A2.4 *Unique technological platform*

At present, the realisation of an electronic device (such as, e.g., a mobile phone) requires the assembly of a variety of components obtained by many different technologies. Graphene, by including many different properties within the same material, may offer the opportunity to build a comprehensive technological platform for the realisation of almost any device component, including transistors, batteries, optoelectronic components, detectors, photovoltaic cells, photodetectors, ultrafast lasers, bio- and physicochemical sensors, etc.

Such an abrupt change in the paradigm of device manufacturing may revolutionise the global ICT industry, opening big opportunities for the development of an entirely new industry. Namely, the European manufacturing industry will have the chance to re-acquire a prominent position within the global ICT industry, by exploiting the synergy of excellent researchers and manufacturers.

A2.5 *Graphene-enabled new technologies*

Graphene may favour not only a radical improvement of existing technologies, such as electronics and optoelectronics, but may also eventually enable the emergence of completely new technologies, hampered so far by intrinsic limitations of the employed materials and processes. The properties associated with graphene, being described by a qualitatively different physics with respect to the other commonly used electronic materials, will permit the practical realisation of promising technological concepts, thus far only proposed by scientists, but never developed.

One example is that of spintronics, which as an emerging technology exploits the spin rather than the charge of electrons as the degree of freedom for carrying information, and has the primary advantage of consuming less power per computation [10]. Although a spintronic effect – namely, giant magnetoresistance [11] - is already a fundamental working principle in hard disk technology [12], the exploitation of spintronic devices as convenient substitutes for standard electronics is still far from being realised. Scientific papers have highlighted some graphene properties that are highly suitable for the development of novel spintronic devices [13,14,15], and many research groups are now involved in such activity.

Radically new technologies could be enabled by graphene, such as the so called "valleytronics" [16], which exploits the peculiar "isospin" of charge carriers in graphene as a degree of freedom for carrying information. Further, there are some still not experimentally proven theoretical predictions, such as a "chiral superconductivity" [17], which may lead to completely new applications which cannot even be predicted at this stage.

Taking these few examples of unique physical phenomena and remembering Kroemer's lemma once again, it is reasonable to expect the rapid development of many new applications due to the development of graphene technology, with a huge impact for ICT industry.

A2.6 *New customised "graphene-inspired" materials*

Graphene is an ideal candidate for engineering new materials, and many examples have already been realised in practice. Indeed, the "all-surface" nature of graphene offers the opportunity to tailor its properties by surface treatments (e.g. by chemical functionalization [ref]). For example, graphene has been converted into a band-gap semiconductor (hydrogenated graphene, or "graphane" [18]) or into an insulator (fluorinated graphene, or "fluorographene" [19]). In addition, graphene can be easily obtained in the form of small nanoflakes dispersions [20]. These retain many of its outstanding properties, and can be used in well-established approaches for the realisation of composite materials (e.g. embedded in a polymeric matrix [21,22]) with improved performance [21,22].

Graphene is important not only for its own properties, but at an even higher level because it provides the first demonstration of a truly two dimensional (2d) material. Therefore, it is the paradigm for a new class of materials, which is likely to rapidly grow following the rise of graphene technology. Some examples have already been reported, such as boron nitride (BN) [3,23] and molybdenite monolayers [3,23]. The assembly of such 2d crystals, *i.e.* by stacking different atomic planes (hetero-junctions) or by varying the stacking order of homogeneous atomic planes, will provide a rich toolset for the creation of new, customised materials. Graphene S&T will drive the manufacturing of many innovative materials. The development of new materials, engineered according to the specific needs of various industries, will strongly impact many different technological fields, even beyond ICT (such as, aeronautics, automotive, etc.). Again, graphene technology will give the opportunity for a synergic action which will be beneficial to competitiveness of European industry.

B. Research in graphene, new 2d materials, and hybrids

One of the reasons for the fast progress of graphene research is the multitude of unique properties observed in this 2d crystal. Graphene is a leader in several disciplines, including mechanical stiffness, strength and elasticity, electrical and thermal conductivity, it is optically active, chemically inert, impermeable to gases, and so on… These properties allow graphene to earn its place in current technologies as a replacement for other materials in existing applications. For instance, high electric and thermal conductivities would work nicely for interconnects in integrated circuits (where copper is being used at the moment), and high mechanical stiffness would allow its use for ultra-strong composites.

However, what makes this 2d crystal really special, and what gives it a chance to become disruptive, is that all those properties are combined in one material. Transparency-conductivity- elasticity will find use in flexible electronics, high mobility-ultimate thinness in efficient transistors for RF applications, transparency-impermeability-conductivity for transparent protective coatings [see Fig. 4]. The list of such combinations is already very long and ever growing. Last but not least, the most important combinations are probably those not yet explored, as they might lead to new, revolutionary applications.

Currently several record high characteristics have been achieved with graphene, some of them reaching theoretically predicted limits: room temperature electron mobility of $2.5\times10^5 cm^2/V\cdot s$ [24] (theoretical limit [25] $\sim 2\times10^5$ $cm^2/V\cdot s$); a Young modulus of 1TPa and intrinsic strength of 130GPa [9] (very close to that obtained in theory [26]); complete impermeability for any gases [27] and so on. It has also been documented to have a record high thermal conductivity [28,29] and can sustain extremely high densities of electric current (million times higher than copper) [30].

Probably the most important consequence of the isolation of graphene is the opening of a floodgate for experiments on many other 2d atomic crystals. One can use similar strategies which were applied to graphene and obtain new materials by mechanical [3] or liquid phase exfoliation of layered materials [23] or CVD growth. An alternative strategy to create new 2d crystals is to start with existing one (like graphene) and use it as an atomic scaffolding to modify it by chemical means (graphane [18] or fluorographene [19]). The resulting pool of 2d crystals is huge, and covers a massive range of properties: from most insulating to most conductive, from strongest to softest. Depending on the particular application one or another might be used. E.g., to cover a range of various conductance properties (but keeping the strength) one might use combinations of graphene and fluorographene, the latter being insulating, but almost as strong as the former.

If 2d materials hold large variations of properties, the sandwiched structures of 2, 3, 4… different layers of such materials can go a long way. We are getting back into the world of 3d crystals, but such that have not been available to us naturally. Since such 2d based heterostructures [29,31] can be tailored with atomic precision and individual layers of very different identity can be combined together, the properties of such structures can be tuned to fit any application. Furthermore, the functionality of such stacks is "embedded" in the design of such heterostructures. There are already examples, e.g. vertical tunnelling transistors based on heterostructures, with promising characteristics [32].

B1. Fundamental research in graphene properties

In order to fully exploit graphene's unique properties, further basic research is needed, as well as studies of other 2d crystals, beyond graphene.

B1.1 *Electronic transport in graphene and graphene-based devices*

Graphene's promise to complement or even replace semiconductors in micro- and nanoelectronics is determined by several factors. These include its 2d nature, enabling easy processing and direct access to the mobile charge carriers, chiral properties of charge carriers, a very high carrier mobility – both at room and low temperature, and high thermal conduction. Graphene crystals have two well-established allotropes, single layer graphene (SLG), where charge carriers resemble relativistic Dirac particles [33], and bilayer graphene (BLG) where electrons also have some Dirac-like properties, but have a parabolic dispersion [33]. Both allotropes are gapless semiconductors. However, unlike SLG, where the absence of a gap is protected by the high symmetry of the honeycomb lattice, BLG is more versatile: a transverse electric field can open a gap [34,35,36] and its low-energy band structure can be qualitatively changed by relatively weak strain [37]. Each of the above-mentioned factors has its advantages, but also some disadvantages, for particular applications, and one has to learn how to control and exploit those in functional devices.

Concerning carrier mobility, further research is needed to understand its limitations and the origin of defect and charge inhomogeneities in both SLG and BLG, as well as development of doping techniques, not damaging its quality and mobility. The influence of various dielectric substrates or overgrown insulators also needs detailed studies, aiming to optimize graphene performance in devices. Further studies of transport regimes and optoelectronic effects in gapped BLG are needed, for FET applications. Having in mind a possible use of electrically induced gap in BLGs for quantum dots and dot/wire circuits (e.g., for quantum information processing [38]), a very detailed understanding of the influence of disorder and electromagnetic environment on the electron transport is required, including the interplay between Efros-Shklovskii and Mott hopping regimes in gapped BLGs.

Besides studies of sample-average graphene parameters, such as R_S, it is highly desirable to get insights into local properties of graphene used in devices. This can be achieved by means of several non-destructive techniques: Raman spectroscopy [39,40], Kelvin probe microscopy [41], local compressibility measurements [42], and non-contact conductivity using capacitive coupling of a probe operated at high frequency [ref]. The application of such techniques to graphene is natural, due to its 2d nature and atomic thickness. They can reveal the role of inhomogeneity in carrier density, the role of particular substrates, and can shed light onto the role of structural defects and adsorbents in limiting device performance.

The peculiar properties of electrons in SLG (their similarity to relativistic Dirac particles) make a p-n junction in graphene (interface between hole- and electron-doped regions) transparent for electrons arriving at normal incidence [43,44]. On one hand, this effect, also known as Klein tunnelling [44] makes it difficult to achieve a complete pinch-off of electric current, without chemical modification or patterning of graphene. On the other hand, it offers a unique possibility to create ballistic devices and circuits where electrons experience focusing by one or several n-p interfaces [45]. The development of such devices requires techniques of non-invasive gating [see, e.g., 46]. Another method to improve quality/purity of graphene is to suspend it over electrodes (also used as support) and then clean it by current annealing [46,47]. This enables one to achieve highly homogeneous carrier density, and micron-long mean free paths in SLG, therefore to investigate in details the properties of electrons at very low excitation energies [47].

Understanding the transport properties of graphene also includes its behaviour in the presence of a strong – quantising – magnetic field. As a truly 2d electron system, graphene displays the fundamental phenomenon of quantum Hall effect (QHE) [48,49,50,51,52], which consists in the precise quantization of Hall resistance of the device. Up to now, both integer and several fractional QHE states have been observed [48,50,53]: the latter requiring very high purity material [53]. The QHE robustness in SLG opens a possibility to explore one, up to now, impossible regime of quantum transport in solid state materials: the interplay between

QHE and superconductivity in one hybrid device made of graphene and a superconductor with a high critical magnetic field (NbTi alloy). Moreover, a particular robustness of QHE in graphene on the Si face of SiC [54] (still waiting for a complete understanding [55]) makes it a suitable platform for the new type of resistance standard [54].

One of the issues in the fabrication of GFETs is electrostatic gating. Atomic layer deposition (ALD) of high-K dielectrics (Al_2O_3, HfO_2) is one possibility worth further exploration, due to the accurate control over layer thickness [56]. After such processing, graphene can be transferred to a Si substrate in which deep trenches are previously filled with metal (e.g., W) for the back-gate, and the source and drain are fabricated on the graphene itself. Such an approach offers a possibility to build devices with complex architectures. However, ALD uses alternating pulses of water and precursor materials, and as graphene is hydrophobic, the deposition of a uniform, defect-free dielectric layer is difficult [57], and requires further work to be optimized. Another promising technological advance is offered by photochemical gating [58]. There are several polymers (e.g., containing chlorine) where UV light converts Cl atoms into acceptors, whereas thermal annealing returns them into a covalently bound state [59]. Due to easy charge transfer between graphene and environment, UV illumination can modulate carrier density in graphene covered by such polymers, enabling non-volatile memory cells.

For device applications, graphene contacts with metals and semiconductors require further studies: charge transfer between materials, formation of Schottky barriers in the environment, and formation of p-n junctions in graphene. The contacts play a crucial role for several devices: for superconducting proximity effect transistors [60], where they determine how Cooper pairs penetrate in graphene, and for transistors used to develop quantum resistance standard, also needing very low resistance contacts to reduce overheating at the high-current performance of the resistance standard. Chosen to match the work functions of graphite and metals, the most common combinations are Cr/Au, Ti/Pt, and Ti/Pd/Au, the latter exhibiting lower contact resistances in the 10^{-6} Ω/cm^2 range [61]. The best results to date, down to $10^{-7}\Omega/cm^2$, were obtained for Au/Ti metallization with a 90s O_2 plasma cleaning prior to the metallization, and a post-annealing at ~ 460ºC for 15 min [62].

B1.2. *Spectroscopic characterization of graphene and defects in graphene*

Spectroscopy is an extremely powerful non-invasive tool in graphene studies. Optical visibility of graphene – enhanced by an appropriately chosen substrate structure [63,64,65] makes it possible to find graphene flakes by inspection in an optical microscope. While a trained person can distinguish single- from few layer graphene by “naked eye” with high fidelity, Raman spectroscopy has become the method of choice when it comes to scientific proof of SLG [39,40]. Indeed, the graphene electronic structure is captured in its Raman spectrum that evolves with the number of layers [39]. The 2D peak changes in shape, width, and position for an increasing number of layers, reflecting the change in the electron bands via a double resonant Raman process. The 2D peak is a single band in SLG, whereas it splits in four bands in BLG [39]. Since the 2D peak shape reflects the electronic structure, twisted multi-layers can have 2D peaks resembling SLG, if the layers are decoupled. The Raman spectrum of graphite was measured 42 years ago [66]. Since then Raman spectroscopy has become one of the most used characterization techniques in carbon science and technology, being the method of choice to probe disordered and amorphous carbons, fullerenes, nanotubes, diamonds, carbon chains, and poly-conjugated molecules [67]. The Raman spectrum of graphene was measured 6 years ago [39]. This triggered a huge effort to understand phonons [39,40], electron-phonon [39,40,68], magneto-phonon [69,70] and electron-electron [71] interactions, and the influence on the Raman process of number [39] and orientation [39,40] of layers, electric [72,73,74] or

magnetic [75,76] fields, strain [37,77], doping [78,79], disorder [40], quality [80] and types [80] of edges, functional groups [81]. This provided key insights in the related properties of all sp^2 carbon allotropes, graphene being their fundamental building block. Raman spectroscopy has also huge potential for layered materials other than graphene.

Angle-resolved photoemission spectroscopy (ARPES) directly probes band dispersions and lattice composition of electron states, which determine the chiral properties [82,83].

These techniques will be used for further investigation of electronic properties of graphene. In particular, studies of the magneto-phonon resonances [84,85] enable to directly measure the electron-phonon coupling constants in SLG and BLG [84,85]. Optical spectroscopy allows to study the split-bands in BLG [86,87], and the analysis of disorder-induced phonon-related Raman peaks provides information on sample quality complementary to that extracted from transport measurements.

Further improvement of the above-mentioned optical characterisation techniques and development of new approaches are critically important for the *in-situ* control and characterisation of natural and synthetic graphenes. Outside the visible-range and IR optical spectroscopy, detailed studies of defects in graphene can be addressed using scanning transmission electron microscopy (SuperSTEM), energy loss spectroscopy, low-angle X-ray spectroscopy, and resonant inelastic x-ray scattering (RIXS) - all methods already available in European research facilities. The issue of spectroscopic characterisation of graphene must be addressed broadly and with the highest priority, since the development of a standardized optical characterisation toolkit with the capability to control the number of layers in graphene, together with their quality and doping level is one of the key elements needed for the progress in graphene mass manufacturing. Since there are several routes towards viable mass production of graphene, which are described in Section C, the suitable energy/wavelength range for the standardised spectroscopic characterisation toolkit is not known, yet, so that spectroscopic studies of graphene will be carried out over a broad energy range, from microwaves and far infra-red to UV and X-ray spectroscopy.

Scanning tunnelling microscopy STM) is another important tool [88]. Since electronic state in graphene can be directly addressed by a metallic tip, STM studies of natural (exfoliated) and synthetic graphene will be instrumental for understanding the morphology and electronic structure of defects: vacancies, grain boundaries in polycrystalline graphene, functionalised faults in graphene lattice, and simply the strongly deformed regions (‘bubbles’) resulted from graphene processing or transfer. Such studies will be necessary for graphenes manufactured using each of the production methods discussed in Section C, and to investigate the result of subjecting graphene to various gases. STM will also reveal the electronic band structure of twisted BLGs, consisting of non-Bernal-stacked SLGs. In addition to standard STM spectroscopy under high vacuum, the use of STM under extreme conditions – such as strong magnetic field – will be used to investigate local properties of electrons in Landau levels in graphene, and their structure in the vicinity of defects.

B1.3. *Magnetism and spin transport in disordered graphene*

The control and manipulation of spins in graphene may lead to a number of novel applications and to the design of new devices, such as spin based memories or spin logic chips. Graphene is uniquely suitable for such applications, since it does not show sizeable spin-orbit coupling [89], and is almost free of nuclear magnetic moments [90]. Graphene is the first material to demonstrate spin transport at room temperature [90], a prerequisite for real world applications [90,91,92]. Further studies require investigation of spin injection, diffusion, and the analysis of interfaces between graphene and magnetic materials.

We need to fully understand the spin relaxation mechanism. Spin diffusion lengths longer than 100μm have been already demonstrated [93]. The next steps for a better understanding of the spin relaxation mechanisms are the identification of the imperfections (ripples, impurities, structural defects, interactions with the substrate) that limit spin lifetime and the optimisation of the spin lifetime (high quality graphene on best substrate). Impurities, contact to the substrate (or a dielectric on the top), and out-of-plane deformations can induces spin-orbit scattering. The analysis of such scattering mechanisms is needed to achieve optimal production methods for graphene-based spin-valves. Graphene should be an ideal material to implement, e.g., large scale "spin only" logic circuits in the "beyond perspective".

The studies of defects in graphene are directly connected to studies of magnetic properties. As a 2d electronic system, graphene is intrinsically diamagnetic [94]. However, defects in graphene, as well as localisation of electrons in or around defects (vacancies, edges, and covalently bonded dopants) may generate local magnetic moments. Recent measurements show an enhanced paramagnetic signal in graphene crystallites [95], and it has been found that magnetism of graphene is enhanced in irradiated samples [95], in a similar way to the behaviour observed in graphite [96]. Strong enhancement of paramagnetism has also been observed in functionalized fluorographene [97]. An unambiguous assessment of the nature and the formation of magnetic moments in graphene and in few layer graphene (FLG) (up to 5-7 layers), and the resulting control of their properties will be a major advance and will significantly expand graphene applications. Related issues are investigation of nanomagnetism of magnetic materials deposited on graphene, and understanding of the interfacial electronic structure of such contacts.

B1.4. *Polycrystalline graphene*

The role of grain boundaries (GB) in transport and optical properties needs to be fully investigated, especially in view of large scale production.

Microscopic studies of grain boundaries are needed to determine the lattice structure and morphology, as well as functionalization of broken carbon bonds by atoms/molecules acquired from environment. Grain boundaries in the 2d graphene lattice are topological line-defects consisting of non-hexagonal carbon rings, as evidenced by aberration corrected high resolution TEM investigations [98]. Although, they are expected to substantially alter the electronic properties of the unperturbed graphene lattice [99], so far there is little experimental insight into the underlying mechanisms. The grain boundaries introduce tension in graphene nanocrystals, which, in its turn, bears influence on the electronic properties, including local doping. From the point of view of electronic transport, grain boundaries generate scattering, possibly with a strongly nonlinear behaviour. Indeed, e.g., CVD grown samples fall behind by about an order of magnitude as compared to mechanically exfoliated graphene [100]. The internal structure of grain boundaries, and the resulting broken electron-hole and inversion symmetry may generate thermo-power [101] and local rectification [102], which may affect high current performance. Depending on their structure GBs can be highly transparent [103], as well as perfectly reflective [103], they are expected to act as molecular metallic wires [104] or filter propagating carriers based on valley-index [105].

GB spectral properties should be also investigated in great details, using STM and atomic force microscopy (AFM), and with local optical probes [106], in view of their possible effect on light absorption and emission. The use of graphene for energy applications, in solar cells, requires also understanding of the role of grain boundaries in the charge transfer between graphene and environment. Moreover, optics, combined with electrochemistry, is needed to figure out ways to recrystallize graphene poly-crystals, and to assess its durability. There is

growing evidence that the presence of grain boundaries is responsible for the degradation of the electronic performance [107].

B1.5. *Thermal and mechanical properties of graphene and graphene durability*

Practical implementation of graphene requires understanding of its performance in real devices, as well as its durability under ambient and extreme conditions. A specialised effort will be needed to study the reliability of graphene-based devices, such as electric or thermal stress tests, device lifetime, etc. To preserve device performance, it is likely that some protection of the graphene and the metals will be needed to minimize environmental effects.

Due to the sp^2 hybridization of carbon orbitals, pristine SLG is very strong, and it takes 48,000 $kN \cdot m \cdot kg^{-1}$ of stress before breaking (compare this to steel's 154 $kN \cdot m \cdot kg^{-1}$). This makes graphene a desirable addition to lightweight polymers, and the enforcer of their mechanical properties. Moreover, as ultrathin stretchable membrane, SLG is an ideal material for nonlinear tuneable electromechanical systems. However, for the practical implementation of realistic graphene systems, a detailed study of mechanical properties of polycrystalline graphene is needed: in vacuum, ambient environment, and of graphene embedded in polymers. Studies of mechanical properties of grain boundaries between graphene nano-crystals will require a further improvement of scanning techniques. The durability of graphene in various systems will also depend on its ability to recrystallize upon interaction with various chemical agents, as well under various types of radiation, ranging from ultraviolet and soft X-rays to cosmic rays.

The application of graphene in electronics and optoelectronics requires detailed understanding of its thermal and mechanical properties. Several early experiments [28,108,109] indicated that graphene is a very good heat conductor, due to the high speed of acoustic phonons in its tight and lightweight lattice. Detailed studies of heat transfer by graphene and the heat (Kapitza) resistance of the interfaces of graphene and other materials (metallic contacts, insulating substrates, polymer matrix) are now needed. Graphene performance at high current may lead to overheating, and quantitative studies (both experimental and theoretical) are needed to compare its performance with the standards set in electronics industry. Moreover, the overheating upon current annealing may lead to its destruction, so that studies of thermal and thermo-mechanical properties are needed to assess its durability in devices, and optimise its use in realistic and extreme conditions. In particular, *in situ* studies of kinetics and dynamics of graphene at the break point (use of HRTEM would be appropriate) are a challenging but necessary step towards practical implementation.

Experimental studies need to be complemented by *ab-initio* and multiscale modelling of nanomechanical and heat transport properties, and modelling of graphene at strong non-equilibrium conditions (see in B5).

B1.6 *Artificial graphene structures in condensed-matter systems*

Recent advances in the design and fabrication of artificial honeycomb lattices or artificial graphene (AG) pave the way for the realization, investigation, and manipulation of a wide class of systems displaying massless Dirac quasiparticles, topological phases, and strong correlations. Such artificial structures have created by means of atom-by-atom assembling by scanning probe methods [110], by nanopatterning of ultra-high-mobility 2DEGs in semiconductors [111], and optical trapping of ultracold atoms in crystals of light [112]. Examples of AG structures realized so far are shown in Fig. 6. The interplay between single-particle band-structure-engineering [113], cooperative effects and disorder [114] can lead to spectacular manifestations in tunnelling and optical spectroscopies.

One of the reasons for pursuing the study of AGs is that these systems offer the opportunity to experimentally reach regimes difficult to achieve in graphene, such as high magnetic fluxes, tuneable lattice constants, and precise manipulation of defects, edges, and strain. These will enable us to probe several predictions made for massless Dirac fermions [115,116]. Studies of electrons confined in artificial semiconductor lattices, as well as studies of cold fermions and bosons in optical lattices should provide a key perspective on strong correlation and the role of disorder in condensed matter science.

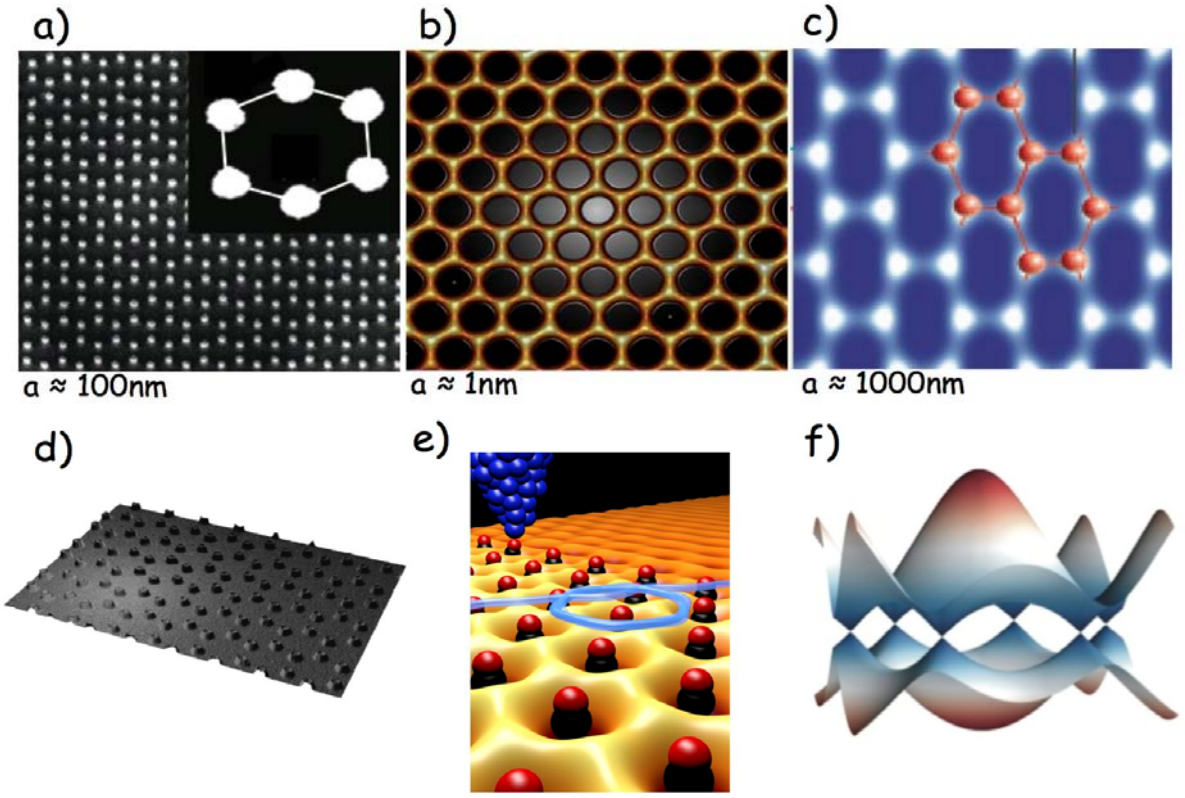

Figure 6: *a) SEM image of an AG realized by e-beam lithography and reactive ion etching on a GaAs/AlGaAs heterostructure. Electrons localize underneath the nanopillars that are also shown in d) [111]. b) STM topography of a molecular graphene lattice composed of 149 carbon monoxide molecules [110]. c) A honeycomb optical lattice for ultracold K atoms [112]. e) Electron moving under the prescription of the relativistic Dirac equation. The light blue line shows a quasi-classical path of one such electron as it enters the AG lattice made of carbon monoxide molecules (black/red atoms) positioned individually by an STM tip (comprised of Ir atoms, dark blue). f) Tight-binding calculations of the Dirac Fermion miniband structure of the AGs in a) and d).*

B1.6.1 Honeycomb lattices in semiconductors

The goal is the creation of structures that have honeycomb geometry imposed on a 2DEG in high-mobility III-V semiconductor heterostructures of different material systems, so that the miniband structure displays well-defined (isolated) Dirac points. The lattice constant in graphene is fixed at~1.42 Å. In contrast, AG structures have tunable lattice period, so that it should be possible to change interaction regimes from one in which Mott-Hubbard physics prevails (with relatively weak inter-site interactions), to another in which inter-site interactions drive the creation of novel phases, and finally to the topological insulator regime in materials with large spin-orbit interaction.

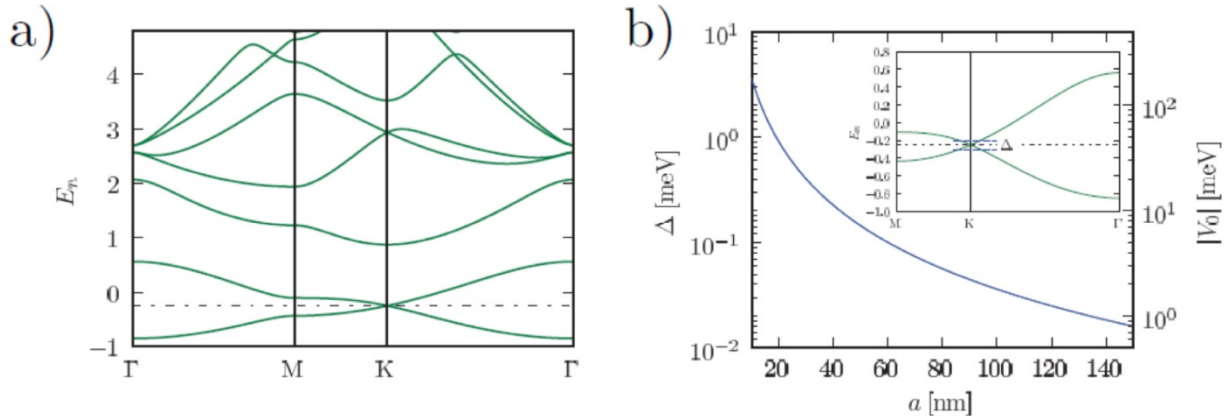

Figure 7: *a) AG Minibands (energy is meV) with a = 60 nm, r_0 =0.2a (r_o is the width of the potential well) and V_0 = 5meV. Γ, M, and K are high symmetry points in the 2d Brillouin zone. The Dirac point is at the K. A dash-dotted line is drawn at the Dirac-point energy. b) Δ of the linear part of the spectrum near the Dirac point as a function of a. In these calculations V_0 was varied correspondingly (see the right vertical axis) in order to obtain an isolated Dirac point, i.e. without any other state inside the bulk Brillouin zone at the Dirac-point energy. Inset: magnification of the energy bands in panel a) around the Dirac point energy. The blue dashed lines mark the energy limits of the linear dispersion approximation.*

AG may also challenge current thinking in ICT, revealing new physics and applications of scalable quantum simulators for ICT based on semiconductor materials already used in real-life electronic and optoelectronic devices. Due to the embryonic nature of the field, the proposed research is of high-risk, but has great potential for breakthrough discoveries. In semiconductor materials the efforts should be directed to the realization of artificial lattices with small lattice constants and with tuneable amplitudes V_0 of the potential modulation. The idea is that the energy range, Δ, in which the bands are linearly dispersing in AGs depends on the hopping energy, therefore this quantity is expected to exponentially increase as we reduce

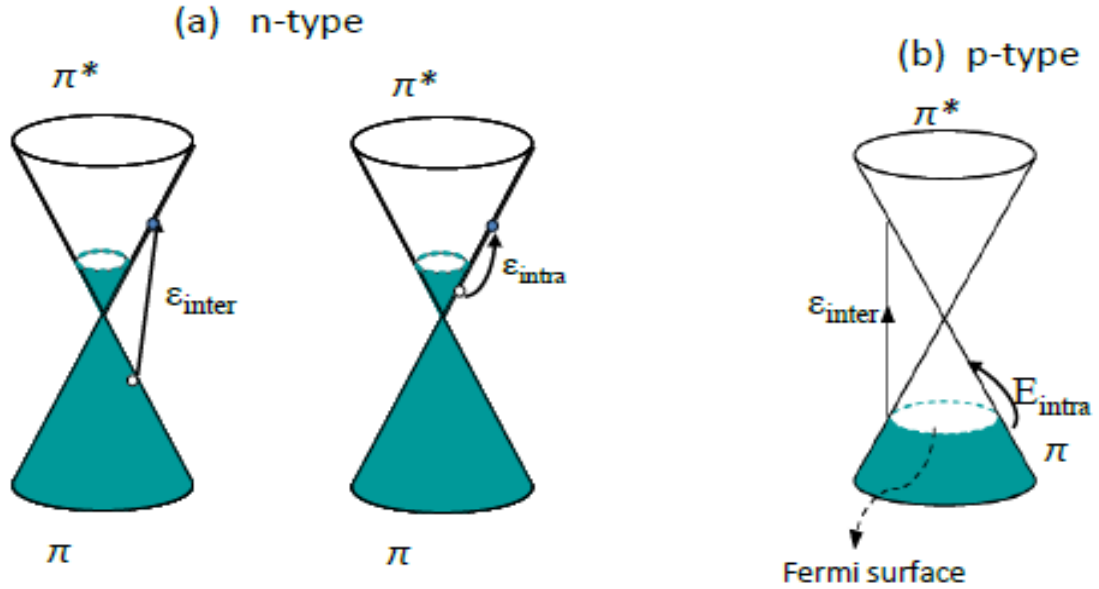

Figure 8: *Schematic representation of single particle transitions of Dirac fermions in the AG lattice. The cones are the states that arise from the dispersive minibands at the K-point shown in Fig. 7. The lower cone is labelled π, the upper cone π*, in analogy with graphene. Typical interband and intraband transitions are shown.*

the lattice constant and/or decrease the amplitude of the potential modulation.

We target the realization of AGs in the regime in which Δ approaches 1meV. This requires lattice constants a~20–40nm (see Fig. 7).

Formation of Dirac cones in AGs can be monitored by measurements of excitations using inelastic light scattering. Fig. 8 shows the single particle transitions expected in n- and p-type structures. The observations of excitations from these transitions will provide direct insights on Dirac-Fermi velocities. Interband and intraband excitations are dispersive, Fig. 9a.

One ambitious goal is to observe the dispersive intrasubband plasmon mode of the AG lattice by resonant inelastic light scattering or far-infrared spectroscopy. Intrasubband plasmons in dilute 2DEGs in GaAs heterostructures were previously studied by inelastic light scattering [117]. These experiments demonstrated the capabilities of light scattering to detect dispersive plasmon modes even in regimes of ultra-low electron densities below $n=10^9$ cm^{-2}.

Peculiar to plasmon modes in graphene, in fact, is the specific dependence of energy on electron density: $\omega_{plasmon}(q) \propto n^{1/4} q^{1/2}$, where q is the in-plane wavevector. The difference with the classical square-root dependence $n^{1/2} q^{1/2}$ of 2d parabolic-band systems is a consequence of the 'relativistic' linear dispersion of Dirac fermions [118, 119]. The manifestations of Dirac fermions are particularly striking under the application of a perpendicular magnetic field. In AGs with lattice constant is much smaller than the magnetic length (a<< lB) this is expected to lead to a graphene-like Landau levels.

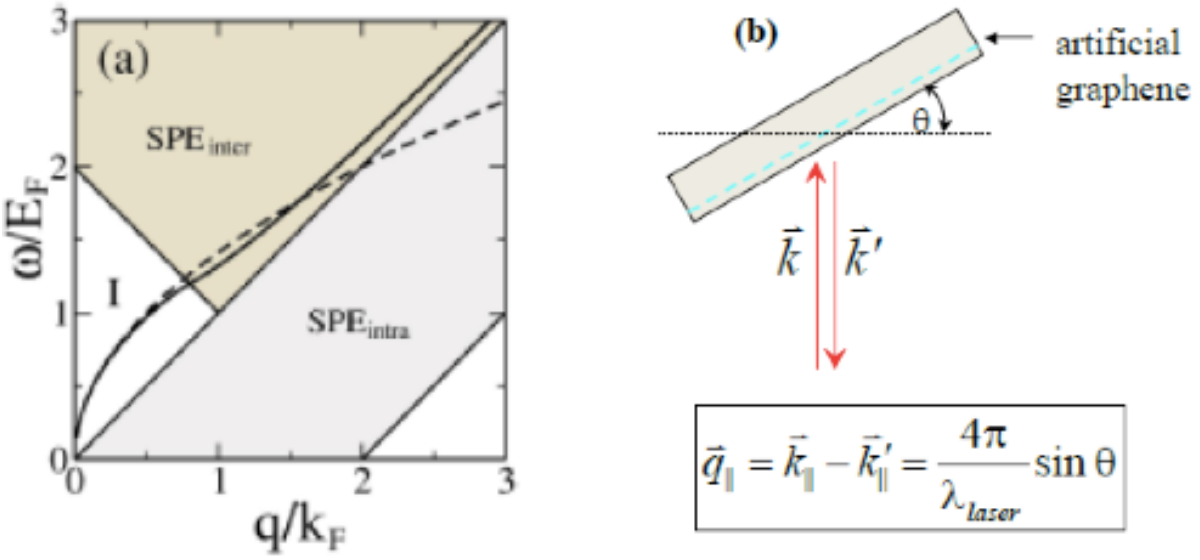

Figure 9: *(a) The thick solid line is the intrasubband plasmon dispersion calculated within the random phase approximation (RPA). The dashed line is an evaluation that goes beyond RPA. The thin solid lines represent the boundaries of respective single-particle transition (SPE), in which there is Landau damping of plasmons. (b) back-scattering geometry for inelastic light scattering experiments. k and k' are the incident and scattered light wave vectors. Typical values of the in-plane wave vector transfer are~$10^5 cm^{-1}$.*

Such peculiar energy level structure and the resulting anomalies in QHE experiments have been largely explored in graphene where the lattice constant is a=0.14 nm ($l_B \approx 25$ nm at 1T in GaAs). In the AG structure, however, the lattice constant is much larger than graphene. Tight-binding shows that the Dirac Fermion physics occurs when $l_B/a>1$. In AGs with a~10-20nm, a Dirac-Fermion Landau level structure is expected for magnetic fields~several Tesla. In molecular AG structures with a~1nm, Dirac Fermion physics should emerge at much smaller magnetic fields. The occurrence of such phenomena can be investigated by

conventional QHE and by optical spectroscopy experiments. For $l_B/a<1$, commensurability effects, such as the Hofstadter butterfly, begin to emerge and compete with the Dirac-Fermion physics of the honeycomb lattice [120]. These commensurability effects prevail when $l_B<<a$. The impact of the Hofstadter physics on the energy spectrum of a 2DEG in semiconductor heterostructures was studied in magneto-transport in a lateral superlattice of anti-dots arranged in a square geometry [120].

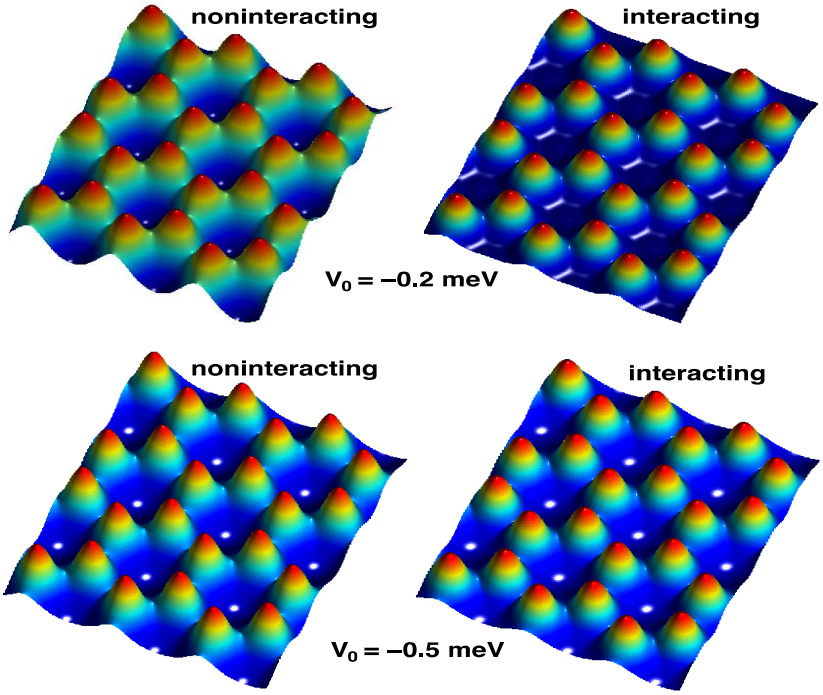

Figure 10: *Spatial distribution of electrons in AG (with one electron per pillar) calculated for two values of the potential well representing the pillar. The left and right panels show the results without and with electron-electron interactions. These calculations have been performed by employing a two-dimensional version of the local-density approximation within a Kohn-Sham density-functional theory scheme [121].*

If met, these demanding limits will enable the occurrence of the physics linked to artificial massless Dirac fermions at temperatures above liquid helium. Finally, the impact of electron-electron interaction can be studied theoretically by exploiting advanced methods such as density-functional theory (DFT) and developing a Kohn-Sham DFT coded for 2d electrons moving in a model periodic potential (see Fig. 10) [121] and experimentally by optical, transport and scanning probe methods. Additionally artificial topological order and spin-splitted counter-propagating edge channels can be pursued by creating honeycomb lattices in 2DEGs confined in InSb and InAs heterostructures, which are characterized by a large spin-orbit coupling. In this area, our long-term vision is to establish a new field of quantum information processing and scalable quantum simulations based on nanofabricated AGs in high-mobility semiconductor heterostructures.

B.1.6.2 *Honeycomb lattices with cold atoms*

Cold atoms in optical lattices also allow for the experimental realization of AG [112,122]. Of particular relevance is the possibility to study the impact of disorder and the interplay between disorder and Dirac Fermion physics. An example related to one-dimensional optical lattices is shown in Fig. 11, where the localization transition for ultracold atoms in a quasiperiodic bichromatic lattice was seen [114]. As the amount of disorder Δ is increased, the atom cloud stops expanding in the lattice, becoming Anderson-localized.

The dynamics of excitations in such cold atoms trapped in honeycomb lattices can be probed by Bragg spectroscopy [123]. This gives access to the dynamical structure factor $S(q,\omega)$ of the atomic system, as shown in Fig. 12. We also note that hexagonal optical lattices, which can be regarded as a triangular lattice with a bi-atomic basis where atoms occupy $\sigma+$ and $\sigma-$ sites, as indicated in Fig. 13 by green and red spheres, can also be created,

as recently demonstrated with cold ^{87}Rb in different hyperfine- and magnetic Zeeman-states [124].

As also stated above these AG systems might open new avenues of research on spin-orbit coupling phenomena, with impact on spintronics, and frontier issues related to novel topological phases. These studies are centred on systems known as topological insulators, because they have protected spin-split conducting states at their edges (in 2DEG's) or on their surfaces (in 3D bulk insulators). Such insulating materials with counter-propagating spin currents are known as quantum spin Hall (QSH) insulators. The QSH effect was also predicted in graphene [125], and linked to the honeycomb topology of the lattice and to the existence of spin-orbit coupling, albeit this turned out to be rather small. AG structures in systems properly engineered to display large spin-orbit coupling represent viable candidates to simulate TI states. It is expected that under the application of a parallel magnetic field the spin-orbit-split bands should resemble a gapped Dirac point at small momentum.

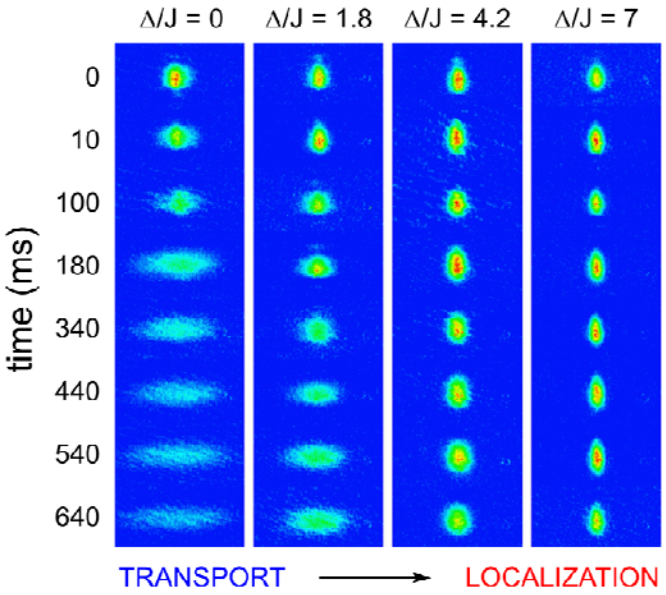

***Figure 11**: Localization transition for ultracold atoms in a quasiperiodic bichromatic lattice [114].*

There are further possibilities for research arising from the demonstration that single atoms can function as atomic-size gates of a 2d electron system at noble metal surfaces [126], whereby simple molecules, such as CO, function as repulsive potentials for surface electrons when shaped into open and closed quantum structures. Recently, individual CO molecules arranged on Cu(111) were used as a tuneable gate array to transform a 2d gas of electrons moving through these lattices [110]. This system recently termed 'molecular graphene' displays specific potentials that induce these quasi-particles to condense into various

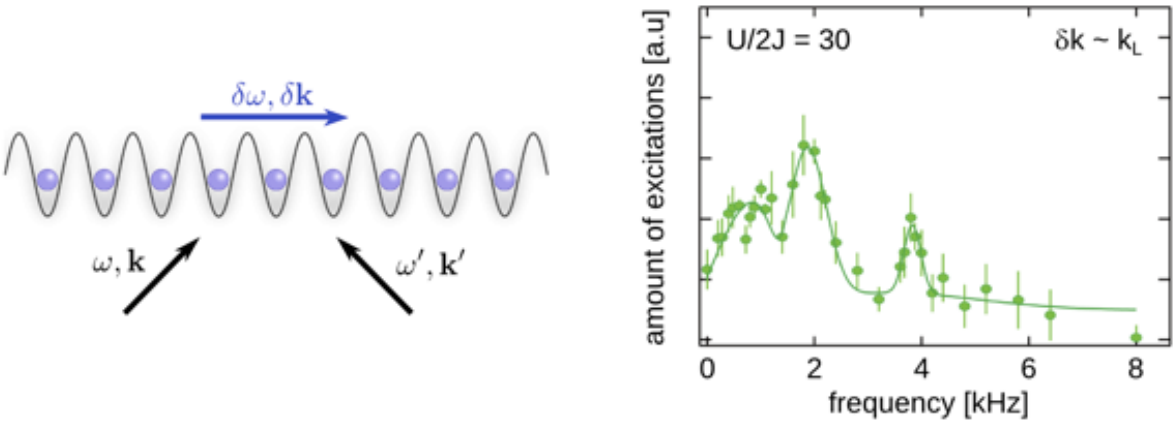

***Figure 12:** a) Scheme of Bragg spectroscopy (stimulated inelastic scattering of light by a system of cold atoms). b) Excitation spectrum measured for a one-dimensional Mott insulator state of repulsive bosons. The main peak corresponds to excitation at the Hubbard gap energy U [123]*

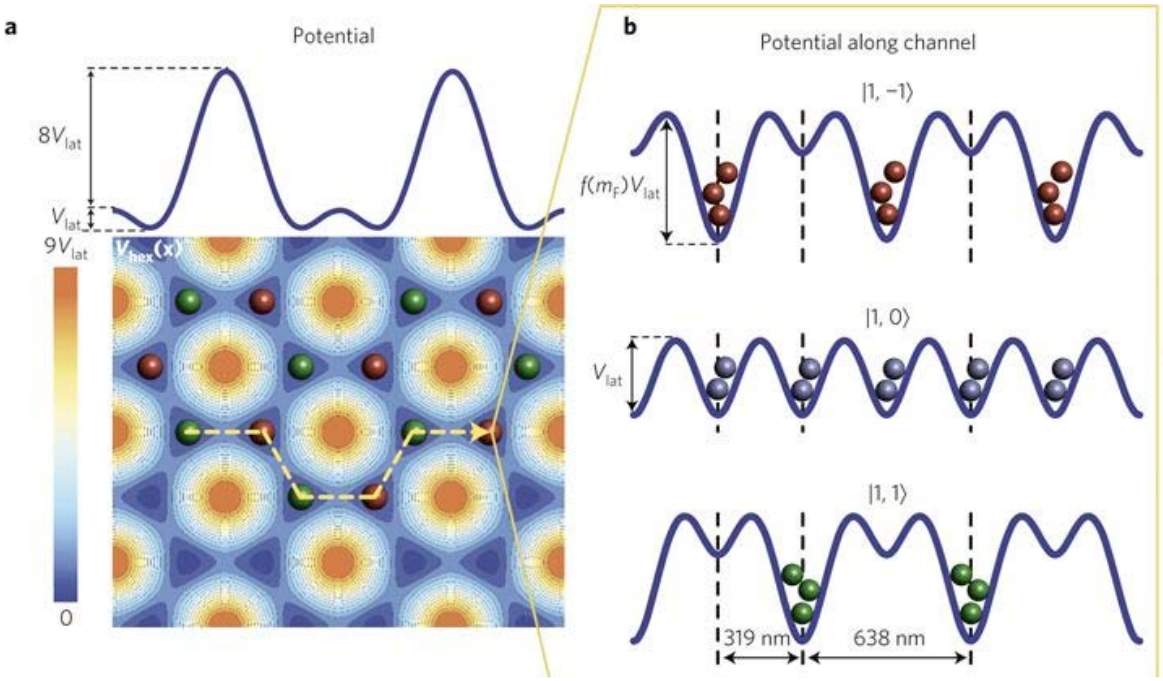

Figure 13: *a) Lattice potential with alternating σ+ (green spheres) and σ− (red spheres) polarization structure. The upper 1d plot shows a cut through the 2d potential. The bottom graph shows the 2d polarization distribution in the lattice, ranging from fully σ+ (green) to σ− (red) polarized. (b 1d potential along the channel indicated by the orange dashed line in (a) for particles in different Zeeman states. The modulation depth of the channel depends on the hyperfine state of the atoms. The lower part shows the corresponding light polarization [124].*

topological phases. Control over every lattice position and potential would result in unprecedented control of the spatial texture of the hopping parameter, ultimately allowing observation of electronic ordering into ground states, rarely encountered in natural systems.

Last but not least, in AGs, molecular graphene, artificial lattices in semiconductors and optical lattices in cold atoms, controlled densities of 'artificial impurities' can be introduced in otherwise perfect lattices. Studies of these artificial structures are expected to provide key insights on localization and mobility degradation occurring in graphene.

B2. Atomic scale technology in graphene and patterned graphene

Tailoring of electronic and optical properties in graphene can be achieved by lateral confinement of the 2d electron gas from the mesoscopic regime down to the molecular scale [127,128,129,130,131,132,133]. The dominant approach consists in using inorganic resist to lithographically define nanoribbons (GNRs) [134,135,136,137]. A resist-free approach can be achived by focused ion beam [138,139]. However, the transport in ion-etched GNRs is strongly dominated by edge disorder and amorphization [138,140,141], which called for alternative approachs. Ultrasonically shredded graphene [142], carbon nanotube opening [143,144], AFM and STM tip-induced oxidation [145,146] and catalytic particle cutting [147,148,149] offer promising routes to 50-500 Å wide GNRs, but only the former has so far led to functional devices.

The ultimate goal of graphene-based nanotechnology is to achieve atomic-scale fabrication through techniques that are rapid enough to bridge the gap with standard nanofabricated features. A promising strategy should probably exploit electron and/or scanning probe microscopy techniques. A challenging objective is to investigate the suspended *vs* supported cases and, in the latter, define the most suitable atomically flat

substrate. However, chemical approaches should also be considered either from the molecular synthetic or colloidal etching viewpoint. Next, atomic-scale imaging of graphene, such as STM, non-contact AFM, aberration-corrected HRTEM, should be developed in the specific realm of atomic-scale graphene devices. Electron transport, optical measurements and local, near-field measurements should be pushed to the limits to assess the properties in atomic-scale devices and identify the degrees of freedom able to control graphene behaviour, such as magnetic field, gate effects, optical excitations, near-field coupling to metallic surfaces, etc. These experimental issues should be guided by a theoretical description and simulations, in particular regarding the bridging between atomic/molecular scale and the mesoscopic regime.

B2.1. ***Graphene nanoribbons***

Nanofabrication applied to graphene has already produced a new physical system: graphene nanoribbons (nanometre wide graphene wires). The On/Off current ratio can reach high values in GNRs [150], including at room temperature [150], with the extra asset that all GNRs are found to be semiconducting, in contrast to nanotube devices [151]. Interestingly, transport measurements in shredded GNRs have shown that scattering by substrate potential fluctuations dominates the edge disorder [152]. One approach that has so far demonstrated the ability to produce GNRs with high crystallinity and smooth edges is based on e-beam etching at high energy (80-300 kV) in a TEM [153,154,155]. Progress was also made in chemical synthesis of GNRs [156,157,158]. This envisions a bridge between top-down patterning and atomically-precise chemical design.

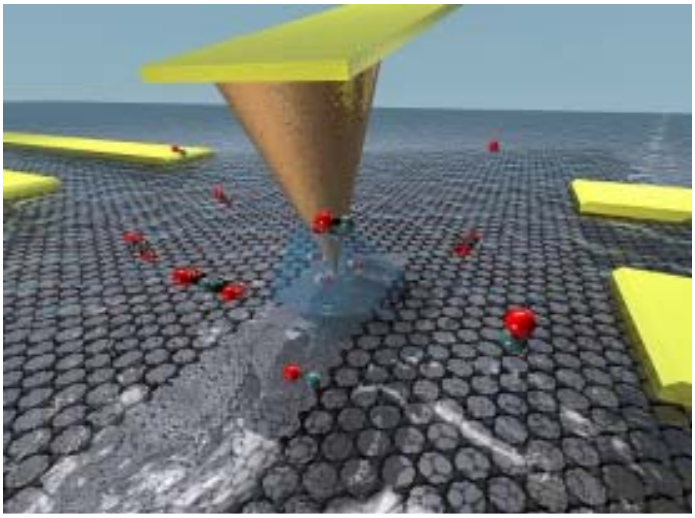

Figure 14*: AFM lithography of graphene*

To achieve patterning of GNRs and bent junctions with nanometer precision, well-defined widths and predetermined crystallographic orientations, one should further improve STM lithography. The latter can be used only for the demonstration of operational principles of new devices, since it is difficult to integrate in a production line; despite the good stability and reproducibility even under ambient conditions [146, 159]. The short de Broglie wavelength of He ions gives He ion lithography an ultimate resolution better than 0.5nm [160], very attractive for GNRs [139,161]. Graphene samples on Si/SiO_2 can be cut using this technique, with computer controlled alignment, patterning, and exposure. Using 30kV He ions, clean etching and sharp edge profiles, 15nm wide were obtained, with little evident damage or doping, so that He-techniques may considered further for GNR production. While many of the very promising applications of graphene do not require precise nanoscale processing, there are numerous applications, for example in digital nanoelectronics and spintronics, for which the precise engineering of GNRs [146] or antidot lattices [162] is mandatory. This is a challenging task, as the properties of GNRs and other graphene nano-architectures depend strongly on the crystallographic orientation of the edges, the width [163], and the edges atomic structure [164], including edge disorder. Precise, reproducible and fast patterning is vital for devices. Patterning of graphene can deeply modify its intrinsic properties, including band-gap and spin properties. Patterning of graphene concerns not

only removal of material (anti-dot lattices, nanomesh, and GNRs) but also suspending it on supports, holes or gates. To date, only few nano-processing methods [165 , 166] have been reported, which can meet the very strict criteria for nanopatterning of graphene, namely crystallographic orientation control and atomic scale precision, see Fig. 14. These rely on local probes (STM, AFM), or crystallographically selective chemical reactions, or their combinations. The usual method for the production of patterns on the 10 - 100nm scale is e-beam lithography, followed by plasma etching. Several groups have used this technique to make GNRs [134], single electron transistors (SET) [167] and FETs [168]. In order to open a practically relevant band gap, graphene must be patterned to critical dimensions in the range of a few nm. However, 20nm is on the threshold of what can easily be achieved using conventional e-beam lithography, due to known electron scattering effects in common e-beam resists [169]. Other top–down approaches, such as reduction of graphite oxide [296], unzipping of CNTs [143,170] Fig. 15a, or liquid-phase exfoliation (LPE) [142] of graphite (Fig.15 b,c), have so far lacked control over the size and edge structure.

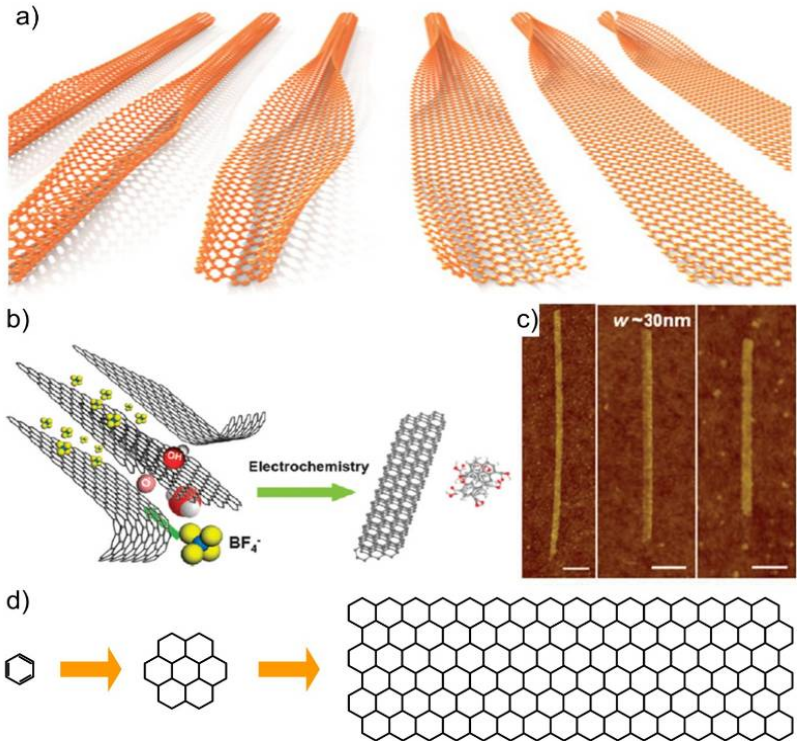

Figure 15*: Top-down fabrication of GNRs via a) unzipping of nanotubes [170] b) exfoliation of chemically modified [166] and c) expandable graphite [263]. d) bottom-up [174].*

The high precision control of graphene edges will create narrow constrictions in graphene wires, down to the atomic size contacts [171,172], and this enables one to operate a GNR as a quantum wire [173], for use in quantum information processing, in conjunction with QDs. Simultaneously, bottom-up synthesis offers an alternative route towards the production of GNRs (see Fig 14 c): GNRs with lengths of 40nm were recently reported [174].

Another goal is to investigate the effects of patterning on graphene, in order to fully control the balance between engineering of desirable properties, against introduction of performance inhibiting defects and artefacts. High-resolution (few nm-scale) lithography enables periodic patterns of voids (‘antidots’) and networks of GNRs [175]. The transport, microwave, and far infrared (FIR) properties of such systems are not yet known, and they require a dedicated investigation. While the study of GNR devices and the optimization of their performances will contribute much to the development of graphene-based nanoelectronics (See Section D) and also THz plasmonics, progress made towards atomic-scale technology, would make graphene an unrivalled platform for non-CMOS approaches to Boolean information processing, by inspiration of monomolecular electronics paradigms [176]. In this context, transport measurement may suggest new ways to implement Boolean logic into designed, atomically-defined graphene nanostructures.

B2.2. *Graphene quantum dots*

QDs are sub-micron-size objects made of conducting materials, which can be incorporated in electronic circuits and then controlled electrically. There are two main physical effects that distinguish the QD electrical properties from any other electronic system: size quantisation of electronic states into a discrete spectrum, and charge quantisation – the phenomenon known as Coulomb blockade. The ability to move electrons in/out the dot one by one makes it possible to use them as SETs. Moreover, by trapping an odd number of electrons (*e.g.*, one) on QDs one can create an electrically controlled localised spin and use it for quantum information processing.

The advantage of graphene as QD material lies in its reduced dimensionality, therefore large charging energy, which protects the quantized charged state of the dot. This enables SET operation at high temperatures. Coulomb blockade effects have been observed in GQDs [167,177,178]. It is now necessary to achieve full control on GQD-based circuits. Besides a further development of atomic scale technologies on graphene, this also requires understanding of the properties of electronic states on graphene edges (functionalized and with dangling bonds).

An additional possibility to create GQDs [38] is related to the unique properties of BLG [34,35,36,51]. In BLG, one can use a transverse electric field created by external electrostatic gates to open a gap, reaching up to 200meV [34]. It has been demonstrated that one can confine electrons in small regions of BLGs using a combination of top/bottom gates, and then, operate the charging states of such QDs electrostatically [179]. Since spin relaxation in high-quality graphene is slow (in particular, due to the absence of a nuclear spin environment, which, on the other hand, is a major problem for the use of III-V semiconductor dots for quantum information processing), further studies of gap control and electron confinement in gapped BLGs are needed.

B2.3. *Patterning- and proximity-induced properties in graphene*

Decoration of graphene with nanoparticles opens up a range of possibilities to modify its charge carrier properties, by proximity effects with superconductors, ferromagnets or coupling to strong spin–orbit entities. From a fundamental point of view, interesting topological transport effects have been predicted for graphene decorated by 5d transition metal adatoms, with very high magnetoelectric ratios [180]. By covering graphene with superconducting island one can induce superconductivity [181,182,183,184] through the Andreev reflection process [185], whereas by changing the carrier density one can control the critical temperature and current of the induced superconducting state [185], as well as induce a superconductor – quantum insulator transition [186,187]. The newly acquired properties of graphene, due to its patterning with other materials, require detailed studies, aiming at determining new functionalities of the hybrid structures. Other routes are: a) to exploit progresses in high critical magnetic field electrodes [188], to inject Cooper pairs in the edge states of graphene QHE; b) combine proximity superconductivity and suspended graphene to extremely high-Q vibration modes, eventually controlled by the ac Josephson effect [181].

Large-scale periodic patterning of graphene may also be done using deposition of nanoparticles, and this would change the high-frequency response of the system, up to the THz range. A superlattice potential can modify the properties of pristine graphene [189,190,191,192,193]. The block-copolymer (BC) technology can be used to create “soft” modulations of graphene, in contrast to “hard” modulations caused by the antidots. In particular, we envisage graphene sheets gently suspended on a regular array of “needles”, fabricated with the BC technology. These novel structures may lead to a plethora of new

phenomena concerning the nature of the achieved modulation, and its tunability. Manufacturing and characterisation of patterned graphene flakes represents both challenging and promising direction of fundamental research in graphene, requiring a combination of graphene-specific techniques with methods developed for more conventional materials, available in a large number of nanoscience centres in Europe.

B3. 2d crystals beyond graphene

There are many examples of 2d materials, besides graphene. A number of studies [3,23] have reported exfoliation of layered materials to atomically thin layers. These include h-BN, transition metal dichalcogenides (TMDs) [194,195,196,197,198,199,200,201,202,203,204,205,206,207,208,209], and possible TIs such as (bismuth telluride) Bi_2Te_3, or (bismuth selenide) Bi_2Se_3 [210,211]. However, other classes of layered material exist. Examples are transition metal oxides, transition metal trichalcogenides, transition metal chalcogenide phosphides, and many others. Each class consists of a range of material types, with its own set of properties. This field is so new that little is known about their physical properties: from insulators (BN) and semiconductors (MoS_2, WS_2) to superconducting metals ($NbSe_2$). Monolayer MoS_2 has a direct band gap [212] (while bulk 2H-MoS_2 has indirect band gap [213]) that allows optical applications and, when used in a lateral FETs [214], On/Off ratios of 10^8 have been achieved. It has excellent electrostatic integrity that allows sub-nanometer thickness, flexible electronics, and may have 100,000 times less power consumption in standby state than traditional Si transistors [214].

Reduced dimensionality is a great advantage for electronic applications. But quantum-mechanical confinement usually translates into different electronic and optical properties from the bulk. Mechanical properties are also tuned by ultra-thin thickness, and the large surface-volume ratio would certainly affect chemical reactivity. With this in mind, it is easy to foresee potential applications in optoelectronics [215], catalysis [216], batteries [217,218] or supercapacitors [219,220], ultrasensitive sensors for pressure changes, gas storage or separation, lubricants [221], inert coatings, lab-on-a-chip substrates, or electrical circuits and molecular electronics in general. Titania nanosheets could be ideal for ultrathin high-k dielectrics, with maximum values for $\varepsilon \approx 125$ for thickness of a few nm [222], better than conventional dielectric oxides. Transition metal oxides, in particular MnO_2 nanosheets, have excellent properties for batteries [223] and supercapacitors [224,225]. They also have photoelectrochemical properties, with photon-to-electron conversion efficiencies comparable to those of dye-sensitized solar cells. The small thickness may facilitate charge separation of excited electron-hole pairs, although the low conductivity could favour recombination if longer migration distances are required. Electrical conductivity can be enhanced by combination of these oxides with graphene, which could enable high-performance energy storage flexible devices. Moreover, the impressive mechanical properties [226,227] of some 2d materials (*i.e.* BN and MoS_2) make them attractive as fillers to reinforce plastics. Thin films prepared from the exfoliation of layered compounds may lead to efficient thermoelectric devices [23,218].

B3.2. *Characterisation of new 2d crystals*

The physical and chemical properties of 2d crystals are yet to be fully understood. In view of the potential applications, in the short term, priority might be given to optimization of band gaps, electron conductivity, chemical activity, and dielectric, magnetic, mechanical and thermal properties. The role of defects (point defects, dopants, grain boundaries, stacking faults, etc) and edge terminations must also be addressed. Due to the reduced dimensions and

large surface-volume ratio, environment effects could be important and need to be studied, especially for reverse engineering of 2d materials to build superstructures (Section C14).

The newly found/produced 2d crystals will be subjected to the same exhaustive studies as graphene. Their structure will be tested using TEM and grazing incidence XRD. Some of these require improvements to get molecular-scale information. Of particular interest would be the development of tools sensible to light elements, enabling chemical differentiation. In this sense recent developments on annular dark-field TEM are very promising. It is most natural to determine the electronic band structure of 2d crystals using ARPES. There are several European facilities with capacity to perform such studies, on a massive scale: BESSY in Germany, Diamond Light Source in the UK, SOLEIL in France, DAFNE in Italy, and several others. Since electronic states in transition metal compounds may feature strong spin-orbit coupling, some of the studies will involve spin-resolved ARPES. Moreover, the development of a scanning ARPES instrument with submicron-resolution is highly desirable for speeding up such studies: this will enable the study of free-standing monolayers left upon a lift-off of a bulk layered crystal, without the necessity to transfer those onto a substrate.

The studies of individual flakes will be performed using a broad range of optical techniques, in particular, absorption, reflectivity, ellipsometry and luminescence measurements on insulating BN and semiconducting MoS_2, WS_2, $MoSe_2$, $MoTe_2$. Raman scattering will be used to investigate phonons, as well as electronic excitations, in order to develop techniques for determining the number of layers in atomically thin films and to characterise their quality. Metallic $NbSe_2$ and $NiTe_2$ will be studied using FIR and microwaves. The doped materials will be subjected to FIR magneto-spectroscopy to characterise the effective masses and to develop non-contact methods for quality assessment.

Transport studies (temperature dependent resistivity, Hall effect) of individual flakes will require the development of methods for non-destructive deposition of metallic contacts and the implementation of the 2d crystals in FET-type devices. These studies may appear to be material sensitive and will require the development of low-temperature deposition processes: some of the dichalcogenides start losing Se and Te already at few hundred ^{o}C. Semiconducting 2d crystals, such as MoS_2, offer opportunities to realize low-power electronic devices and circuits. Because of their atomic-scale thickness and lower dielectric constant than in Si, 2d semiconductors offer large degree of electrostatic control and could overcome issues related to short – channel effects in Si [228].

All of the new 2d materials will be studied using surface scanning techniques, such as AFM and STM. STM studies will be used to shed light onto the spatial structure of the electronic states near the Fermi level, as well as their accessibility from the environment. STM will also provide information on the electronic structure of defects in dichalcogenides (such as S, Se, or Te vacancies) and on the influence of oxygen on these compounds.

B3.3. *Modelling of physical properties of new 2d crystals*

To understand the physical properties of the new 2d materials, a multi-scale modelling approach is needed for each particular material: a combination of microscopic modelling based on first principles, effective minimal tight-binding models, and effective Fermi liquid theory for electrons at low energies. The existing literature on electronic properties of TMDs addresses band structure, Fermi surface nesting, and lattice reconstruction in bulk crystals, but very few studies were devoted to isolated monolayers and bilayers of such crystals, and the properties of the truly 2DEG in them.

From the simulation point of view, there is a need for development of new models of electronic interactions for studies of transport at the mesoscale, effects of disorder, and device simulation. DFT and quantum Monte Carlo simulations will be performed to determine the

band structure and microscopic charge distribution in monolayers of various TMDs, and chemically modified graphene. Developments in the computational physics community (see in B5) will enable to predict optical properties, electronic correlations, and photochemical reactions, as well as to interpret the experimental findings. Multi-scale approaches such as QM/MM can be applied for 2d crystals in solution, or interactions with macromolecules (for example for lab-on-a-chip applications that require control on nanosheet decoration with molecular sensors). New possibilities to find stable TMDs with ferro- and antiferromagnetic properties will be tested. Stability and model of the electronic properties of monolayers and bilayer of ternary compounds $B_xN_yC_{1-x-y}$ will be studied. This will be done both *ab-initio* and by developing phenomenological models for the alloy properties.

Using the input from the *ab-initio* band structure, minimal tight binding models will be developed for each particular compound and used to describe their optical properties (see B5). Effective Fermi liquid theories for electrons at low excitation energies for each 2d compounds will be developed and used to analyse transport and correlation properties, including the Landau level spectrum and transport in the QHE regime.

Using DFT and effective low-energy theories, the electronic properties of the edges of the layers and states formed around defects will be studied. These low-energy models, in conjunction with the group theory analysis of the highly symmetric lattice of the hexagonal crystals, will also be used to study the electron-phonon coupling.

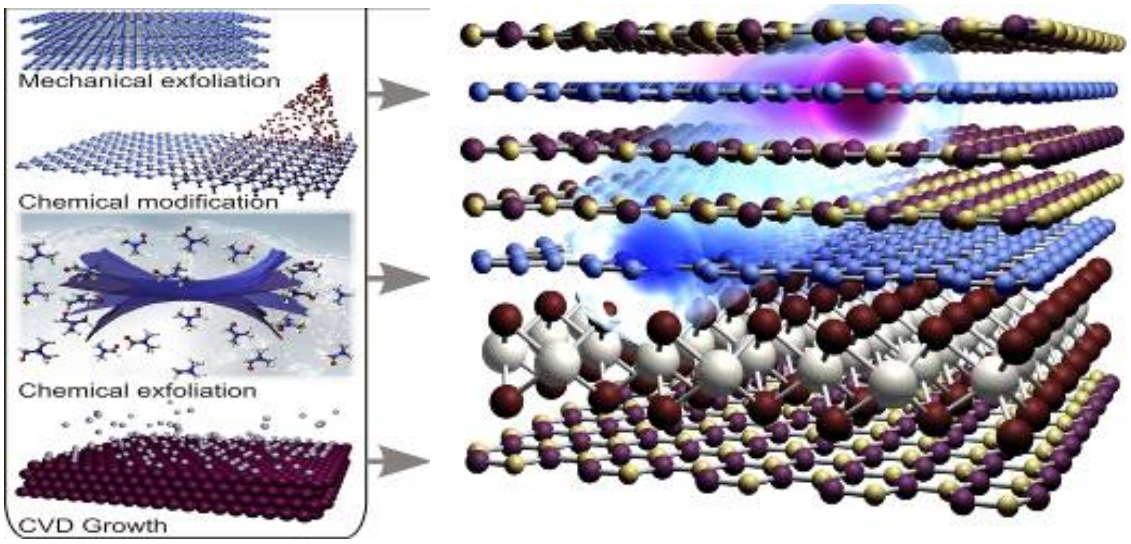

Figure 16*: From 2d crystals to superstructures*

B4. Hybrid structures and superstructures of graphene and other 2d materials

We will explore the concept of "materials on demand": an assembly of graphene and other individual 2d crystals into hybrid superstructures, Fig. 16. This would allow practically infinite number of different multilayers with properties tailored for novel, multitasking applications.

B4.1. *Electronic transport in lateral and vertical hybrid superstructures*

Vertical and lateral transistors are the first and most natural application of atomically thin heterostructures and multilayer systems. Vertical heterostructures and tunnel devices have been used for many years, from the Esaki diode [229] to cascade lasers [230]. 2d-based heterostructures offer a unique prospect of extending the existing technologies to their

ultimate limit of using monolayer-thick tunnel barriers and quantum wells. At the same time, since the doping-dependent screening properties of graphene can be controlled electrically, graphene sheets and thin ribbons in multilayers can be used as gates with widely variable properties – a functionality hardly offered by any other material. New heterostructures, built by one of the methods listed above, will offer unique opportunities to study transport properties of complex, interacting systems (e.g. exciton condensation [231]) and to use such structures for transistor with significantly improved transfer characteristics, sensors and other applications. Vertical devices can also be scaled to one nm laterally, as far as lithography techniques allow.

B4.1.1. *Tunnelling and resonant tunnelling devices*

The feasibility of using multilayer structures for tunnelling devices has recently been demonstrated [32] (Fig. 17) showing that BN can act as an excellent defect-free tunnel barrier [32]. BN monolayer separating two graphene electrodes provide a high-quality tunnel barrier and allow biases as large as 1V without electrical breakdown [32]. The first experiments on exfoliated Gr/BN/Gr structures ("Gr" stands for "graphene") demonstrate non-linear tunnelling I-V curves [32].

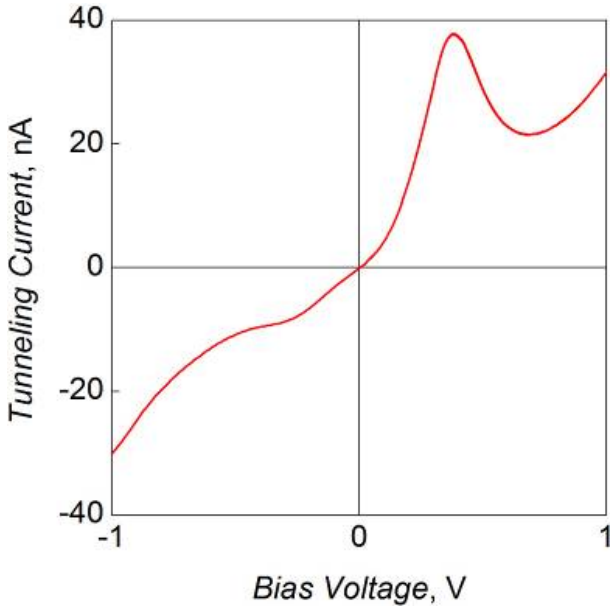

***Figure 17**: I(V) characteristics of a Gr/$(BN)_4$/Gr device. Here $(BN)_4$ stands for 4 BN layers [32].*

Theoretical understanding of transport properties of such vertical FETs, leading to the full control of their operation, will require a substantial dedicated effort. Here, one challenge is to develop quantitative microscopic description of single-particle tunnelling processes, based on atomistic approaches. The other is to take into account several factors important for different parts of the I(V) spectrum: orientation mismatch of Gr flakes, contribution of the phonon-assisted inelastic tunnelling, and the defect-assisted tunnelling.

Aiming at practical applications, further investigation is needed of the possibility of using vertical tunnelling structures of graphene, BN and materials from the TMD family in various nonlinear electronic elements, such as frequency multipliers. Furthermore, tunnelling experiments will be the first step towards the production of other devices, as they will allow to find optimum thickness and to learn about achievable quality of one-atom-thick barriers. There are various types of devices where quantum tunnelling is used (e.g. tunnelling magnetoresistance devices or resonant tunnelling diodes). Atomically thin, smooth and continuous barriers offered by the use of 2d crystals can dramatically improve quality and characteristics of any existing or considered scheme involving quantum tunnelling. Investigation of resonant tunnelling is a logical continuation of the tunnelling experiments. Modulating the tunnelling barrier height by using different materials (for instance using heterostructures like *Gr/BN/MoS_2/BN/Gr* or *Gr/BN/Gr/BN/Gr*) will create additional states in the barrier, which would allow resonant tunnelling, see Fig. 18 [32]. Such devices are most interesting to get negative differential resistance conditions, which can be used in various

non-linear components. Furthermore, resonant tunnelling through impurities and defects enables to map the wavefunction of the latter [232].

Vertical graphene-based structures represent a new approach to develop functional electronics. Rapid response and ultra-small sizes can also be achieved in vertical transistors. Indeed, electron transfer through nm thick barriers can be extremely fast (and, possibly, coherent). Ballistic tunnelling transistors may allow one to overcome the most significant drawback of GFETs: the low On/Off ratios. The tunnelling devices would have a highly insulated off state with no dissipation, which should allow not only individual transistors but integrated circuits at room temperature. The latter is difficult to achieve for horizontal transport in graphene and remains a distant goal. The ideas currently under consideration include several architectures for tunnelling/hot electron transistors. The simplest is *metal/BN/Gr/BN/Gr*, where the metal contact (separated from the bottom graphene by thick, tunnelling non-transparent BN) serves as a gate and the two graphene layers (acting as emitter and collector) are separated by thin BN layer. The operation of the device relies on the voltage tuneability of the tunnelling density of states in graphene, and of the effective height of the tunnel barrier adjacent to the graphene electrode. It will be worth experimenting with several different dielectrics in heterostructures, such as *metal/BN/Gr/MoS_2/Gr*. Higher quality heterostructures and dielectrics with smaller tunnelling barrier will bring the On/Off ratio to 10^5-10^6, as required by modern electronics.

Another interesting idea is to attempt the development of a hot electron transistor, similar to those discussed in semiconductor electronics [233]. Few-atom-thick transistors based on a 2d tunnelling barrier and graphene may allow much better quality, and become more successful in applications. The transit time through such sandwiches is expected to be <<1 ps, whereas there are no limits for scaling down in the lateral dimension to true nm sizes. In a *metal/BN/Gr_B/BN/Gr_T* system, the thickness of the active part of the devices would be less than 10 atoms (~3nm) and should allow a ballistic current controlled by the central graphene electrode. The assembly of 2d crystals into superstructure may also allow stacks of several transistors in series (*metal/BN/Gr_B/BN/Gr_T*)$_N$, thus a vertical integrated architecture.

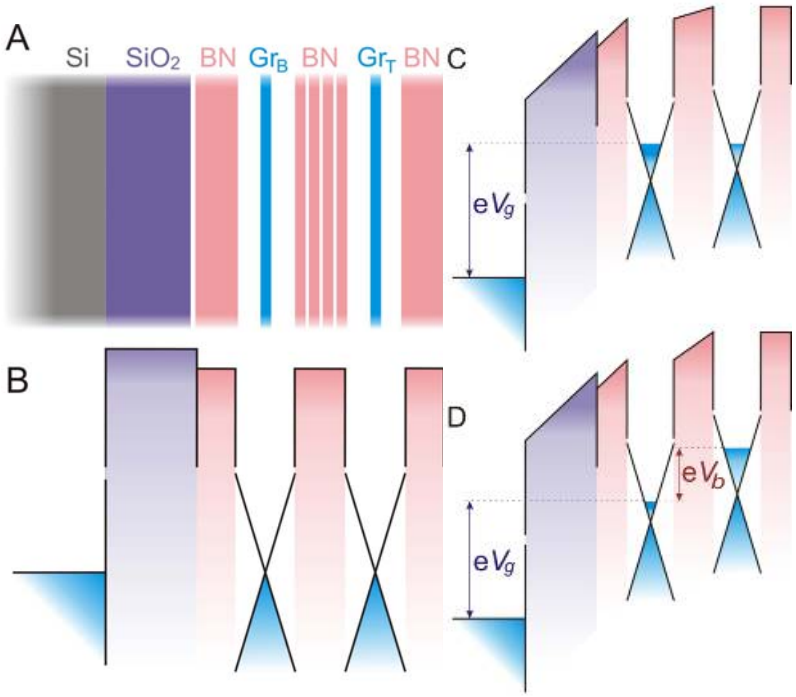

***Figure 18**: Graphene field-effect tunneling transistor. (A) Schematic structure of the proposed experimental devices. (B) The corresponding band structure with V_g=0. (C) The same band structure for a finite V_g and zero V_b. (D) Both V_g and V_b are finite. The cones illustrate graphene's Dirac-like spectrum [32].*

B4.1.2. *Light emission and photovoltaics*

Superstructures of 2d crystals will be used to develop tunnelling LEDs and photovoltaic cells. Here, we refer to superstructures composed of two conducting layers separated by a barrier with a modulated profile. Type-I quantum wells (Fig. 19) can be used for injecting electrons and holes, with subsequent recombination leading to light emission.

Using more complicated structures, both type-I and type-II quantum wells of various configurations can be created. As the band-structure of 2d materials depends on the number of layers, simply by changing the thickness of one component, we could tune the optical properties. Using various thicknesses of different materials one can target LEDs of different colours. As individual heterostructures can be combined in one stack with individually contacted layers, LED at different wavelengths could be combined in one structure.

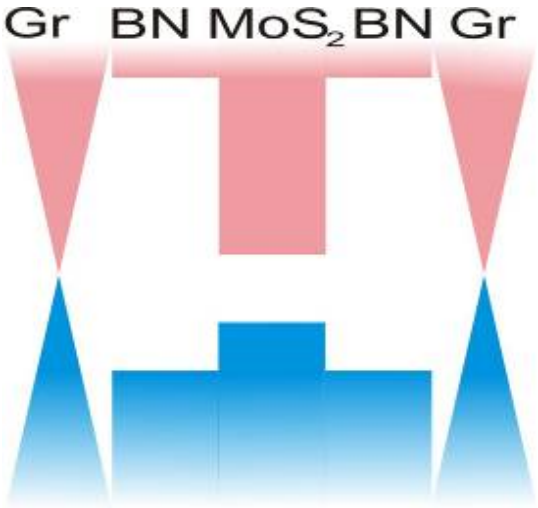

***Figure 19**: Gr/BN/MoS_2/BN/Gr structure: blue is the valence band and pink is the conduction band [32].*

Similarly, photovoltaic devices can be created by placing two metallic 2d crystals (for instance graphene) within tunnelling proximity of each other. By applying bias voltage (or by using proximity effect of other metallic 2d crystals) electric field will be created inside the barrier. Any e-h pair excited by light will be separated and contribute to photocurrent. Similarly to the case of LED, it should be possible to create heterostructures with various band gaps, sensitive to photons of different energies. Moreover, plasmonic nanostructures can improve the performance of graphene photovoltaic devices [234].

B4.1.3. *Hybrid superstructures for active plasmonics*

Combinations of 2d heterostructures with plasmonics would allow for creation of active optical elements. 2d heterostructures are ideally suited to be used with plasmonic structures, as they can be positioned exactly at the maximum of electric field. Such elements are of great importance in different areas of science and technology: from ubiquitous displays, to high tech frequency modulators. Despite great progress in optical disciplines, active optics still relies heavily on either liquid crystals, which guarantee deep modulation in inexpensive and small cells, but are quite slow, or non-linear optical crystals, which are fast, but bulky and expensive. Thus, the development of inexpensive, fast and small active optical elements would be of considerable interest.

The target is the design and fabrication of a new generation of active plasmonic metamaterials with optical properties electrically controlled by 2d heterostructures. Plasmonic metamaterials of various configurations will be sandwiched between *Gr/BN* heterostructures (see Fig. 20). The conductivity of graphene can be changed by two orders of magnitude using electrostatic doping. This could modulate the optical properties of the under-lying plasmonic structure. The combination of 2d heterostructures with plasmonics could result in fast, cheap and small active optical elements.

The optimisation of active plasmonic materials will require multiscale modelling of their properties, taking into account plasma modes and single-particle excitations, as well as their coupling with flexural vibrations of individual layers. Further studies will include modelling of heating of superstructures and their cooling by lateral and vertical heat transfer.

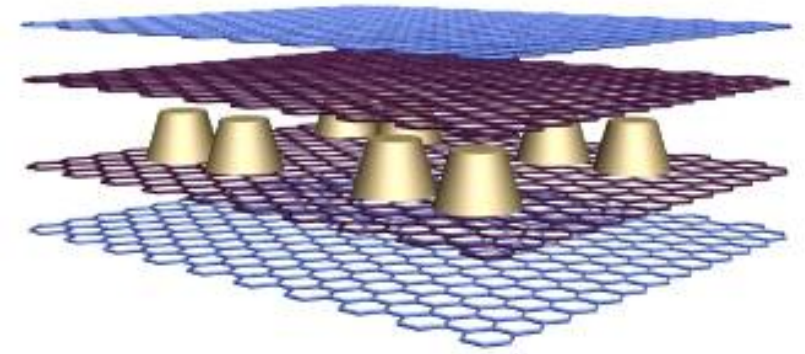

***Figure 20**: Active plasmonic superstructure: Au dots sandwiched between Gr/BN layers.*

B4.1.4. *In situ characterization methods*

Graphene hybrid systems will require advanced characterization, which should involve both high spatial and/or point resolutions and coupling preferentially in-situ. This will limit the contact with air, preventing contamination. Two kinds of in-situ coupling are worth considering: (i) coupling several characterization methods to investigate a single object, for instance HRTEM + Raman spectroscopy + electrical measurement, in order to accurately correlate the structural features and the physical behaviour. (ii) Coupling one or several characterization methods (e.g., HR-TEM imaging and electrical measurement) with one or several treatment methods (e.g., mechanical and/or thermal stresses) in order to correlate the variation of the behaviours with the structure changes. Considering in-situ TEM experiments, the above considerations will be typically allowed by using sample holders equipped with various facilities (e.g., able to apply thermal or mechanical stresses to the specimen). However, we plan to develop other sample holders that will allow a larger panel of possible tests to be applied to the samples under study. When the in-situ coupling is technically difficult (e.g., coupling TEM and UV-Raman, which cannot be done through an optical fiber, or coupling TEM and high magnetic field inducer), the chip-based sample holder technology will be highly preferred. Indeed, the latter will allow the chip to be transferred from a characterization method to another, each of them being equipped with the appropriate sample holder bearing the same in-situ treatment methods. This will allow carrying out various investigations on the same hybrid graphene specimen under the same conditions.

The chemical functionalization of graphene with reactive molecules and the deposition of supramolecular assemblies requires studying the self-organization process and the molecule/graphene interface in several conditions: At the liquid-solid interface, by wetting-dewetting processes but also in connection with ultra-high vacuum (UHV) conditions. This is already possible with UHV systems in different European laboratories, combining several sources of molecule deposition (sublimation, liquid-valve injection), with surfaces characterization techniques such as STM and X-ray and UV Photoelectron Spectroscopy. Several STM techniques are currently used: low temperature STS, Spin-polarized STM and Fourier-Transform Scanning Tunnelling Spectroscopy, which can allow a local dispersion and surface Fermi measurement. Synchrotron sources can be used for high resolution ARPES, X-ray magnetic circular dichroism (XMCD) and also spin-polarized low-energy electron microscopy particularly useful for the ferromagnet /graphene interfaces.

B5. Multiscale modelling of graphene-based structures and new 2d materials

Modelling of physical properties of new 2d materials and graphene-based devices constitutes an important research direction. Specialised modelling effort is needed to provide timely interpretation of the characterisation of new 2d materials, assessment/prediction of functional properties, and guidance of technological effort in creation of hybrid superstructures ('materials on demand', see in B4). This will require the implementation of a multiscale modelling approach, in which the materials band structure and local microscopic parameters computed using *ab initio* simulations are incorporated in the mesoscale description of electronic transport, thermal, mechanical, and optical characteristics, which, then enter into the finite-element modelling of operational devices or technological processes.

Many fundamental questions are open in the field of nano-electronics and new materials. Due to the complexity of both, these cannot be answered by conventional simplified approaches. The research of novel functional materials is highly interdisciplinary covering the domains of chemistry, material science, physics, and engineering with their methods and scope of length scales. Advanced knowledge of such fields has necessarily to be combined. In addition the complexity of quantum laws in nano-electronics complicates upscaling attempts, to the point that, at the cross-road of new materials and nanoelectronics (especially for beyond-CMOS applications), only multiscale modelling approaches can progress knowledge sufficiently fast in the near future. The development of the necessary theoretical and computational methods, as well as improvement of the existing technologies are therefore needed and will be a local part of the S&T Roadmap.

B5.1. *Ab initio computations*

Quantum laws are very well covered by *ab initio* methods. *Ab inito* modelling provides an atomistic viewpoint by computing the atomic structure from monomers to larger clusters of atoms and molecules with larger systems treated with lower accuracy (which is commonly accepted practice). The suitable *ab initio* methodologies encompass the following approaches, all of which will require further development: Hartree-Fock theory (HF) and Post-Hartree-Fock (PHF) quantum chemistry methods. Usually, HF has insufficient accuracy for most purposes, but it provides a good starting point for quantum chemistry configuration interaction methods, Møller-Plesset perturbation theory and coupled-cluster methods. PHF is highly accurate, but scales extremely poorly with system size [O(N6) or worse] [235]. Almost always used localised basis sets. Codes generally allow optimisation of geometry and calculation of a wide range of other properties.

DFT is the "standard" ab initio approach. Either plane-wave or localised basis sets can be used. Conventional DFT calculations scale as O(N3), but linear-scaling [O(N)] DFT methods are available for insulators. DFT results can be mapped to tight-binding theory, to enable transport calculations. Most DFT codes allow molecular dynamics and lattice dynamics calculations (using density functional perturbation theory, DFPT, or finite displacements). Limitations include failure to describe van der Waals forces and band gap underestimation.

GW theory: Approximation to the self-energy of quasi-particles in a many-body system, to obtain accurate excitation energies. The methods generally scale as O(N4), although a paper describing an O(N3) implementation recently appeared [236]. GW theory can use the Bethe-Salpeter equation [237] to describe excitonic effects [238,239], but scaling is O(N6).

Time-dependent density functional theory (TDDFT): Time-dependent formulation of Kohn-Sham equations, for calculating response functions [240]. Poles of density-density response function correspond to excited states. TDDFT is a cheaper, but less accurate than GW, for determining excited-state energies.

Quantum Monte Carlo (QMC): Most accurate total energy method for condensed matter. Scaling is O(N3), like standard DFT, but with a much greater prefactor. Quadratic scaling algorithms have been developed. QMC is able to exploit massively parallel computers. Excitation energies are accurate, but must be calculated one by one as differences of total energy. QMC molecular and lattice dynamics will be available in the near future.

There is a manifold of codes suitable for modelling new 2d materials and hybrid structures, developed and maintained by European research groups:

ABINIT: Plane-wave DFT code, also able to perform TDDFT and GW calculations.
ADF: Slater-function basis DFT code. Also able to perform TDDFT calculations.
CASINO: Quantum Monte Carlo code.
CASTEP: Plane-wave DFT code.
CHAMP: Quantum Monte Carlo code.
CONQUEST: Linear-scaling DFT code (using B-spline basis).
CPMD: Plane-wave DFT code for performing molecular dynamics simulations. It can be used to perform TDDFT calculations.
CRYSTAL: Gaussian-basis Hartree-Fock/DFT code.
FLEUR: Full-potential linearized augmented plane-wave DFT code.
GAMESS-UK: Gaussian-basis quantum chemistry code, post-Hartree-Fock.
OCTOPUS: TDDFT on real-space grids.
ONETEP: Linear-scaling DFT code.
QUANTUM ESPRESSO: Package of first-principles codes including DFT in a plane-wave basis (PWSCF), with TDDFT and GW codes (YAMBO).
SIESTA: Linear-scaling DFT code.
VASP: Plane-wave DFT code.

Despite the intensive software development, the computational cost of *ab initio* methods is still very expensive. This originates from the complexity of electrons represented by wavefunctions, hence, possessing an inner structure with widely variable properties compared to simple particles used in classical molecular dynamics. The requirement of self-consistency is only one consequence of the quantum nature which slows down such methodology. Although many concepts exist to weaken this impact, there is a practical limitation to sizes of systems, at present of about 1-2 nm, treatable ab-initio. This, however, is not the lengthscale on which one discusses functional materials (at least one-two orders of magnitude above).

B5.2. *Mesoscale modelling*

The characteristics and fundamental properties of interest of functional materials are co-defined on a larger length scale beyond the *ab initio* scope. This is because they are additionally influenced by other facts governing properties on such length scales, such as low concentration dopants, impurities or structural defects, or simply that the relevant structures may reach these dimensions themselves. Special attention has to be paid to the interfaces or interaction of layers in multilayer systems.

Multiscale modelling is capable of bridging the introduced length scales. The concept is based on the observation that not all interactions must necessarily be treated within the first principles framework. This allows one to introduce a hierarchy of interactions, which might be founded either on very general considerations or just adapted and valid for the presently studied properties. Based on this, a hierarchy of levels of treatment may be introduced. The lowest (microscopic) level deals with the smallest objects at the highest accuracy. It can be identified with the full *ab initio* level. Multiscale modelling defines first the models on each level and second the interfaces of transferring relevant information to the respective upper (or even lower for feedback loop) level where they are further processed. The advantage is that

not all information available on the computationally heavy lower level enters the upper-level modelling, but only relevant condensed information which is precisely where multiscale modelling is benefiting from. In addition, modelling of interactions on the upper macroscopic level replaces respective couplings on the more refined lower level. This allows one to reduce the work at the lower level by treating smaller parts (non-interacting subsystems) there.

For instance a finite range impact on electrostatics and on electronic properties can be expected from impurities or dopants depending on the local surrounding of a host crystal. Additional long-range parts such as the Coulomb interaction might be separable and can be treated on the upper level. The information on local electronic properties can still be obtained with massively parallel ab-initio methods using large supercells. On the other hand, the evolution of a system as a whole composed of millions of atoms including a certain distribution of such dopants is unpredictable by *ab initio* methods when the whole system is included at the same level. The problem is solved by combining local *ab inito* codes with specialised solvers addressing mesoscale range of distances. Such combined codes, developed and maintained by European research groups include:

LOTF: Hybrid quantum/classical molecular dynamics code;
SMEAGOL: DFT-based Transport code developed;
TranSiesta: Extension of SIESTA with recursive Green functions solver.

For a broader range of applications, including electronic and heat transport, optics, optoelectronics, thermomechanics, etc, alternative hybrid codes will be needed, and their development will be a natural part of a scientific Roadmap.

B5.3. *High Performance Computing*

In the longer term, having a strong and realistic simulation capability will provide a strategic tool to support product development in all fields of applications, including ICT and beyond. In this perspective, supercomputing will be very useful for material characterization and device simulation at a realistic level. The use of High Performance Computing (HPC) is certainly necessary for making advances in frontier developments in the fields of first-principles calculations and multiscale methodologies. To make these new computational schemes useful, supercomputers must be used intensively. However, one should note that the grand challenge in the development of multiscale computational tools for simulating ICT is not just a question of computing faster and faster. E.g., for simulating complex graphene-based devices (NEMS, sensors, transistors, or circuits), in additional to high performance computing resources, more physical inspection of models and suitable use of first principles are needed. This will apply to all types of devices (realistic tunnelling FET, memresistors, sensing devices, NEMS…).

There already exists an infrastructure of European supercomputers named PRACE [241], gathering the leading platforms. Graphene research will greatly benefit from a connection to supercomputers facilities, especially for material simulation to serve as guidance applications. Improvements are required for multiscale modelling and reverse engineering, such as decreasing the problem complexity, ideally to O(N). In DFT this has already been achieved for insulators with the advent of O(N) codes. For other methods it is a far greater challenge. Furthermore, it is essential to add functionality (the ability to calculate a range of properties) to these codes, whilst retaining the favourable scaling.

Other improvements include the increasing the ease of use (availability of documentation, support, examples, well-designed and clear input and output, ease of installation, etc.), robustness (lack of bugs and numerical reliability), "reverse engineering" tools

Broad cooperation between European groups authoring the existing codes will be needed, for comparison between codes for testing and optimisation purposes, development of better

interfaces between codes, including better data standards, developments of methods that can exploit massively parallel computer facilities, development of "code libraries" and allowing problems to be distributed among members of a community.

Developments made to first-principles algorithms and codes will be equally useful in other areas of physics, chemistry and materials science. First-principles codes and algorithms aim to be general. For example, the first principles methods already used to study graphene have been developed for many other materials.

B5.4. *Further development of field-theory and kinetic theory methods*

Analytical methods will play an equally important role in the multiscale modelling of new 2d materials and graphene-based systems, providing a consistent scalability of materials parameters and a systematic description of 2d materials in strongly non-equilibrium states.

The effects of e-e correlations, as well as the interplay between e-e interaction and disorder can be efficiently addressed using the renormalisation group approach. The latter enables one to follow non-trivial (non-linear) scaling of effective materials parameters upon the variation of the length scales at which the electron system is studied. It is based upon the microscopic input (phenomenological or provided by DFT modelling), permitting one to formulate a medium-energy effective field theory describing the physical system, and it is followed by the analysis of the renormalisation flow of essential constants in the theory, which may (or may not) be length scale dependent. The renormalisation group approach may and will be applied to the studies of both quantum effects, like localisation in graphene, the interactions-driven phase transitions into states with spontaneously broken symmetry, and to studies of classical problems related to the renormalisation of flexural deformations of graphene considered as a flexible membrane.

The development of efficient methods of kinetic theory is also necessary, in order to treat graphene in strongly non-equilibrium conditions. As a one/two-atom thin material with a weak coupling to the substrate/environment, graphene may be easily overheated. Moreover, the energy relaxation of non-equilibrium carriers in graphene (photoexcited or injected by tunnelling) has not been fully understood and requires extensive modelling effort. Tackling graphene at high current, reaching the conditions of the flake breakdown, is even a more challenging theoretical problem, which requires the use of a combination of the microscopic dynamics computation with the mesoscale kinetic theory.

B5.5. *Correlations in multiple graphene layers*

e-e interaction is relevant in BLG [242], where novel phases are expected. A similar situation is expected in FLG with (translational or rotational) stacking faults.

Apart from fundamental questions, a deeper understanding is relevant for potential applications, because of possible bandgaps induced by correlations that may compete with gaps in graphene nanostructures due to their spatial confinement.

The role of electronic correlations in graphene systems is yet poorly understood, and its understanding will thus be a major issue during the next years. These e-e interactions lead to novel, yet unexplored phases, with possible magnetic order or unusual topological properties due to an expected time reversal symmetry breaking. The interplay between topology and interactions opens a new research field in theory (advanced analytical and numerical techniques, such as DMFT extensions) and experimental physics, where novel experimental techniques are required for probing these phases (e.g. Kerr rotation measurements).

C. Production of Graphene, related 2d crystals and hybrids

The industrial exploitation of graphene, related 2d crystals and hybrids will require large scale and cost-effective production methods, while providing a balance between ease of fabrication and final material quality. One advantage of graphene is that, unlike other nano-materials, it can be made on large and cost-effective scale by either bottom up (atom by atom growth) or top-down (exfoliation from bulk) techniques.

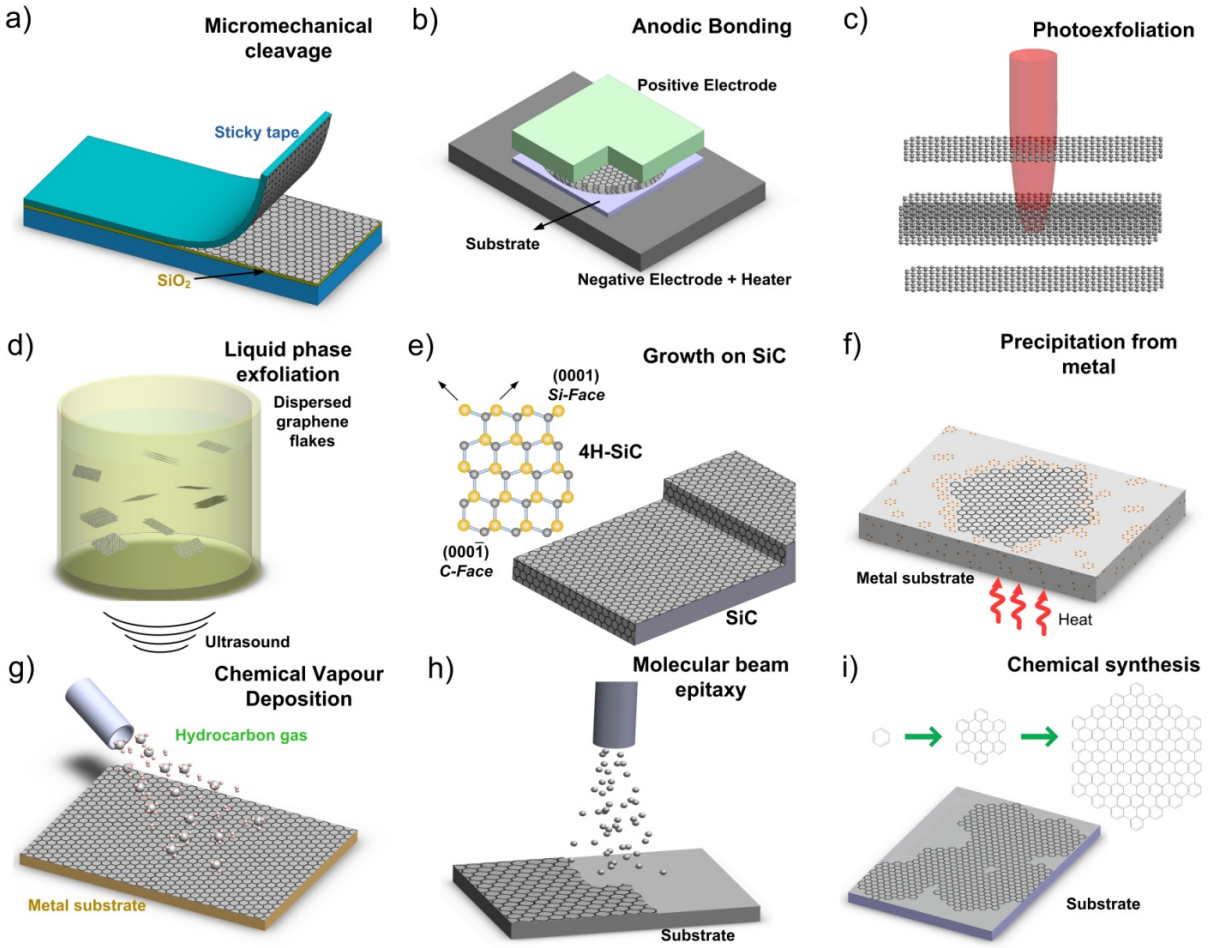

Figure 21*: Schematic illustration of the main experimental setups for graphene production. (a) Micromechanical cleavage (b) Anodic bonding (c) Photoexfoliation. (d) Liquid phase exfoliation. (e) Growth from SiC. Schematic structure of 4H-SiC and the growth of epitaxial graphene on SiC substrate. Gold and grey spheres represent Si and C atoms, respectively. At elevated temperatures, Si atoms evaporate (arrows), leaving a C-rich surface that forms graphene. (f) Precipitation from carbon containing metal substrate. (g) CVD process. (h) Molecular beam epitaxy. Different carbon sources and substrates (i.e. SiC, Si, etc.) can be exploited. (i) Chemical synthesis using benzene as building blocks.*

C1. Mechanical exfoliation for research purposes and new concept devices

Micromechanical cleavage (MC) [3] consists in repeatedly peeling off a piece of graphite by means of an adhesive tape, Fig. 21a. MC has been optimized to give SLG up to mm in size [33], of high structural and electronic quality (mobility>10^6 cm^2/Vs). Although MC has low yield and throughput, and is impractical for large scale applications, it is the method of choice

for fundamental research, and most key results on individual SLG were obtained on MC flakes. MC is ideal for making prototype devices and will always be essential to investigate both new physics and concept devices.

C2. Anodic bonding

In anodic bonding [243,244] graphite is attached to a glass substrate by means of electrostatic forces and then cleaved to leave SLG, see Fig. 21b. This technique is widely used in microelectronics to bond Si wafers to glass [245]. Anodic bonding makes it possible to apply MC on a larger scale, while still giving high quality samples. Only the first or first few atomic layers remain bonded to the substrate, while the bulk can be peeled off. Anodic bonding allows the production of flakes with μ~6000 cm^2/V s [243] and up to millimetres in size [243]. Because the samples are bonded to a rigid glass substrate, this technique can produce larger samples than MC. This method may also be used for other layered materials.

C3. Laser ablation and photoexfoliation

Laser ablation is the removal of material, via evaporation and/or sublimation, from a solid surface by a laser beam irradiation, (Fig. 21c), [246]. In the case of layered materials such as graphite, if the laser beam irradiation does not determine evaporation and/or sublimation of the carbon atoms, but the detachment of an entire or a part of a layer, the process is called photoexfoliation [247].

***Table 2**: State of the art of the main production strategies and foreseen applications*

Method	Crystallites Size, μm	Sample Size, mm	Charge Carrier Mobility (@R*T*)	Applications
Mechanical Exfoliation	1,000	1	2×10^5 $cm^2/V\cdot s$ $10^6 cm^2/V\cdot s$ (@low *T*)	Research and proof of principle devices
Liquid Phase Exfoliation	0.1	0.1 (∞ as overlapping flakes)	100 $cm^2/V\cdot s$ (for a layer of overlapping flakes)	Coating, paint, batteries, supercaps, solar cells, composites, sensors, TCs, photonics flexible electronics and optoelectronics, bio-applications
Chemical Exfoliation via Graphene Oxide	1	1 (∞ as overlapping flakes)	1 $cm^2/V\cdot s$ (for a layer of overlapping flakes)	Coating, paint, batteries, supercap, solar cells, composites sensors, TCs, photonics flexible electronics and optoelectronics, bio-applications
Growth on SiC	50	100 (6'')	10^4 $cm^2/V\cdot s$	RF transistors other electronic devices
CVD	500	1000	10^4 cm2/V·s	Photonics, nanoelectronics, TCs, sensors,bio-applications

Tuning the ablation threshold energy density permits patterning of graphene with high spatial control [248]. Selectivity, *i.e.* the ablation of a defined number of layers, is obtained thanks to energy density windows existing between the minimum required for ablating SLG, and the energy density required for ablating FLGs [248]. Photoexfoliation could be used to detach intact SLGs from a graphite surface, one at a time, in principle free of contaminants and defects, at a high rate, both on wafer and in liquid. Photoexfoliation can be alternative and complementary technique to LPE.

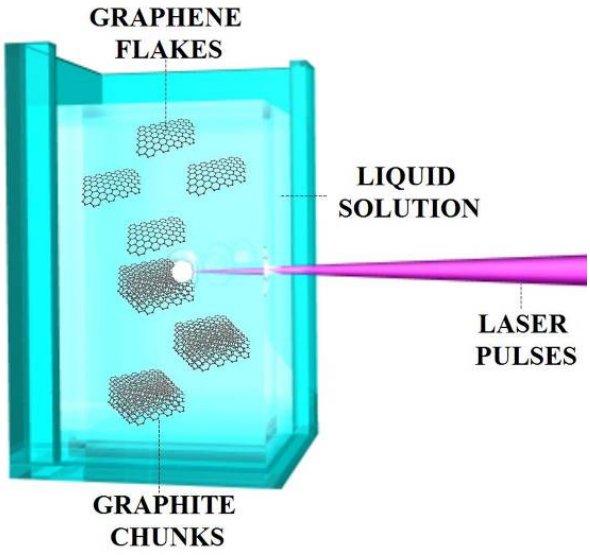

***Figure 22**: Photoexfoliation of graphite in liquid environment.*

Laser irradiation (Fig. 22) has room for further optimization. This technique was tested to produce flakes from direct laser irradiation of graphene oxide (GO) [249]. New protocols are needed to prepare graphene flakes in liquid, overcoming the limitations of LPE, exploiting high boiling point solvents and surfactants. Laser ablation is still in its infancy, and all the parameters require further optimization.

The laser irradiation approach is of general validity. It can be extended to other layered materials with weak interlayer coupling.

C4. Chemical exfoliation of pristine graphite, graphite oxide; graphene derivatives

Graphene flakes can be produced by exfoliation of graphite via chemical wet dispersion followed by ultrasonication (Fig. 21d), both in aqueous [250,251] and non-aqueous solvents [20,251]. This technique offers many advantages in terms of cost reduction and scalability.

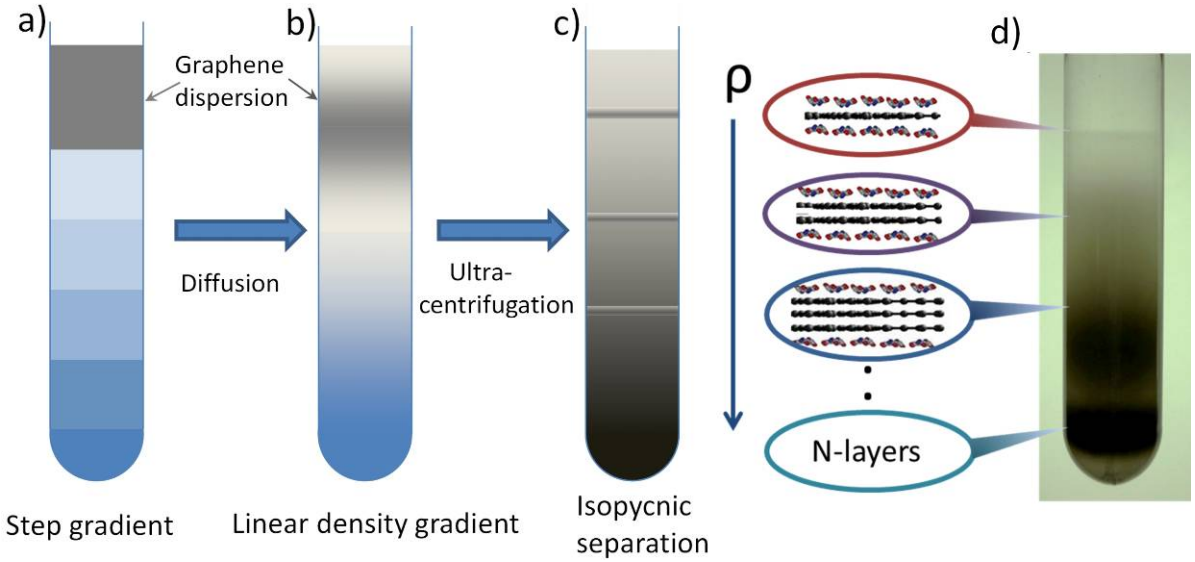

***Figure 23**: Sorting of graphite flakes via isopycnic separation. Formation of (a) step gradient and (b) linear density gradient. (c)The flake-surfactant complexes move along the cuvette, dragged by the centrifugal force, until they reach their corresponding isopycnic points. The buoyant density of the flake-surfactant complexes increases with the number of graphene layers. (d) Photograph of a cuvette containing sorted flakes.*

Thick flakes can be removed following different strategies based on ultracentrifugation in a uniform [252] or density gradient medium (DGM) [253]. The first is called differential ultracentrifugation (sedimentation based-separation, SBS) [252], while the second density gradient ultracentrifugation (DGU) [253]. SBS separates various particles on the basis of their sedimentation rate [252] in response to a centrifugal force acting on them. Up to ~70% SLG can be achieved by mild sonication in bile salts followed by SBS [106]. Graphene flakes with lateral sizes ranging from few nm to a few microns can be produced with concentration up to a few mg/m in up to litre batches [254,255]. Control on the number of layers is achieved via DGU: graphitic flakes are ultracentrifuged in a preformed DGM [253,256], see Fig. 23 a,b. During the process, they move along the cuvette, dragged by the centrifugal force, until they reach the corresponding isopycnic point, *i.e.*, the point where their buoyant density equals that of the surrounding DGM [253]. The buoyant density is defined as the density of the medium at the corresponding isopycnic point [256]. Isopycnic separation has been used successfully to sort nanotubes by diameter [257], metallic vs semiconducting [258] and chirality [259]. However, unlike nanotubes of different diameter, graphitic flakes have the same density irrespective of number of layers, so another approach is needed to induce a density difference. This is provided by the surfactant coverage. Indeed, in the presence of an uniform surfactant layer, the GSC buoyant density increases with number of layers, see Fig. 3c. Fig. 23d is a photograph of the cuvette after the isopycnic separation with Sodium Deoxycholate (SDC) surfactant. To date, up to ~80% SLG yield was reported by using isopycnic separation [260]. Other routes based on chemical wet dispersion have been investigated, such as exfoliation of fluorinated graphite [261], intercalated compounds [262], expandable graphite [263] ultrasonication of graphite in ionic liquid [264], and non-covalent functionalization of graphite with 1-pyrenecarboxylic acid [265].

LPE is cheap and easily scalable, and does not require expensive growth substrates. A range of applications for graphene lie in conducting inks [266] (Fig. 24a), thin films [20] (Fig. 24b) and composite materials [250] (Fig. 24c). For these, graphene is best prepared as flakes, so that the active surface is maximised. The resulting material can be deposited on different substrates (rigid and flexible) following different strategies, such as drop and dip casting (Fig. 24d), rod (Fig. 24e) and spray coating (Fig. 24f), ink-jet printing (Fig. 24g), etc.

High quality graphene inks and ink-jet printed thin film transistors with mobility ~100cm^2/Vs have been demonstrated, paving the way towards a fully graphene-based printable electronics [266].

The aim is to further develop LPE to get control on-demand of layer number, flake thickness and lateral size, as well as rheological properties of the resulting dispersions. A combination of theory and experiments are needed to fully understand the exfoliation process in different solvents, in order to optimise the separation of graphene flakes in centrifugal fields, so to achieve SLG and FLG with well-defined morphological properties at a high rate.

A very desirable step in graphene technology is the development of techniques capable of manipulating individual flakes. Optical tweezers (OT) can trap, manipulate, control and assemble dielectric particles, single atoms, cells and nanostructures [106,267,268,269]. These can be used to trap graphene layers and/or GNRs in liquid environments. The coupling of OT with a Raman spectrometer (Raman Tweezers [106]), can test solutions composition and sort layer number in optofluidic channels. The assessment of exfoliation yield is essential to allow further improvements. Detailed structural characterisation of the exfoliated sheets can be done by aberration-corrected HRTEM and STEM, EELS and in-situ TEM. These can characterise the exfoliated materials down to the atomic level. The effect of structural defects on the electrical properties can be investigated in-situ.

Chemical derivatives of graphene, e.g. graphite intercalated compounds (GICs [270]) and GO [271,272], are useful for various applications. GICs are formed by periodic insertion of atomic or molecular species (the intercalant) between the graphene layers [270]. This modifies the band structure. GICs are typically characterized in terms of a 'staging' index *n*, i.e. the number of graphene layers between two adjacent intercalant layers. GICs have a long history since the first recorded production by Schaffautl in 1841 [270]. For GIC production, a number of approaches have been developed over the years, starting from solid [273], liquid [274] or gaseous reagents [275]. Intercalation takes place at high vapour pressure (*i.e.* at ~3-5 atm) of the intercalant material [275]. Using these methods, hundreds of GICs with donor (alkali, alkali earth metals, lanthanides, metal alloys or ternary compounds, etc.) or acceptor intercalants (*i.e.* halogens, halogen mixtures, metal chlorides, acidic oxides, etc.) have thus far been produced [276,277,278,279,280,281]. In general, the intercalation process increases

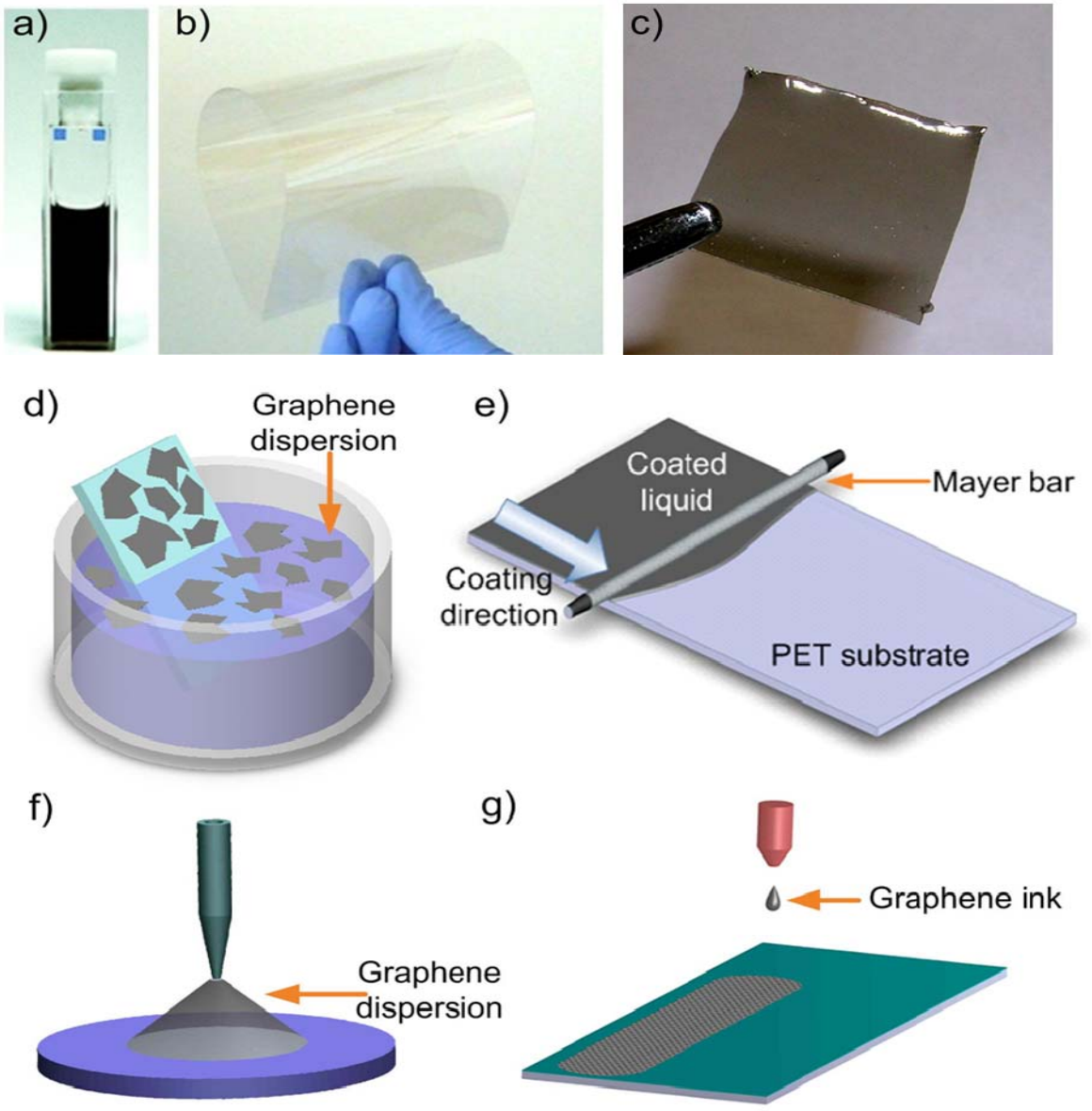

***Figure 24**: (a) Graphene ink. (b) Graphene-based TCF and (c) graphene polymer composite. (d) Dip casting and (e) rod coating of LPE graphene. In rod coating, a wire-covered metal bar (Meyer bar) applies the graphene dispersion onto the substrate. (f) Spray coating and (g) ink-jet printing.*

the interlayer spacing in graphite. This is particularly true for GICs with low stage index [276,282]. E.g., K, Rb, Cs-GICs have interlayer distance ~0.53-0.59nm, while more complex intercalants, such as dimethylsulfoxide, increase it to 0.9nm [276]. These values are 1.5 to ~3 times larger than the spacing in graphite, making GICs ideal for LPE, even without ultrasonication [276,277,282]. To date it is possible to exfoliate GICs (produced from graphite oxide) with lateral size on the order of 20 μm and a yield of ~90% single layer [277].

GICs have potential as highly conductive materials. Indeed, metal chloride or pentafluoride GICs like antimony pentafluoride (SbF_5) have been intensively investigated since the '70s [278,279,280]. For example, SbF_5 GICs can offer up to ~70 times increase in electrical conductivity compared to bulk Cu [279,280]. They have also interesting superconducting properties [283], with transition temperatures of up to 11.5K for C_6Ca GICs [279,280]. They are also considered potential hydrogen storage materials, yet again due to their increased interlayer spacing. GICs were commercialized in batteries, in particular, for Li-ion batteries in the 1970s [284,285,286,287] GICs got further boost as negative electrodes (anode during discharge) with the introduction of solid electrolytes [288,289].

Aspects of the intercalation mechanism, key for applications, still need to be clarified. This has implications for life duration of Li-ion batteries [290,291,292]. The role of the solvent and the search for novel strategies for intercalation are also crucial, particularly to achieve large quantities of LPE graphene. Some GICs were shown to be spontaneously soluble in polar solvents without need of sonication or high shear mixing [262,293].

Other open questions are: what is the role of the intercalant, the charge transfer to the graphene layer and the modification of the graphene band structure. The effects of commensurability and types of intercalation (homogeneous superstructure) can rule Tc.

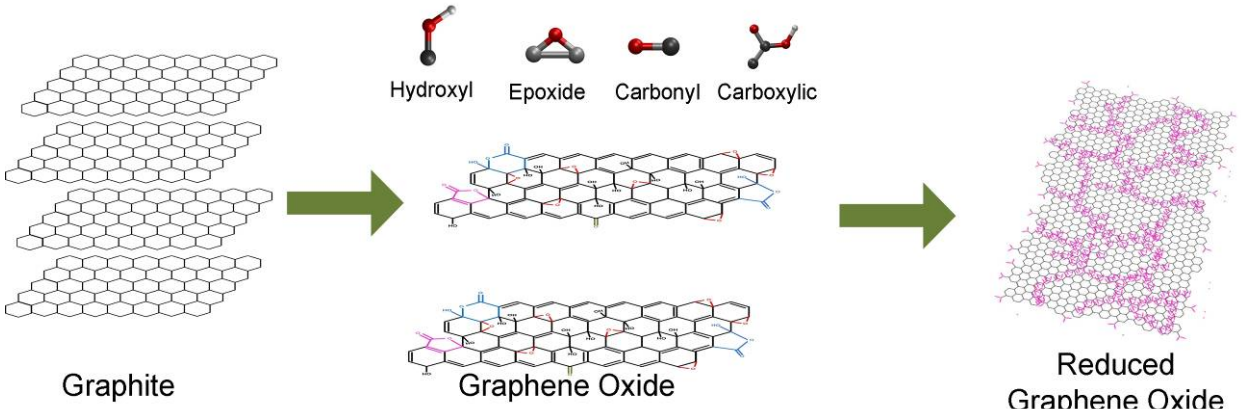

***Figure 25**: GO synthesis and reduction. Graphite can be oxidized with different procedures in the presence of strong acids. The GO flakes have the basal plane functionalized with epoxy and hydroxyl groups, both above and below it, and the edges with a variety of functional groups. This makes GO sheets defective. A partial restoration of the electronic properties is obtainable following different reduction strategies.*

LPE was first achieved through sonication of graphite oxide [294], Fig. 25, the oxidation of graphite following the Hummers method [295]. This makes GO sheets readily dispersible in water [296] and several other solvents [297]. One advantage of GO based dispersions is that the flakes tend to be predominately SLG. However, although large GO flakes can be produced; these are intrinsically defective and electrically insulating [298]. Despite several attempts [298,299], reduced GO (RGO) does not fully regain the pristine graphene electrical conductivity [299].

Nevertheless, RGO, as well as pristine graphene dispersions, can be deposited on different substrates with all the aforementioned techniques. Moreover, GO is ideal for mass

production of material that can be used in composites. RGO may also be employed as electro-active layer [300,301,302] or transparent layer [303] in FETs and solar cells [304].

Heating-driven reduction has the potential to produce good quality graphene structures. Laser heating in an oxygen-free environment (Ar or N_2) can be done with a spatial resolution down to a few μm and temperature as high as 1000ºC. This will enable graphene micro-patterns fabrication (also monolayer thick). This methodology paves the way to large-scale production of patterned graphene. GO is also luminescent [305]. GO could be used in low-cost optoelectronic devices, display and lighting applications [306]

Other strategies to create reactive dangling bonds directly on edges or GNRs have been developed [301]. Thus GO and chemically modified graphene (CMG) are also attractive for bio/medial applications, for the development of new biosensors, for bio-labelling and bio-imaging [307], for tissue engineering, for drug delivery and as antibacterial.

Another option is to induce magnetism property by chemical functionalization. Theoretical studies predicted that defective graphene could be semiconductive and magnetic [308,309,310]. Ref. [311] reported a mixture of disordered magnetism regions (ferro, super-paramagnetic and antiferromagnetic) on graphene using nitrophenyl functionalization. The aim is to induce long-range ferromagnetic order by controlling the chemisorbed sites for spintronics [311].

Functionalized graphene could be used as substrate for the deposition and organization of supramolecular layers and (or) enhance the local reactivity by inducing a curvature. Molecules are used either simply for the doping [312,313] or to use the graphene itself as substrate for the self-organization of supramolecular layers or simple molecules [314,315] and (or) using Moiré pattern for example in the case of graphene/Ru(0001) [316,317].

The outstanding issue is to understand the electronic interaction between molecules and graphene and the balance between molecule-molecule and molecule-substrate interaction for the realization of supramolecular network.

An important demonstration of the possibility to functionalize graphene with individual molecules is the recent realization of a prototype of molecular spin valve device made by decorating a graphene nanoconstruction with $TbPc_2$ magnetic molecules [318]. These experiments open a wide research field and several intriguing questions on spintronics.

C5. Epitaxial graphene on SiC

Graphene can also be made through Si sublimation from SiC [319,320,321] (Fig. 21 e) following high-temperature annealing. Acheson reported a method for producing graphite from SiC in as early as 1896.

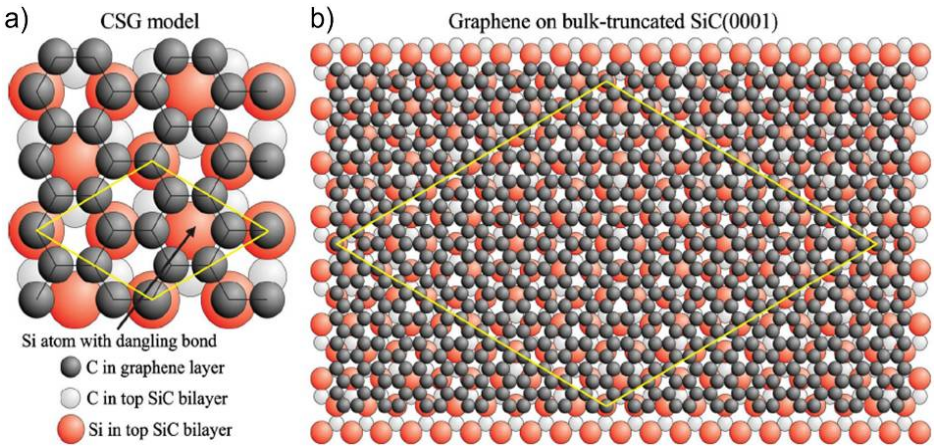

***Figure 26**: a) Top view of CSG model on SiC(0001). b) graphene on bulk-truncated SiC(0001) surface [325].*

Both surfaces (Si(0001)- and C(000-1)-terminated face) annealed at high temperature under UHV tend to graphitize, because of the evaporation of Si atoms from the topmost layers of the crystal [322,323]. Refs. [320,321,324] reported the production of

graphene films by thermal decomposition of SiC above 1000 °C. This is not a self-limiting process and areas of different film thicknesses may exist in the same layer [321].

On the Si(0001)-face (see Fig. 26) the graphene layer is grown on top of a C-rich $6\sqrt{3}\times6\sqrt{3}R30°$ reconstruction with respect to the SiC surface, which is called the buffer layer [325]. This consists of carbon atoms arranged in a graphene-like honeycomb structure [325]. The buffer layer has the same σ bands as graphene, but not the same different π bands [325]. The buffer layer can be decoupled from the Si(0001)-face by hydrogen intercalation [326,327].The topmost Si atoms are now saturated by hydrogen bonds. The buffer layer is turned into a quasi-free-standing graphene monolayer with its typical linear π bands [326]. In contrast, the interaction between graphene and the C(000-1)-terminated face is much weaker [325].

The graphene growth rate depends on the specific polar SiC crystal face [328,329]. Indeed, graphene forms much faster on the C-face than on the Si-face [328,329]. On the C-face, larger domains (~200 nm) of multilayered, rotationally disordered graphene are produced [330,331]. On the other hand, on the Si-face, UHV annealing leads to small graphene domains, typically 30-100nm in diameter [331]. The small-grain structure is attributed to morphological changes of the surface in the course of high-temperature UHV annealing [321]. Indeed, Ref. [332] via energy-resolved maps of the local density of states of graphene grown on Si-face revealed modulations on two different length scales, reflecting both intra-valley and inter-valley scattering due to in-plane atomic defects. These defects in UHV annealed SiC are related to the relatively low growth temperatures and the high graphitization rates in the out of equilibrium UHV Si sublimation process [328].

Different strategies have been proposed in order to control the Si sublimation rate. Ref. [333] used Si in a vapor phase establishing thermodynamic equilibrium between the SiC sample and the external Si vapor pressure to vary the temperature of phase transition from the Si-rich (3 × 3) to the C-rich ($6\sqrt{3}$ × $6\sqrt{3}$ R30°) structure, the buffer layer, and the final graphene layer. The obtained graphene samples were an order of magnitude larger with respect to samples obtained in UHV conditions [326].

Ref. [321] used the “lightbulb method”, exploiting an 80-year old process at first developed to extend the lifetime of incandescent lightbulb filaments [334]. This relies on the use of Ar, in a furnace at nearly ambient pressure (1 bar), to reduce the Si sublimation rate. This is driven by the dense cloud of Ar molecules hindering transport of Si atoms away from the SiC surface [321]. Indeed, in Ar atmosphere, no sublimation of Si from the surface is observed at temperatures up to 1500°C, whereas Si desorption commences at 1150 °C in UHV[321]. This increases the graphitization temperature by several hundred °C, enhancing surface diffusion, obtaining complete surface restructuring before graphene formation [321].

Graphene films on the Si-face have smooth surfaces with tens of micrometres (~50μm) domains [321], almost 3 orders of magnitude larger than via UHV annealing [331].

Si sublimation can also be controlled by confining the SiC in a graphite enclosure (either in vacuum [328] or in an inert gas [328]) limiting the escape of Si, thus maintaining a high Si vapor pressure. This procedure permits graphene growth, close to thermodynamic equilibrium, both on Si-[328] and C-face [328], producing either SLG [328] or FLG [328] films over macroscopic areas. The advantage is the control of the graphene formation rate by introducing inert gas (*i.e.* Ar) into the graphite enclosure. High temperature annealing of SiC can also bring to the production of GNRs and GQDs on demand [335,336].

To date, graphene grown on the Si-face has mobility at RT in the range 500-2000 cm^2/Vs [328], while much higher values are achieved on the C-face (10 000 - 30 000 cm^2/Vs) [326,328,329].

Graphene transistors can be manufactured from epitaxial graphene on a wafer scale [337]. The use for sensors and RF devices is interesting [337], but a clear advantage with respect to other materials and existing technology still needs to be demonstrated.

A key metrological application of epitaxial graphene is as QHE-resistance standard [54]. Disadvantages of epitaxial graphene are the high cost of SiC wafers, their limited size compared to Si wafers, and high processing temperatures, well above current CMOS limits. Although the growth of graphene on SiC improved considerably over the years, the layers are not perfect yet due to step edges.

The main aim is to control the layer thickness homogeneity (currently not 100% monolayer) probably via better control of unintentional mis-cut angles, the understanding and control of unintentional doping caused by the substrate, together with a better understanding of the effect of structural in-homogeneities (e.g. steps, wrinkles, BLG inclusions) on transport, and the mechanisms limiting mobility. Other targets are the growth of graphene on pre-patterned SiC substrates, and a better control of growth on the SiC C-face, so to have SLG also on this face. The aim is also to tune epitaxial graphene properties via interface engineering (e.g. SiC surface hydrogenation, etc.) and better understanding of defects generated during growth and/or interface manipulation and identification of methods to heal them. Doping of graphene by insertion of heteroatoms will also be addressed, with the aim to have a full control on the procedures and consequently on the properties of the graphene flakes. The achievement of many of the aforementioned goals will require a careful investigation and improvement of the substrates. Other points to be addressed are routes to improve growth of cubic SiC as substrate, and the growth of insulating SiC layers on cheap on-axis n-type substrates, in order to replace expensive semi-insulating substrate materials.

The graphene quality and the number of layers are strongly dependent on the growth and annealing conditions. The advantage over standard CVD is the graphene quality control achievable via tuning of carbon source thickness and annealing conditions. In addition, all the process steps occur in fully semiconductor compatible environment. Thus, the semiconductor industry can then take benefit of the versatility of this method to integrate graphene in their process flow. The long term goal is a totally controlled graphene nano-structuring, so to produce GNRs and GQDs on demand. This is motivated by the prospect of band gap creation in graphene.

Different techniques can be used for the characterization of epitaxial graphene such as Raman, (STM), X-ray photoelectron spectroscopy (XPS), ARPES, spectroscopic ellipsometry, etc.

C6. High temperature segregations from carbon-containing metals and inorganic compounds

Segregation from carbon-containing metal and inorganic substrates is another approach [338,339,340], see Fig. 21 f). This exploits the temperature-dependent solubility of interstitial carbons in transition metals (i.e. Ni(111) [341], Ru(001) [342], Ir(111) [343], Pt(111) [344], Pd(100) [344], etc) or inorganic chemical compounds (i.e. LaB_6 [345]) to achieve layer-by-layer growth of graphene on the surface. The transition metal is first annealed to high temperature (>1000° C) in UHV, where the bulk solubility of interstitial carbon is high, then cooled to decrease solubility, resulting in its segregation as a graphene film [346].

Significant attention has been devoted to the use of relatively inexpensive metals such as Ni [100,347,348,349] and Co [350]. Growth on noble metals, Ir [343], Pt [344], Ru [342], and Pd [344], aimed at a better understanding of the growth mechanisms. It would be desirable to have a stable metal that can promote “graphene single crystal growth”. The use of (111) oriented Ni or Co could facilitate the hexagonal arrangement of carbon atoms.

To get large metal grains with crystalline orientation *i.e.* Ni(111)[351], an annealing of the metal surface is often performed. The carbon segregation in Ni(111) was investigated in Ref [100], with control of number of surface C atoms by adjusting the annealing temperature.

The graphene-metal distance and its nano-rippling on the metallic substrate determined by the so-called graphene-metal Moiré superstructure [100,343]. The latter is due to mismatch between the substrate graphene lattices, and depends on the metal substrate. For lattice mismatches between graphene and substrate below 1%, commensurate superstructures, where the resulting broken symmetry is a doubling of the unit cell along one axis (*i.e.* 1/2, 0,0), are formed [352]. This is the case for Ni(111) [346] and Co(0001) [353]. On the other hand, larger mismatches yield incommensurate (total loss of symmetry in a particular direction, *i.e.* (0.528,0,0)) moiré superstructures, such as in Pt(111) [88], Ir(111)[354], or Ru(0001) [355]. Indeed, graphene grown on Ir(111) yields flakes of well-defined orientation with respect to the substrate [343]. On the contrary, graphene obtained via high-temperature segregation of C on Ru(0001) has a spread of orientations [355]. Moreover, the graphene/Ru lattice mismatch results in a distribution of tensile and compressive strains [356]. This causes corrugation, due to buckling, and the formation of~1.7 Å humps [356].

The Moiré superstructure could be eliminated by the adsorption of oxygen on the metal surface acting as intercalant [357].

The aim is to have a full control on the graphene quality and the number of layers. These are strongly dependent on the growth and annealing conditions and a full control on the latter is still missing. Moreover, the production of high quality graphene via carbon segregation first requires that defects, such as grain boundaries, pentagon-heptagon pairs, point defects [358], wrinkles [359], or local deformations are avoided. Another open issue is the transfer of graphene produced via carbon segregation onto arbitrary substrates. An optimized procedure has not been developed yet.

C7. CVD growth on metals in vacuum, atmospheric, and high pressure

CVD proceeds by exposure of a catalyst to a carbonaceous precursor at suitable reaction temperatures. SLG and FLG can be readily grown on metal substrates (see Fig. 21 g), such as Ni, Cu, Ir, Ru, etc. [100, 360 , 361 , 362 , 363]. Many carbon sources have been used, such as Methane, Ethylene, and Acetylene. Graphene grown on Cu was reported with mobilities exceeding 16400 cm^2/V s at room temperature [364]. Since it is not possible to measure the films while still on Cu, it is difficult to determine if there is degradation as a result of transfer.

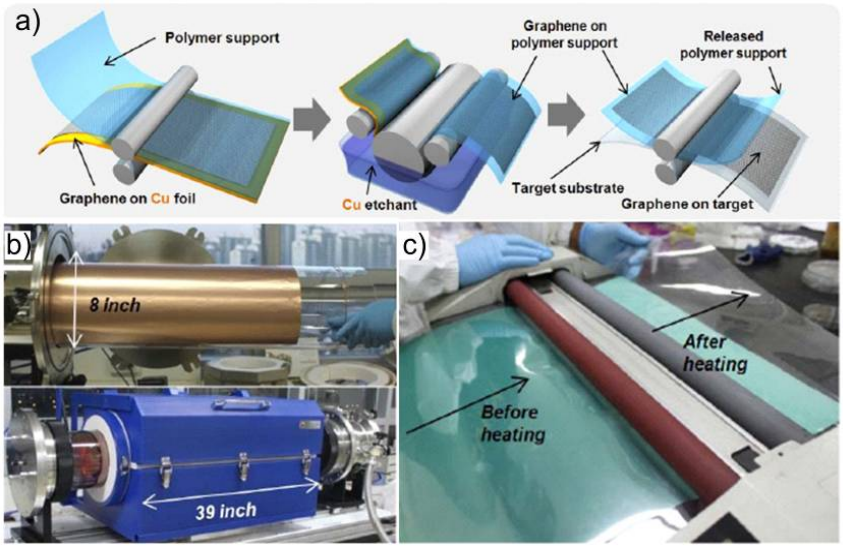

***Figure 27**: Roll-based production of graphene. a) Schematic of the process. b) A Cu foil is wrapped on a 7.5 inch quartz tube, then placed into an 8-inch quartz reactor. c) R2R transfer of graphene from to a PET film [4].*

Graphene films with lateral size ~50cm and μ>7000 cm^2/Vs can be produced on Cu and transferred via a roll-to roll (R2R) process, see Fig. 27 [4].

The goal is now to grow high quality samples (with crystal size>10-100μm) over large areas via R2R. Growth on metallic alloys will be investigated, as well as the optimisation of CH_4-H_2-Ar mixtures. Alternative precursors will be tested and screened. There is increasing evidence GBs and wrinkles are responsible for the degradation of the electronic performance [365]. However, so far there is little experimental insight into the underlying GB formation mechanisms, crucial to understand and control charge propagation across/within these line-defects. On one hand, there is a need for quick and easy characterization methods, able to reveal the grain structure of the CVD grown samples [366]. On the other hand, grain boundaries can be highly transparent as well as perfectly reflective [367], they are expected to act as molecular metallic wires [368] or filter the propagating charge carriers based on the valley-index [369]. In order to explore and exploit these properties the investigation of the electronic properties of individual GBs with known atomic configuration is needed. STM is a versatile tool for investigating both the structure of individual GBs at atomic resolution and their electronic (and magnetic) properties on the nanometer scale [146]. Substrates and dielectrics with optimized properties will allow devices with high mobility.

CVD growth has also been demonstrated from liquid sources, such as benzene, and various solid sources, including polymers, such as PMMA and polystyrene [370]. Different precursors will be investigated, as well as the effect of growth parameters such as temperature and pressure.

Growth of graphene on single crystal substrates is another route towards the improvement of its electronic properties, although the high cost of such substrates makes them less suitable for large scale applications. This requires *in-situ* growth monitoring. TEM will be fundamental to obtain atomic images of domain boundaries, as well as macroscopic images of the relative domain orientations in a film [371]. Graphene nucleation needs to be investigated, to control and enhance domain size, via controlled and multi-step exposures.

Reducing the growth temperature is desirable in order to cut production costs, and directly integrate graphene with standard CMOS processing. Growth of FLG at 650°C was demonstrated on Fe [372]. However, the optimization of layer control and growth temperatures below 450°C is required for CMOS integration. Although the growth of nanographene at 325°C has been shown on MgO [373], its suitability for applications is yet to be elucidated. Graphene grown on Cu foils at temperatures as low as 300°C using benzene as a precursor was also reported [370].

Plasma-enhanced CVD (PECVD) is a scalable and cost effective large area deposition technique, with numerous applications ranging from electronics (IC, interconnects, memory and data storage devices), to flexible printable electronics and photovoltaic. PECVD has also been proposed for low temperature growth of thin graphitic films [374, 375, 376] and nanowalls (CNWs) [377, 378, 379, 380]. This might address the key issue of growth at low temperatures, to prepare graphene directly on substrates compatible with applications and

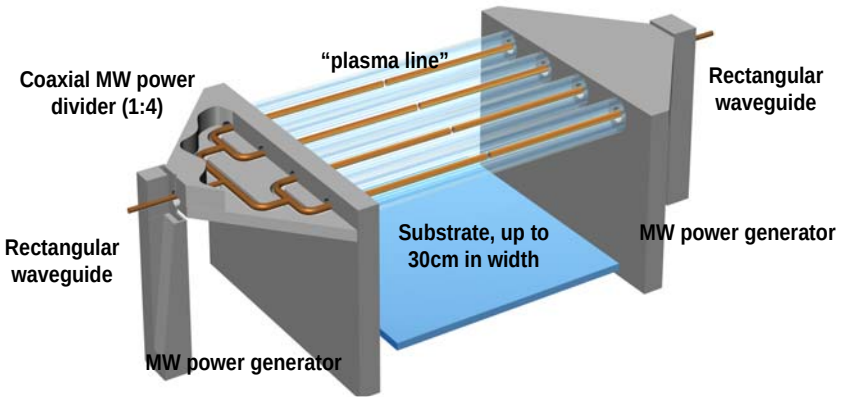

Figure 28: *Schematic of large area pulsed MW system*

processing technologies listed above. An example is direct deposition on plastic. The advantage of plasma methods with respect to thermal CVD is the production of graphitic materials without metal catalyst over a wide range of growth conditions, both as surface-bound and freestanding materials [378].

However, large domains are needed, together with a reduction of damage caused by direct plasma during growth that might limit the quality of graphene that can be achieved with this approach. Nevertheless, this approach seems to be promising for TCs [4].

MWCVD has also been proposed as a method for graphene growth [381,382]. Ref [382] reported growth at 150-300° C. However, to date SLG grown has not yet been demonstrated, with the deposited films consisting of sub-micrometer flakes [382]. Nevertheless, this approach was successfully used for the production of TCs [382]. With further developments it could be a viable strategy for large scale, low temperature graphene production [382].

A key target is thus the development of low temperature growth on large area, by understating and optimising plasma chemistry.

Low temperature high density pulsed micro wave plasmas (electron density close to 10^{12} cm^{-3}) are not only usable for large are growth, but also surface processing and work-function engineering, important for chemical functionalization, and for mobility control. Systems scalable to large areas should be investigated (see Fig. 28).

The production of unsupported flakes using alcohols as carbon feedstock was also demonstrated [383,384], with the potential for up-scaling.

The target is to further up-scale the CVD graphene-growth, developing a protocol for a batch reactor, producing m^2-sized graphene. The development of new routes to achieve stable doping is another key need for commercialization. Different approaches will be investigated, either during growth, by exploiting alternative precursors (i.e. pyridine), or post-growth, via "molecular doping" by stable hydrazil- and nitroxide- organic radicals and metal grids.

Another key point is the development of reliable, fast, economic and environmentally friendly transfer techniques. Methods for the recovery of the metal substrates are also needed for cost reduction and environmental issues. The presence of the substrate generally modifies the graphene electronic properties, thus it is of paramount importance to optimize the interaction between graphene and substrate. This interaction can be tuned by applying surface treatments that, in turn, can provide additional control on the graphene properties. Substrates and interfacial dielectrics with optimized properties will enable high mobility devices. Basic reaction kinetics and layer-by-layer growth will be investigated by dedicated surface science experiments. Real-time spectroscopy will be used to monitor CVD-graphene growth to understand the thickness distribution and optimize the growth conditions.

C8. CVD on insulators, CVD/PECVD deposition of functional coatings

Growth of high-quality graphene layers on insulating substrates, such as SiO_2, SiC, sapphire, ect., would be a major factor step forward towards the application of graphene in nano-electronics. The use of SiC wafers in microelectronics is becoming increasingly popular [385] (see, e.g, the new SiC MOSFET developed by CREE [385]) which should result in lowering of their prices. Moreover, SiC substrates of up to 150mm diameter should become available in the short term.

CVD of carbon thin films on insulators has been known since 1971 [386]. However, thus far it was optimized to give highly sp^3 bonded diamond-like carbons. Recently this approach has been developed to achieve graphitic films [387,388]. Growth on SiC [389], sapphire [390] and Si_3N_4/Si [391] was reported, as well as on metal oxides such as MgO [373], and ZrO_2 [392]. However the domain size and quality so far produced is inferior to CVD grown graphene on transition metal catalysts.

h-BN has also been shown to be effective as a substrate for graphene CVD [393], and graphene produced by this method appears comparable to that grown on transition metal catalysts [352,362]. As well as achieving direct growth on an insulator, this approach has the additional benefit of an atomically smooth substrate, with few dangling bonds and charge traps [394]. Direct growth of graphene/h-BN stacks, by both CVD and metal-organic CVD (MOCVD), is the ideal alternative to tedious successive exfoliations of rare BN single crystals (mostly one source in Japan [395]). CVD can also give C-BN composite layers with various topologies. Different B and N precursors (solid, liquid, gaseous) should be tested in a variety of environments, aiming at optimum quality and layer control, and privileging less costly and harmful ones. Wafer scale extension of BN/graphene encapsulation techniques will pave the way to transport in high-frequency electronics [396], a regime exploiting Dirac Fermion optics, with no counterpart in semiconductor electronics. Substrate tailoring will optimize these properties in a broad (and economically relevant) spectrum, from microwave to optics including millimeter waves (THz) and IR.

The aim is to produce graphene on smart substrates in a single CVD run. At present, however, only FLGs were grown by CVD on h-BN, thus improved thickness control is needed. Understanding basic growth processes is needed, with the help of both in situ and ex situ characterizations. These procedures should then be adapted to more scalable conditions.

PECVD has the potential to synthesize graphene at lower temperatures than conventional CVD in a graphene-on-insulator (GrOI) environment.

The long term target plan (>10 years) is to achieve on-demand graphene deposition on insulator/Si and other materials on 300–450mm wafer size, in-line with the fabrication projections in the electronic industry. The challenge is to develop an integrated atomic layer deposition ALD-PECVD process that would allow deposition of compatible insulators at the same time as synthesising graphene. This should be done without compromising the quality of the graphene layer.

C9. Molecular Beam Epitaxy growth of graphene on insulating surfaces

Molecular Beam Epitaxy (MBE) is an Ultra-High-Vacuum (UHV)-based technique for producing high quality epitaxial structures with monolayer control. Since its introduction in the 1970s [397] as a tool for growing high-purity semiconductor films, MBE has evolved into one of the most widely used techniques for epitaxial layers of metals, insulators and superconductors, both at the research and the industrial level. MBE of single crystal semiconductors, e.g. GaAs, is a well-established technique and has produced hetero-junctions with the current record value of mobility (3.5×10^7 cm^2/Vs [398]). MBE has also produced record low threshold current density multi-quantum-well lasers [399]. MBE can achieve precise control of both the chemical composition and the doping profile. MBE can use a wide variety of dopants compared to CVD epitaxial techniques.

MBE can be used to grow carbon films (see Fig. 21 h) directly on Si(111) [400], and is a promising approach to achieve high-purity graphene heterostructures on a variety of substrates such as SiC, Al_2O_3, Mica, SiO_2, Ni, ect. MBE graphene will have applications in RF, THz electronics, heat management and could enable novel functionalities by producing hybrid structures.

MBE is more suited to grow 2-6 inch wafers rather than 30-inch ones [4]. MBE graphene will find industrial applications in niche markets where highly specialised devices are required. Despite the conceptual simplicity, a great technological effort is required to produce systems that yield the desired quality in terms of materials purity, uniformity and interface control. The control on the vacuum environment and on the quality of the source materials should allow higher crystal quality compared to non-UHV-based techniques. Although MBE

of graphene is still very much in its infancy, there are a number of groups working on it, some in Europe. Multi-crystalline graphene has been reported, with crystal grain size up to 20–400nm [401]. The higher end of this range is comparable to CVD grown graphene. In-situ growth of heterostructures could produce devices based on hybrid structures, combining graphene and semiconductors. Graphene can be grown directly on a wide variety of dielectric and metallic substrates as well as h-BN. Growth on MBE-grown h-BN is a possibility.

The aim is to develop atomic beam epitaxy techniques for high-quality large-area graphene layers on any arbitrary substrates. In particular, targeted characteristics of MBE graphene are: high-mobility samples – at least as good as exfoliated graphene on h-BN, i.e. ~ a few 10^5 cm^2/Vs (at small carrier densities) and precise control over the number of layers, *i.e.* SLG/BLG/TLG. Although to date the growth process gives mainly polycrystalline graphite-like films [400], with future optimizations, it may be possible to produce large area single crystal sheets on a wide variety of dielectric and metallic substrates. The fine control of doping, and the growth of hybrid semiconductor/graphene heterostructures –e.g. for heat management applications, will be investigated. MBE is also interesting for semi-transparent large-area electrodes, most of all in view of integration with Si technology.

Another benefit of MBE is that it is compatible with in-situ vacuum characterization. Thus, the growth can be controlled by in-situ surface sensitive diagnostic techniques, such as reflection high-energy electron diffraction, STM, XPS, etc.

C10. Heat-driven conversion of amorphous carbon and other carbon sources

Heat-driven conversion of amorphous carbon (a-C) is emerging as an alternative method for synthesis of graphene [402,403,404]. The process, carried out at high temperature (>2000 K) could transform a-C or hydrocarbons in crystallized graphene domains.

In the case of a-C conversion, small a-C clusters rearrange and crystallize due to the high temperatures reached during current annealing without the involvement of any catalyst [402]. The a-C rearrange through a phase of glasslike carbon into high-quality graphene before the temperatures are high enough for the a-C evaporation [402].

The transformation of physisorbed hydrocarbon adsorbates into graphene requires an intermediate step [403]. At annealing temperatures around 1000K the hydrocarbon transforms into a-C initiating the crystallization phase [403]. At temperatures exceeding 2000 K the transformation terminates in the formation of polycrystalline graphene [403]. The high temperature removes contaminants [402,403].

Heat-driven conversion can also be applied to aromatic self-assembled monolayers (SAMs), composed of aromatic carbon rings [405]. A sequence of irradiative and thermal treatment of SAMs, cross-links them, and then converts them into a nanocrystalline graphene sheet, after the annealing step carried out at 1200 K [405].

However, to date the graphene produced via heat-driven conversion has structural defects and low carrier mobility (0.5 cm^2/Vs at RT) [405].

The aim is to develop reliable protocols to improve and exploit this process for a cheap and industrially scalable approach.

C11. Synthesis of graphene and its derivatives from molecular precursors

In principle graphene can be chemically synthesized, assembling benzene building blocks [406,407], see Fig. 21 i. In such approach, small organic molecules are linked together through surface-mediated reactions at relatively low temperature (<200^{o}C). The resulting materials include nanostructured graphenes, which may be porous, and may also be viewed as 2d polymers. Graphene nanostructures could be obtained after polymerization of graphene-

like molecular precursors in the form of polyphenlenes [158]. By designing and synthesizing appropriate precursors, one should be able to scale up the formation towards i) micron-sized graphene islands; ii) nano-ribbons and nano-graphene(s) with a large variety of structures [408]. The aforementioned methodology can be generalized to (1) sp^2-like monolayers of BN, (2) nano-porous, "graphene-like" two-dimensional structures, and (3) "graphene-like" organometallic co-polymers lattices based on phtalocynanines, for their applications in molecular spintronics [409]. The chemical approach offers opportunities to control the nano-graphenes with well-defined molecular size and shape. Thus properties that can be tuned to match the requirements for a variety of applications, ranging from digital and RF transistors, photodetectors, solar cells, sensors, etc. GNRs with well-defined band gap and/or QDs with tuneable absorption can already be designed and produced, Fig. 29 [410]. Such approaches will ultimately allow a degree of control truly at the atomic level, while still retaining the essential scalability to large areas. Reliable production and control on the properties of synthetic graphenes is needed to reach these goals.

Chemical graphenes tend to form insoluble aggregates [263]. A common strategy to solubilise conjugated systems is the lateral attachment of flexible side chains [410]. This was very successful in solubilising small graphene molecules, while failing for graphenes with increasing size [410], because the inter-graphene attraction rapidly overtakes the solubilisation forces, making the current strategy less and less effective [410]. A possible approach relies on supramolecular interactions that can be used to cover SLG with PAHs composed of i) an aromatic core able to interact strongly with graphene and ii) flexible side chains to make them soluble in most organic solvents. NGs adsorb reversibly forming ordered layers, with precise control of orientation and spacing [406,407]. These interact with the graphene backbone allowing in principle to control and tune its optoelectronic properties [406], while the NG flexible side-chains makes the graphene-NG composites soluble [411].

Supramolecular interactions have the advantage of keeping intact the sp^2 network, without compromising the transport properties [410]. Possible applications include the integration of graphene with other chemical functionalities, such as metal containing dye molecules or reactive sites for the attachment of biological molecules.

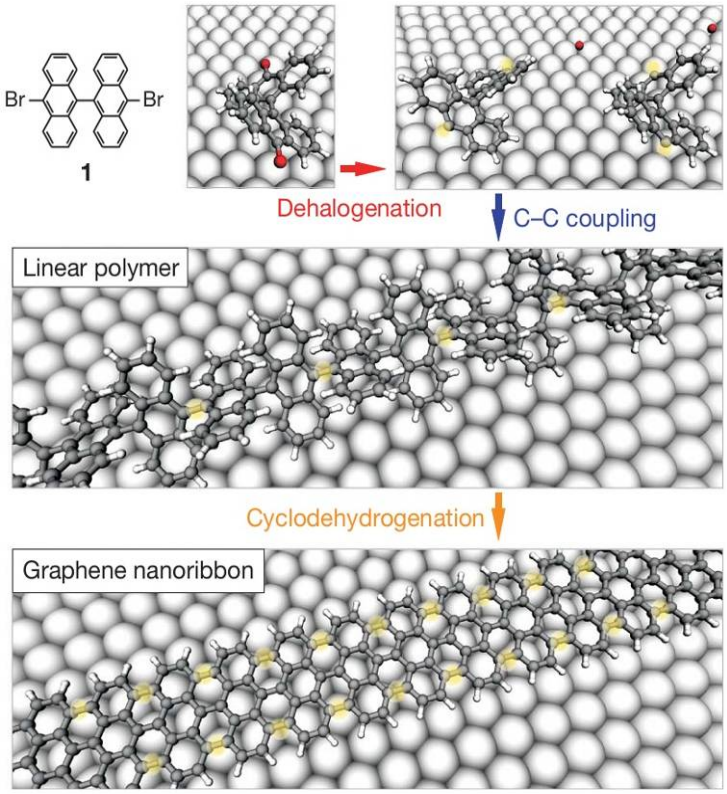

***Figure 29**: Bottom-up fabrication of synthetic graphene and GNRs starting from 10,109-dibromo-9,99-bianthryl monomers (1). Top, dehalogenation during adsorption of the precursor monomers. Middle, formation of linear polymers by covalent interlinking of dehalogenated intermediates. Bottom, formation of fully aromatic GNRs by cyclodehydrogenation [158].*

Chemical synthesis is also particularly suited for the formation of superstructures, whose physics is very rich. For instance, the rotation angle between graphene layers controls the carrier velocity [412]. There is much more to do in terms of designing and tuning the strength and type of interaction with the substrate. None of the superstructure-induced effects have been thus far harnessed in real devices. Several directions as starting points for the realization of such structures and effects can be planned. E.g. the induced growth across atomic islands of insulating materials deposited by nano-stencilling in regular patterns on catalytic, atomically flat metallic surfaces. Alternatively, exploring routes (e.g. thermally, electric field controlled or through electronic excitations) for the initiation of cascade chemical reactions and assembly from NG precursors on insulating monolayers and nanostructures to form graphene origami and GNRs. Such assembly has only been demonstrated so far on atomically flat metallic surfaces, but molecular self-assembly processes show considerable promise and versatility. Novel, volatile metallo-organic and organometallic complexes could be used as the precursors for this process which will provide a route at the molecular level.

The aim is to explore synthetic graphenes starting from the compatibility with a very large range of substrates and the easy association of organic and inorganic layers. The target is to control with atomic precision the shapes and edges, in order to tune continuously the band gaps and conductivity, as well as control doping, obtaining a spatial distribution of dopants with ultimate resolution. Indeed, as the device size is pushed down, the dopant distribution needs to be precisely tuned, which is very difficult to achieve by post-treatment of large area graphene, such as hydrogenation or fluorination (or even doping during thin film growth). Precise and tailored dopant distribution will be assured by means of a hetero-(dopant) atom that is readily part of the precursor molecule. The effect of local doping will be investigated. This could be in principle achieved functionalising graphene using acceptor/donor molecules that would self-assemble precisely on its surface.

C. 12 Transfer and placement

The deterministic placement (Fig. 30) of graphene on arbitrary substrates is key for applications and characterization. The ideal approach would be to directly grow it where needed. However, to date, we are still far from this goal, especially in the case of non-metallic substrates. We thus need to develop alternative approaches. Transfer of SLG and FLG from SiO_2/Si to other substrates using poly(methyl methacrylate) (PMMA) as sacrificial layer has been demonstrated [347] as well as a dry-methods based on a polydimethylsiloxane (PDMS) stamp [100].

The process has been scaled up to a roll-based layer-by-layer transfer onto plastic substrates [4]. Large scale placement of LPE samples can be achieved via vacuum filtration [20], spin coating [413], Langmuir-Blodgett [414], spray coating [415], rod coating [416] and screen printing [417]. Surface modification by SAMs can enable targeted placement on a large scale. Dielectrophoresis can also be used to control the placement of individual graphene flakes between pre-patterned electrodes [418].

Inkjet printing is another attractive technique, since it can be directly integrated in processing of polymer optoelectronic devices. It allows selective deposition [266]. Deposition of fluidic droplets to form patterns directly on substrates offers a mask-less, inexpensive and scalable low-temperature process for large area device fabrication.

The resolution can be enhanced by pre-patterning substrates, so that the functionalized patterns can act as barriers for the deposited droplets [419]. Resolution of 100–400 nm was demonstrated by a self-aligned method [419]. This is versatile, has a limited number of process steps, and a range of components can be printed on a variety of substrates [266].

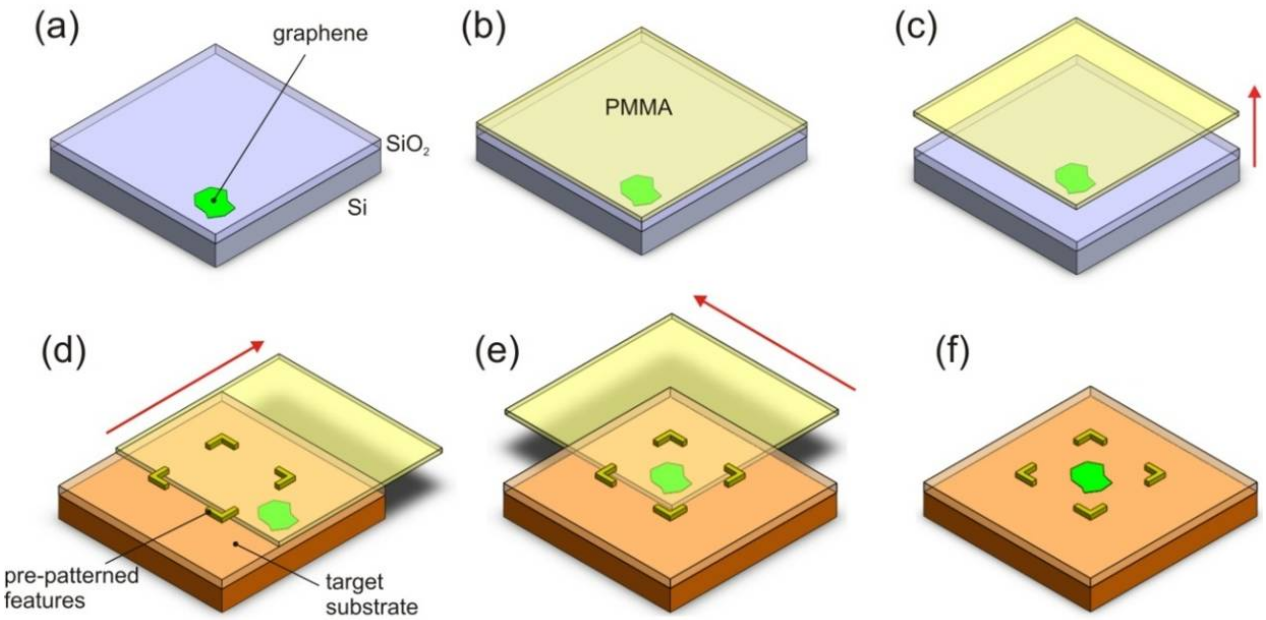

***Figure 30**: Determinist transfer. (a) Graphene samples are prepared onto Si/SiO_2 by MC. (b) PMMA is deposited by spin coating. (c) PMMA is detached from the hydrophilic substrate by immersion in DI water. Graphene adheres to the polymer and is removed from the $Si+SiO_2$ substrate. (d) PMMA+graphene film is moved onto the (arbitrary) target substrate, where features of interest (electrodes, cavities, etc.) have been pre-patterned. (e) A thin layer of water at the interface allows the film to be slid onto the substrate, and the graphene can be aligned with the feature of interest. (f) Once the water evaporates, the PMMA is dissolved by acetone, releasing graphene in the desired target position.*

A big challenge is the development of a dry transfer technology for ultrahigh quality graphene up to 450mm, avoiding the wet conditions with polymer coating, which suffer from polymer contamination. The development of dry processes for large area graphene on insulator will be extremely useful for long term sustainability in device engineering.

Optical trapping can also be exploited to manipulate (translate, rotate) and deposit trapped graphene [106] and 2d layered materials on solid substrates in a controlled fashion.

Optical binding, the formation of extended periodic self-organized (optically bound) structures, could be used for patterning and controlled deposition on a substrate over an extended area for parallel nano-lithography. Another promising application of radiation forces is optical stamping lithography [420], where the repulsive force exerted by a laser beam is exploited to deposit flakes at desired positions on a substrate. Exploiting this, graphene flakes could be optically stamped on substrate using holographic patterns (using a Spatial Light Modulator), and combined with any other nanomaterial. This paves the way for integration in microfluidic environments, expanding the range of applicability for biosensing.

We will also explore the other possible alternative for large scale (suitable for industrial level) placement of graphene, such as R2R coating, flexographic, gravure printing, etc.

C. 13 Inorganic layered compounds

Studies of new 2d crystals should start from developing methods of their production. This will be realised following the following routes.

C13.1. Mechanical exfoliation of layered 3d crystals

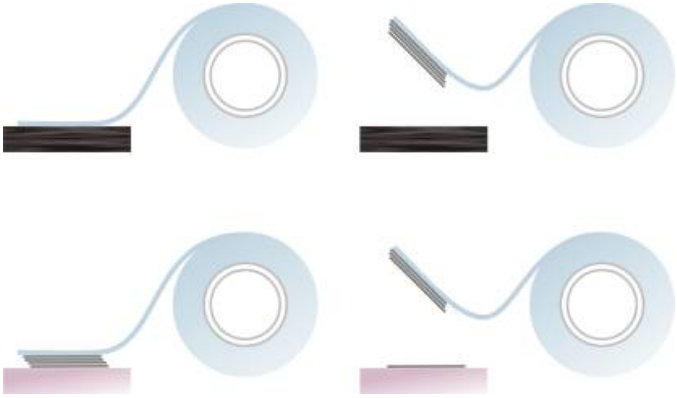

***Figure 31**:Micromechanical cleavage for producing 2d crystals.*

Under normal circumstances, nanosheets stack together in layered crystals. However as with graphene [3], a number of researchers have found that individual inorganic nanosheets can be removed from their parent crystal by micromechanical cleavage [3,421,422,423], see Fig. 31. This has allowed the structural characterisation of BN by high resolution TEM [421] and its use as a substrate for high performance graphene devices [394]. Similarly, for MoS_2 a number of advances have been demonstrated including the production of sensors [424], transistors [3,214,425] and integrated circuits [426], the measurement of the mechanical properties of individual nanosheets [226] and the observation of the evolution of the vibrational [422] and electronic structure [213,423] with number of stacked nanosheets.

Other top-down techniques already used for the exfoliation of graphite such as photoexfoliation and anodic bonding will be extended to inorganic layered materials.

C.13.2 Liquid phase exfoliation (LPE)

It was recently shown that both BN [23, 427 , 428 , 429 , 430 , 431] and TMDs [23,218,432,433] can be exfoliated in liquids (solvents or aqueous surfactant solutions) by ultrasonication. The exfoliated sheets can then be stabilised against re-aggregation either by interaction with the solvent [23], or through electrostatic repulsion due to the adsorption of surfactant molecules [259,434]. In the case of solvent stabilisation, it was shown that good solvents are with surface energy matching that of the exfoliated materials [23]. This results in the enthalpy of mixing being very small [23,433]. Because these exfoliation methods are based on van der Waals interactions between the flakes and either the solvent molecules or surfactant tail group, stabilisation does not result in any significant perturbation of the flake properties. These dispersions can easily be formed into films or composites [23] and facilitate processing for a wide range of applications.

However, much work remains to be done. Exfoliation techniques must be extended to a wider range of materials. Both solvent [23] and surfactant-exfoliated [218] TMDs tend to exist as multilayer stacks with few individual sheets. Thus the exfoliation must be improved. The dispersed concentrations (up to tenth of grams per litres) and the lateral flake size (up to mm) must be increased considerably. The development of a sorting strategy both in lateral dimensions and number of layers will be essential for the full exploitation of their optical and electronic properties.

Quantitative analysis for monitoring the exfoliation (yield and quality of the as-produced material) of transition metals dichalcogenides (TMDs) and TMOs will be based on a range of appropriate techniques such as AFM, TEM, Raman spectroscopy, etc.

The number of layers can also be controlled via separation in centrifugal fields or by combination with DGU, Fig. 32b [260]. The availability of dispersions opens up a range of applications in composites, thin films and inks. Inks can be printed in a variety of ways, and

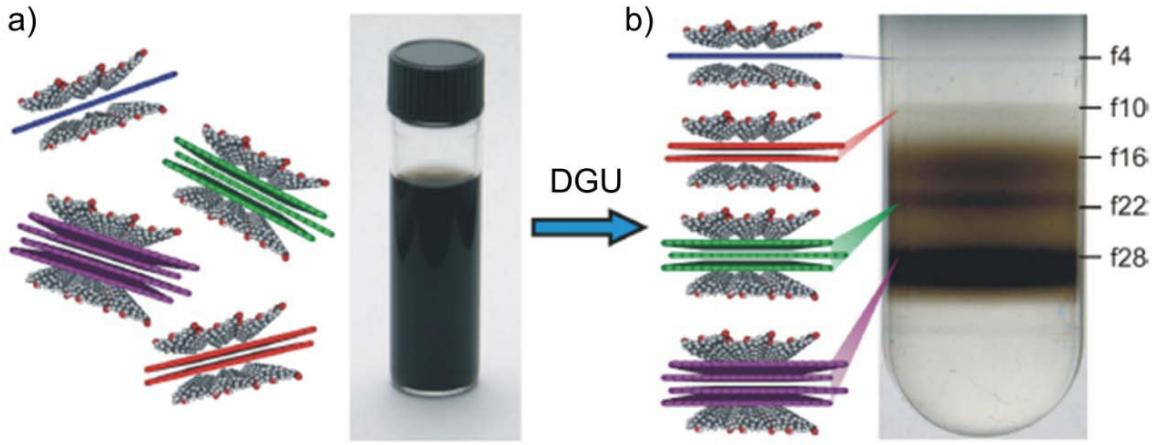

***Figure 32**: Liquid phase exfoliation and DGU selection of monolayer crystals [260].*

mixed to create hybrids. Many applications in photonics and optoelectronics, such as TCs, third generation solar cell electrodes, and optical-grade polymer composites will benefit from LPE produced and assembled materials.

LPE can also produce ribbons with widths <10 nm [142], allowing a further in-plane confinement of the 2d materials, thus an extra handle to tailor their properties. LPE does not require transfer techniques and the resulting material can be deposited on different substrates (rigid and flexible) following different strategies such as dip and drop casting, spin, spray and rod coating, ink-jet printing, etc. Several layered materials (including BN, MoS_2, WS_2, $MoSe_2$, $MoTe_2$, $TaSe_2$, $NbSe_2$, $NiTe_2$, and Bi_2Te_3) have been successfully exfoliated using this simple, yet efficient method [23]. This approach may also influence the chemical stability, as the layer of liquid might protect those crystallites from oxidation. Such suspensions allow easy assembling of the materials into superstructures, as discussed in C14.1.

C.13.3 Direct growth and deposition

2d crystals can also be produced using different approaches. For instance, films of WS_2 can be deposited by a variety of deposition methods like magnetron sputtering from both WS [435] and WS_2 targets [436], sulfurization of W [437] or WO_2 films [438], ion beam mixing [439], etc. For instance, for tribological applications magnetron sputtering is the preferred production strategy due to low substrate temperatures, high chemical reactivity of the species due to plasma-assisted dissociation and excitation [440]. Magnetron sputtering is also suited for large area deposition on the order of m^2 [441]. This is also ideal for PVs application, especially for building-integrated PV systems.

CVD is emerging as a promising strategy to grow 2d crystals. Growth of *h*-BN [442] and MoS_2 [443] was already demonstrated. Ref. 442 reported growth of single layer *h*-BN by thermal decomposition of borazine ($B_3N_3H_6$) on Ni (111). Ref. [443] demonstrated that the CVD growth of MoS_2 is scalable and films of any size can be made because the lateral size of the layers is simply dependent on the size of the substrates used. Moreover, also the thickness of the MoS_2 film can be controlled being directly dependent on the thickness of the pre-deposited Mo metal on the substrate and the as-grown layers can then be transferred onto arbitrary substrates [443].

The aim is to produce a large range of 2d crystals on large scale and with control on demand number of layers. Low-temperature CVD and CMOS compatible substrate will be investigated as well all the transfer strategies already developed with graphene.

2d crystals can also be produced as nanoribbons with tunable electrical and magnetic properties. MoS_2 nanoribbons were made via electrochemical/chemical synthesis [444], while zigzag few- and single-layered BN nanoribbons were obtained unzipping multiwall BN nanotubes through plasma etching [445]. The target is to produce, within the next 10 years, nanoribbons with totally controlled electrical and optical properties.

C13.4 Chemical modification of 2d crystals

Chemical modification of graphene (Fig. 33) is a powerful method for the synthesis of new members of graphene family (e.g., graphane [18], chlorinated graphene [446] or fluorographene [19]). Applying this to other 2d crystals offers a chance to create new varieties with versatile physical properties. Clearly it is only the beginning and many other materials with very different properties are possible. Moreover, methods for the separation of chemical modification of the two sides of a 2d crystal are desirable. This way, an electric

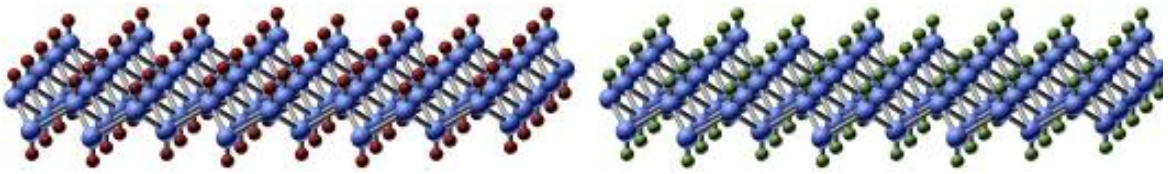

Figure 33: *Chemically modified graphene. One can add different species (hydrogen or fluorine) to graphene scaffolding.*

moment can be created across the crystal and lead to new, unexpected properties. Also, chemical modifications can provide a fine control over the distance between neighbouring planes in the 2d heterostructures. This can also be done by intercalation or by placing other metallic and semiconducting nanostructures between the planes.

C13.5 Intercalated structures

The possibilities of modification of the band structure by intercalation meet the historical research community of the "graphite intercalation compounds" (GICs). The most famous application of GICs is energy storage with the Li-ion battery [284]. The research in GICs has considerably intensified after the discovery of high T_c superconductivity for GIC Calcium graphite (CaC_6) [285,286,287].

C14. Hybrid structures and superstructures of graphene and other 2d materials

We will explore the concept of "materials on demand": an assembly of graphene and other 2d crystals into hybrid superstructures. This would allow practically infinite number of different multilayers with properties tailored for novel, multitasking applications.

C14.1. *Superstructure assembly*

The properties of 2d crystals acquire new qualities and functionalities when those are combined in heterostructures, or multi-component superstructures. Three methods can be utilised to generate atomically thin heterostructures: (i) layer by layer mechanical stacking [24,394,447]; (ii) layer by layer deposition of chemically exfoliated 2d crystals by vacuum filtration [20], dip and drop casting, spin [413], spray and rod coating [416], inkjet [266] and screen printing, and Langmuir-Blodgett [448]; (iii) direct growth of 2d-heterostructures by CVD [449]. All these are already being developed and, as the field develops, others will emerge, more suitable for mass production.

Mechanical transfer

Transfer individual 2d crystals into heterostructures was already been demonstrated [24,450]. Graphene – BN heterosystems have enabled the observation of several interesting effects, including fractional QHE [394], ballistic transport [24] and metal-insulator transition in graphene [450]. An advantage of 'dry' mechanical transfer is the possibility to control/modify each individual layer as it is being deposited, including chemical modification, at any stage of the transfer procedure. Also, any atomic layer in the multilayer stack can be individually contacted, offering unprecedented control on the properties of the stack (effectively we have a material with individual contacts to every conducting atomic plane). Furthermore, one can apply local strain to individual layers. It has been demonstrated that local strain can significantly modify the band structure of graphene and other 2d crystals [451,452,453]. Also important is the control of the relative orientation of the layers, which may affect electronic properties of the stack in certain intervals of the energy spectrum [412].

Heterostructures deposited from dispersions

Large-scale placement of LPE samples can be achieved by spin coating and Langmuir-Blodgett (Fig. 34). Surface modifications by self-assembled monolayers enable targeted large-scale deposition. High uniformity and well defined structures on flexible substrates can also be obtained. Di-electrophoresis can also be used to control the placement of individual crystals between pre-patterned electrodes. Inkjet printing allows to mix and print layers of different materials and is a quick and effective way of mass-production of such systems. Although the quality of the resulting structures would be significantly lower than that obtained by mechanical or CVD methods, it would still be suitable for a number of photonics and optoelectronics applications, as well as for applications in thin film transistors, RF tags, solar cells, batteries and supercapacitors.

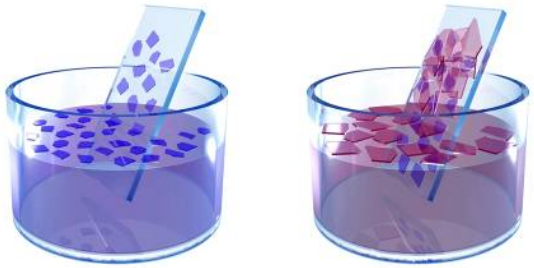

Figure 34: *Superstructure assembly by Langmuir-Blodgett.*

Direct CVD growth

CVD is a method suitable for mass production of heterostructures, though it requires the largest investment and effort in terms of developing the necessary expertise and machinery. There are several indications that such growth is indeed feasible [454]. h-BN has already been shown to be effective as a substrate for graphene CVD, see Fig. 35. CVD graphene on h-BN has shown remarkable mobilities, much higher than for graphene grown on metal substrates (though, after transfer).

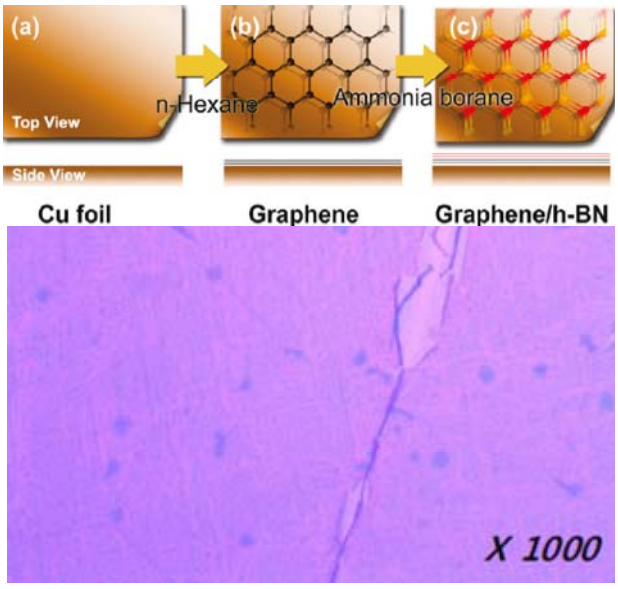

Figure 35: *Example of CVD-grown graphene/BN heterostructures*

Nanosheet bonding using polymers

2d polymers offer large structural diversity through different possible connections between the monomers. Different synthesis routes are possible: using small fragments covalently bonded (difficult), self-assembly approaches (maximum sizes of the order of a few nanometers), knitting polymeric strands (planarity difficult to achieve), polymerization at air/liquid or liquid/liquid interfaces, SAMs, stacked (3d) multilayer polymerization, etc.

C15. Silicene

Recently silicene sheets [455], *i.e.*, the Si equivalent of graphene [456], have been synthesized by in-situ epitaxial growth on silver (Ag) (111) surfaces. A honeycomb atomic structure with a Si-Si distance of 0.23 nm was revealed in STM, with a long-range epitaxial order confirmed by sharp Low Energy Electron Diffraction patterns. Conical band dispersions at the corners of the silicene Brillouin zone (K and K' points), evidenced in High-Resolution ARPES measurements, point to Dirac fermions, *i.e.*, massless relativistic carriers, with a Fermi velocity of 1.3×10^6 ms^{-1}, as theoretically predicted [457], quite the same as graphene, and four times higher than previously obtained on a one-dimensional grating of silicene nano-ribbons [458]. GGA-DFT calculations including the Ag(111) substrate-confirm the stability of the epitaxial arrangement.

Silicene is predicted to have non-trivial topological properties [459]. Hence, it could offer the possibility, if interfaced with a s-wave superconductor, for advances in the long quest for Majorana fermions [460]. Furthermore, being Si the workhorse of electronics, this synthesis could have a major impact for novel devices because of the compatibility with existing Si technologies. Indeed, a key issue in this direction will be the transfer -or even better the growth- on an insulating substrate, like, possibly AlN [457].

The epitaxial growth of silicene paves the way to the synthesis of germanene, the equivalent of graphene for Ge, also with nontrivial band topology and a gap induced by effective spin orbit coupling for the π orbitals at the K point in low-buckled geometry corresponding nearly to room temperature [459,460].

D. Functional graphene and graphene-based devices

Graphene has already demonstrated high potential to impact most ICT areas, ranging from top end high performance applications in ultrafast (> 1 THz) information processing, to consumer applications using transparent or flexible electronic structures (see Fig. 36).

The great promise of graphene is testified by the increasing number of chip-makers now active in graphene research. Most importantly, graphene is considered to be amongst the candidate materials for post-Si electronics by the ITRS [8].

D1. Opening a band-gap in graphene

The target is to fully explore the performance of graphene transistors in both logic and RF applications. Graphene will be used to develop new applications based on stretchable electronics, such as conformal biosensors and rollable displays. These are required to meet the increasing needs of human-interface technology. Graphene can solve the standstill of stretchable electronics, due to the difficulty in developing semiconducting materials with the high stretchability required for such applications.

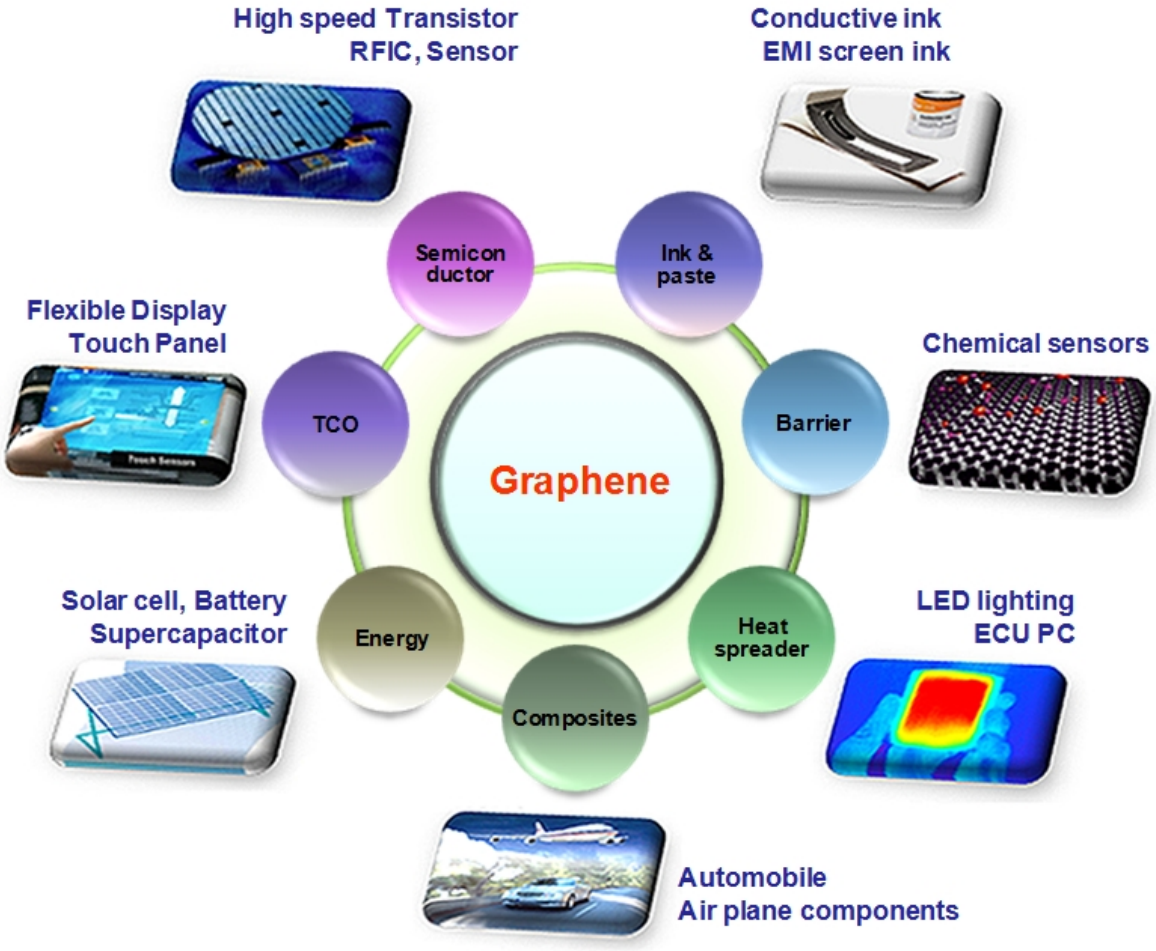

***Figure 36**: Overview of Applications of Graphene [461]*

The combination of its unique optical and electronic properties, in addition to flexibility, robustness and environmental stability, can be fully exploited in photonics and optoelectronics, even in the absence of a band-gap, and the linear dispersion of the Dirac electrons enables ultra-wideband tunability. We target applications of graphene in the emerging field of photonics and optoelectronics, ranging from solar cells and light-emitting devices to touch screens, photodetectors, ultrafast lasers, etc. Fig. 37 and Table 3 show some possible applications and the time that we might anticipate graphene based devices.

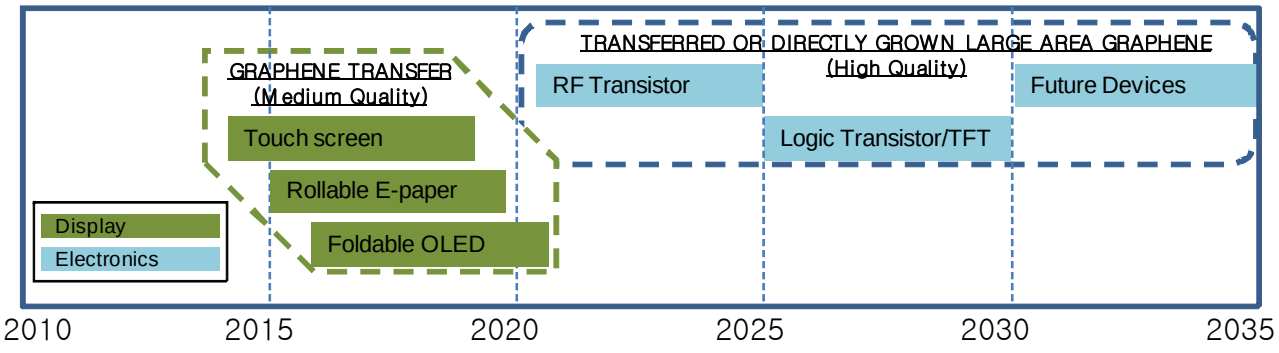

***Figure 37:** Graphene electronics' application timeline*

Table 3: *Drivers leading the implementation of graphene for different electronic applications and issues to be resolved with current graphene technology.*

Year	Application	Drivers	Issue to be addressed
2014~	Touch screen	- Better endurance with graphene as compared to other materials	- Need to better control contact resistance
2015~	E-paper	- High transmittance of monolayer graphene; Visibility	- Need to better control contact resistance
2016~	Foldable OLED	- Graphene with high electrical properties and bendability - Efficiency improved due to graphene's work function tunability - Atomically flat surface of graphene helps to avoid electrical shorts and leakage current.	- Need to improve the sheet resistance - Need to control contact resistance - Need a conformal coverage of 3D structures
2021~	RF Transistor	- No manufacturable solution for InP HEMT (low noise) after 2021 according to the 2011 ITRS	- Need to achieve current saturation - f_T = 850GHz, f_{max}= 1200GHz should be achieved
2025~	Logic Transistor	- High mobility	- New structures - Need to resolve the band-gap / mobility trade-off - Need an On/Off ratio>10^6

Graphene can replace materials in several existing applications, but the combination of its unique properties should inspire completely new applications, which is the ultimate target.

The major obstacle of graphene in transistor applications, especially for integrated circuits as potential Si replacement, is its zero band-gap. This is responsible for the low On/Off ratio in GFETs. Thus, opening a band gap without compromising any of its other outstanding properties, such as high-field transport and mobility, is one of the most active research areas in graphene. Apart from quantum confinement (GNRs and GQDs), many other techniques have been developed for this goal. Substrate induced band-gap opening was investigated [462]. Band-gap opening in epitaxial graphene, both on epitaxial h-BN and h-BN/Ni(111) with band gap up to 0.5eV was reported [463]. Theory suggests that a band gap ~0.52eV can be opened in graphene deposited on oxygen terminated SiO_2 surfaces [464]. A bandgap is observed for epitaxial BLG [465].

Substitutional doping is another promising route for opening a band gap. Nitrogen doping can be used to convert graphene into a p-type semiconductor [466].

Small band gap opening was observed in large area hybrid films, consisting of graphene and h-BN domains synthesized on Cu substrates by CVD [467].

A few other approaches also exist for band gap engineering. Formation of GNRs with finite band gaps is possible using conventional block copolymer lithography [175]. A band gap~0.7eV was recently demonstrated by selective hydrogenation of graphene on Ir [192]. Molecular doping and charge transfer methods could also modulate the electronic properties via paramagnetic adsorbates and impurities that can effectively dope graphene [468]. Selective chemical functionalization can also be used for band gap engineering [18,19]. Complete hydrogenation of graphene forms graphane, an insulator [18], while a similar process using Fluorine, originates fluorographene [19]. The latter is optically transparent with a gap~3eV [19]. BLG is also gapless, however, if an electric field is applied perpendicular to it, a gap opens, with size dependent on the strength of the field [469,470,471].

The organic synthesis of GNRs seems to be a powerful tool [158]. However, as reported in Section C11, a reliable approach for on-demand bandgap engineered GNRs needs to be developed. Moreover, we aim to exploit all others feasible ways to open a band gap in graphene. For instance, although band-gap opening in epitaxial graphene on SiC sparked a lot of interest because of the viability of the growth process, to date it is controversial [472]. Indeed, epitaxial graphene on SiC is electron doped and the Fermi level lies above the gap. To make graphene viable for electronics requires hole doping, or the Fermi level must be moved by applying a gate voltage.

All these methodologies are at their infancy, and need be further developed. For instance, B substitutional doping, which is one of the most promising ways of opening a band gap in free standing graphene [473], increases defects and disorder. Moreover, uniform doping over large areas has not been successfully achieved yet.

Techniques will be studied, to locally functionalize graphene on an atomic length-scale employing a Scanning Catalyst Microscope (SCM). A catalyst particle attached at the end of a scanning tip is positioned close to the sample and then a local chemical reaction is triggered by local heating in the presence of a reaction gas [149]. For instance, Ni particles preferentially cut graphene along specific crystallographic directions [149]. Atomic precision is assured by the limited contact area between tip and sample.

Another aim is to achieve control over domain size and shape in graphene-BN hybrids. This is essential for tuning the gap and other electronic properties. Tuneable band gap and spintronic properties in graphene-graphane superlattices will be addressed. Strain as a means of opening a bandgap in large-area graphene and the effect of uniaxial strain on the band structure will be investigated, as well as other types of strain, such as biaxial strain and local strain that can modify the band structure of graphene.

D2. Graphene-based microelectronics and nanoelectronics

The progress in digital logic relies in down scaling CMOS devices through the demand for low voltage, low power and high performance. This size scaling has permitted the complexity of integrated circuits to double every 18 months [474 , 475]. The decrease of gate lengths corresponds to an increase of the number of transistors per processor chip. Nowadays, processors containing two billion MOSFETs, many with gate lengths of just 30 nm, are in mass production (Fig. 38) [472].

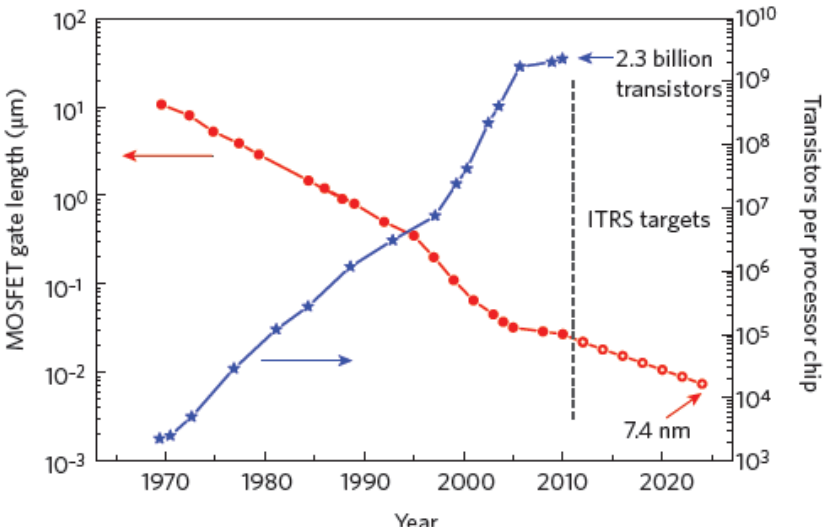

***Figure 38**: Evolution of MOSFET gate length integrated circuits (filled red circles). The ITRS targets a gate length of 7.4nm in 2025 (open red circles)[8]. With the decrease of gate lengths, the number of transistors per processorincreased (blue stars). New materials, like graphene, are needed to maintain these trends [472].*

However, CMOS scaling is approaching fundamental limits due to various factors, such as increased power density, leakage currents

and production costs, with diminishing performance returns. For instance, static (leakage) power dissipation in state-of-the-art Si microprocessors has already reached more than one-third of the total power, and is expected to increase further with the continuation of the aggressive scaling of CMOS technology.
Faster computing systems need access to large amounts of on-chip memory and Si technology scaling limits create bottlenecks in realizing high density memories. Thus, a significant challenge for the semiconductor industry is the development of a post-Si age, with new materials, such as graphene. However, the potential performance of graphene-based transistors is still unclear. It is not the extremely high mobility of graphene, but rather the possibility of making devices with extremely thin channels that is the most forceful feature of GFETs. Indeed, these devices may be scaled to shorter channel lengths and higher speeds, avoiding the undesirable short channel effects that restrict the performance of current devices. Moreover, with the continuous downscaling of electronic devices and increasing dissipation power density in downscaled circuits, materials that can conduct heat efficiently are of paramount importance [28]. The outstanding thermal properties [28] of graphene provide an extra motivation for its integration with CMOS technology, as well as beyond-CMOS, with the possibility to overcome state-of-the-art Si and III-V semiconductor based high frequency FETs at the ultimate scaling limits [476].

The first graphene back-gate MOS device was reported in 2004 [2]. However, such back-gate devices, although very useful for proof-of-concept purposes, suffer from very large parasitic capacitances and cannot be integrated with other components. Consequently, practical graphene transistors need a top-gate. The first graphene top-gate MOSFET was reported in 2007 [477]. From that important milestone, huge progresses have followed. Top-gated graphene MOSFETs have been made with graphene produced by MC [57,477,478,479,480,481] carbon segregation [396,482,483] and CVD [484]. Different top gate high-k dielectrics have been used such as SiO_2 [477], Al_2O_3 [485], and HfO_2 [486] for the preservation of the high carrier mobility [487].

The first GFETs to exhibit voltage gain arger than one (~ 6) were recently realized by utilizing ultra-thin AlO_x gate dielectrics [488,489]. The gate stack was fabricated by evaporation of Al followed by exposure of samples to air. This naturally forms a very thin (< 4 nm) AlO_x layer at the interface between graphene and the Al layer evaporated on top [488]. However, fabricated FETs exhibited over-unity voltage gain only at cryogenic temperatures as strong hysteresis observed in their transfer characteristics suppressed the voltage gain at room temperature [489]. Hysteretic behaviou of graphene FETs under ambient conditions stems from water charge traps adsorbed on the substrate [490,491,492] which has a detrimental impact on their transconductance and therefore the voltage gain. The first over-unity voltage gain under ambient conditions [493] was obtained by deploying misoriented BLG as active material and using a solid polymer electrolyte as gate dielectric. However, these devices exhibited over-unity voltage gain only in direct current (DC) mode, as a consequence of a large overlap between the polymer gate and source/drain contacts. DC gain is of no interest in realistic electronic applications, as logic gates and voltage amplifiers operate in dynamic, AC mode. An AC voltage gain larger than unity was recently demonstrated at room temperature in a complex 6-finger-gate FET configuration [494]. The obtained gain was relatively small (1:7) and measured on an infinite load in a high-frequency transmission-line environment. The demonstrated devices are very complicated to fabricate and are not integrated (they require external inductors and capacitors to operate).

Soon thereafter integrated graphene voltage amplifiers were demonstrated [495]. They exhibit the highest AC voltage gain reported so far in sub-micron graphene FETs at room temperature (3.7). In contrast to standard graphene FETs in which there are ungated parts of graphene channel on either side of the gate [472], those in Refs. [488,493] did not have

ungated parts, due to a self-aligned fabrication process. This also eliminated hysteresis in the FET transfer curve, thus far detrimental in obtaining over-unity AC voltage gain in graphene FETs at room temperature. Such a unique blend of transistor properties combined with the use of very thin gate insulators resulted in voltage gain that can readily be utilized both in analog and digital electronics. However, these devices were fabricated from exfoliated graphene, unsuitable in commercial applications. The highest AC voltage gain reported so far in wafer-scale graphene under ambient conditions, 2.2, has just been reported [496]. Such gain allowed graphene integrated complementary inverters to exhibit digital signal matching at room temperature. Cascading of digital inverters in which the previous stage is capable of triggering the next stage, were also demonstrated [497]. The highest voltage gain of 35 has just been reported [497], but in exfoliated BLG under large perpendicular fields in large devices [497].

The channels of most top-gated transistors were made of large-area graphene, with a minimum conductivity (~$4e^2/h$), even within the limit of nominally zero carrier concentration. This is too high for applications in logic elements, as it leads to high leakage in the off state. This poses a serious limitation for the switching ability of these devices. Thus, the future of graphene in digital logic relies on bandgap opening, as reported in section D1.1. To date, the formation of GNRs seems the most promising route and nanoribbons MOSFETs with back-gate control have been demonstrated [498]. Such devices operate as p-channels with On/Off ratios~10^6 [499]. Recently, the first top-gated graphene nanoribbon MOSFETs with HfO_2 top-gate dielectric was reported [479], with a room-temperature On/Off ratio of 70.

Proof of principle devices have also been demonstrated in BLG MOSFETs, with On/Off ratio of 2000 at low temperature, and 100 at room temperature [500].

The high mobility coupled with high thermal conductivity and high current density makes graphene ideal as a replacement for Cu interconnects [501]. Theoretical projections suggest that graphene with low line-shapes (< 8nm) may outperform Cu [501]. Thus, although for digital electronics the entry of graphene is expected on a longer timescale, Fig. 39, the first components, such as interconnects, will likely be fabricated within the next few years. The long term target plan (>10 years) is to transform graphene transistors, from being excellent tools to probe the transport properties of this material, to viable devices to compete and replace/integrate state-of-the-art Si and compound semiconductor electronics. Promising routes for realizing graphene based digital electronics will be explored and assessed to fully exploit the potential of this material to bringing the semiconductor industry beyond the 7.4nm node, which the ITRS expects to be reached in 2025 [8].

GFETs with controlled threshold voltage and both n-channel and p-channel need to be demonstrated for CMOS logic. The contact resistance between the metallic source and drain and graphene channel should be investigated deeply and more focussed research is needed to understand the contact properties. New graphene device concepts, such as tunnel FETs and bilayer pseudospin FETs (BISFET [502]) need to be extensively studied, and different design options must be explored, evaluated and optimized. Moreover, the integration with exiting CMOS technology is a critical step in establishing a pathway for graphene electronics.

Another crucial point concerns the steady increase in power dissipation demand per unit area (despite the reduction of the supply voltage). This is becoming a major issue for the design of next-generation devices: it is mandatory to add large thermal conductivity functionalities in the device structures, to efficiently remove heat. Besides its practical importance, the investigation of heat transport in graphene and graphene-based systems offers other rewards, more closely related to fundamental physical issues like, e.g., the role of the reduced dimensionality and/or different shaping on transport features.

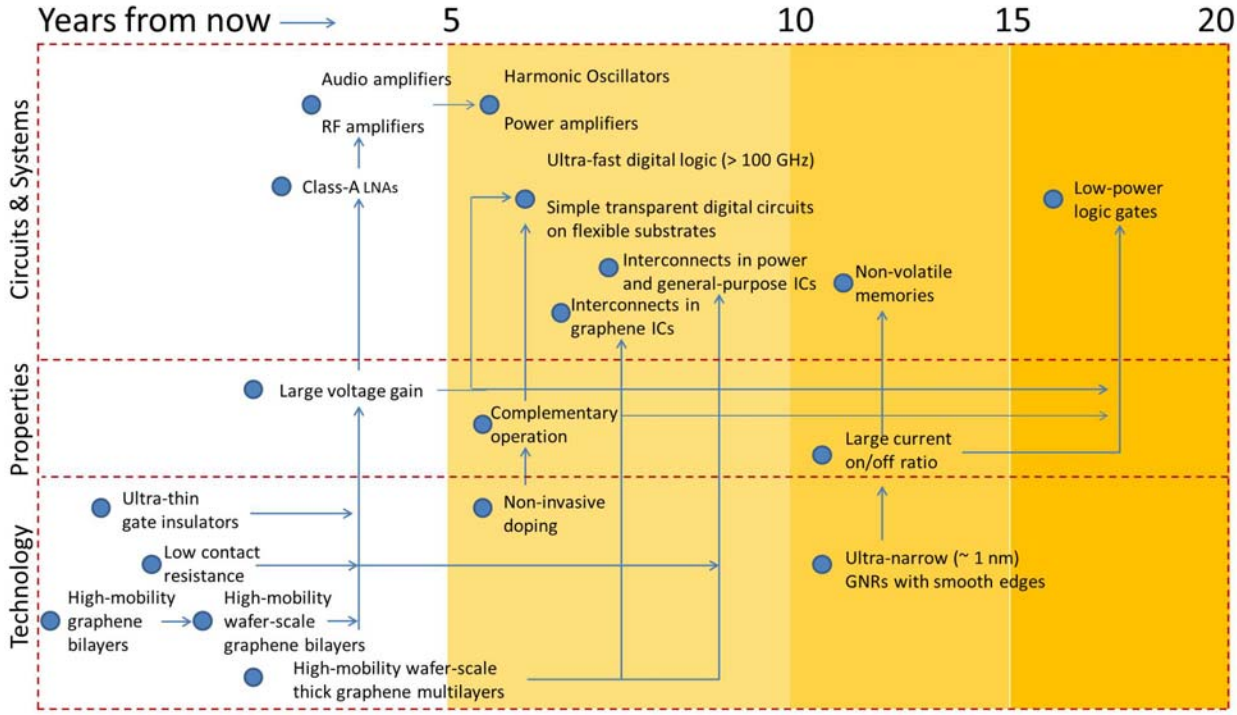

Figure 39: *Graphene electronics' roadmap.*

Thermal transport properties will be investigated both experimentally and theoretically. In particular, it is possible, through computer simulations, to understand how/to-what-extent in-plane thermal conductivity is affected by structural defects, stretching and bending deformations and lateral dimensions (in GNRs). Also, by simulations, proof-of-concept studies can be executed on possible thermal rectification effects in GNRs.

D2.1. Digital Logic Gates

Application of graphene in digital logic gates is limited by the zero bandgap which prevents depletion of charge carriers. Inability to completely turn off GFETs increases static power dissipation with respect to traditional, *i.e.*, Si-based CMOS logic. This also limits the control of gate voltage over the drain current, *i.e.*, it reduces the transconductance g_m with respect to conventional semiconductor FETs, which can be turned off at suitable gate biases [503]. Moreover lack of depletion leads to a weaker drain current saturation regime in graphene FETs, which in turn increases their output conductance g_d. Hence most graphene FETs so far have intrinsic gain g_m/g_d much smaller than unity [492,504,505,506,507,508,509] which results in the inability to directly couple digital logic gates (due to a mismatch between input and output voltage logic levels) [504,505]. Current modulation in graphene devices can be increased by patterning GNRs, which increases the On/Off ratio [134,510,511]. However this also significantly reduces the ON current [142,492], which in turn reduces voltage gain. Similarly, very large ON/OFF ratios obtained in recently reported GTFETs [32] are unusable in digital logic due to very low on currents.

GFETs must satisfy two additional requirements in order to be considered as building blocks of future logic gates: large intrinsic gain (>10) and ON/OFF ratios (>10^4). The short-term goal in the development of graphene logic should be the requirement for a large intrinsic gain, to sufficient in realistic applications where high-speed operation is desired, but power dissipation is not a concern, similar to SiGe and InP emitter-coupled logic (ECL), the fastest logic family [512].

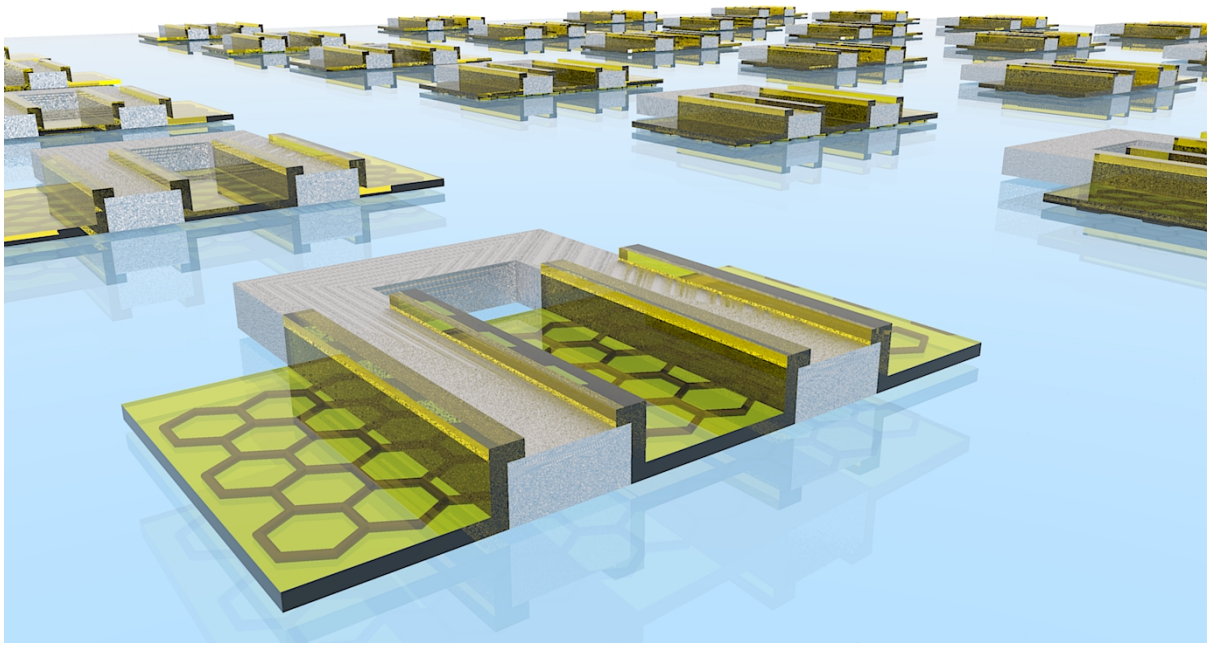

Figure 40: *Digital complementary inverters integrated on wafer-scale graphene.*

The long-term goal should be based on both requirements, as only in this way graphene could be considered as a replacement for Si CMOS in future ubiquitous logic gates (e.g., in microprocessors). This is not a far-fetched goal because the Si CMOS is also experiencing some fundamental difficulties, as reported in section D2.

In order to achieve the short-term goal it will be necessary to realize top-gated GFETs with ultra-thin (< 4nm) gate insulators as over-unity voltage gain has already been demonstrated in graphene devices with similar gate thicknesses (~ 4nm) [493,494,495]. The next step should be incorporation of such highly-efficient gate stacks in BLGFETs, in which perpendicular electric field opens a bandgap [36] allowing large voltage gain in dual-gate configurations [497]. In order to further improve mobility misoriented (instead of Bernal-stacked) BLG should be used. Misorientation electronically decouples the two graphene layers in a BLG. The bottom layer acts as a pseudosubstrate, which electrostatically screens the top layer from the substrate, thus giving enhanced carrier mobility within the top layer [513,514]. The final stage in the technological development should be technology transfer to wafer-scale misoriented BLG. Once wafer-scale high-gain graphene logic gates become available, their application in ultra-fast logic circuitry should be investigated.

The long-term goal is more challenging, as no satisfactory solution has been found so far in order to open a bandgap in graphene without reduction of mobility. Bandgap engineering of graphene should be attempted by patterning into GNRs. However, state-of-the-art GNRs have very low mobilities (~200cm^2/Vs) as a consequence of carrier scattering on disordered ribbon edges. In order to eliminate unwanted scattering, GNRs should have crystallographically smooth edges [147,149,158] and be deposited on insulating substrates. This leads to an enormous fabrication challenge as GNR widths~ 1nm are required in order to reach the Si bandgap (~1eV), as necessary for reliable switching. Finally, complementary logic (Fig. 40) is currently realized through electrostatic doping [496] which imposes limits on supply voltages in logic gates. In order to lift this restriction, GNRs should be chemically doped [506,515,516] but this doping should not introduce additional scattering centres in order to maintain high-mobility of crystallographically smooth GNRs.

GFETs cannot be turned off in either of the two logic states and a typical in/out voltage swing is 17% of the supply voltage at room temperature [516]. Although this is less than the

voltage swing in Si CMOS (capable of rail-to-rail operation with the voltage swing reaching almost 100% of the supply voltage) [512], it is still more than the swing in ECL gates. Similar to graphene logic gates, ECL gates are also comprised of overdriven transistors in order to achieve ultra-fast operation. For this reason a typical swing of the ECL gates is 0.8~V at a supply of 5.2 ~V, *i.e.*, only 15% of the supply voltage [512]. ECL gates are at the core of the fastest SiGe and InP bipolar-CMOS ~ (BiCMOS) or heterojunction bipolar transistor (HBT) chips and are used for digital signal processing at ultra-high frequencies (f>100GHz), inaccessible with conventional state-of-the-art CMOS technology. E.g., they are used in high-speed integer arithmetic units [517], static ultra-high frequency dividers [518], high data rate (> 50Gb/s) serial communication systems for demultiplexing [519] and phase detection for clock and data signal recovery [520,521]. Hence graphene logic gates could find uses in applications not suitable for traditional Si logic, such as ultra-fast logic applications where power dissipation is not a concern, or transparent circuits on flexible substrates.

GNR FETs should be considered as a replacement for Si FETs in CMOS logic once they reach sufficiently large intrinsic gain and ON/OFF ratio, as discussed above. However, at this stage it is not clear whether this would be sufficient to migrate from Si to graphene logic. In the very optimistic scenario in which charge carrier mobility in GNR FETs would exceed that in Si FETs by an order of magnitude, it would still require a FET to comprised 100 GNRs (W=1nm) connected in parallel in order to reach the same current drive a Si FET (W=1μm).

The roadmap is shown in Fig. 39 and the main deliverables for digital logic gates are: **5-10 years:** Ultra-fast (> 100 GHz) integrated digital logic gates replacing ECL gates. **5-10 years:** Simple digital logic gates on flexible or transparent substrates. **15-20 years:** General-purpose low-power GNR digital logic gates replacing Si CMOS.

D2.2. *Digital Non-volatile Memories*

Non-volatile memories are the most complex and advanced semiconductor devices following the Moore's law down to the 20nm feature size. State-of-the-art non-volatile memories consist of floating-gate flash cells, in which the information is stored by charging/discharging an additional floating gate embedded between the standard control gate and semiconductor channel of a MOSFET. Aggressive scaling of CMOS technology has a negative impact on the reliability of non-volatile memories. Parasitic capacitances between the adjacent cells increase with scaling, leading to a cross-talk [522]. Diminished lateral area leads to reduced gate coupling and lead to higher voltages [523], increasing the number of array cells leads to a reduced sensing current and increased access times [524].

For these reasons, alternative materials and storage concepts have been actively investigated, include implementation of graphene in non-volatile memories, see Fig. 41, [492,525,526,527,528,529]. However, the most important figures of merits of non-volatile memories are often neglected or incompletely addressed in graphene literature: no endurance and program/erase (P/E) curves are reported [526,527,528,529], questionable extrapolations are carried out to evaluate the retention, and so on. Moreover, similarly to logic gates discussed above, non-volatile memories also require large enough ON/OFF ratio for memory states to be unambiguously resolved from one another. The following parameters should be thoroughly investigated: the P/E curves as a function of time, the available P/E window (*i.e.*, difference in threshold voltage or current between the two logic states), the retention (capability to retain a programmed state over time), and the endurance (maximum number of cycles that the memory cell can withstand). In addition, if graphene is to be used as a conductive channel in flash FETs, bandgap engineering should be pursued, as in case of graphenelogic gates (see above).

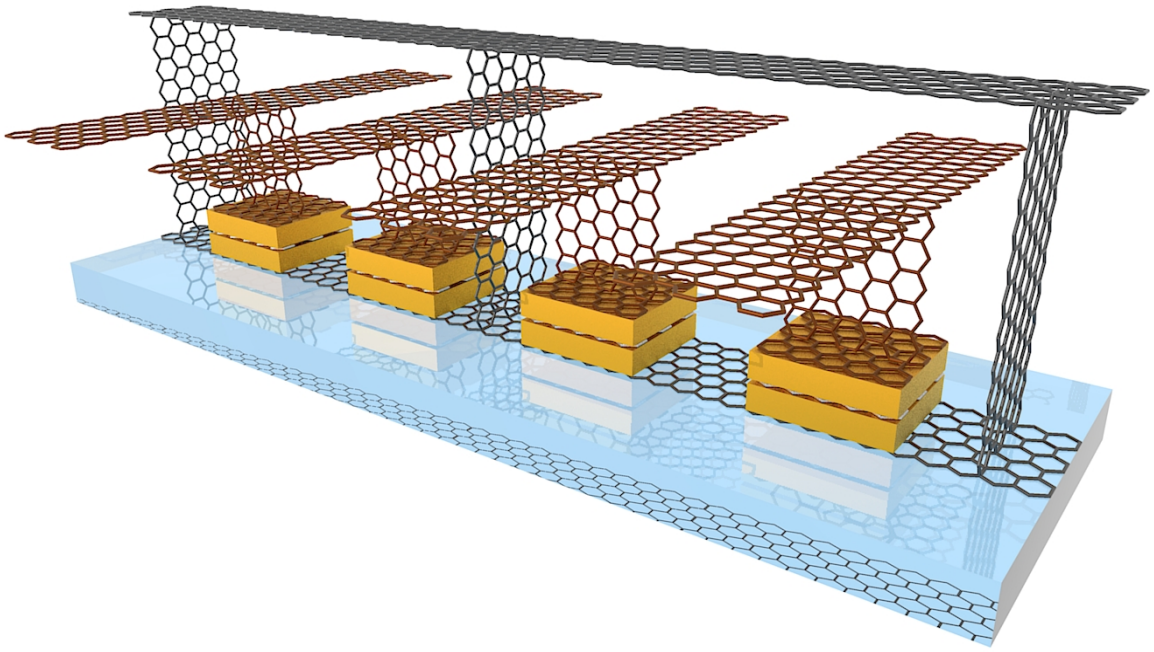

Figure 41: *Two cells graphene NOR gate flash memory. Graphene is used for conductive FET channels [492,528] and bit line (black), control gates [527] and word lines (brown), and floating gates [526] (white).*

Use of graphene in non-volatile memories is facing less challenge than in logic gates, because memory operation requires only large ON/OFF ratio (assuming that the ON current is not too low). In this case the voltage gain of memory GFETs is irrelevant, as reliability of a memory state readout depends only on the sensitivity of the sense amplifiers connected to the bit lines. Graphene could be used in non-volatile memories as channel [492,528], resistive switch [525529], and storage layer, *i.e.*, replacement of floating [526] or control gates[527].

The roadmap is shown in Fig 39, and graphene non-volatile (flash) memories could reach the market in **10-15 years**.

D2.3. *Analog Voltage Amplifiers*

The main building block of analog electronics is a voltage amplifier: an electronic device capable of amplifying small alternating current (AC) voltage signals. For the same reasons discussed in section D2.1 in case of digital logic gates, AC voltage gain is usually much less than unity in graphene circuits. The use of graphene FETs in analog electronics is currently limited to niche applications, such as analog mixers [530], but even these require voltage amplifiers for signal processing. Room T operation of GFETs with a high intrinsic gain has remained elusive, meaning that graphene circuits and detectors should rely on Si FETs for signal amplification and processing [531]. This is not favourably viewed by semiconductor industry, which generally does not like such more expensive hybrid technologies.

One of the main factors contributing to a low gain is the use of back-gated Si/SiO_2 devices, which also suffer from large parasitic capacitances and cannot be integrated with other components. For this reason, top-gated GFETs with thinner gate insulators have been extensively investigated, as in case of digital logic gates.

The future investigation of graphene voltage amplifiers partly overlaps with that of digital logic gates, as in both cases the short-term goal is the same: large voltage gain (>10) should be obtained in wafer-scale SLG and BLG grown by CVD or epitaxially on SiC substrates. In

order to further increase the voltage gain, FETs should be fabricated from wafer-scale misoriented BLG. Finally, several remaining challenges of GFETs, most technological rather than fundamental in nature, should be addressed. E.g., graphene circuits remain sensitive to fabrication induced variability. Higher mobility, g_m and lower g_d and contact resistance should increase the voltage gain for both analog and digital applications. The long-term goal should be the integration of graphene amplifiers in more complex analog circuits.

GFETs are well suited as building blocks of low-noise amplifiers (LNAs) as they exhibit very low levels of the electronic flicker noise (or 1/f noise, where f is the frequency) which dominates the noise spectrum at low frequencies [532,533,534]. Such voltage amplifiers are also expected to benefit from graphene's high mechanical and chemical stability and high thermal conductivity [535]. Graphene LNAs are needed in high-frequency electronics [7,396,536,537], as their realization would allow seamless integration with graphene analog mixers, thus eliminating need for Si FETs in these applications. As present day GFETs cannot be turned off, class-A amplifiers with low harmonic distortions should be developed. Large voltage gain should also allow realization of electronic harmonic oscillators, combining a high-gain voltage amplifier with a passive feedback network.

Finally, the development of graphene voltage amplifiers could pave the way for the development of graphene power amplifiers. These are usually found in the final stages of more complex amplifiers. They operate with a unity voltage gain and have a sole purpose to match the previously amplified signals (provided by the voltage amplifiers) to a low-impedance load such as a loudspeaker (~4 Ω) in high-fidelity audio systems [538] or antenna of a transmitter (~50 Ω) in RF applications.
The roadmap is shown in Fig. 39. Timescales: **3-4 years:** Class-A LNAs. **4-5 years:** Audio and RF voltage amplifiers. **5-6 years:** Harmonic oscillators. **5-10 years:** Power amplifiers.

D2.4. *Interconnects in Integrated Circuits*

State-of-the-art ICs contain large number of FETs (e.g., a typical microprocessor contains $>10^9$ FETs) which must be interconnected in order to perform required functions. Interconnection of such large number of FETs requires a complex multi-level metallization network (e.g., 9 metal levels are used in typical microprocessors) which consumes most of the die volume. This network is especially large in power ICs, in which interconnects must withstand large currents (typically > 10 A). State-of-the art interconnects are usually made of Cu whose maximum current density of 1 MA/cm^2 is limited by electromigration. Graphene is currently being considered as an alternative to Cu because it has very large current-carrying capability [539], which offers possibility for size reduction of interconnects.

Exfoliated SLG can sustain 1.2 mA/μm = 12 A/cm under ambient conditions [539]. Assuming that each SLG (0.33 nm) within a multilayer stack can sustain the same current density, the breakdown current density of a multilayer stack is~360 MA/cm^2, *i.e.*, 360 times more than that of Cu. However, initial investigations of wafer-scale multilayer graphene stacks revealed an order of magnitude lower breakdown current densities (40 MA/cm^2) [540]. Although this is still 40 times more than in Cu, the Rs (> 500 Ω/sq) of these 20nm thick graphene stacks corresponds to $\sigma<0.1\times10^3$S/m, much less than Cu ($\sigma=60\times10^3$S/m). Therefore, further development in wafer-scale graphene synthesis should be undertaken in order to increase the conductivity of thick graphene films, and therefore reduce parasitic resistances of graphene interconnects.

Graphene interconnects should be first introduced in ICs in which FETs are also made of graphene, in order to eliminate initial problems of contact resistance between graphene interconnects and contacts in non-graphene FETs. Eventually graphene interconnects should be introduced both in power and general-purpose ICs. The roadmap is shown in Fig. 39.

Timeline: **5-8 years:** Interconnects in graphene ICs. **5-10 years:** Interconnects in power and general-purpose ICs

D2.5. High frequency electronics

High frequency electronics is a cornerstone of today's high-tech economy, currently supporting more than 50.000 direct and a multitude of indirect jobs in Europe. The continuous downsizing of components in ICT sustained the electronics industry for more than three decades. Indeed, this field was first dominated by defence applications, until the late 1980s, and then it moved into the mainstream in the 1990s owing to advances in wireless communications. Not only because miniaturization reaches fundamental physical limits, which are not solvable with conventional Si technology, but also because emerging applications, such as THz-spectroscopy [541], require higher and higher operation frequencies, hardly achievable with established technology platforms. Thus, a radical new approach is needed. Graphene as material platform for both digital and analog electronics could overcome most obstacles: scaling beyond the Si limits is possible with graphene because it is ultimately thin and the material's enormous carrier mobility allows transistors to operate at frequencies even beyond 1 THz.

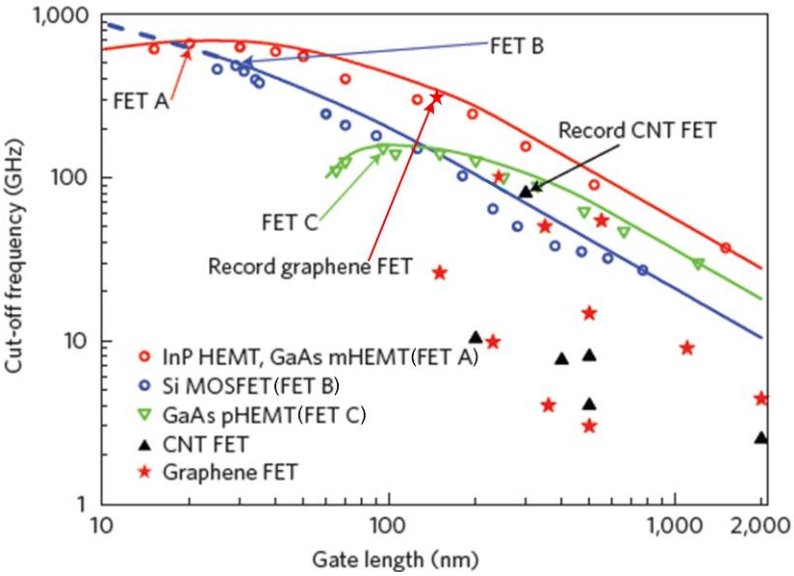

***Figure 42**: Cut-off frequency versus gate length for GMOSFETs, nanotube FETs and three types of RF-FETs (Adapted from Ref. 472)*

The first industrial entry points for graphene will be in analog high frequency electronics, as there the advantages are most distinct in comparison with established technologies. Graphene will allow much higher operation frequencies for frequency doubling and mixer applications than possible with Si or Si/Ge, avoiding the disadvantages of III/V materials, such as high production costs, limited substrate size, toxicity and poor integrability into a cost efficient Si technology.

In addition, ambipolar devices can significantly reduce the number of transistors needed in these applications. Simpler circuits mean less power consumption and smaller chip area. Moreover, considering that RF circuits are much less complex than digital logic ones, makers of RF chips are more open to new device concepts. Indeed, a large variety of different transistor and materials are today used in RF electronics, such as Si n-channel MOSFETs, high-electron-mobility transistors (HEMTs) based on III–V semiconductors (GaAs;InP), and different types of bipolar transistors [542].

Graphene transistors with a 240 nm gate operating at frequencies up to 100 GHz were demonstrated in early 2010 [396]. This cut-off frequency is already higher than those achieved with the best Si MOSFET having similar gate lengths [472].

Recently, cut-off frequency over 300 GHz were demonstrated with graphene transistors with a 140nm channel length, comparable with the very top HEMTs transistors with similar gate length [543], see Fig. 42. These results are impressive, comparing the young age of

graphene with the longer timescales of other devices. This is a clear indication that GFETs have the potential to pass the THz-border in the near future. Thus graphene will offer a cost efficient platform for novel applications in a variety of fields, such spectroscopy or automotive RADAR in analog high frequency electronics. Significant impact in analog RF communication electronics in areas as diverse as low noise amplifiers, frequency multipliers, mixers and resonators is already expected within the next 5 years, see the roadmap in Fig 43.

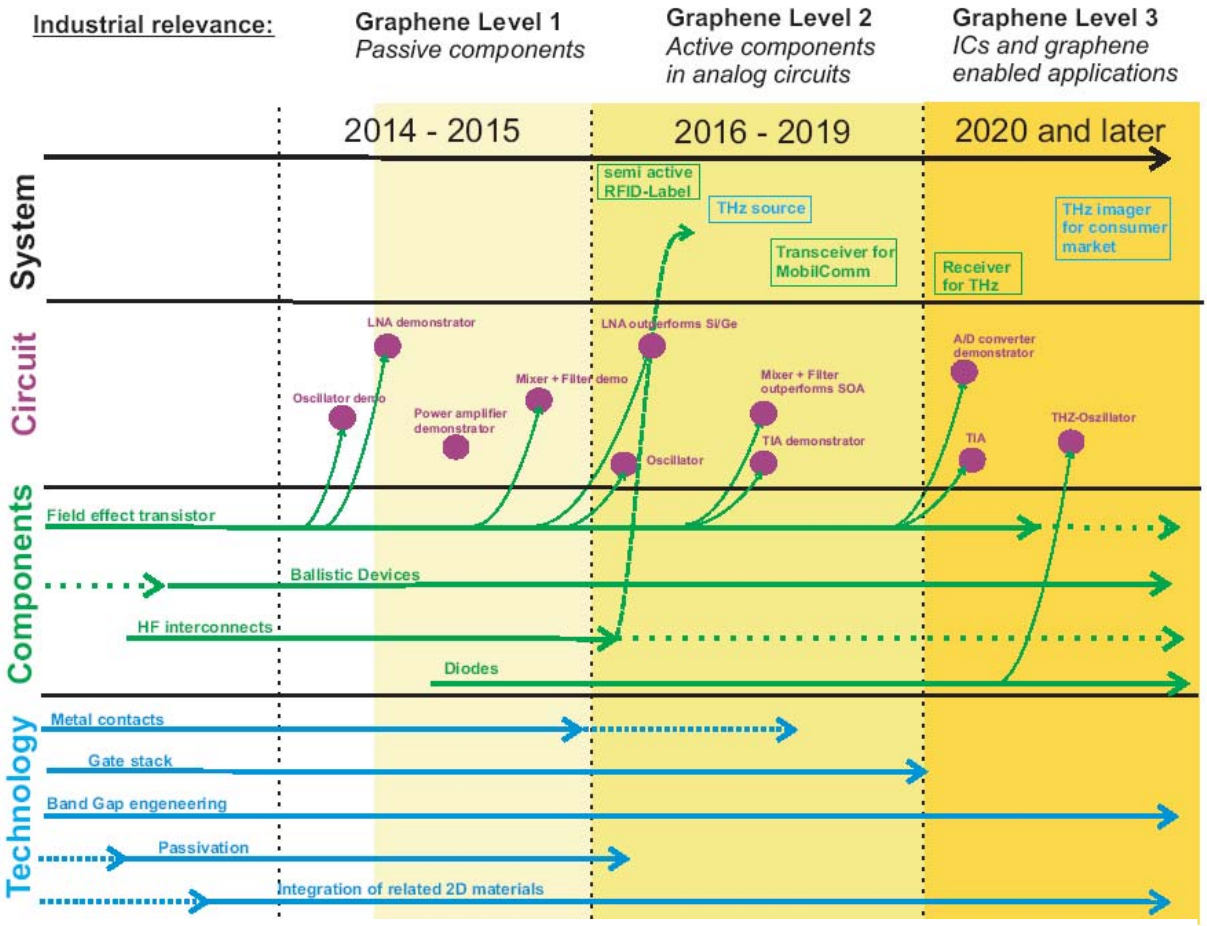

***Figure 43**: High frequency electronics roadmap.*

At present, laboratory-level graphene electronics projects are limited to single device systems. Research efforts will not only be required for the optimization of graphene based devices, but mainly for the development of circuit designs that can fully exploit the unique properties of graphene based devices. The absence of a band-gap, therewith the un-incisive current saturation, the ambipolarity and the targeted operation frequencies going beyond 100GHz require revolutionary concepts on system level and circuit design, which could also open the door towards novel functionalities. Thus, to take advantage of the full potential of graphene devices, the aim is to combine more basic research with improved material growth and device technology. A better understanding of parameters such as breakdown voltage, electron velocity, and saturation current is needed to allow a complete benchmark of this material and an evaluation of its potential performance. In addition, these new applications will have to overcome the limitations that arise from the lack of band-gap.

Once the growth and fabrication technology of these new devices matures, the main challenges for RF applications are the integration of graphene devices in Si technology, and the increase of their trans-conductance by, e.g., introducing a band gap, and ensuring sufficient voltage gains and output currents so that components can be integrated to circuits.

Advanced graphene devices have the potential to transform communication systems in a broad array of new applications in the next ten years. Graphene is therefore in an excellent position to help RF systems become even more ubiquitous and versatile than they are today.

D.2.6 *Novel vertical and planar transistors and devices*

2d superstructures offer dramatically richer opportunities in terms of physics and transport properties than each of the individual 2d crystals. The most obvious device to develop is the TFET [19] . There are already some preliminary results indicating that such devices will indeed offer required parameters in terms of ON/OFF ratio and mobility. Other directions to explore, both experimentally and theoretically, are hot electrons transistors, resonance tunnelling, formation of minibands, etc.

Planar devices will include double quantum wells; drag in parallel 2d electron gases, Bose-Einstein condensation in such systems, etc. Also, effects of enhancement of electronic properties (improved mobility) for each individual conductive layer need to be addressed.

We also need to investigate exotic combinations, such as superconductor/insulator/normal metal or superconductor/insulator/ferromagnet, or even more complex structures, providing we can find suitable 2d materials. Such devices would allow us to explore quasi-particles spin and valley degrees of freedom. Finally, by embedding nanoclusters of conventional metals, ferromagnets, and semiconductors between the layers, we will combine the opportunities for quantum technologies offered by the quantum dot physics and the unique electronic properties of 2d heterostructures. Intercalated superstructures are ideal building blocks for thermoelectric devices and batteries and could give rise to novel capacitive elements. We will investigate the fundamentals of Li-ion and electron ion transport in different nanostructures aiming at an optimum balancing of energy and power density. Solution processed materials will be combined with R2R web-coating on polymeric substrates to fabricate flexible and, potentially, optically transparent/translucent energy storage devices.

D2.6.1 Vertical tunnelling transistors and vertical hot electron transistors

This is a viable alternative to the current approach to graphene-based electronics. We need to exploit vertical transport, instead of juts the horizontal one currently under scrutiny

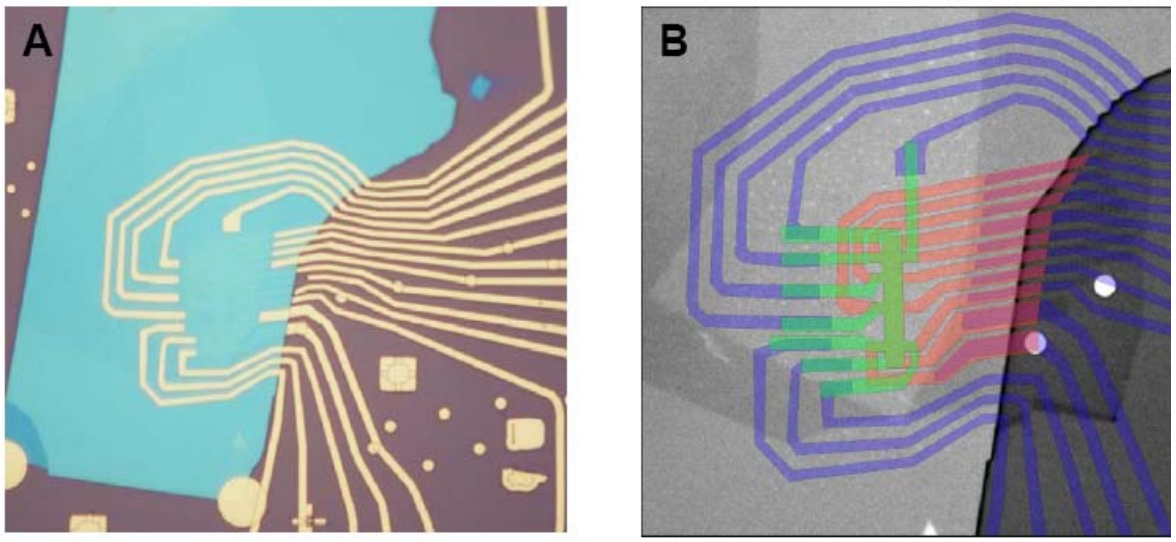

Figure 44*: BN/Gr/BN/Gr/BN devices [32]. (A) Optical image of the final device. (B) Electron micrograph of the same. Two 10-terminal graphene Hall bars are shown in green and orange. The scale is given by the 2μm Hall bar width.*

worldwide. Rapid response and ultra-small sizes can also be achieved in vertical transistors. Indeed, electron transfer through nm thick barriers can be extremely fast (possibly coherent). Ballistic tunnelling transistors may allow us to overcome the most significant drawback of the present approach to graphene electronics, its low ON/OFF ratios. Tunnelling devices would have a highly insulated off state with no dissipation, which should allow not only individual transistors, but integrated circuits at room temperature. The latter is difficult to achieve for horizontal transport and remains a distant goal.The aim is to explore, by experiments and modelling, several architectures for tunnelling/hot electron transistors. The simplest one is metal/BN/Gr/BN/Gr, where the metal contact (separated from the bottom graphene by thick, tunnelling non-transparent BN) serves as a gate and the two graphene layers (acting as emitter and collector) are separated by thin BN layer, Fig. 44. The operations of the device rely on voltage tuneability of the tunnelling density of states in graphene, and on the effective height of the tunnel barrier adjacent to the graphene electrode. We will experiment with several different dielectrics and will use other heterostructures, such as metal/BN/Gr/MoS_2/Gr. Proof of principle devices with BN tunnelling barriers have already demonstrated room temperature On/Off ratio~50 [32], Fig. 45, better than any other graphene transistors to date. We expect that with an improvement of the quality of the heterostructures and use dielectrics with smaller tunnelling barrier – the ON/OFF ratio will be brought close to that required by modern electronics (10^5).

We will also investigate, by experiment and modelling, other possible geometries for vertical transistors, including hot electron transistor similar to those discussed in literature previously [25]. They were typically 100nm-thick and their transfer characteristics were not good enough to inspire further development. Few-atom-thick transistors based on a 2d tunnel barrier and graphene may allow much better quality, and become more successful in applications. The transit time through such sandwiches is expected to be<<1 ps, whereas there are no limits for scaling down in the lateral direction to true nm sizes. We will use metal/BN/GrB/BN/GrT where both BN barriers in are transparent for tunnelling, and the bottom graphene electrode (GrB) serves as the control electrode. The thickness of the active part of the devices would be less than 10 atoms (~3nm) and should allow ballistic current that is controlled by the central graphene electrode. We will also attempt to produce stacks of

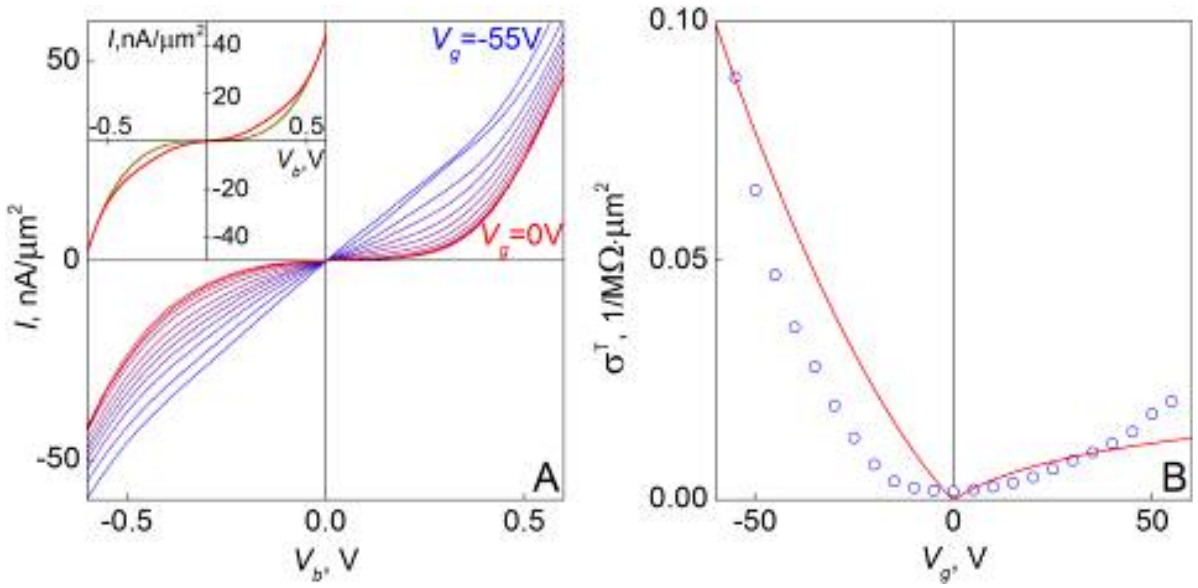

Figure 45: *(A) Tunneling I-Vs and their response to gate voltage (in 5V steps) for a*BN/Gr/$(BN)_4$/Gr/BN *device [32]. Temperature: 300 K. (B) Changes in low-bias tunneling (symbols) and the theory fit for 4 hBN layers (solid curve) [32].*

several transistors in series (metal/BN/GrB/BN/GrT)$_N$, thus introducing a vertical integrated circuit architecture. We will also search for other possible architecture and electronic components as well as for the different ways of integration into vertical integrated circuits.

D.2.6.2 In-plane transport in 2d superstructures

The aforementioned devices (with atomically thin tunnel barriers, graphene and other materials) are a completely new experimental system and offer an enormous range of opportunities for fundamental and applied research. For instance, in terms of fundamental research, two graphene layers separated by a thin dielectric offer an opportunity to look for excitonic condensation and other phenomena mediated by e-e interaction between closely spaced graphene layers. Coulomb drag is an exquisite tool to probe many-body interactions, hard to discern in conventional transport measurements.

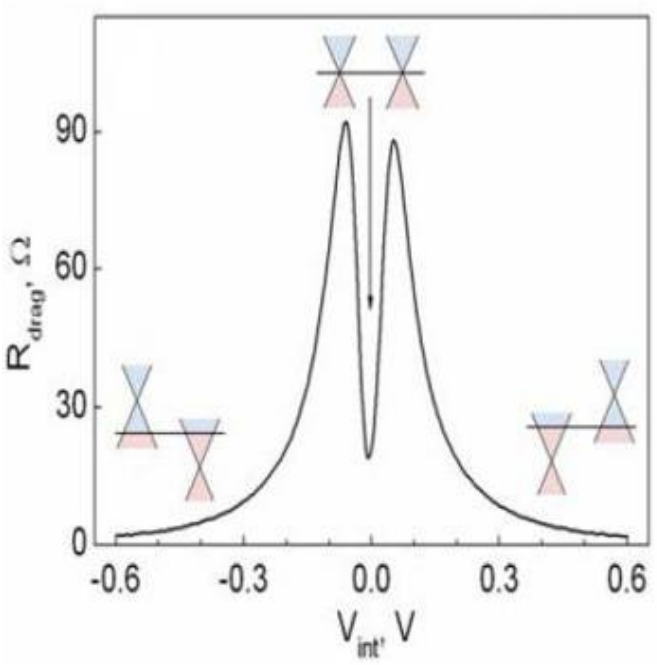

Figure 46: *Coulomb drag in Gr/BN/Gr heterostructure in the regime of matching e-h densities: the bias between two graphene layers is varied at zero gate voltage.*

The advent of Gr/BN and other heterostructures offers a new venue for investigation of interlayer interaction. First, the 2d charge carriers in graphene are confined within a single atomic plane, whereas a few atomic layers of h-BN are sufficient to isolate graphene electrically. This allows extremely small (nm) separation between the graphene layers, which favourably compares with the smallest effective separation ≈15 nm achieved in GaAlAs heterostructures. Second, charge carriers in graphene can be continuously tuned between e and h from densities n $>10^{12}$ cm^{-2} all the way through the neutral state, where the inter-particle distance nominally diverges. This makes it possible to access the limit of strongly interacting 2d systems. First results demonstrate very strong Coulomb drag in BN/Gr/BN/Gr/BN systems (Fig. 46) [32]. Optimisation of the parameters of the structures will lead to myriads of interesting effects.

On the theory side, there is need to impose rigor onto widely varying conflicting predictions for the Coulomb drag and a related issue of exciton condensation [24]. In both problems, we shall use the method of 1/N expansion (N=8), recently developed for two-layer graphene systems, taking into account screening, disorder, and doping inhomogeneity. Additionally we also shall evaluate the contribution of the phonon drag, related to the emission/absorption of vibrations in the separating insulating layers.

We shall explore, experimentally and theoretically, an opportunity to generate new or to enhance the earlier discussed correlation effects in structures with a complex architecture. The formation of the excitonic insulator in the *e-h* two-layer graphene systems is hindered by screening of the Coulomb interaction, which appears to be sensitive to the electron spin and valley degeneracy. In MoS_2, the valley degeneracy in not characteristic to the band structure, hence the temperature of the excitonic insulator transition in MoS_2/(BN)n/MoS_2 sandwiches

may be higher and fall into the experimentally accessible range. Also, we shall search for correlated states in $NbSe_2$/(BN)n/$NbSe_2$ sandwiches, which, by extrapolating from bulk properties of $NbSe_2$, may form both charge density waves and superconductivity.

D3. Graphene nanoelectronics beyond CMOS

There are increasing incentives to explore new avenues to follow the ever increasing need for computational speed and storage capability. While some of the directions look at new types of devices (such as cross-nanowire transistors [544]), others explore novel physical phenomena (using electron spin [545] instead of charge) and alternative materials such as graphene, to build electronic devices and circuits for ICTs. Spintronics is a relatively young field. Electronic devices that use the spin degree of freedom hold unique prospects for future ICT, and graphene is emerging as promising candidate to achieve unprecedented innovation in the generation, storage and processing of the spin-based information.

Due to weak spin-orbit and hyperfine interactions, ultra-long spin coherence lengths could offer a true capability for efficient spin manipulation, with the innovative design of a full spectrum of spintronic nanodevices, including (re-)writable microchips, transistors, logic gates, and more. To date, the advent of spintronics-based logic devices has been impeded by the difficulty to achieve both long spin lifetimes and proper spin control simultaneously. Spin control is usually associated with a sizable spin-orbit coupling. However, a large spin-orbit coupling tends to lead to fast de-coherence. Novel approaches to circumvent this seemingly insurmountable problem by taking advantage of the intrinsic properties of graphene could permit both to obtain long spin lifetimes, and to manipulate the spin information locally.

The large use of interconnections and their power dissipation are limitations for downscaling CMOS technology. Graphene provides solutions to integrate several elements (active and passive) on the same platform. The intrinsic properties of graphene will be used to make a new generation of Magnetoresistive random-access memory (MRAM) with enhanced properties and higher density. While graphene- or GO- hybrids have been demonstrated to have memory effects, the underlying microscopic mechanisms still need to be clarified. Non-volatile GFETs with ferromagnetic gates have been demonstrated to operate as three terminal resistive memories [546], while graphene-based memristors (two terminal resistance) [547] are interesting since they may act both as memory and logic elements.

D3.1. Graphene spintronics

Graphene consists of light atoms, thus exhibits negligible spin-orbit coupling [548] and a possible absence of nuclear spins in isotopically pure material [89]. This leads to long spin relaxation and spin coherence times, the central benchmarks for spintronic devices. Graphene also allows efficient spin injection due to the tunability of the Fermi level [549]. The large electron velocity implies that graphene has unique properties for the transport of spin polarized currents to exceptionally long distances. Moreover, the proximity with other active monolayers, molecules or nanoparticles, can allow to selectively tune its properties at the (molecular-) nano-scale, while high charge mobility and thermal conductivity imply low power consumption and efficient heat

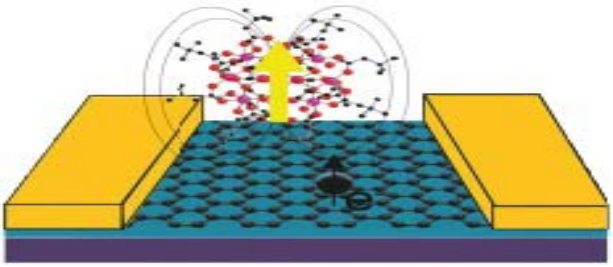

Figure 47*: Molecular spin valve made by decorating a graphene nanoconstriction with $TbPc_2$ magnetic molecules [409].*

dissipation.

Thus, graphene's intrinsic features appear truly suitable not only for downscaling of conventional devices, but also to demonstrate radically new concepts that will allow for spin manipulation without the trade-off related to the reduction of spin coherence time. New concepts to be explored include tailoring spin degrees of freedom through magnetic proximity effects (magnetic gating), torque effect, mechanical strain or molecular/atomic functionalization, all aspects demanding the networking of interdisciplinary research communities. The development of advanced device fabrication and innovative spin manipulation protocols would advance spin injection efficiency at the ferromagnet/graphene interfaces, data recording and spin information processing, but even more exciting is the design of novel spintronic devices at molecular scale (<10nm). Here, components enter in the quantum regime, and graphene may exploit the crossover between the classical to the quantum features of such nano-elements.

Spin injection is currently performed and deeply investigated in both SLG and BLG [90,550]. Measurements on FLG have also been reported [551]. While in early devices spin injection was achieved using transparent contacts (Co/SLG) [552], a great improvement on both injection efficiency and spin lifetime has been obtained with tunnelling contacts (Co/Insulator/SLG) [553]. One of the main issues in conventional interfaces is the matching of conductances. In this respect, interfaces of graphene with graphite intercalated with magnetic impurities or molecules (similarly to magnetic semiconductors [554,555]) seem viable and have to be explored more deeply. The spin valve [556], the simplest spintronic device made by a spin injector and a spin analyser sandwiching a non-magnetic spacer, is the natural bench to test the efficiency of spin injection with graphene hybrids (Fig. 47) [409]. The spin scattering length in graphene was determined to be ~1-2μm [90], enabling the use of graphene in spintronic devices, and in particular spintronic based magnetic sensors. Indeed it has recently been shown [557] that graphene has a large non-local spin current effect near the Dirac point [740] up to room temperature, and at relatively small magnetic fields (0.1T) [740].

As a major advance, graphene spintronics has the potential to revolutionize the development of magnetic sensors with sensitivity ranging from the nT to the pT ranges (for comparison, the Earth’s magnetic field is in the mT range), reaching the domain of mine detection and magnetic anomaly detection. The potential of lab-on-chip spintronic sensors for magnetic nanoparticles would also impact on onsite drug delivery control or tumour disease fight medicine. Additionally, breakthroughs in the fields of MRAM and reconfigurable logic have a transverse interest for ICT. The present trend towards multi-cores processors and the evolution towards massively-parallel computing systems as well as new non-von-Neumann paradigms may thus greatly benefit from graphene spintronics and have a deep impact on ICT in general. Intrinsic non-volatility of spintronics technologies presents a significant advantage in terms of power consumption. The power consumption reduction will benefit as much for tightening supplies of energy and global warming electronics, as for the digital societal revolution of ever more demanding portable electronics. The radiation hardness of spintronics metal-based technologies is also an advantage, in particular in aerospace; the coupling of spin information with optics could lead to spin information transmission by optical links. Finally, spintronics concepts already mainly rely on low-dimensional quantum limit and can be downscaled without increasing power consumption.

We aim to explore the potentialities of GQDs, where individual spin states can be coherently controlled allowing the implementation of so-called spin qubits. In particular, the ratio between operational time and coherence time of the graphene will be optimized, by shortening the former and prolonging the latter. An intriguing challenge is to couple GQDs with other quantum systems. Among these, molecular nanomagnets (e.g. single molecular magnets, spin transition compounds) have shown considerable potential, due to the control of

their quantum features at the molecular level. Moreover the ability to control/functionalize the external shell of such molecules, that allow grafting them on carbon surfaces, makes the realization of molecule-graphene hybrids feasible. The choice of the substrate and of the spin state of the deposited molecule make hybrid carbon based – molecular architectures a flexible platform to design novel spintronic devices. For instance, we will aim to design and fabricate molecular spin valves in vertical geometry made by graphene sandwiched between a magnetic substrate and a magnetic molecule. Another possibility is to investigate -at higher temperatures- the spin split of the energy band induced by magnetic molecules deposited on top of graphene. These are just few examples of the opportunities that the new field of molecular quantum spintronics based on low dimensional carbon materials may open.

The advantage of graphene over conventional materials is the sensitivity of the electronic/magnetic properties to adatoms, adsorbed molecules, interfaces, vacancies, nanomeshes, edges. Several ways will be explored to manipulate spin currents. Interfaces with magnetic materials, magnetic impurities, magnetic adatoms or adsorbed molecules to induce spin splitting of the electronic levels in graphene and spin filtering effects. Since electric transport can be ballistic in the (sub-) micron scale in graphene, there are high hopes for a much more precise spin manipulation. We will analyse the basic ingredients for such purposes, starting from investigation of the possible mechanisms for spin-orbit coupling, and evaluating the spin relaxation time and g factor (i.e. the position of the spin resonance), by taking into account the relevant scattering processes close to and away from the Dirac point (short and long range scatterers, e-e and e-ph interaction etc.). Alternative mechanisms that induce spin polarization directly on graphene have been theoretically proposed and need to be tested. High mobility graphene with reduced sources of spin relaxation is envisaged, but both fundamental mechanisms of spin relaxation and the technological paths to achieve this need to be fully investigated. Improvements are expected by controlling edges and impurities, thus optimization is largely a materials issue.

D3.2. *Graphene single-electron transistors*

The advantage of using graphene as material for QDs is its large charging energy, which protects the quantized charged state of the dot [167,177,178]. This enables GQD-SET operation at higher temperatures, possibly, even at room temperature. Using SETs based on Coulomb blockade in GQDs as classical memory units would both reduce the size of the electronic circuit as well as energy losses.

D3.3. *Graphene qubits*

By trapping an odd number of electrons on the dot one can create an electrically controlled localised spin state, which can be used for quantum information processing [558]. Several proposals to use GQDs for quantum information processing have already been made [16,559], based on the long spin memory of electrons in graphene (in particular, due to the absence of nuclear spin environment which is a major problem of the use of III-V semiconductor dots for quantum information processing).

An additional possibility to create GQDs is related to the unique properties of BLGs [34,35,36,51]. In BLGs, one can use a transverse electric field created by external electrostatic gates to open a gap. It has been demonstrated that one can confine electrons in small regions of a BLG using a combination of top/bottom gates, and, then, operate the charging states of such QDs electrostatically [179]. Further studies of gap control and electron confinement in gapped BLGs are needed.

D4. Flexible electronics, optoelectronics and transparent conductive coating

New nanomaterials, including graphene, related 2d crystals and hybrids, will have a disruptive impact on current optoelectronics devices based on conventional materials, not only because of cost/performance advantages, but also because they can be manufactured in more flexible ways, suitable for a growing range of applications [Fig. 48].

In particular, modern human interface technology requires the development of new applications based on printed and flexible electronics and optoelectronics, such as stretchable displays, touch-screens, light emitting diodes, conformal biosensors, photodetectors and new generation solar cells. Such devices are mostly based on transparent conducting electrodes (TCEs) that require materials with low R_s and high optical transparency (T) throughout the visible region, other than physical and chemical stability, appropriate work function, uniformity, thickness, thermal durability, toxicity and cost [560].

Current TCs are semiconductor-based [561]: doped Indium Oxide (In_2O_3) [562], Zinc Oxide (ZnO) [563], Tin Oxide (SnO_2) [561], as well as ternary compounds based on their combinations [560,561,563, 564]. The dominant material is ITO, a doped n-type semiconductor composed of ~90% In_2O_3, and ~10% SnO_2 [561]. The electrical and optical properties of ITO are strongly affected by impurities [561]. Sn atoms act as n-type donors [561]. ITO is commercially available with T ~80% and R_s as low as 10Ω/□ on glass [563], and ~ 60−300Ω/□ on polyethylene terephthalate (PET) [564].

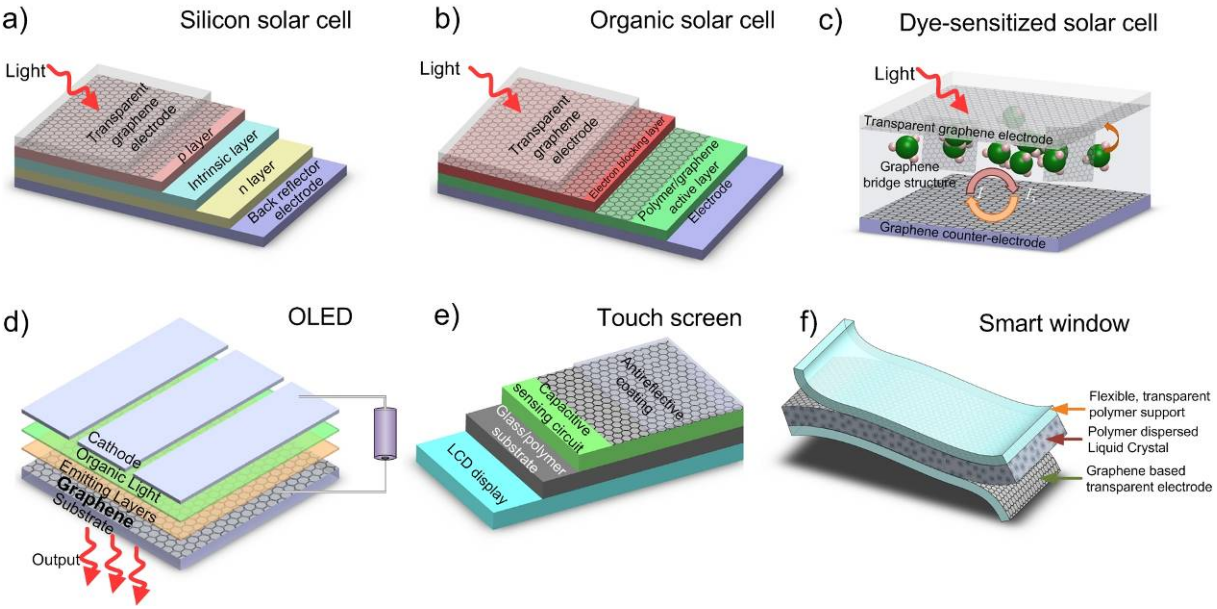

Figure 48: *Graphene-based optoelectronics. (a) inorganic, (b) organic, (c) dye-sensitized solar cells, (d) organic LED, (e) capacitive touch screen, (f) smart windows [306].*

ITO suffers severe limitations: an ever increasing cost due to In scarcity [561], processing requirements, difficulties in patterning [561,564], sensitivity to acidic and basic environments. Moreover, ITO is brittle and can wear out or crack when used in applications where bending is involved, such as touch screens and flexible displays [565].

Metal grids [566], metallic nanowires [567], or other metal oxides [564] have been explored as alternative. Metal nanowires, e.g. Ag NWs have been demonstrated as TCEs on polymeric substrates using different methods, such as vacuum filtration, rod coating, transfer printing, and spray deposition. However, they suffer from stability and adhesion issues.

On the other hand, 2d layered nanomaterials are ideal candidates offering a cost-effective, flexible alternative to ITO and other TCs, paving the way for a new generation of fully flexible displays and optoelectronic devices. In particular, graphene in principle can combine high T with high conductivity, maintaining these properties even under extreme bending and stretching, ideal for easy integration in polymeric and flexible substrates. In many cases (e.g. touch screens or OLEDs), this increases fabrication flexibility, in addition to having economic advantages. For instance, present liquid-crystal-based devices face high fabrication costs associated with the requirement for large transparent electrodes. The move to a graphene-based technology could make them more viable. New forms of graphene-based TCEs on flexible substrates for solar cells can add value and a level of operational flexibility, not possible with current TCs and rigid glass substrates. Moreover 2d layered materials such as h-BN, MoS_2, WS_2 etc., have complementary physical and chemical properties to those of carbon-based nanomaterials and have the potential to fill a wide range of important applications either in isolation or as hybrids with graphene.

Doped and substrate bound graphene (*i.e.* unintentionally doped) offers comparable T and R_s to ITO on flexible substrates. Graphene and GO are being extensively investigated using deposition techniques similar to the ones mentioned in Section C.

Graphene films have higher T over a wider wavelength range with respect to nanotube films [568,569,570], thin metallic films [566,567], and ITO [561,563], Fig. 49a. The flat absorption spectrum determines a neutral colour compared to the yellowish colour of ITO, and the often bluish tint seen in conducting polymers. However, the 2d dc conductivity $\sigma_{2d,dc}$ does not go to zero, but assumes a constant value [89] $\sigma_{2d,dc}\sim 4e^2/h$, resulting in R_s ~6kΩ for an ideal intrinsic SLG with T ~97.7%.

Thus, ideal intrinsic SLG would beat the best ITO only in terms of T, not R_s. However, real samples deposited on substrates, or in thin films, or embedded in polymers are never intrinsic. Exfoliated SLG has typically $n\geq 10^{12}cm^{-2}$ (see e.g. Ref. [79]), and much smaller R_s. The range of T and R_s that can be realistically achieved for graphene layers of varying thickness can be estimated taking $n=10^{12}$-$10^{13}cm^{-2}$ and $\mu=10^3$-$2\times10^4 cm^2/Vs$, as typical for CVD grown films. Figs. 49b,c show that graphene can achieve the same R_s as ITO, ZnO-Ag-ZnO [571], TiO_2/Ag/TiO_2 and CNTs with a much reduced thickness (Fig 48b) and a similar or even higher T. Fig. 48c plots T versus R_s for ITO [566], Ag nanowires [566], CNTs [568] and the best graphene-based TCFs reported to date [4], again showing that the latter is superior. For instance, taking $n=3.4\times10^{12}cm^{-2}$ and $\mu=2\times10^4 cm^2/Vs$, it is possible to get T=90% and R_s = 20Ω/□, with better values achieved with hybrid graphene-metal grids [572].

Different strategies can be used to prepare GTCFs: spraying [573], dip [574] and spin coating [575], vacuum filtration [20], roll-to-roll processing [4].

Different methods to reduce GO [298] have been investigated to further decreased R_s, down to 800Ω/□ for T=82% [576]. Ref. [415] reported, thus far, the best GTCF from LPE of graphite. This was fabricated by vacuum filtration, followed by annealing, achieving Rs=5kΩ/□; T ~90%. GTCF from LPE of graphite produced by rod coating with T higher than 90% and R_s below 1kΩ/□ was also reported [577].

A key strategy to improve performance is stable chemical doping. Ref. [415] prepared GTCFs, produced by MC, with T ~98% and R_s=400Ω/□, exploiting a PVA layer to induce n-type doping. Ref. [4] achieved Rs ~30Ω/□; T~90% by nitric acid treatment of GTCFs derived from CVD grown flakes, one order of magnitude lower in terms of R_s than previous GTCFs from wet transfer of CVD films [4]. Acid treatment permitted to decrease the R_s of hybrid nanotube-graphene films to 100Ω/□ for T=80% [578]

Figure 49d overviews current GTCs. It shows that GTCFs derived from CVD, combined with doping, could outperform ITO, metal wires and SWNTs. Note that GTCFs and GOTCFs produced by other methods, such as LPE, albeit presently with higher R_s at T=90%, have

already been tested in organic light emitters [576,579], solar cells [574] and flexible smart window [306] . These are a cheaper and easier scalable alternative to CVD films, and need be considered in applications where cost reduction is crucial.

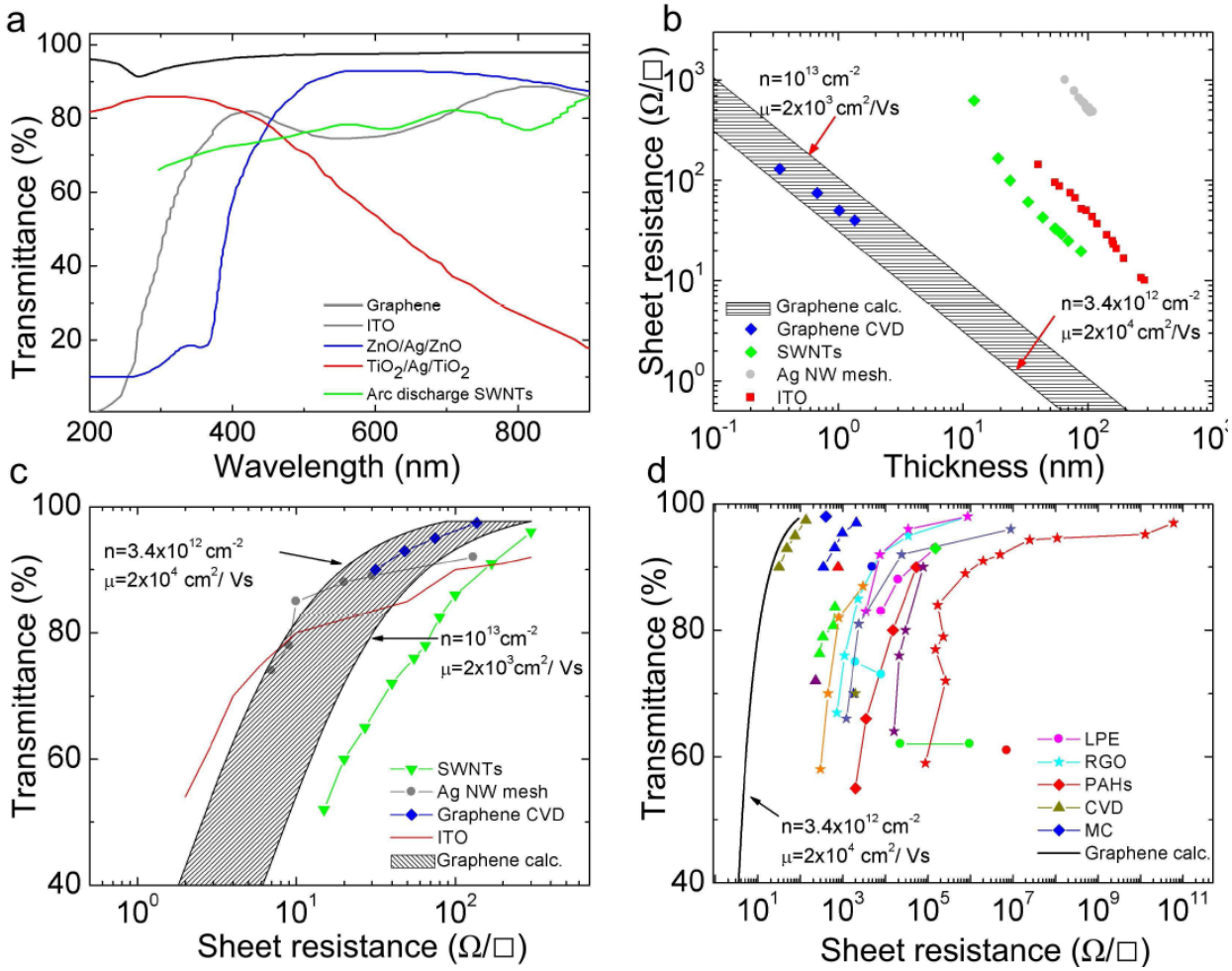

Figure 49: *a) Transmittance of graphene compared to different TCs; b) Thickness dependence of sheet resistance, Rs, for graphene compared to some common materials; c) Transmittance vs sheet resistance for different TCs compared to graphene; d) T vs Rs for GTCFs grouped according to production strategies: LPE, RGO, organic synthesis using PAHs, CVD, and MC. A theoretical line is also plotted for comparison [306].*

The current graphene transparent conductive electrodes (GTCEs) performance are extremely promising in view of commercial applications, already matching industrial requirements [580] for many of them, Fig. 50

Graphene can be used as window electrode in inorganic (Fig. 48a), organic (Fig. 48b) and dye-sensitized solar cells (Fig. 48c).

OLEDs can also take advantage of graphene. They consists in an electroluminescent layer between two charge- injecting electrodes, at least one of which transparent. In these diodes, holes are injected into the highest occupied molecular orbital (HOMO) of the polymer from the anode, and electrons into the lowest unoccupied molecular orbital (LUMO) from the cathode. For efficient injection, the anode and cathode work functions should match the HOMO and LUMO of the light-emitting polymer. Traditionally, ITO is used as TCF. However, besides cost issues, ITO is brittle and limited as a flexible substrate. In addition, In tends to diffuse into the active OLED layers, which reduces device performance over time. Graphene has a work function of 4.5 eV [306,581], similar to ITO. This, combined with its

promise as a flexible and cheap TC, makes it an ideal candidate for an OLED anode (Fig. 48d), while also eliminating the issues related to In diffusion.

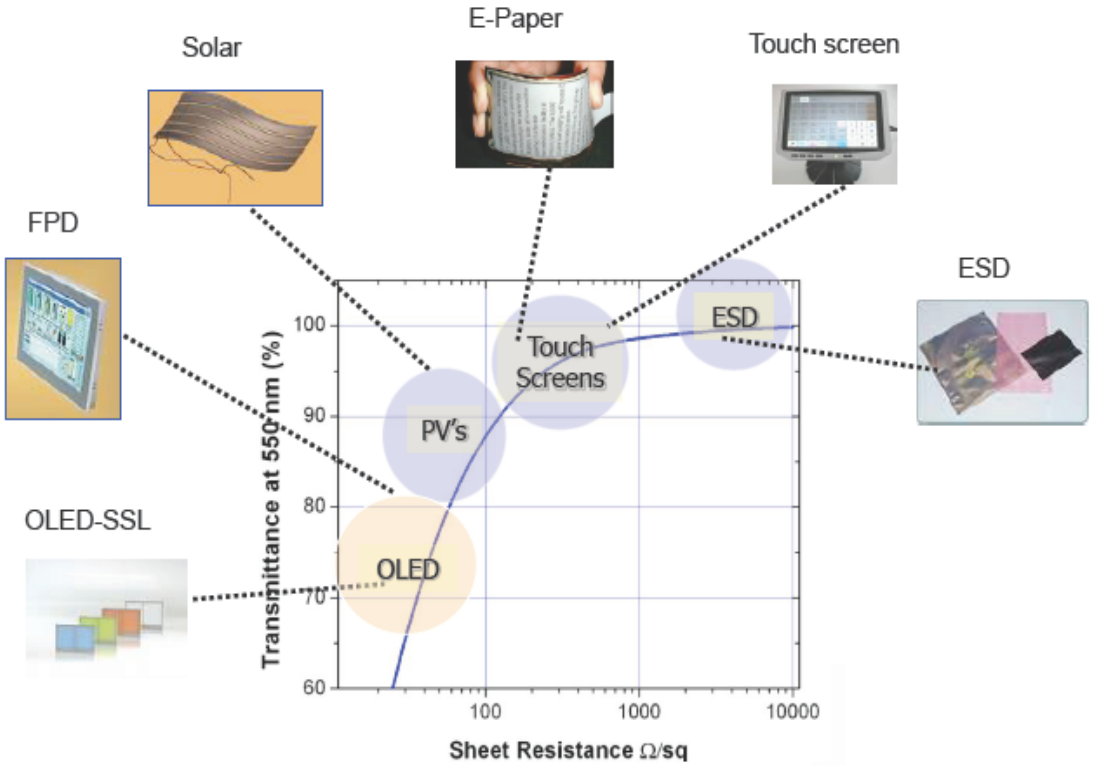

Figure 50*: Industrial requirements for TC applications [580].*

It is also to be expected that other 2d crystals will have interesting optoelectronic properties. For example, individual MoS_2 layers are photoluminescent [213,582,583,584]. We can thus foresee electroluminescent devices based on these materials. These will have a considerable advantage over traditional systems. They will be processable from solution like organics. However, they will not photo-oxidise like organics. This means they may be processable in ambient conditions, a considerable advantage.

Human Computer Interaction (HCI) is a very important aspect of portable electronics, and new interaction technologies are being developed, including touch screens. These are visual outputs that can detect the presence and location of a touch, by a finger or other objects, such as a pen, within the display area, thereby permitting the physical interaction with what shown on the display itself [585]. Touch panels are used in a wide range of applications, such as cell phones and cameras, and where keyboard and mouse do not allow a satisfactory, intuitive, quick, or accurate interaction by the user with the display content.

Resistive and capacitive (see Fig.48e) touch panels are the most common. They comprise a conductive substrate, a LCD frontpanel, and a TCF [585]. When pressed by a finger or pen, the front panel film comes into contact with the bottom TC and the coordinates of the contact point are calculated on the basis of their resistance values. The TC requirements for resistive screens are Rs~500−2000Ω/□ and T>90% at 550nm [585]. Favourable mechanical properties, including brittleness and wear resistance, high chemical durability, no toxicity, and low production costs are also important. GTCFs can satisfy the requirements for resistive touch screens in terms of T and R_s, when combined with large area uniformity. Ref. [4] reported a graphene-based touch panel by screen-printing a CVD sample. Considering the R*s* and T required by analogue resistive screens, GTCF or GOTCF produced via LPE also offer a viable alternative, and offer further cost reduction.

Capacitive touch screens are emerging as the high-end version, especially since the launch of Apple's iPhone. These consist of an insulator such as glass, coated with ITO [585]. As the human body is also a conductor, touching the surface of the screen results in an electrostatic field distortion, measurable as a change in capacitance. Although capacitive touch screens do not work by poking with a pen, thus mechanical stresses are lower with respect to resistive ones; the use of GTCFs can improve performance and reduce costs.

However, these solutions do not yet provide 100% satisfaction in terms of user experience, as touch screens tend to be inert in the way they interact with a user. Also, the proliferation of icons, virtual keys and densely packed browsing menus on mobile touch screens require increasing cognitive efforts from the user in order to be located, distinguished and manipulated. Solutions for low-cognitive effort user interfaces (UI), such as vibration enabled tactile feedback, are currently gaining market momentum by improving usability, interaction interoperability, and user acceptance.

Thus far, the most active tactile feedback solutions have been implemented through simple monolithic vibrations of the entire device driven by a single or very few vibrating actuators, typically electromechanical or piezoelectric [586]. The types of tactile feedback that can be provided by such traditional techniques are limited to relatively basic feedback patterns, only partially correlated to finger position, perceived audio-visual information and actions. Such solutions do not yet provide complete satisfaction in terms of user experience. Key to this is the inability of monolithic vibrations to provide localized tactile feedback associated with visual images, and this is related to the difficulty in implementing tactile feedback directly from a display surface. To address the problem of providing localized tactile feedback directly from the display of a device, a flexible and optically transparent graphene-based programmable electrostatic tactile (ET) system was developed [587,588] capable of delivering localized tactile information to the user's skin, directly from the display's surface and in accordance with the displayed visual information (Fig. 51) [589].

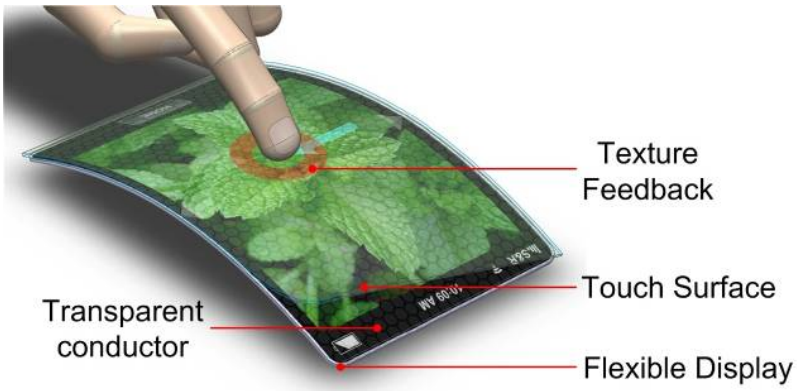

***Figure 51**: Graphene-based electrotactile display [589].*

Aside these "*high end*" applications, TCEs are used in several other every-day appliances, such as low-emissivity windows in buildings, electrochromic mirrors and windows, static dissipation, electromagnetic shielding, invisible security circuits, defrosting windows, oven windows, improving the durability of glass etc. It is clear considering the diversity of applications for TCs that different materials are most suitable for all uses. Depending on which material property is of most importance, different choices are possible [560]. However, considering that the majority of these applications do not require very low R_s and that graphene can be produced in many different ways with diverse properties, GTCEs are likely to revolutionize completely the TCEs market. In particular, GTCFs produced by LPE are most appealing in "*low tech applications*" for ease of fabrication and low cost.

Electrically switchable optical shutters or similar structures, generally known as 'smart windows' [590] are other devices that can take full advantage from the exploitation of graphene as TCEs. Smart windows consist of thin films of optically transparent polymers with micron-sized liquid crystal (LC) droplets contained within pores of the polymer. Light

passing through the LC/polymer is strongly forward scattered, producing a milky film. If the LC ordinary refractive index is close to that of the host polymer, the application of an electric field results in a transparent state [591]. The ability of switching from translucent to opaque makes them attractive in many applications, e.g. where privacy at certain times is highly desirable. There are other potential applications of PDLCs in flexible displays such as an organic thin film transistor driven flexible display with each individual pixel controlled by an addressable PDLC matrix [591]. Conventionally, ITO on glass is used as TCF to apply the electric field across the PDLC. However, one of the reasons behind the limited market penetration of smart windows is the significant ITO cost. Furthermore, flexibility is hindered when using ITO, reducing potential applications, such as PDLC flexible displays [591]. For transparent or coloured/tinted smart windows, the required T and R_s range from 60 to 90% and above and 100 to 1kΩ/□, depending on production cost, application and manufacturer. In addition to flexibility, the electrodes need to be as large as the window itself and must have long term physical and chemical stability, as well as being compatible with the R2R PDLC production process. LCs could also be used for next-generation zero-power monochromatic and coloured flexible bi-stable displays, which can retain an image with no power consumption. These are attractive for signs and advertisements or for e-readers, and require TCs for switching the image. The present ITO devices are not ideal for this application, owing to the limitations discussed above.

All these deficiencies of ITO electrodes can be overcome by GTCFs [306], as shown by the prototype of a flexible smart window with PET used as substrate, see Fig. 48f.

Increasing the carrier density by doping is a means to reduce R*s*. However, in most cases the stability of the dopant is unknown. The aim is to investigate and apply innovative doping routes to achieve stable n-type and p-type doping of graphene, preserving electrical properties over extended time scales. Doping simultaneous to growth can be achieved exploiting alternative precursors (e.g. pyridine, a molecule structurally related to the benzene ring but already with a donor nitrogen atom in the ring). Another route is the "molecular doping" by stable hydrazil- and nitroxide- organic radicals and doping by metal grids.

Up-scaling and developing a graphene-growth protocol for a batch reactor producing graphene on a large scale (size over 50cm x 50cm) is a key target, as outlined in Section C.

Reliable transfer of large-area graphene onto arbitrary substrates is a critical step in the use of CVD-grown graphene. In many cases, the transfer process results in loss of material, and it is difficult to avoid contamination, wrinkling and breakage of the samples. Dry transfer techniques have also been developed, but need to be optimized for different substrates and conditions. The presence of the substrate generally modifies graphene's electronic properties and thus it is important to optimize interaction between graphene and substrate. One way is the modification of the substrate surface by applying surface treatments. The question is how the bonding of graphene to the various substrates affects the electronic properties of the graphene film. It turns out that the interaction depends to a surprising extent on the support. The variations with the support can, in turn, provide additional control of the graphene properties. The target is to broaden our understanding and use these effects for tailoring the chemical reactivity of supported graphene. For many aforementioned applications, thermal expansion and conductivity are crucial. The goal is to investigate the underlying physics and to optimize these properties. Moreover, the combination of graphene and related 2d crystals (*i.e.* MoS_2) should lead to significant charge redistribution at the interface. Thus, tuning of different parameters such as mobility and work function will be investigated.

Another aim is to develop processed LPE graphene deposited on a variety of flexible polymeric substrates to realize TCFs using an up-scalable, R2R coating. The goal is to achieve T~90-95%, with Rs<100Ω/□ and tuneable work function. The achievement of these targets will permit the full integration of GTCFs in many of the aforementioned applications.

Characterization methods that are compatible with large areas are required to monitor quality and consistency of as-produced GTCFs. Scanning probe microscopies as well as TEM are very suitable for investigation of selected regions with small to moderate areas, however, not practical for fast mapping of large areas. Apart from micro-Raman mapping and optical inspection, large-area mapping could include conductivity probes and THz probes.

In the 10-year perspective, the vision for flexible electronics and optoelectronics is built upon five key technology enablers (TE), which are then unified around two streams of applications and summarized in Fig. 52. Key TEs are *T1 Fabrication and integration, T2 Energy, T3 Connectivity, T4 Sensing,* and *T5 TCO.* The two streams of applications identified by industry are *D1 Smart Portable Devices* and *D2 Energy Autonomous Sensors*.

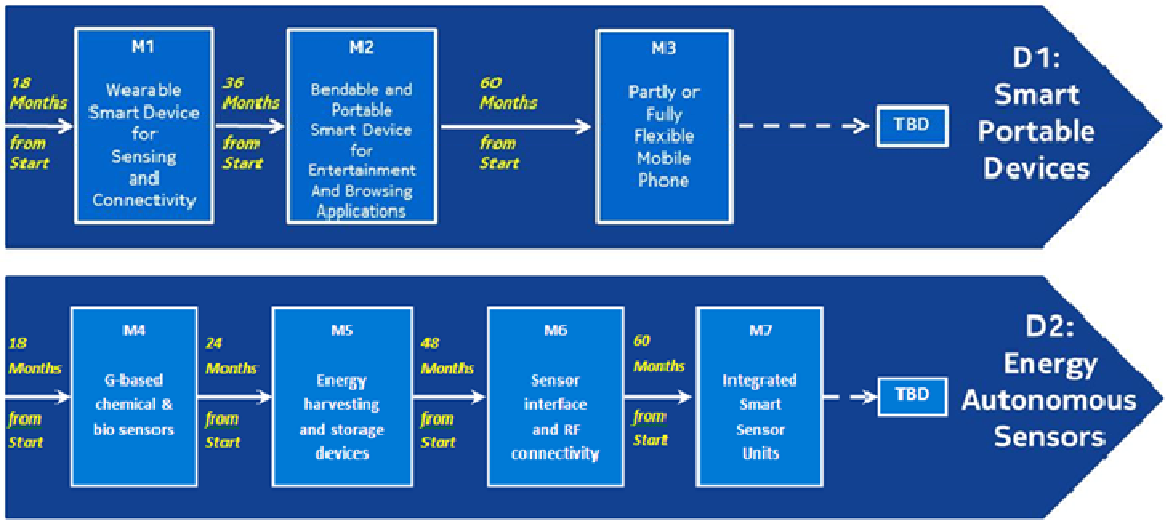

Figure 52: *Two identified streams of applications targeted for flexible electronics and optoelectronics.*

The graphene flagship consortium will aim in the first 30-month period towards the development and the increase in maturity of the TEs listed above. The first period will be succeded by the realization of demonstrators. For instance different fabrication approaches will be developed such as printing of graphene inks, but also the scaling up the manufacturing of integrated components will be investigated. The consortium will address also the need for developing flexible versions of essential energy related technologies, but the flexibility creates also new requirements and opportunities for dedicated connectivity solutions such as radio communication. Biocompatible large area sensors and flexible version of these will also be one of the key technology enablers developed in this area. Finally, electromechanical and reliability tests of individual layers, substrates, devices and full systems will be performed.
In the first **D1 (“Smart Portable Devices”)** application stream we expect the following major prototype demonstrators to be realised: ***Year 2:*** *Wearable Smart Device for Sensing and Connectivity* – Leveraging both existing and new, graphene based technologies this demonstrators will show the potential for cost advantage and/or performance enhancement in wearable, connected devices for the emerging market fitness and wellness application. ***Year 3****: Bendable and Portable Smart Device for Entertainment and Browsing Applications*– Combining advanced material, energy, connectivity and integration/manufacturing technologies developed within the Flagship projects with display and logic processors from external suppliers, this demonstrators will showcase radically new solutions for game control and user interaction and manipulation of content. **Year 4** and Beyond: Partly or Fully Flexible Mobile Phone – The most advanced and challenging demonstrator that can be

envisaged at this stage will attempt to reproduce important functionalities of a smart phone in a partly or fully flexible format.
In **the D2 ("Energy Autonomous Sensors")** stream we expect the following major prototype demonstrators to be realised: ***Year 2:*** *G-based chemical and bio sensors* – Exploiting both existing and new sensing devices with high or ultra-high sensitivity and chemical stability, based on graphene functionalization chemistry, intrinsic biocompatibility and ambipolar characteristics of G-FET devices. ***Year 3:*** *Energy Harvesting and Storage devices*– Developing energy related technologies tailored for flexible substrates such as flexible batteries, super-capacitors and their integration with harvesting devices. This milestone aims to provide the "engine" to propel the autonomous sensor devices. **Year 4** and beyond: Integrated Smart Sensor Units with RF connectivity – At first, we will combine RF device and circuit applications based on ambipolar non-linear graphene electronics for RF connectivity with Analog Sensor Interfaces, and integrating both on a flexible foil substrate. Finally, we will develop and provide the necessary infrastructure towards "graphene-augmented" smart integrated sensors on flexible substrates, with the necessary energy harvesting and storage capability to work autonomously and wireless connected to the environment.

D5. Graphene Photonics and Optoelectronics

Graphene is emerging as a viable alternative to conventional optoelectronic, plasmonic and nanophotonic materials. It has decisive advantages such as wavelength-independent absorption, tuneability via electrostatic doping, large charge-carrier concentrations, low dissipation rates, extraordinary electronic properties, and the ability to confine electromagnetic energy to unprecedented small volumes.

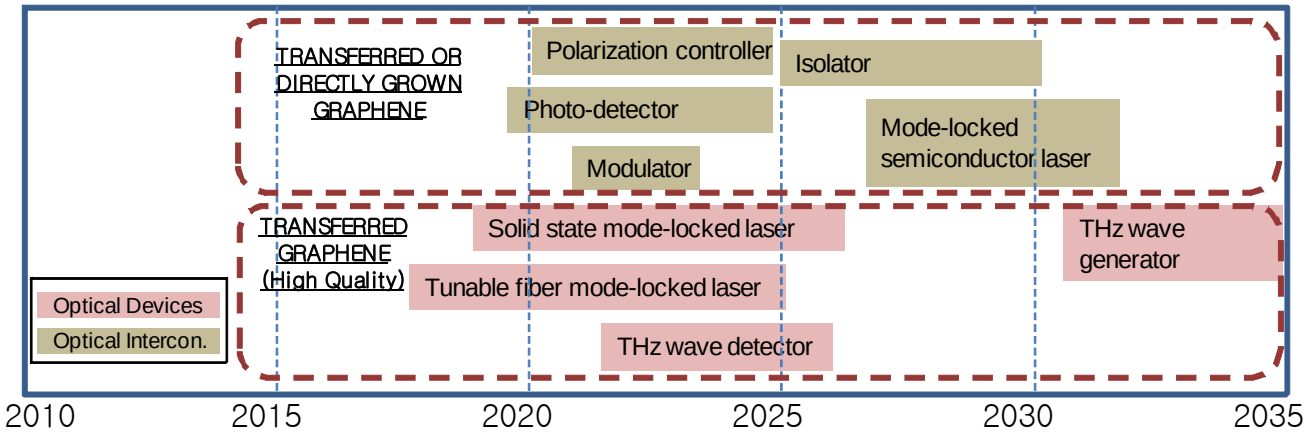

Figure 53*: Graphene photonics application timeline.*

Fig. 53 and Table 4 show some possible applications, the drivers and timeline. We envision breakthroughs in highly-integrated and high-speed graphene optoelectronics, long-wavelength photodetection and THz operation, ultrafast pixelated photodetection, high efficiency photodetection and PVs, and graphene optical metamaterials and plasmonics, see Fig. 54, for a roadmap outlining the timeline from the realization of individual demonstrators passing through integration with aiming to be on the market in ~ 10 years.

Table 4: *Drivers and issues for implementation of graphene in photonics.*

Year	Application	Drivers	Issue to be addressed
2019~	Photo-detector	- Fast increase of bandwidth between chip to chip/intra-chip. - Higher bandwidth per wavelength not possible with IV or III-V detector in 2020 - Graphene photo-detector can increase bandwidth per wavelength to 640GHz.	- Need to increase responsivity, which might require a new structure and/or doping control. - Modulator bandwidth has to follow suit.
2017~	Mode-locked semiconductor laser	- Bandwidth increase between core to core and core to memory requires DWDM optical interconnect with over 50 wavelengths, not possible with a laser array. - GSA enables passively mode-locked semiconductor and fibre lasers, candidates for D-WDM.	- Market will be open in 2020's. - Competing technologies: actively mode-locked lasers or external mode-lock lasers - Interconnect architecture should consume low power.
2018~	Solid-state mode-locked laser	- GSA can be simpler and cheaper and easy to integrate into the laser system.	- Need cost effective graphene transfer technology.
2017~	Tunable fiber mode-locked laser	- Wide spectral range of graphene is suitable for widely tunable fiber mode-locked laser.	- Need a cost effective graphene transfer technology.
2022~	Optical modulator	- Si operation bandwidth limit~50GHz. Graphene is a good candidate without using complicated III-V epitaxial growth or bonding	- High quality graphene with low Rs is key for increasing bandwidth over 100GHz.
2020~	Polarization controller	- Current polarization controlling devices are bulky and/or difficult to integrate. - Graphene can realize compactness and integration of these devices with low volume.	- Need to improve controllability.
2025~	Isolator	- Graphene can provide integrable and compact isolators on Si substrate, only possible with bulky magneto optical devices	- Decreasing magnetic field and processing are important to products

The most prominent properties of graphene for photonics/optoelectronics are: 1) The dispersion relation remains quasi linear for energies up to approximately ±1eV from the Fermi energy [44]. It is therefore possible to generate charge carriers in graphene by optically stimulating inter-band transitions over a wide energy spectrum, unmatched by any other material. This includes commercially important telecommunication wavelengths and the FIR/THz and MIR regimes (see Fig. 55a). 2) The high carrier mobility enables ultrafast conversion of photons or plasmons to electrical currents or voltages (Fig. 55b). By integration with local gates, this process is actively tunable and allows for sub-micron detection resolution and pixelization.

Graphene electronic and photonic devices can be fabricated using standard semiconductor technology, which facilitates monolithical integration into Si-based mass-production platforms. This is a decisive advantage over most other promising nanotechnologies.

At elevated carrier densities, graphene supports surface plasmons (electromagnetic waves strongly confined to the surface) with unprecedented properties [592]: (i) Extreme confinement, 1−3 orders of magnitude smaller than the wavelength, much smaller than the confinement of plasmons in noble metals in the considered spectral regime. (ii) The optical response of graphene is strongly dependent on the doping level, *i.e.* the Fermi energy relative to the Dirac point. This can be changed electrostatically, providing a tool for ultrafast electro-optical switching and modulation. (iii) Crystallinity and defect-free structures over large distances due to the strength of the carbon chemical bond, in contrast to conventional plasmonic metals, in which fabrication imperfections constitute a bottleneck in the performance of nano-metallic structures. (iv) Low losses, resulting in surface plasmon lifetimes reaching hundreds of optical cycles [592].

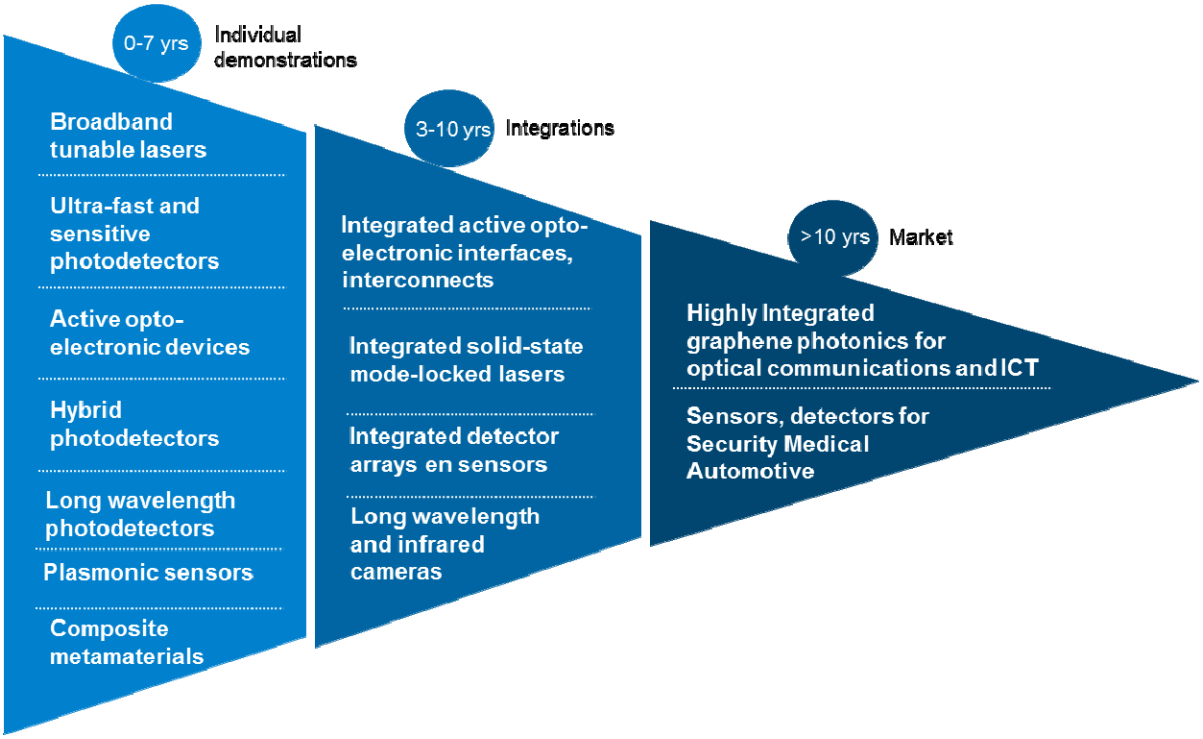

***Figure 54**: Graphene photonics roadmap.*

Electrostatically controlled Pauli-blocking of optical transitions and controlled damping of plasmon propagation enables the realization of ultra-high bandwidth electro-optical modulators [593], optical switches, and similar devices.

Graphene is an excellent candidate for high-gain photodetection by employing the photogating effect. Because of its very high mobility and its 2d nature, its conductance is very sensitive to electrostatic perturbation by photogenerated carriers close to the surface.

The graphene properties that may appear to hinder its development for purely electronic devices, such as the absence of a band-gap, are not critical for photonics and optoelectronics. In fact, they can be beneficial, enabling ultra-wideband accessibility provided by the linear electronic dispersion, allowing efficient, gate controllable, e-h pair generation at all wavelengths, unlike any other semiconductor.

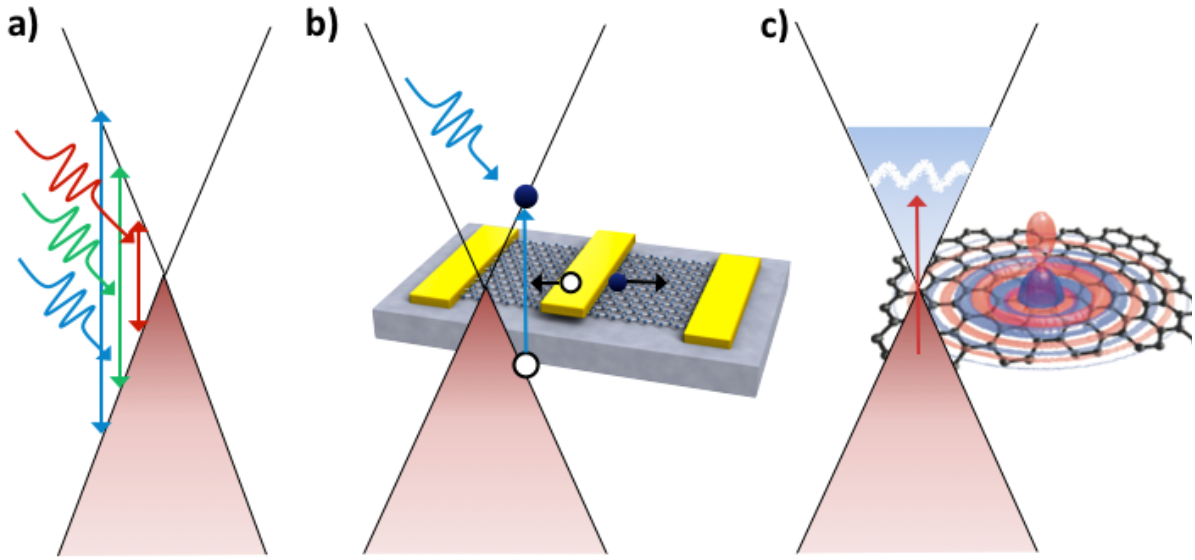

***Figure 55**: Schematics of (a) wavelength-independent absorption, (b) broadband photodetection, (c) plasmon generation by a dipole or through a plasmon resonance.*

We will aim at the following breakthroughs:
Highly-integrated graphene photonics. The compatibility of graphene with standard CMOS processes at wafer scale makes it a promising candidate for high data-rate (inter- and intra-chip) optical interconnects. Graphene will allow the realization of high-speed, compact-footprint electro-optical modulators, switches and photodetectors integrated with Si waveguides or plasmonic circuits. The mechanical flexibility of graphene will also enable the integration with bendable substrates and plastic waveguides.
Long-wavelength light detection. Graphene enables light detection at wavelengths beyond the current limit set by the band gap of traditional semiconductors, opens up new applications in the FIR (THz) and MIR regimes (e.g. bolometers and cameras), and has potential for ultrafast pixelated detection with ballistic transport of generated charge carriers.
Terahertz operation. This will enable products such as portable sensors for remote detection of dangerous agents, environmental monitoring or wireless communication links with transmission rates above 100 Gbit/s.
High-efficiency photodetection. We will target the realization of highly efficient photocurrent generation by providing a gain mechanism where multiple charge carriers are created from one incident photon.
Graphene plasmonics and metamaterials. We will explore graphene surface plasmons as well as tailored metal nanostructures to enhance and control the coupling between light and graphene. This paves the way to ultra-fast optical switching, ultra-strong light-absorption, PVs, and single bio-molecule sensing.

The vision is to establish a new field of graphene photonics, sustained by the convergence and co-integration of graphene-based electronic and photonic components such as lasers, optical waveguides, cavities, modulators, photodetectors, and solar cells.

Graphene will be employed as active optoelectronic material to achieve light-matter interaction, convert incident light energy into detectable electrical signals, and, vice versa, use electrical signals to modulate light and realize optical switches. For this purpose, graphene will be integrated with established and mature technologies such as dielectric (Si or plastic) waveguides, optical antennas, plasmonic structures (e.g. gratings or nanoparticles), metamaterials, quantum dots, etc. Graphene's constant optical absorption over a spectral range covering the THz to the UV allows light detection over a wavelength range superior to any other material. Combined with its ultra-high carrier mobility and Fermi velocity, this implies that devices operating in the hundreds of GHz range are feasible.

Despite graphene's absorption of 2.3% being large once its monoatomic thickness is considered, it is still necessary to increase this value to allow more efficient light-matter interaction and realize highly efficient optoelectronic devices. For that purpose, several routes will be pursued. One is the combination of graphene with plasmonic nanostructures [234,592], whereby the near-field enhancement due to localized surface plasmons can significantly increase the light absorption [234]. In principle structures can be designed to achieve 100% light absorption [234]. Semiconducting nanoparticles of various shapes and forms can also be used to hugely improve the quantum efficiency. Light harvesting and concentration with these nanostructures into graphene leads to an increased absorption and more efficient conversion of light into electrical signals, with an increase of quantum efficiency.

Another concept involves the integration of graphene with highly confined optical waveguides, such as Si-on-insulator (SOI) waveguides, widely used in highly-integrated Si photonics. As the light propagates along the waveguide, it is absorbed along the length of the propagation and 100% light absorption is possible. Graphene may also be inserted between two mirrors to form microcavity-integrated optoelectronic devices. The incident light is reflected by the top and bottom mirrors and passes through the graphene multiple times. At

the resonance condition, constructive interference enhances the optical field in the cavity, leading to enhanced light-matter interaction and strong optical absorption.

We will also target the exploitation of plasmons in graphene itself. This strong light-matter interaction can be further utilized to enhance detector performance as well as enabling radically new light sensing concepts.

The ever increasing demand for higher-bandwidth communications brings along the need for higher-bandwidth devices on the transmitting, as well as the receiving side, of the communications link. As large parts of the internet traffic are already transmitted optically, the need for high-speed modulators and photodetectors in the telecommunications wavelength range (1.3–1.55μm) is ever more pressing. Moreover, optical interconnects are currently being introduced as a way to link computers to mobile devices, as well as ultra-high bandwidth links for inter- and even intra-chip communication. It has been experimentally demonstrated that graphene photodetectors are capable of supporting bandwidths of up to 262 GHz [594], a huge value, but still far below the intrinsic limit, thus far estimated in the THz range [595]. We will determine the speed limit of graphene-based photodetectors, at the same time optimizing the devices in terms of responsivity, by enhancement with plasmonics and quantum structures, as well as integration into optical cavities and waveguides. Electro-optical modulators will be realized and benchmarked in terms of speed and other parameters.

The FIR (THz) and MIR regions are fairly unexploited parts of the electromagnetic spectrum, and especially light detection is difficult. However, many interesting applications can be thought of, due to the non-ionizing and low-energy characteristics of THz and MIR radiation. Ranging from medical applications, such as cancer diagnostics, to security, such as explosive detection, since all materials have characteristic fingerprints in the THz/MIR region, a very wide application range is feasible. Further, active devices working in the THz/MIR range are crucial to convert very high frequency signals (in particular, the THz/MIR part of the solar radiation spectrum) into DC voltage – a feature which could eventually lead to self-powered devices. Being a zero-band gap semiconductor, graphene offers huge potential to outperform all available semiconductor technologies in the THz and MIR range, to reach THz operation frequencies, and to enable future wireless THz systems.

The 2d nature of graphene makes it also feasible to use CMOS-compatible processing techniques with CVD grown large-area graphene, in order to achieve highly-integrated arrays consisting of numerous individual devices. This may allow the fabrication of pixelated graphene-based cameras working over an ultra-wide spectral range, enabling image capture from the visible to the more unexplored THz/MIR range. Potential targets include medical, automotive and security, with applications such as tissue imaging, driver supporting head-up displays, and explosive/biological species detection.

Current solar cell technologies use only a rather small part of the solar spectrum due to their intrinsic band gap limiting the maximum detectable wavelength. The absence of a band-gap in graphene translates into the absence of this maximum detectable wavelength limit and combined with its constant absorption, solar energy over a much wider spectral length can be converted to energy. Solar cells based on graphene, as well as combined with plasmonic and quantum nanostructures will be explored.

Finally, we will combine graphene with other nanostructures. We will take advantage of the strong light absorption in QDs and the 2-dimensionality and high mobility of graphene to merge these materials into a hybrid system for photodetection with extremely high sensitivity. Further, the integration with plasmonic metamaterials will allow for the realization of a new class of optical switches for displays.

Surface enhanced Raman Spectroscopy (SERS) can in principle achieve signal enhancements of up to 10^{15} [596]. We expect that plasmonic nanostructures enhanced sensing may lead to detection limits on the single-molecule level. The near-field enhancement

resulting from the combination of graphene with plasmonic nanostructures will increase the signal sufficiently. Such structures will also benefit from graphene's compatibility with biological species. Combined with graphene's single-electron charge sensitivity, we expect this technology to become a new platform for medical applications, not only providing enhancement at the single-molecule sensing level, but also being bio-compatible.

Integration of graphene into a cheap, flexible sensing platform based on plastics will be explored. It is envisaged to integrate and merge the aforementioned medical and THz/MIR sensors with plastic electronics to achieve a sensing-platform for wearable electronics, as well as low-cost one-time use sensors for use in developing countries.

D5.1. *Graphene saturable aborbers and related devices*

Materials with nonlinear optical and electro-optical properties are needed in most photonic applications. Laser sources producing nano- to sub-picosecond pulses are key components in the portfolio of leading laser manufacturers. Regardless of wavelength, the majority of ultrafast laser systems use a mode-locking technique, where a nonlinear optical element, called a saturable absorber (SA), turns the continuous-wave output into a train of ultrafast optical pulses [597]. The key requirements are fast response time, strong nonlinearity, broad wavelength range, low optical losses, high power handling, low power consumption, low cost and ease of integration into an optical system. Currently, the dominant technology is based on semiconductor SA mirrors (SESAMs) [597,598]. However, these have a narrow tuning range, and require complex fabrication and packaging [597,603]. The linear dispersion of the Dirac electrons in graphene offers an ideal solution: for any excitation there is always an e–h pair in resonance. The ultrafast carrier dynamics [599,600] combined with large absorption [65,601] and Pauli blocking, make graphene an ideal ultrabroadband, fast SA [603,602]. Unlike SESAMS and nanotubes, graphene does not require bandgap engineering or chirality/diameter control [603,602].

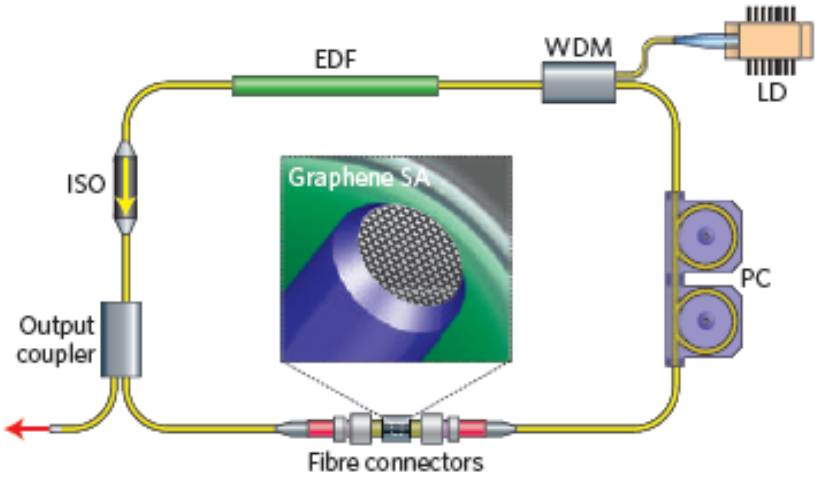

Figure 56**: Graphene fiber laser [603]. WDM, wavelength division multiplexer; PC, polarization controller; EDF, erbium-doped fiber; ISO, isolator [**Error! Bookmark not

Since the first demonstration in 2009 [603] (Fig. 56), the performance of ultrafast lasers mode-locked by graphene has improved significantly. For example, the average output power has increased from a few mW [603] to 1 W [604]. Some of the aforementioned production strategies (e.g. LPE [603,602,605,606,607,608,609], CVD [610,611], carbon segregation [612], MC [609,613]) have been used for GSA fabrication. So far, GSAs have been demonstrated for pulse generation at 1μm [619,604], 1.2μm [620], 1.5μm [603,602,610,611,613,616] and 2μm [614]. The most common wavelength so far is ~1.5μm, not due to GSAs wavelength restriction, but because this is the standard wavelength of

optical telecommunications. Ref. [606] reported a widely tuneable fiber laser mode-locked with a GSA. The laser produces picoseconds pulses in a tuning range of 1525-1559nm, demonstrating its "full-band" operation performance.

Fiber lasers are attractive due to their efficient heat dissipation and alignment-free format [615]. GSAs have been successfully used to mode-lock fiber lasers [603,605,606,607,610,611,613,602,616]. For fiber lasers, the simplest and most economical approach for GSA integration relies in sandwiching directly the GSA between two fiber connectors (Fig.33) [606,610,611,613,616,602]. Other options (e.g. evanescent-wave based integration [617]) have also been demonstrated for high-power generation. Sub-200fs pulses have been achieved using a stretched-pulse design, where the cavity dispersion is balanced to stretch the pulse for the limitation of nonlinear effects [605].

Solid-state lasers are typically used for high-power output, as alternative to fiber lasers [618]. GSAs have also been demonstrated to mode-lock solid-state lasers [604,619,620,621]. In this case, CVD graphene (>1cm^2) has been directly transferred to quartz substrate for solid-state laser mode-locking [620]. Ref. [620] reported 94fs pulses with 230mW output power. Another approach for GSA fabrication relies in spin-coating LPE graphene either on quartz substrates or high-reflectivity mirrors. GSA can then be inserted into a solid-state cavity for ultrafast pulse generation achieving average power up to 1W using a solid-state Nd:YVO_4 laser [604]. The output wavelength is ~1 μm with power energy of ~14nJ.

Graphene is also an optimal material also for other photonic applications, such as optical limiters and optical frequency converters. Optical limiters are devices that have high transmittance for low incident light intensity and low transmittance for high intensity [622]. There is a great interest in these for optical sensors and human eye protection, as retinal damage can occur when intensities exceed a certain threshold [622]. Passive optical limiters, which use a nonlinear optical material, have the potential to be simple, compact and cheap [622]. However, so far no passive optical limiters have been able to protect eyes and other common sensors over the entire visible and near-infrared range [622]. Typical materials include semiconductors (*i.e.* ZnSe, InSb), organic molecules (*i.e.*, phthalocyanines), liquid crystals and carbon-based materials (*i.e.*, carbon-black dispersions, CNTs and fullerenes) [622,623]. In graphene-based optical limiters the absorbed light energy converts into heat, creating bubbles and microplasmas [623], which results in reduced transmission. Graphene dispersions can be used as wideband optical limiters covering visible and NIR. Broad optical limiting (at 532 and 1064nm) by LPE graphene was reported for ns pulses [623]. Ref. [624] reported that functionalized graphene dispersions could outperform C_{60} as an optical limiter.

Optical frequency converters are used to expand the wavelength accessibility of lasers (for example, frequency doubling, parametric amplification and oscillation, and four-wave mixing) [622]. Calculations suggest that nonlinear frequency generation in graphene (harmonics of input light, for example) should be possible for sufficiently high external electric fields (>100 V cm^{-1}) [625].

Second-harmonic generation from a 150fs laser at 800nm has been reported for a graphene film [626]. In addition, four-wave mixing to generate NIR tunable light was demonstrated using SLG and FLG [627]. Graphene's third-order susceptibility $|\chi_3|$ was measured to be ~10^{-7} e.s.u. [627], up to one order of magnitude larger than CNTs [627]. Other features of graphene, such as the possibility of tuning the nonlinearity by changing the number of layers, and wavelength-independent nonlinear susceptibility [627], still could be potentially used for various photonic applications (e.g. optical imaging).

The main parameters of a pulsed laser are output power (or single pulse energy), output spectral coverage (e.g. operation wavelength, wavelength tuneability), pulse duration and repetition rate. The requirements for ultrafast laser applications are highly application-dependent. E.g., for fiber-optical communications, the operation wavelength is ~1.5μm as

optical fibers have low loss and low dispersion around this spectral range. For medical applications (e.g. laser surgery), the required laser operation wavelengths mainly depend on the peak absorption of different tissues waiting for surgery. These range from MIR for minimally invasive surgery of skin cutting, to UV for a-thermal photoablation. For high-speed fiber-optical signal transmission and processing, high-repetition rate (>GHz) allows the signal to carry more data, while for industrial material processing (e.g. micro-machining), kHz pulses are commonly used to decrease the cumulative heating caused by multiple laser pulses. In general, high output power, wide spectral coverage, short pulse width, and high repetition rate are desirable, because it is easy to reduce the output power (e.g. by attenuators), narrow the spectral coverage (e.g. by optical filters), broaden the pulse duration (e.g. by dispersive fibers) and decrease the repetition rate (e.g. by optical choppers), but not vice-versa. Furthermore, stability, cost, compactness and efficiency (e.g. electrical-to-optical or optical-to-optical efficiency) also are key for applications.

D5.1.1 Output power/pulse energy

Currently, solid-state lasers and fiber lasers are the major commonly used for high output power/pulse energy applications, mainly because they allow high-power pump. Solid-state lasers are advantageous in terms of high pulse energy and peak power, as fiber lasers suffer from nonlinear effects. For example, Watt-level ultrafast Ti:sapphire lasers and their low-repetition-rate (<kHz), high energy and high peak power amplifiers are widely used for academic research. The primary limitation of solid-state lasers to achieve high average power is thermo-optic effects, such as thermal lensing. Compared to solid-state rod and slab lasers, solid-state thin-disk designs significantly reduce thermal effects and nonlinearities, due to the pump configuration and small thickness (~a few hundred μm of the gain medium). This could be a solution to high average power and high energy pulses. GSAs could be used in thin-disk design for this purpose. The main challenge is the relatively large non-saturable loss of these SAs, which can be addressed by further devices.

Compared to solid-state laser, fiber lasers have a greater potential for high average power because of their better heat dissipation, due to large surface- to-volume ratio. However, the nonlinear effects, enhanced by strong mode confinement and the long fiber required for fiber lasers (typically~10m), may distort the pulses, and restrain the maximum peak power. Recently, large-mode-area fiber (e.g. photonic crystal fiber, PCF) based ultrafast lasers working in a dissipative solution regime have been demonstrated [628] for high average power ultrafast pulse generation with MW peak power (e.g. 11W average power and 1.9MW peak power from a SESAM mode-locked Yb-doped PCF laser [628]). In principle, large-mode-area fiber lasers mode-locked with GSA may deliver better performances (e.g. high average power, high peak power, system simplicity). E.g., coating GSAs on the fiber surfaces with evanescent-wave interaction can preserve the alignment-free waveguide format by removing the free-space components, necessary for traditional SA coupling. It is also possible to put GSAs inside the fiber (e.g. holes of PCFs). These integration strategies (i.e. graphene on the surfaces or inside the devices) can be applied with various lasers: waveguide (e.g. laser inscribed waveguide and polymer waveguide) and semiconductor (e.g. vertical external cavity surface-emitting semiconductor lasers and optically pumped semiconductor disk lasers) for high power/energy pulse generation.

For applications, it is not necessary to generate high average power ultrafast output only using one oscillator, as external cavity processing can easily increase the output power. For example, external amplification of graphene mode-locked lasers or coherent combination of various lasers could boost output power and energy.

D5.1.2 Spectral coverage

Operation wavelength is an important parameter. In particular, a range of applications (e.g. ultrafast PL) require resonant excitation, thus ultrafast lasers covering a broad wavelength range are attractive. Wavelength tunable or switchable lasers are another solution to access broadband spectral range. Combination of wide-band gain materials (e.g. Ti:sapphire) and GSAs could provide novel broadband tunable ultrafast sources to meet the requirement for wideband range.

The output wavelength or tuning spectral range of a traditional laser will be ultimately constrained by the gain medium. For example, Ti:sapphire typically only works between 0.65 and 1.1μm [629]. Nonlinear effects (e.g. optical parametric generation and Raman scattering) can be used to broaden the spectral range. They can provide gain covering from UV to THz.

Nonlinear frequency conversion (e.g. harmonic frequency generation, parametric oscillation and amplification, four-wave mixing, supercontinuum generation) is also useful to expand the wavelength accessibility after the oscillator.

D5.1.3 Pulse width

Shorter optical pulses can provide better temporal resolution and high-speeds (e.g. pulse widths of 200-400fs can enable 1.28TB/s optical communications). In general, solid-state lasers facilitate shorter pulse generation (e.g. 4.4-fs pulses from a Ti:sapphire laser oscillator [630]), as the shortest pulse that fiber lasers can generate is typically limited by enhanced nonlinearity [630]. Indeed, so far the shortest pulse duration for GSAs (94fs from a Cr:forsterite laser [631]) was achieved with solid-state lasers [632]. These could be shortened further by using broadband solid-state gain materials (e.g. Ti:sapphire). E.g., with wideband gain media and laser design optimization (e.g. dispersion management), graphene mode-locked lasers could generate pulses as short as those produced by any other SAs, but possibly with reduced system complexity. One of the limitations to get shorter pulses is the medium narrow gain bandwidth. Nonlinear effect-based gain has much broader bandwidth, which also supports ultrafast pulse generation. E.g., the combination of broadband Raman gain and GSAs can enable shorter pulse duration than ever before.

External-cavity methods (e.g. nonlinear compression, or coherent combining) could also be used to generate shorter pulse down to a few optical cycles (a cycle is defined as the time needed for light to travelling over a distance equal to the light wavelength) (e.g. 4.3-fs).

D5.1.4 ***Repetition rate***

The repetition rate is inversely determined by the cavity length. This means that shorter cavities permit higher repetition rates, and vice versa. Pulsed lasing with short cavities generally requires high-gain materials, low-loss cavity, and low-loss SAs. So far, multi-GHz pulse sources have been demonstrated for mode-locked semiconductor lasers (e.g. 50GHz from a 3mm SESAM mode-locked semiconductor laser [633]), and compact solid-state lasers (e.g. 157GHz from a 440μm Nd:YVO_4 laser mode-locked with SESAMs [634]). Waveguide lasers also allow high repetition rate (e.g. ~400MHz). GSAs have low non-saturable losses, which makes them suitable for short cavity lasers. Coating graphene on surfaces/facets of the cavity components (e.g. fiber, waveguide, semiconductor, monolithic solid-state materials, or mirrors) could enable compact lasers with repetition rates up to hundreds of GHz.

Another option to push the output repetition rate is to exploit harmonic mode-locking [635]. This requires complex design to achieve precisely equidistant pulses, as the fluctuations of the temporal positions of pulses from those in a perfectly periodic pulse train

(also termed timing jitter [636]) is detrimental for various applications, such as fiber-optic communication and optical sampling measurements.

D5.1.5 *Other considerations*

Solid-state lasers are superior for high pulse quality (e.g. smooth spectral profile and low chirp) ultrafast pulse generation, since other waveguide formats (e.g. fiber lasers) are subject to dispersion and enhanced nonlinear effects and have low pulse quality (e.g spectral side-band, high chirp). Waveguide-based ultrafast lasers also suffer from birefringence (as it is dependent on temperature and bending), which can be eliminated by using polarization-maintaining fibers. Unfortunately, nonlinear polarization evolution based mode-locking (the mode-locking using optical intensity dependent polarization direction rotation) cannot be applied to polarization-maintaining fibers (PMF), as the polarization in the PMF does not change with optical intensity. GSAs have potential for polarization-maintaining fiber lasers.

Fiber lasers and other alignment-free waveguide based lasers (e.g. waveguide lasers) can offer excellent beam quality even when operated at high average power, because of reduced thermal effects. In addition, they are compatible with fiber delivery, which offers flexibility in system design and use. In terms of fabrication cost, it is also comparably inexpensive to fabricate fiber lasers to meet applications with low demand on pulse energy (~1nJ), polarization, emission bandwidth, pulse quality, etc., as most fiber devices are economically available due to their mass-production for fiber-optical communications. GSAs are interesting for this type of fiber lasers, as they can further decrease the fabrication costs and reduce system complexity compared to traditional SA technologies (e.g. SESAMs).

In order to increase the damage threshold, graphene-based optical limiters need to be developed on two fronts. The first is to grow on-demand graphene with the desired characteristics, while the other is to design new optical geometries that maximize the range of protection. For instance, the use of two focal planes offers new possibilities for the optimization of graphene-based optical limiting.

The aim will also be to enhance the frequency conversion effect. Special graphene samples as large as tenth of cm for ICT applications and as small as a few mm for microchip laser applications need to be routinely produced. The combination of growth capabilities, device design and assembly, will result in products with superior performance.

The target is also to exploit the properties of graphene toward new applications and devices in the fields of quantum nano-photonics. We will develop novel devices at the interface between graphene and quantum technologies, focusing on nonlinear optical devices that operate at the single-photon level, using tightly confined surface plasmons in graphene.

D.5.2 Graphene Photodetectors

Photodetectors measure photon flux or optical power by converting the absorbed photon energy into electrical current. They are widely used in a range of devices [637], such as remote controls, televisions and DVD players. Most exploit the internal photoeffect, in which the absorption of photons results in carriers excited from the valence to the conduction band, outputting an electric current. The spectral bandwidth is typically limited by the absorption [637]. Graphene absorbs from the UV to THz [601,638,639]. As a result, graphene-based photodetectors (GPD) (Fig. 57) could work over a much broader wavelength range.

The response time is ruled by the carrier mobility. Graphene has huge mobilities, so it can be ultrafast [637]. Graphene's suitability for high-speed photodetection was demonstrated in a communications link operating at 10Gbit s^{-1} [640].

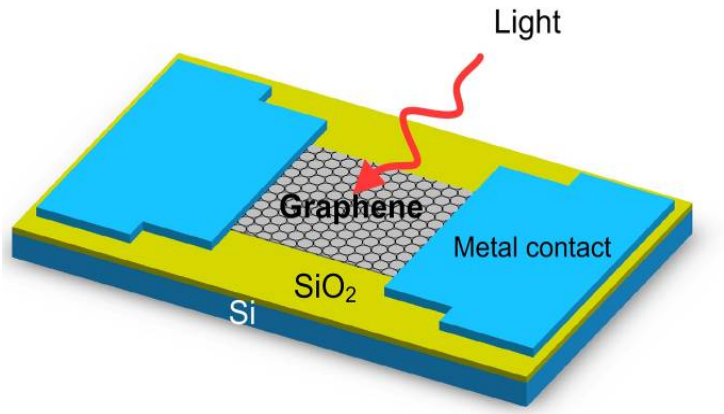

Figure 57**: Graphene-based photodetector [**Error!

The photoelectrical response of graphene has been investigated both experimentally and theoretically [640,641,642,643,644]. Although the exact mechanism for light to current conversion is still debated [642,651], a p–n junction is usually required to separate the photo-generated e–h pairs. Such p–n junctions are often created close to the contacts, because of the difference in the work functions of metal and graphene [581, 645]. Responses at wavelengths of 0.514, 0.633, 1.5 and 2.4μm have been reported [640]. Much broader spectral detection is expected because of the graphene ultra-wideband absorption. A GPD with a photoresponse of up to 40GHz was reported [644]. The operating bandwidth of GPDs is mainly limited by their time constant resulting from the device resistance, R, and capacitance, C. An RC-limited bandwidth of about 640 GHz was reported for graphene [644], comparable to traditional photodetectors [646]. However, the maximum possible operating bandwidth of photodetectors is typically restricted by their transit time, the finite duration of the photogenerated current [637]. The transit-time-limited bandwidth of GPDs could be over 1,500 GHz [644], surpassing state-of-the-art photodetectors.

Although an external electric field can produce efficient photocurrent generation with an e–h separation efficiency of over 30% [642], zero source–drain bias and dark current operations could be achieved by using the internal electric field formed near the metal electrode–graphene interfaces [640,646]. However, the small effective area of the internal electric field could decrease the detection efficiency [640,646], as most of the generated e–h pairs would be out of the electric field, thus recombining, rather than being separated. The internal photocurrent efficiencies (15−30% [642,643] and external responsivities (generated electric current for a given input optical power) of ~6.1 mA/W so far reported [640] for GPDs are relatively low compared with existing photodetectors [637]. This is mainly due to limited optical absorption when only one SLG is used, short photocarrier lifetimes and small effective photodetection areas (~200 nm [644]).

We will target the low light absorption of graphene (2.3% of normal incident light [601,647]); difficulty of extracting photoelectrons (only a small area of the p–n junction contributes to current generation); and the absence of a photocurrent for the condition of uniform flood illumination on both contacts of the device. Unless the contacts are made of different materials, the voltage/current produced at both contacts will be of opposite polarity for symmetry reasons, resulting in zero net signal [640,642,648].

The optimization of the contacts needs to be pursed both theoretically and experimentally. Other possible ways of overcoming these restrictions is to utilize plasmonic nanostructures placed near the contacts as recently demonstrated [234]. Incident light, absorbed by such nanostructures, can be efficiently converted into plasmonic oscillations, with a dramatic enhancement of the local electric field [234]. Such a field enhancement, exactly in the area of the p–n junction formed in graphene, can result in a significant performance improvement. The role of the plasmonic nanostructures is therefore to guide the incident electromagnetic energy directly to the region of the p–n junction. Thus far, plasmonic effects enabled a 20 times increase in the efficiency in hybrid GPDs [234].

Nanostructures with geometries resonant at desired wavelengths need to be investigated for selective amplification, potentially allowing light filtering and detection, as well as polarization determination in a single device at high frequencies. The frequency performance can be even improved in comparison with traditional devices, as the plasmonic structures add only negligible contribution to the capacitance (fractions of fFs), but can significantly reduce contact resistance. Further optimization (e.g., making use of coupled or cascaded plasmon resonances [649,650]) could increase the photovoltage enhancement.

The photothermoelectric effect, which exploits the conversion of photon energy into heat and then electric signal [637], may play an important part in photocurrent generation in graphene devices [642,651].

Another approach to increase the responsivity is to integrate a GPD a highly confined optical waveguide and increase the optical absorption, Fig. 58. NIR light is coupled to a Si waveguide, which is embedded in SiO_2. A graphene sheet is located on top of the Si waveguide and there is a thin isolation oxide layer in between. The fundamental TM (transverse magnetic) mode would get almost completely absorbed in the graphene, as the light propagates along the waveguide. The local field gradient at the metal/graphene interface drives a photocurrent towards the ground leads. The metal electrodes may also be replaced by poly-Si to reduce optical mode damping. The expected foot-print of such device is~30 μm^2, thus comparable to state-of-the-art Ge photodetectors, nowadays used in highly-integrated Si photonics for on-chip interconnects. The simple device geometry, less complex processing and compatibility with Si technology could make graphene indeed an alternative to other semiconductors such as Ge, even for large-scale integrated photonics.

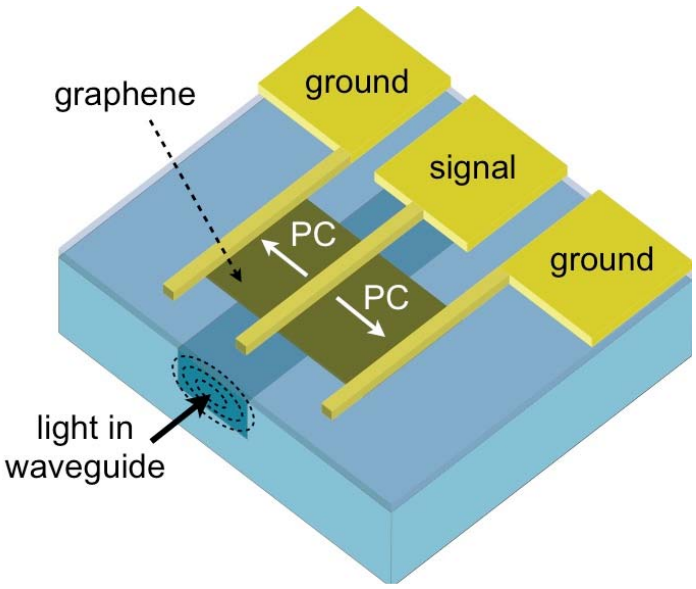

Figure 58*: Schematic of an integrated waveguide GPD*

The 2d character of graphene and the possibility of large-area fabrication allows up-scaling from single devices into arrays. This could enable a pixelated, camera-like structure, where each pixel may be read out individually. Co-integration with Si transistors as amplifying elements is envisaged. The goal is to achieve gated photodetector arrays with strongly enhanced responsivity.

The energy spectrum and optical properties of graphene can be modified through an electrostatic field. This can be utilized to realize a waveguide-integrated electro-optical modulators at 1550 nm, based on optical absorption for photon energies $2E_F <$ Eph (Eph is the photon energy, E_F denotes the Fermi energy) and absorption suppression for $2E_F >$ Eph due to Pauli blocking [602]. Graphene-based modulators can be realized on a much smaller foot-print than devices using semiconductor materials for electro-absorption or electro-refraction by the Pockels, Kerr [652] and Franz–Keldysh effects [653,654].

We will target integration of graphene electro-absorption modulators into Si waveguide ring resonators and Fabry-Perot cavities with grating mirrors, to further decrease the foot-print. This will also lead to higher modulation depth and speed than previously reported.

When it comes to high demand applications, requiring photon detection at very low levels, even approaching single photon detection, photodiodes cannot be chosen, because their

quantum efficiency is limited to unity, accounting for 1 carrier per photon. Therefore, the electrical signal suffers from read-out electronic noise, which overwhelms the photocurrent at low intensities. In view of this constraint, gain has been sought in PDs: a mechanism that can provide multiple electrical carriers per single incident photon.

Four PD classes exist that may provide for gain: photomultiplier tubes (PMTs), avalanche photodiodes (APDs), photoconductive detectors, and phototransistors. PMTs and APDs are extensively used in high sensitivity metrology. PMTs may provide a 10^5 gain, however they require the application of voltages~ hundreds V. In addition to this, PMTs are bulky devices and therefore cannot be integrated in CMOS electronics, let alone allow the development of PMT arrays for imaging applications. APDs on the other hand are solid-state detectors that exploit the phenomenon of impact ionization and carrier multiplication upon application of high reverse bias in a photodiode. APDs can provide gains~100 for applied bias~ hundreds V, whereas they yield gain~10^3 when operated in Geiger mode, with voltages exceeding 10^3 V. These extremely high voltages thus far prevented the integration in arrays for imaging.

Photoconductive detectors are based on the effect of carrier recirculation providing Ohmic contacts to the semiconductor and appropriate sensitizing centres that can prolong the carrier lifetime. Photoconductive gain is then possible, with a value given by the ratio of the carrier lifetime over the transit time. Photoconductive detectors have recently regained attention with the advent of colloidal QDs photodetectors [655]. Photoconductive gain~10^3-10^5 has been reported for PbS, ZnO or CdSe QDs [655,656,657], limited, however, by the low mobility of QD films. Phototransistors have also been proposed to provide for photoconductive gain [656]. Phototransistors may rely on the two transistor configurations of bipolar transistors or FET transistors. Recently a FET-like phototransistor has been reported with single-photon counting potential, based on a 2DEG channel and QDs as the photosensitive gate, in an epitaxially grown structure. The 2DEG was formed in an AlGaAs substrate by cooling the device at 4 K and it was critical in achieving high sensitivity due to the very high carrier mobility that can be achieved in a 2DEG.

Graphene is an excellent candidate for high-gain photodetection because the charge carriers in graphene exhibit very high mobility and since graphene is 2d. Thus its conductance is very sensitive to electrostatic perturbation by photogenerated carriers close to the surface. This makes graphene a particularly promising material for high gain photodetection by employing the photogating effect. Additionally, graphene is a very thin, flexible and durable, and can be fabricated in a large scale and easily deposited on Si, offering integration to standard integrated circuits. Thus, the demonstration of photodetection gain with graphene would be the basis for a plethora of applications such as graphene-based integrated optoelectronic circuits, biomedical imaging, remote sensing, optical communications, and quantum information technology.

We will target ultra-sensitive photodetector arrays for visible and IR imaging. These are based on sensitized graphene: a film of semiconducting particles or QDs is deposited on the graphene sheet [658], see Fig. 59. Through sensitization, strong absorption ~50-100% can be achieved. The detection mechanism is based on

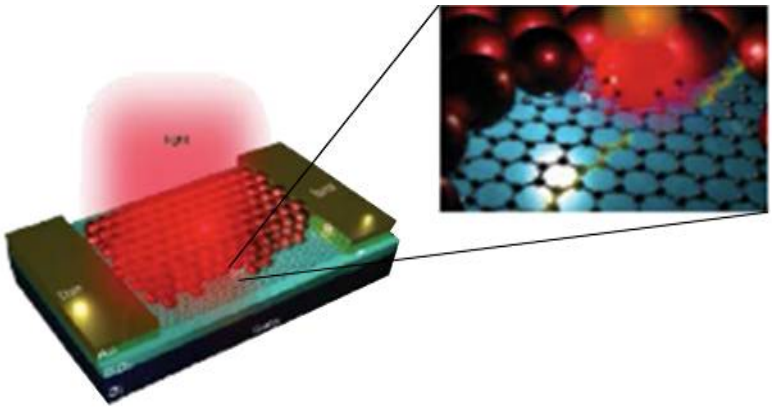

Figure 59: *Graphene-QD photodetector [658].*

photogating [659], where light induced trapped charges in the QD change the resistance of the graphene sheet. The photoconductive gain associated to this mechanism can be quantified by the ratio of the lifetime of the trapped carriers in the QD over the drift time of the charge carriers in the graphene sheet.

Applications of long-wavelength radiation are manifold. The term "long-wavelength" is here used to refer to the FIR (THz) and MIR, i.e. the wavelength range between 3 and 1000μm. Many chemical agents, explosives or narcotics feature spectral fingerprints in this range. Optoelectronic devices operating in the THz and MIR range can thus be employed in homeland-security-related applications, e.g. in security systems at airports monitoring dangerous substances, but also in environmental-related applications, e.g. gas spectrometers for air-quality control, whereby traces of threat chemicals have to be detected against a spectral background. Graphene-based systems can offer a new route towards the realization of these efficient long-wavelength photodetectors and sensors.

D5.3. *Graphene plasmonics*

Photonic technologies, based on light-matter interactions, already own a significant slice of today's markets. With the advent of nanofabrication techniques, light-matter interactions can now be studied and tailor-designed at a fundamental level. Of recent interest is the use of metallic nanoparticles (MNPs), where due to the surface plasmon resonances (SPRs) light-matter interactions are greatly enhanced and/or facilitated [660]. Indeed, the SPRs are characterized by a large extinction cross section and the electromagnetic field is amplified by several orders of magnitude in the nearby of the resonant MNPs [660]. Because of the near field focusing at the SPR, every photoelectrical activity, such as absorption and emission, gets enhanced on the MNP surface. At high enough intensity these two effects get coupled in a nonlinear manner exhibiting novel phenomena. Plasmon resonance can be tuned by acting on the shape and on the mutual interactions of the MNPs. The dynamics of the plasmon resonance is extremely fast. Furthermore, plasmonic nanostructures are usually characterized by high thermal and chemical stability and can be functionalized by chemical reactions on the surface very easily. Finally, the noble metals are excellent electrical conductors [661].

The combinations of semiconductor quantum dots (SQD) with MNP [662] allows the study of the strong coupling regime and its physics at the interface of classical and quantum mechanics, with possible applications in a broad range of fields, including quantum information, interfacing of electronic and photonic components, surface plasmon lasers, solar energy harvesting, sensors and actuators. Over the past few years, hybrid SQD-MNP structures have been manufactured in order to combine the discrete excitonic response with the strong optical response of plasmons [663]. In these structures, long-range Coulomb interaction couples the two subsystems creating hybrid exciton-plasmon excitations, resulting into Förster energy transfer, Rabi charge oscillations, nonlinear Fano resonances and bistability [663,664,665]. Surface plasmon amplification by stimulated emission of radiation, where rather than amplifying light in a conventional laser cavity a plasmonic 'spacer' amplifies it with the help of plasmons, was used to develop nanolasers [666].

Graphene is poised to make a significant impact in modern photonics applications. A large part of this will be enabled by the advent of plasmonics to enhance and facilitate light-matter interactions. Recent work has shown the benefit of MNP in graphene-based photonic applications such as graphene PVs [234] and SERS [667]. Graphene plasmons provide a suitable alternative to noble-metal plasmons due to their much larger confinement [592] and relatively long propagation distances [592], with the advantage of being highly tunable via electrostatic gating [592]. Graphene also has extraordinarily large Purcell factors [592].

Compared to conventional plasmonic metals, graphene can lead to much larger field enhancement and extreme optical field confinement [592].

The combination of graphene photonics with plasmonics, whereby the light interaction is modulated and enhanced by placing arrays of metal particles or antennas on the graphene surface, can improve the performance of existing devices, overcoming some limitations associated with the transparency of graphene in the visible-NIR. SQD-sensitised GQDs (Fig. 57) can lead to huge photovoltage enhancements [234,658]. The new field of graphene-plasmonics could pave the way towards the realization of novel sensing routes, by modulation of the metal dielectric function.

We expect graphene-MNP-SQD complexes to play an important role in future optoelectronic and quantum information technologies. The applied research in photonics and electronics will have the relevant goal of developing hybrid graphene-plasmonic devices with higher performance than equivalent non-hybrid devices. The interaction between graphene nanodisks or ribbons with metallic nanostructures can be exploited for the realization of optical switches and single photon devices [668], taking advantage of the graphene SA and the local electromagnetic field amplification induced by localized surface plasmons. Such hybrid nanostructures are promising candidates for the realization of nano-optical devices, such as ultrafast nano-optical switches, surface Plasmon-polariton amplifiers, lasers infrared detectors, single-photon quantum devices, and ultrasensitive detectors. Enhancement of energy transfer is also important in solar energy applications such as in dye-sensitized solar cells (DSSCs), where facilitation of dye-MNP interactions may play an important role in improving performance. Graphene can be made luminescent [669], thus its interaction with metallic nanoparticles can be exploited to greatly enhance and tailor its emission properties. The realization of such graphene devices containing plasmonic nanostructures will be one of the main strategies to improve the performance of photodetectors, photovoltaic systems, thin TCs and ultrafast optical components.

Moreover, sensitive photodetection in the short wavelength infrared (SWIR) enables passive night vision [670,671] from 1 to 1.7μm, and biomedical imaging for tumour detection [672], exploiting the tissue transparent windows around 900 and 1100nm [673,674]. Additional applications of SWIR imaging can be found in astrophysics [675], in remote sensing for climate and natural resources monitoring [676], in food and pharmaceutical industries for quality control and product inspection [677] and identification [678].

Sensing and imaging in the visible is currently facilitated by Si photodiodes. The first imaging arrays were based on charge-coupled devices (CCD). This approach involves the photoactive sensor array with several stages of photo-charge transfer to the read-out circuit for electronic processing. CCDs suffer high fabrication and integration cost due to multiple chip interconnections and the incompatibility of CMOS with the process required for the CCD platform. It was not until 1997 when the first integrated CMOS image sensor was reported on a single chip for light sensing and signal processing. However the fill factor is limited due to the coexistence of photoactive elements sand read- out circuitry on the same chip. For sensing and passive imaging in the SWIR the use of InGaAs photodiodes leads the market. However, MBE and MOCVD techniques, required for the growth of InGaAs have high cost. This, in conjunction with lattice mismatch of InGaAs with Si, makes InGaAs very expensive. In addition, interconnection of the light sensing InGaAs array requires complex bump-bonding techniques that increase the cost further and also limit the pixel resolution to a few hundred kpixels. A typical price for a night vision camera based on InGaAs is~20-40 k€. The competing image intensifier technology is somewhat lower cost, but the cameras are more bulky, due to the intensifier tube.

We aim to develop top-surface PDs and image sensors for visible and SWIR imaging applications. PbS colloidal QDs offer high absorption and bandgap tuneability from UV to

SWIR, and will be employed as a vehicle to demonstrate the potential of this technology. Phototransistors based on a graphene channel with a QD layer used a photogating layer. As a result, a photoconductive gain of 10^8 and responsivity of 10^7A/W can be achieved, thanks to the high mobility of the graphene channel and the long carrier lifetime of the photogenerated carriers in the QD layer. In combination with the high quantum efficiency >25% and low noise-effective-power~10^{-17} W, this hybrid QD-GPD is an excellent platform for large-scale sensitive SWIR detection.

A prerequisite for achieving these goals is the efficient modelling of the optical properties, such as extinction, absorption, and scattering cross-sections, as well as local field enhancement in the proximity of metallic nanostructures due to plasmon resonances [667,679] of these hybrid materials, in order to predict their functions and to engineer their properties. It is thus important to create a thorough understanding of the interaction between the subsystems and how their individual optical properties contribute to the formation of novel effects. We will thus target advanced computer models for the optical response of the constituent subsystems, incorporating both photonic and electronic degrees of freedom in a direct time-domain semi-classical approach both for graphene and different graphene derivatives. Finite element methods such as the Discrete Dipole Approximation (DDA) [680] and time domain methods, such as the Finite-Difference Time-Domain (FDTD) [681], represent some of the most effective and versatile solutions for modelling the optical properties of nanostructures with complex form and hybrid composition.

Another important issue that needs to be addressed is the response of molecules or SQD that are very close to the MNP or graphene surface, due to the nonlocal response of the metallic and graphene dielectric functions. This may have an important role on the actual field enhancement and energy transfer rates. We will introduce detailed models of nonlocal response in FDTD, and explore their effect on the performance of graphene-based applications. Finally, while stimulated emission is naturally inserted in the proposed scheme, spontaneous is not, and so an explicit scheme for taking it into account will also be implemented. Such a rich model inventory to describe graphene, metals and active materials will enable the detailed time-resolved simulation of novel graphene-based photonic and plasmonic devices. This modelling capability will facilitate the design of future graphene-based photonic and plasmonic applications.

The pursuit of a scalable and cost competitive production technique for such devices is the next objective. The large scale realization of hybrid devices will require versatile preparation techniques with high control on the surface of metal nanostructures. In some cases, a high degree of purity will be required for the metal-graphene contacts, while in other cases the ability to self-assemble the metal and graphene components will be needed. This can be obtained by the insertion of appropriate synthetic mediators, such as molecules anchored on the surface of plasmonic nanostructures. The control of the surface of the plasmonic nanostructures will play a key role in the realization of hybrid devices. Some devices will require ultra-clean interfaces between graphene and metal nanostructures, which can only be obtained through ultra-clean chemical free techniques of synthesis. In other cases, the creation of ordered structures on a large scale may be achieved through self-assembly of plasmonic nanostructures and graphene, which can be guided by an intermediate molecule, eventually bound to the surface of metal nanostructures by exploiting the easy surface chemistry of noble metals [682]. The laser ablation synthesis in solution of plasmonic nanostructures has the potential for fulfilling a large part of the above requirements [683].

Plasmonic metamaterials have recently been established as a versatile tool for the creation of new optical devices. Their optical properties can be controlled by changing the electric coupling of plasmonic nanoresonators. We will aim to use graphene for this purpose. The electric conductivity of graphene can be changed by several orders of magnitude using gates

operating at relatively low voltages. This will induce dramatic changes of the optical properties of the underlying metallic plasmonic nanostructure. We aim to efficiently couple graphene to plasmonic nanoresonators and to control the optical properties of such composite metamaterials using electric fields. The combination of graphene with metamaterials could result in fast, cheap and small active optical elements, for example for displays.

We also aim to efficiently couple graphene to plasmonic nanoresonators and control the optical properties of such composite metamaterials using electric fields. The active plasmonic elements will then be optimized for response time and modulation contrast. The experimental work will be accompanied and guided by simulations to optimize modulation parameters (contrast of modulation, frequency range, etc.) through the geometry of metamaterials and graphene properties. This will lead to large-area displays based on this type of elements.

Nanostructures functioning as optical antennas will be used to couple long-wavelength radiation to graphene. Due to the long wavelength, the lithography requirements are relaxed, even in the MIR. More advanced plasmonic geometries may be used to further concentrate the radiation at the metal/graphene interfaces. The detector performance will be benchmarked with conventional technologies (HgCdTe detectors, QWIPs, etc.).

Plasmonic effects in graphene itself can be exploited for resonant photoconductive detectors in the THz range. The aim is to find resonances in the photocurrent (as a function of an external parameter, such as the voltage applied to a gate) due to the confinement of the plasmon modes in a channel defined by the gate on the graphene systems. Graphene THz photodetectors can perform well up to room temperature, as recently shown [684]. In addition, these devices will also shed light on the subtle nature of plasmons in this material. The term “plasmon” in the THz related work refers to the collective density oscillations of the electron gas in graphene, not to surface plasmon polaritons, which are electromagnetic waves trapped at the interface between a dielectric medium and an electron gas supporting plasma waves.

Graphene plasmons in real space have been recently visualized [685]. By

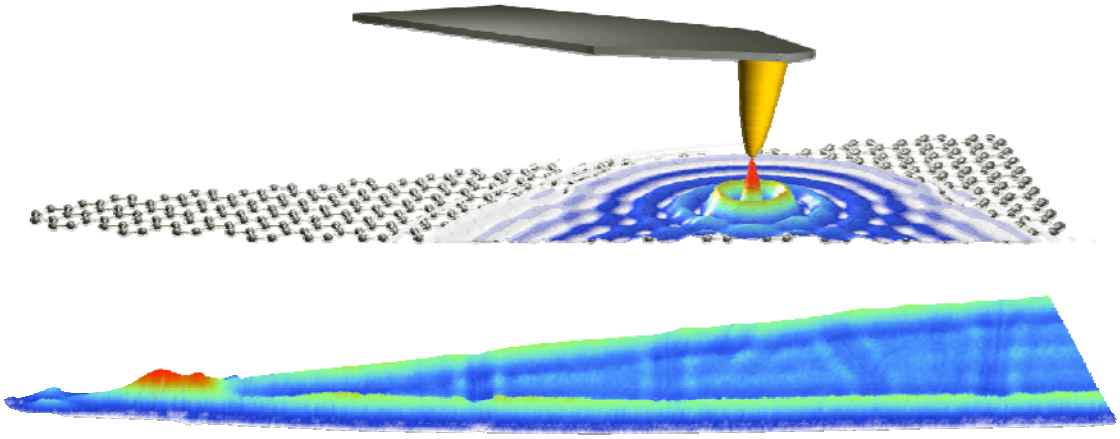

Figure 60: *Imaging propagating and localized graphene plasmons by s-SNOM. a) Schematic of configuration used to launch and detect propagating surface waves. b) Near-field amplitude image acquired for a tapered GNR on top of 6H-SiC. The imaging wavelength is λ_0=9.7um. The tapered ribbon is 12 um long and up to 1 um wide [685].*

employingscattering-type near-field microscopy (s-SNOM) the authors excited and spatially imaged propagating and localized plasmons in tapered GNRs at IR frequencies. They placed the s-SNOM metallic tip [686,687,688] over the sample while illuminating both tip and sample with IR light. The tip acts as an optical antenna that converts the incident light into a localized near field below the tip apex [688]. The nanoscale field concentration provides the required momentum [689] for launching plasmons on graphene, as illustrated in Fig. 60. Plasmon reflection at the graphene edges produces plasmon interference, which is recorded

by collecting the light elastically scattered by the tip via far-field pseudo-heterodyne interferometry [690]. The detected signal as function of tip position yields a spatially resolved near-field image with nm-scale resolution. The extracted plasmon wavelength is remarkably short: over 40 times smaller than the illumination wavelength [685]. The strong optical field confinement is exploited to turn a graphene nanostructure into a tuneable resonant plasmonic cavity with extremely small mode volume [685]. The cavity resonance is controlled in-situ by gating the graphene. Completes ON/OFF switching of the plasmon modes was demonstrated, thus paving the way towards graphene-based optical transistors [685]. This successful alliance between nanoelectronics and nano-optics enables the development of unprecedented active subwavelength-scale optics and a plethora of novel nano-optoelectronic devices and functionalities, such as tuneable metamaterials [691], nanoscale optical processing and strongly enhanced light-matter interactions for quantum devices [592] and biosensing.

From the theoretical point of view, plasmons in doped graphene have been studied by many authors [118,692]. These studies, however, employ RPA [693,694,695], a very well-known theory that has been successfully applied to normal Fermi liquids with parabolic bands in metals and semiconductors. Most of these studies focused on SLG, save a few exceptions. Recent theoretical work demonstrated that RPA misses some important physics in graphene, even in the long-wavelength limit [696]. The plasmon dispersion in this material is indeed affected by potentially large many-body effects due to “broken Galilean invariance” (BGI) [696]. The pseudo-spin texture that characterizes the ground state of the Dirac-Weyl Hamiltonian provides indeed an “aether” against which a global boost of the momenta becomes detectable. In a plasmon mode, the Fermi circle oscillates back and forth in momentum space under the action of the self-induced electrostatic field. This oscillatory motion is inevitably coupled with an oscillatory motion of the pseudo-spins [696]. Since the exchange interactions depend on the relative orientation of pseudo-spins, they contribute to plasmon kinetic energy and renormalize its frequency even at leading order in momentum.

We aim to study the impact of BGI on the plasmon energy-momentum dispersion of the electron gas in SLGs and FLGs. This can be suppressed by e.g. inserting a sufficient number of BN layers between two SLGs. Since Coulomb interactions are long-ranged, one can achieve a regime in which inter-layer tunnelling is negligible, while e-e interactions are not. The intrinsic plasmon lifetime due to e-e interactions also needs to be calculated.

The study of plasmons and magneto-plasmons in graphene will be performed by means of electronic Raman experiments. This approach has been extensively used for the investigations of plasmons and magneto-plasmons in ordinary semiconductor heterostructures [697], but its application to graphene has been limited by the absence of favourable inter-band or intra-band resonant conditions matching the energy of available lasers. Indeed, light scattering can probe magneto-plasmons and coupled phonon-magneto-plasmons in SLG.

The extension of these efforts to the study of plasmons and plasmon dispersions, in connection to the theoretical analysis discussed above, would provide new advances in fundamental understanding of graphene and will set the physical basis for the development of the THz detector technology.

Metamaterials and transformation optics provide schemes for devices such as nanoscale waveguides, and superlenses [698]. Graphene metamaterials are promising, since electromagnetic field patterns can be tailored with nanoscale resolution and ultra-high speed through gate-tunable potential landscapes.

D5.4. *Graphene based nanoantennas*

Throughout the last decades, communication has been enabled among different entities, ranging from mainframes, laptops to sensors. Along with the progressive shrinking in the size

of the devices, engineers have developed efficient communication means tailored to the peculiarities of each type of device. The resulting networks have enormously expanded the applications of the individual nodes by providing them a mechanism to cooperate. A good example of such applications is the Internet. Nowadays, nanotechnology is providing the set of tools to build nanomachines. The main issue to enable communications among nanomachines, and at the nanoscale, is that reducing the size of a classical metallic antenna down to a few hundred nm would impose the use of extremely high resonant frequencies.

Graphene-based nanoantennas (width: few nanometres, length: tens of micrometres) could be a key technology to overcome this issue, since this material supports the propagation of tightly confined SPP waves [699,700]. Due to their high effective mode index, the SPP propagation speed can be up to two orders of magnitude below the EM wave propagation speed in vacuum [701]. The main consequence is to reduce the resonant frequency of the antenna [702]. Recent works [703,704] point to THz bands at short ranges, an unexplored range which allows wireless communications, thereby enabling Graphene-enabled Wireless Communications (GWC) [508].

The particularities of wireless communications at the nanoscale, their applications, and those aspects specifically inherent to GWC, such as the THz band, require that well-established communication protocols and network architectures undergo a profound revision in order to be applied to this scenario. We must develop radically new medium access control (MAC), routing and addressing protocols along with network paradigms for GWC.

GWC will enable a variety of ICT applications. For example, GWC may enable embedding nano-antennas into multi-core processors, allowing them to scale up to thousands of cores, and overcoming the important challenge of global wiring and the associated delay. This multi-core architecture is known as Wireless Network-on-Chip (WNC).

Second, GWC may allow creating networks of small sensors that can measure nanoscale magnitudes with unprecedented accuracy. Nanosensors can measure physical characteristics of structures just a few nanometres in size, chemical compounds in concentrations as low as one part per billion or the presence of biological agents. Such networks of sensors, known as Wireless NanoSensor Network (WNSN), are, *per-se*, a new networking paradigm. WNSN require the integration of several nanoelectronic components and could be commercially feasible in 20 years from now.

Third, GWC may enable communications in any device, regardless of its size. In this context, long-awaited applications such as true Ubiquitous Computing or Programmable Matter may be possible with GWC. These applications will radically change the way in which society understands and interacts with technology, and push the boundaries of what technology can achieve to unprecedented levels.

Moreover, the flexibility of graphene coupled with the extremely high electrical conductivity [89] and high transparency [601], make it a good candidate for printed antennas on top of touch screens on smartphones. Traditionally, these types of antennas are based on ITO [705]. Furthermore, the variable resistivity can also lead to graphene's extensive use in antenna design applications, as a smart material where its conductivity can be adapted according to external stimuli. Reconfigurable antennas will be designed controlling the radiation pattern and efficiency, depending on the application. For instance, stacking several layers of graphene, and therefore making BLG or TLG structures, conductivity and bandgap could also be tuned. Therefore, graphene's properties can be tuned either by an external electric field or through an interaction-induced symmetry breaking between several layers thus leading to atomically-thin insulators or conductors.

We forecast the implementation of graphene in antennas/companies in short and medium-long term, with the following timeline. **Year 1-2**: Electromagnetic properties of graphene across the MW band with an extension to sub-THz bands will be investigated and understood.

Year 1-3: Efficient modelling tools for characterizing its MW properties, incorporating the effective medium model, quantum model and the transmission line model will be developed for industrial production of antennas. **Year 2-4**: Novel graphene based MW antennas and devices including ON/OFF switchable graphene shielding, self-mixing antennas and optically transparent devices will be studied and designed. **Year 5**: All-graphene radio with antennas and devices could be implemented and demonstrated. **Year 10**: WNC prototype. **Year 20**: WNSN will appear on the market.

D5.5. *Hybrid graphene nanocrystal devices for light emitting applications*

Shape controlled semiconductor core/shell NCs show advantageous luminescent properties [706] including high quantum yield in emission and the possibility to precisely tailor their emission wavelength by tuning the core size [707]. The organization of such NCs into ordered arrays, e.g. micro scale ensembles of laterally and vertically aligned nanorods, has been achieved, with promising optoelectronic properties [708].

Graphene will open up new horizons in terms of designing hybrid architectures consisting of light emitting semiconductor NCs [709,710] and plasmonic MNPs [711], Fig. 61. Apart from being the scaffold for complex assembly structures, graphene will contribute to the functionality due to its extraordinary electrical properties, which can be used for charge transport, but also for the modulation of the electrical interaction between metal and semiconductor nanoparticles.

The aims are: (i) fabrication of homogenous and preferably ordered NC layers on graphene, (ii) using graphene as a template for more complex NC assemblies, (iii) implementing graphene as a interface between metal NPs for plasmonics and semiconductor NCs for enhanced light emission, (iv) optimizing the graphene-NC interface for achieving efficient charge injection into semiconductor NCs while maintaining their bright emission, (iii) design of novel device architectures exploiting the flexibility of graphene.

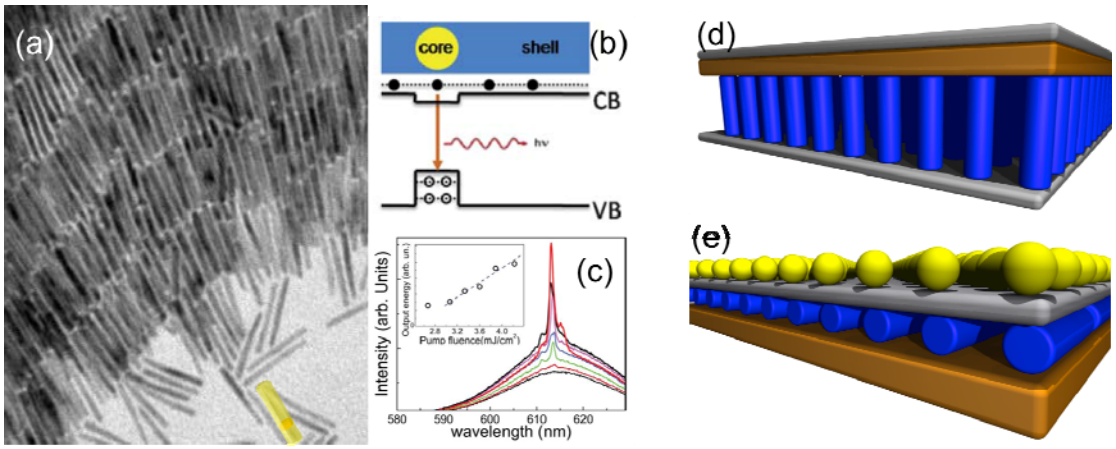

Figure 61: *(a) TEM of laterally aligned nanorods; (b) band diagram for core-shell CdSe/CdS nanorods; (c) laser emission observed from stripes of densely assembled nanorods under optical pumping; (d) Ideal stacked layer architecture with graphene (grey) as surface for nanorod assembly and electrical injection, and an additional electron or hole stopping layer (orange); (e) graphene (grey) as an interface in between plasmonic metal NPs (yellow) and semiconductor nanorods (blue) deposited onto a substrate (orange).*

In a 3 years perspective we aim at controlled fabrication of NC layers on graphene surfaces in bilayer and multilayer configurations for light emitting applications, and at efficient charge injection from graphene into the NC layer. In a 10 years perspective we

target bottom-up approaches towards graphene-NC based electrically-pumped LEDs and lasers, in which the optical gain material also constitutes the resonant cavity.

D6. Electron emission

Large-area field emission (FE) research known as "vacuum microelectronics" has been of interest since the 1970s [712,713]. Its development was initially driven by the aspiration to create new, more efficient, forms of electronic information display known as "FE displays" or "nano-emissive displays". Even though numerous prototypes have been already demonstrated [714], the development of such displays into reliable commercial products has been hindered by a variety of industrial production problems, not directly related to the source characteristics. However, after considerable time and effort, many companies are now shutting down their effort to develop this technology commercially. This is essentially connected with the huge development of both flat-panel LCD and OLED displays. Nevertheless, in January 2010, AU Optronics acquired essential FE display assets from Sony continuing the development of this technology [715]. However, large-area FE sources involve many other applications ranging from microwave and X-ray generation, space-vehicle neutralization and multiple e-beam lithography to plastic electronics.

The early devices were essentially the "Spindt array" [712], and the "Latham emitter" [716]. The first used Si-integrated-circuit fabrication techniques to create regular arrays where molybdenum cones were deposited in cylindrical voids in an oxide film, with the void covered by a counter-electrode with a central circular aperture. In order to avoid IC fabrication the Latham emitters were developed [716]. These comprise two different devices, the metal-insulator-metal-insulator-vacuum and the conductor-dielectric-conductor-dielectric-vacuum [663]. The latter contained conducting particulates in a dielectric film and the field emission is assured by the field-enhancing properties of the micro/nanostructures.

To date this research area is known as "vacuum nanoelectronics" [717,718] and is devoted towards the development/investigation of new nanomaterials that could be grown/deposited on suitable substrate as thin films with appropriate field-enhancing properties. In a parallel-plate arrangement, the field between the plates (FM) is given by FM = V/W, where V is the applied voltage and W is the plate distance. If a sharp object is grown/deposited on one plate, then the local field F at its apex is greater than FM and can be related to FM by: F = γFM. The parameter γ is called the "field enhancement factor" and is essentially determined by the object's shape. Because field emission characteristics are determined by F, then the higher γ, then the lower FM and, for a given W, the lower V at which field emission occurs.

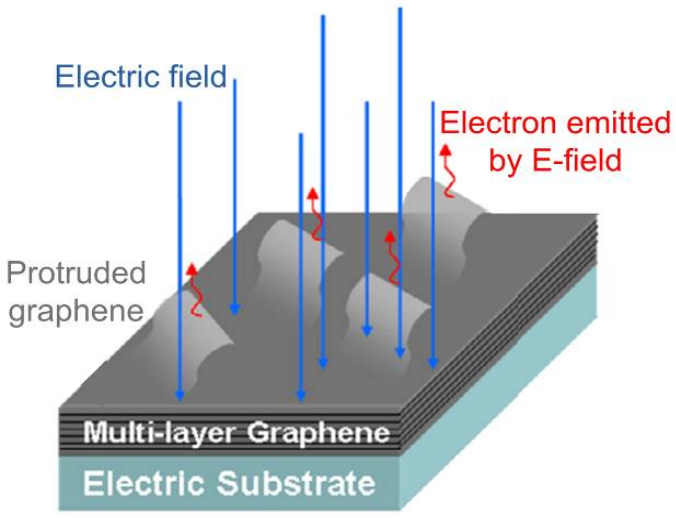

Fig. 62: *Screen-printed Graphene 'emitting device'.*

FE from amorphous and "diamond-like" carbon has been demonstrated [719,720]. The introduction of CNT-FEs [721,722,723,724] was a significant step forward, with extensive research carried out both for their physical characteristics and possible technological

applications [714]. In recent years there has also been massive growth in interest in the development of "high-γ" nanostructures, with a sufficiently high density of individual emission sites based on other carbon forms such as "carbon nanowalls" [725] and on various forms of wide-band-gap semiconductor [718]. In particular, graphene has atomic thickness, high aspect ratio (ratio of lateral size to thickness), excellent electrical conductivity, and good mechanical properties, which qualify it as an attractive candidate as FE source [726,727,728,729]. Moreover, carbon has one of the lowest sputter coefficients [730], which is an advantage as an electron source is usually bombarded by positive ions. Consequently, thanks to the aforementioned properties, a remarkably enhanced local electric field and good electron-emission stability can be expected for graphene (Fig. 62). The excellent FE properties of graphene films can also be attributed to other aspects. The presence of edges may render graphene superior to CNTs for tunnelling of electrons, being another key factor responsible for the excellent FE under a comparatively small bias [727]. Indeed, the atoms at graphene edges can have an unconventional electronic structure [731] and may form a distorted sp^3-hybridized geometry [727], instead of a planar sp^2-hybridized configuration [89], with the formation of localized states at graphene edges, with possible barrier decreasing for electron emission [727]. The orientation of graphene deposited on the substrate is another key factor for high rate FE. Indeed, graphene sheets deposited flat on the substrate surface show low field enhancement [728]. Moreover, both the interface contact and adhesion between graphene and substrate need be optimized to facilitate electron transport, and consequently improve FE performance.

The target is to position graphene as the reference material for vacuum nanoelectronics. We plan to develop new concept devices, to make graphene a key material in applications such as lighting element, high-brightness luminescent elements, FE lamps, cathode-ray lamps, X-ray-tube sources, electron sources for high-resolution e-beam instruments such as e-beam lithography machines and electron microscopes, EM guns and space applications, such as the high-precision thrusters needed for the next generation of space telescopes. However, whichever is the application, FEs work best in conditions of good ultrahigh vacuum. We have to address the problem of emission performance that is degraded by the adsorption of gas atoms. This is a common problem with all FE devices, particularly those that operate in "industrial vacuum conditions". The emitter shape and work function can in principle be modified deleteriously by a variety of unwanted secondary processes, such as bombardment by ions created by the impact of emitted electrons onto gas-phase atoms and/or onto the surface of counter-electrodes. Moreover, impurities such as oxygen, water, and organic residue are unavoidably absorbed on the graphene-emitter and the substrate during the transferring process FE chamber. The impurities could form dipole and apply an additional disturbance on local electrical field near graphene edge. The disturbance may change the local work function of the graphene edge [41]. In addition, a number of electrons emitted from the cathode could be trapped in the impurities in front of cathode, reducing its local electrical field. Therefore, the emission performance could be degraded. Emission stability, lifetime and failure mechanisms, energy spread, reduced brightness are properties that need to be addressed by the graphene consortium, seen the novelty of graphene as FEs.

The FE properties of graphene films can be further improved by optimizing the intrinsic structure of graphene, the deposition processing, and the morphology and thickness of the films. Reliable methods for the deposition of FEs graphene and/or graphene/polymer composite thin films on different substrates need to be investigated and developed opening up avenues for a variety of applications. Uniform morphology, high graphene density, and optimum graphene sheets orientation with respect to substrate surface (graphene edges normal to the substrate) will ensure emission uniformity and sufficient field-emission tips on

the film surface in order to lower the threshold fields (<1V μm^{-1}). A successful strategy could rely on the growth of vertically aligned graphene sheets

D7. Graphene for high-end instrumentation

D7.1. *Graphene for high energy physics instrumentation, Tokamaks and Stellarators*

In addition to the well-known impermeability of graphene to any gas [27] or liquid [27], some other properties of graphene, regarding radiation damage [732], may be used for high-end applications. These characteristics can be used in various fields such as containers used for nuclear repositories or high energy experiments that require ultra-low background noise. Specifically, graphene could be used as the container of Liquid Xenon in experiments searching for dark matter or double beta-decay without neutrinos. Graphene hardly contributes to the background noise due to presence of small traces of radioactive elements (radiopurity). It only around~10% of UV light, the sparkling wavelengths for Xenon when a charge particle passes through, and it is an excellent conductor, which enables the container itself to act as detector.

Another option is to the substitution of graphite as first wall in nuclear fusion reactors (as the Tokamak ITER, presently under construction). Graphite is used to prevent the injection of heavy ions, with a large number of electrons, as impurities into the plasma. These ions are the result of sputtering processes at the reactor walls. Graphite can only provide light C ions as impurities which translate into lower losses of the plasma energy.

D7.2 *Graphene for Metrology*

Quantum resistance standard

The unique existence of QHE at room temperature in graphene [89] paves the wayto using graphene as a new standard for Electric Resistance [54]. Electric resistance measurements in metrology are always referred to the Von Klitzing constant (25,812.807449 Ω) [52,733], measured in QHE experiments of semiconductors [52]. Only few large metrology Institutes have developed electric resistance standards based on QHE, due to the enormous difficulties and cost of setting up the equipment and low temperature and high magnetic field conditions required to measure the effect in semiconductors. The room temperature accurate QHE observed in graphene at lower magnetic fields would enable the realization of new QHE standard of resistance simpler and cheaper that would spread easily to any metrology institutions and calibration benches (Fig. 63). The Von Klitzing constant could also be measured in graphene and compared to semiconductors, enabling the verification of the Von Klitzing relation [52] with a quantum Wheatstone bridge.

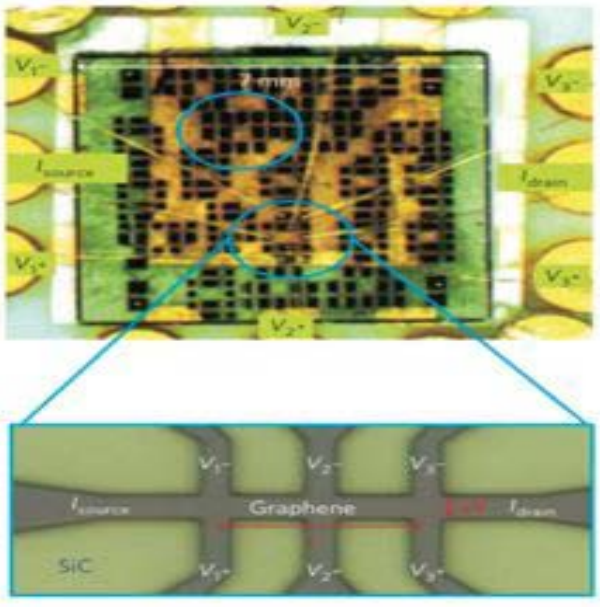

***Figure 63**: 7×7mm² wafer with 20 devices. The contact configuration for the smaller device is shown in the enlarged image [54].*

Quantum current standard

Due to the robust Coulomb blockade in GQDs, those can be used in SET nano-circuits [167,177,178]. When driven by high-frequency field applied to the metallic gates, such SETs can be operated as single electron turnstiles, which pass exactly one electron charge through the QD per each external field cycle. This enables a fundamental current standard based on charge quantization.

Standard for optical absorption coefficient

Another use of graphene in metrology is as a standard for the optical absorption coefficient (≈2.3% for SLG in visible light [601]). It is for some time now that CNTs are used in radiometry [734] and photometry. The useful property in this case is the high absorption in a broad spectral range, from UV to IR and THz frequencies. These materials are, therefore, interesting as coating in thermal detectors and this enables the measurement of optical power in spectral regions where there are not detectors based on semiconductor. The extension of these applications to graphene is straightforward.

D7.3. ***Signal processing in ballistic graphene-based devices***

The peculiar properties of electrons in SLG (their similarity to the relativistic Dirac particles) make a p-n junction in graphene transparent for electrons arriving at normal incidence [43,44]. Moreover, in ballistic p-n junctions electrons experience focusing by the n-p interface [45], which offers a new way to process signals in ballistic graphene devices, by controlling electrostatically how electrons injected by one probe focus on the other (Fig. 64).

Detection of tiny magnetic signals finds several applications. In particular, the bio-compatibility of graphene, its non-toxicity and the enhanced sensitivity due to proximity of the graphene sensor with the biological elements can be exploited in bio-technology [735]. Graphene has higher Hall resistance with respect to conventional magnetic sensors, such as InAs [740]. This coupled with the fact that graphene can sustain high current densities and is not buried beneath additional layers unlike conventional semiconductor systems, makes it a promising candidate for Hall effect sensing.

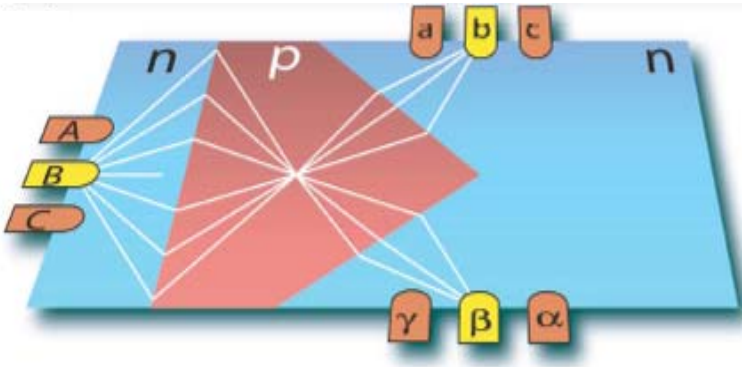

Figure 64*: Prism-shaped focusing beam-splitter in the ballistic n-p-n junction in graphene-transistor [45].*

A graphene-based tuneable magnetic sensor and an extraordinary magneto-resistance device, which relies on the magnetic field causing current flow through the device to be partially excluded from the shunt electrode which increases the non-local resistance, has already been demonstrated [736]. High mobility of carriers, as well as lower carrier density is needed to provide a larger Hall resistivity relative to the diagonal resistivity value. Graphene (especially graphene in BN/Gr/BN multilayers) can satisfy these two requirements, as well as offer devices of much smaller sizes than those possible in

conventional III-V semiconductor structures. The sensitivity of such a devices can be further improved [737], and a 26dB signal to noise ratio in a 1GHz bandwidth may be achieved.

We will target the exploitation of this effect for future magnetic field sensing devices. More importantly, the large non-local spin current near the Dirac point shows that graphene can be used in spintronics without using ferromagnetic materials to inject spin currents. This concept has been already demonstrated in a graphene-based spin capacitor [738]. The time evolution of spin polarized electrons injected into the capacitor can then be exploited as a measurement of external magnetic fields at room temperature. E.g., assuming a 100ns spin relaxation time, magnetic fields on the order of 10mOe may be detected, with measurement accuracy depending both on density of magnetic defects and spin relaxation time.

We also aim to develop graphene-based magnetometers, such as arrays of Hall nano-probes for the detections of magnetic nanoparticles, which may work as magnetic markers in biomolecules. Hall nanoprobes can also be used as non-invasive heads in scanning magnetic probes. For low temperature applications, combination of graphene with superconductors leads to Quantum Interference Devices with extreme sensitivity to magnetic flux. These can also be used to probe neural activity [739] in combination with other GFET biosensors.

D8. Graphene sensors

The exceptional properties of graphene will have huge potential for developing sensors of various types [740]. Indeed, each atom in the graphene sheet interacts directly with the sensing environment; the electronic properties of graphene can be modified by this interaction. Many different types of sensing applications will be explored, including, optical sensors, magnetic and electric field sensors, strain and mass sensors as well as chemical and electrochemical sensors.

D8.1. *Graphene mass sensor*

Nano-electromechanical (NEM) mass sensing is another viable alternative for highly sensitive devices. NEM resonators can be described as harmonic oscillators. Mass sensing consists of monitoring the shift of the mechanical resonance frequency induced by the adsorption onto the resonator of the particles. The mass of a graphene sheet is ultra-low, so even a tiny amount of deposited atoms makes up a significant fraction of the total mass. Changes in mass due to adsorbed molecules can be sensed by their effect on the resonant frequency of a membrane or cantilever [741]. Mass sensors can be fabricated from graphene membranes and cantilevers [742], with principal frequencies sensitive to changes of mass even of the order of 10^{-6} fg [743]. Circular drum structures of FLG were found to have linear spring constants ranging from 3.24 to 37.4 Nm^{-1} and could be actuated to about 18-34% of their thickness before exhibiting nonlinear deflection [744].

One application area for NEM mass-sensing is monitoring the aerosol contents in the environment, important both for public health as well as for a better understanding of climate factors. This requires that the mass and size distribution of nanoparticles can be accurately determined. While current commercial sensors can determine the distribution of particles with sizes down to~0.1μm, there is a need to find compact techniques which can accurately and conveniently determine the distribution of particles in the 10-100nm range. With an increasing need for urban areas to continuously monitor the atmospheric environment as well as the importance of companies working with nanotechnology to ensure high safety standards, such a novel detector is expected to have high commercialisation potential.

Graphene resonators also hold promise for biological and chemical analysis of very small amounts of liquid-phase solutions. A possible application is to e.g. analyse a blood solution

by detecting its different bio-molecules. For this, the solution can be electro-sprayed and the bio-molecules are sent onto a wafer with resonators [745]. In order to detect as many bio-molecules as possible, it will be important that the wafer is covered by a large array of resonators and that the surface of each resonator is as large as possible. Graphene resonators are excellent for such applications: their surface is large and their mass sensitivity is expected to be outstanding. Previously, measurements using CNT resonators [746,747,748] have achieved 0.2-1zg sensitivity (1zg=10^{-21}g), due to the low CNT mass. For the same reason, graphene resonators are expected to be outstanding resonators and already zg sensitivities have been estimated [749]. For commercial purposes, graphene resonators are more promising than CNTs, since large-scale arrays of graphene resonators have been produced [750] using top down techniques. As each resonator will have a small capture cross section, large arrays of resonators will be needed. A problem one may foresee is to multiplex the readout of such a large-scale array. An equally important problem is to establish fabrication techniques that will produce resonators with uniform and controlled parameters.

To fully assess the potential for graphene mass-sensing, we aim to establish proof-of principle integration of graphene resonators with commercially available analysis front ends. Equally important is then to tackle the problem of multiplexing large scale arrays and developing large scale fabrication methods to yield devices with small spread in parameters. For this, there is a need for research ranging from graphene resonator readout and resonator fabrication to studies aimed at obtaining an understanding of how the interactions between graphene and nanoparticles on the graphene affect resonators. Also further research on how to optimize graphene resonator properties, such as quality factor and resonant frequency will be important. If successful, the use of graphene resonators as detectors in spectrometric tools will provide a commercially sustainable means for nano-particle detection in academia, industry and society, filling an important gap in the ability to effectively detect particles in a critical and environmentally important size range.

D8.2. *Electro-chemical and gas sensors*

These sensors are widely used for environmental, security and safety, and transport-mobility applications. The main disadvantage of Si technology is the weakness of Si in harsh environments, which makes other semiconductors, such as diamond or SiC attractive alternatives. However, all these semiconductors based devices are not flexible and novel electrochemical sensing applications are calling for flexible electronics.

The use of graphene should allow an improvement of selectivity and sensitivity. However, the two main advantages would be the possibility to implement flexible sensors, using graphene as sensing layer as well as interconnect lines. Alternatively, it could also be used as a passivation/protection layer.

The main applications are as gas or contaminant sensors, pH sensors, electronic nose, lab on chip, food quality. This application requires transferable SLG or FLGs for optimal performances. For gas sensors, graphene on SiC could also be used. Good electrical properties such as high carrier mobility are not compulsory. The most critical aspect is the functionalization for optimal sensing, contacts optimization and passivation optimization.

Graphene lends itself as a strain sensor [37] and potentially also as a mass sensor with chemical selectivity. With improved edge control one may envision sensor applications which may combine physical and chemical sensing functions.

Similar to CNTs, graphene has no dangling bonds on its surface. Gaseous molecules cannot be readily adsorbed onto its surface [751]. The sensitivity of graphene chemical gas sensors can be enhanced by functionalizing graphene, for example, coating with a thin layer of certain polymers. This will act as a concentrator for gaseous molecules. The molecule

absorption will introduce a local change in electrical resistance. While this effect occurs in other materials, graphene is superior due to its high electrical conductivity (even when few carriers are present) and low noise, making even small changes in resistance detectable [752].

MoS_2 is one of the most stable layered metal dichalcogenides and has historically found applications as a dry lubricant [221] and a catalyst in the petrochemical industry. It can also form tubes [753] and fullerene-like structures [754]. Bulk MoS_2 is an indirect semiconductor [212], but quantum confinement leads to a large direct band gap (~1.8eV) in a monolayer [213]. A MoS_2 monolayer strongly emits light [213] and exhibits an increase in luminescence quantum efficiency by more than a factor of 10^4 over the bulk material [213]. This suggests applications as photostable markers and sensors.

D8.3. *Infrared sensors*

IR sensing is another hot topic in electronics, initially strongly aimed at Military systems, but with a huge number of novel civil applications.

The main advantage of graphene for IR sensing is the possibility to tune the frequency of adsorption with the electric field, sensitivity in the range 0.2-3 THz and room temperature operation. Applications such as bolometers and sensors for automotive, aerospace and telecoms will benefit from these developments

This requires transferable or epitaxial (on SiC) SLG for optimal performances. In this case, good electrical properties such as high carrier mobility are necessary. The most critical aspect concerns contacts optimization.

D8.4. *Nano-optoelectromechanical systems*

The excellent mechanical properties provided by the combination of ultrahigh Young modulus, 1TPa [27], and mono-atomic thickness, together with its unique optoelectronic characteristics, make graphene a very good candidate to implement NOEMS (nano-optoelectromechanical systems) based energy harvesting nanodevices, which convert efficiently the energy from environmental sources, as ambient noise or electromagnetic radiations (from RF to light), to mechanical vibrations. The ultralow dimensions of such graphene based nanodevices would enable mechanical compliances and resonant frequencies matching the energy levels and characteristic frequencies of non-explored energy sources arising at the nanoscale. The convenience of using non-linear MEMS as energy harvesters when the energy source is noisy, with a broadband or a low frequency spectrum, has been recently predicted based on the mechanical non-linearities of suspended GNRs.

Particularly interesting is the merging of the energy harvesting and graphene optoelectronic concepts and technologies, when envisaging the enhancement of light to nanomechanical vibrations conversion on a NOEMS device by using the high optical absorption properties of doped graphene nanostructures.

D8.5. *Microwave detectors*

MW detectors are devices used to convert amplitude-modulated microwave signals to baseband (or video) signals. To date, the current technology is based on Ge diodes because Si diodes are not ideal, due to their much higher barrier potential and consequent need of larger signals for efficient rectification.

We aim to investigate both theoretically and experimentally graphene-based MW detectors with the aim to improve the resolution of transistors for radar (W-band: 90GHz) and telecommunication applications. The mid-term target is to push the working limits of

transistors to the sub-THz domain (500-1000GHz) [684] where sensitive photon sensors are lacking both for security and medical applications. The main issues are i) the increase of mobility for larger transit frequencies, ii) the achievement of current limitation by optical phonons so as to increase the power gain, and iii) the understanding of the role of acoustic phonons which control hot-carrier temperature which limits sensor resolution.

D8.6. Fast charge detectors

Following the general trend to track, investigate and exploit elementary charge transfers in condensed matter, chemistry or biology, there is need for ultra-broad band and real time charge detectors. These are achieved today by SETs, which are ultrasensitive but bandwidth limited Coulomb blockade devices, or less sensitive quantum point contact transistors (QPC-FETs). Indeed, charge detection techniques [755] have been shown to significantly extend the experimental possibilities with QD devices. QD-based devices demonstrated the ability to measure very low current and noise levels [756].

Due to the excellent gate-channel coupling and low noise properties, graphene nanotransistors are promising route to optimize the sensitivity-bandwidth product, thus paving the way to single shot on-the-fly detection of quantum coherent devices.

D9. Thermoelectric devices

Inorganic layered compounds are promising as thermoelectric materials [757]. These are materials that can be fabricated into devices to extract electrical energy from a temperature gradient (*i.e.* waste heat). Such materials need high Seebeck coefficient, S, high electrical conductivity, σ, and low thermal conductivity, κ [757,758]. These properties are found in some layered compounds such as Bi_2Te_3. It was shown that the thermal conductivity can be suppressed by reducing the grain size [759]. The ideal way to do this would be LPE [20]. Thus LPE-Bi_2Te_3 devices could be made with figure of merit ($zT = TS^2\sigma/\kappa$) exceeding 1 (*i.e.* that required by industry). In addition, many layered materials have high S and low thermal conductivity [195]. The low electrical conductivity generally means they are unsuited to thermoelectric applications. However, since layered compounds can be exfoliated in liquids, it will be possible to blend them with nanoconductors such as CNTs or graphene. This will greatly increase σ while retaining S [757]. The challenge will be to keep the thermal conductivity at low values. To reach zT=1 with typical layered materials, σ/κ needs to increase by 3×10^8 [757]. To achieve this we will need to understand the physics of thermal transport in nanostructured disordered networks.

D10. Energy storage and generation

Storage and generation are essential for energy production and saving. Energy can be stored in a variety of ways depending upon the intended use, with each method having its advantages and disadvantages. Batteries, capacitors, and fuel cells have been used and studied for over a century to store energy. The need to develop sustainable and renewable energy sources is leading society to develop energy from sources that are not continuously available, such as Sun and wind. In addition there is a significant need to have portable energy not only for portable devices, but also for transportation to decrease the reliance on fossil fuels. Batteries and electrochemical capacitor storage devices are the most common means of storing energy, and fuel cells are also coming into their own. However, there are a number of challenges that need to be addressed in order to improve their performance and also be economically viable. Therefore, high energy electrodes are increasingly important.

The Ragone plot [760] shown in Fig. 65, plotting power against energy density, is a useful way of comparing different technologies and judge their usefulness for a particular application.

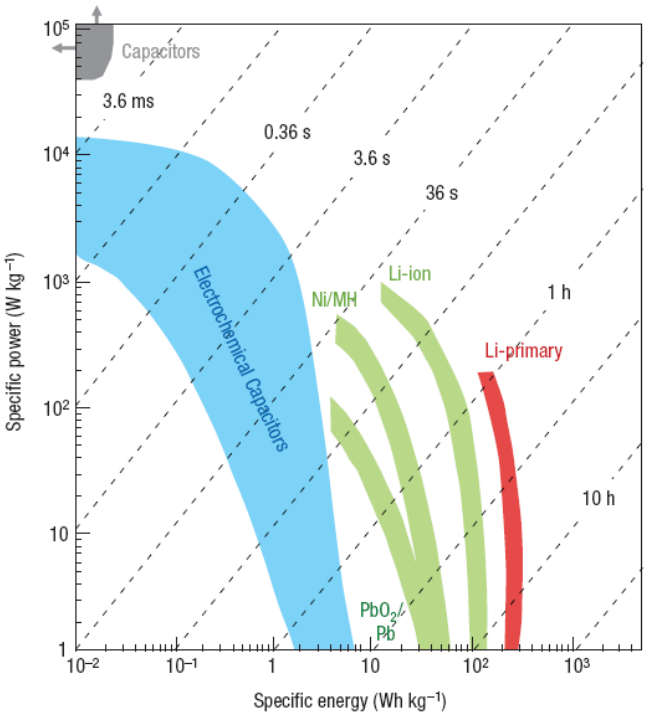

***Figure 65**. Specific power as a function of specific energy, also called Ragone plot [760], for various electrical energy storage devices.*

D10.1. *Graphene batteries*

Renewable electricity from wind, wave, tidal and solar is inherently intermittent; therefore it is imperative to seek efficient energy storage systems. Electrochemical energy storage received great attention for applications in electric vehicles and renewable energy systems from intermittent wind and solar sources. Many forms of storage are important, including large scale storage such as hydroelectric power and compressed air, as well as fly wheels and electrochemical energy storage (Li-ion batteries, redox flow batteries and supercapacitors).

At present, Li-ion batteries, using the chemistry of a $LiCoO_2$ cathode and graphite anode [761,762,763,764], are considered the leading candidates for hybrid, plug-in hybrid, and all electrical vehicles, and for utility applications. The energy density and performance of Li-ion batteries largely depend on the physical and chemical properties of the cathode and anode materials. Conventional Li-ion batteries utilize graphite as the anode. The low theoretical capacity of graphite (372mA h/g) makes it important to find alternative negative electrodes. Si (4200 mA h/g) [765] or Sn (994 mA h/g) [766] attract much interest because of their high capacity. However, their application as anodes in Li-ion batteries has been limited by their poor cycling characteristic caused by large volume changes during the repeated alloying and de-alloying process with Li. The search for suitable cathode and less passivated anode materials has proved challenging. The possibilities for the improvement of cathode materials are quite limited due to the stringent requirements such as high potential, structural stability, and inclusion of Li in the structure [767,768]. Many potential electrode materials (e.g., oxide materials) in Li-ion batteries are limited by slow Li-ion diffusion, poor electron transport in electrodes, and increased resistance at the interface of electrode/electrolyte at high charge/discharge rates [763,764]. To improve

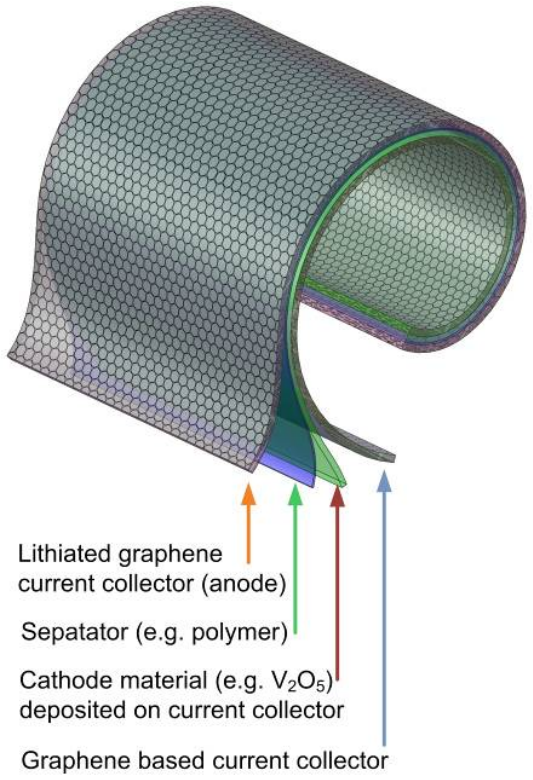

Figure 66: *Schematic of graphene based flexible thin film Li-ion battery*

the charge-discharge rate performance of Li-ion batteries, extensive work focused on improving Li-ion and/or electron transport in electrodes [769]. The use of nanostructures (e.g., nanoscale size or nanoporous structure) has been widely investigated to improve Li-ion transport in electrodes by shortening the Li-ion insertion/extraction pathway [769,770].

Table 5: *Summary of graphene-based batteries.*

Material	Surface Area (m^2/g)	Performances Discharge/charge capacity Current density	[Ref]
RGO-SnO_2 composite	N/A	Discharge and charge capacities of 2140 and 1080 mAh/g, and 649 mAh/g capacity after 30 cycles	[771]
RGO-Fe_2O_3 composite	N/A	Discharge and charge capacities 1693 and 1227 mAh/g (normalized to the mass of Fe_2O_3 in the composite), and 1355 and 982 mAh/g (based on total mass of composite)	[772]
Carbon coated GO-SnO2	N/A	757 mAh/gm after 150 cycles with 200 mA/gm.	[773]
GO and graphene film transferred on Cu foil	GO 275; N-doped 290 B-doped 275	680 mAh/g after 10 cycles with 100mA/gm. ~500 mA h/g after 40 cycles.	[774]
GO mixed with $Mn(No_3)_2$, carbon black and PVDF coated on Cu foil	N/A	770 mAh/gm at 100mA/gm after 90 cycles OR at 202 mA h/g with 5A/gm.	[775]
Graphene/superp/PVDF hybrid electrode	N/A	>1040 mAh/g at 50 mA/gm for both N and B doped graphene. 199 mA h/g at 25 A/gm N doped graphene 235 mA h/g at 25 A/gm B doped graphene	[776]
Commercial graphene nanosheet (GNS)	N/A	Specific capacity of GNS 540 mAh/g. increased to 730 mAh/g and 784 mAh/g, by incorporation of CNTs and C60	[789]
RGO electrode	186 (RGO) 590 (starting GO)	Specific capacity 15000 mAh/g	[777]
RGO electrode	N/A	Discharge and charge capacities of 2179 and 955 mAh/g for graphene, 1105 and 817 mAh/g for Co_3O_4 and 1097 and 753 for Co_3O_4 /graphene composite	[778]
CVD Graphene	N/A	Reversible discharge capacities of 0.05 and 0.03 mAh/cm^2 for pristine and N-doped graphene respectively.	[779]
Hybrid electrode graphene/Super-P/TFE	Up to 900	N/A	[780]
1) RGO electrode 2)Graphene-PANI composite	N/A	RGO: Specific capacity~820 mA h/g. Irreversibile capacity loss (685 mA h/g) Graphene-PANI composite: Specific capacity~800 mAh/g. Irreversible capacity loss (545 mA h/g).	[781]
Reduced GO (via pyrolitic and E-beam) electrode	N/A	GO: 758 and 335 mA h/g discharge and charge capacity Pyrolitic reduction:1544 and 1013 mA h/g E-beam reduced GO:2042 and 1054 mA h/g, respectively	[782]
CMG electrode	N/A	Discharge capacity~528 mAh/g. Discharge capacity~298 mAh/g for CMG electrode. Specific energy density of 1162 W h kg^{-1}	[783]
RGO electrode	N/A	Specific capacity~945 mAh/g in the initial discharge. Reversible capacity~ 650 mAh/g. Specific capacity~460 mAh/g after 100 cycles.	[784]
GO/ TiO_2/Super p hybrid electrode	N/A	Specific capacity of the hybrid material of 87 mAh/g (35 mAh/g for rutile TiO_2 only); specific capacity of anatase TiO_2/graphene of 96 mAh/g (compared with 25 mAh/g of anatase TiO_2). Graphene only initial capacity of 100 mAh/g,	[791]

In addition, a variety of approaches have also been developed to increase electron transport in the electrode materials, such as conductive coating (e.g., carbon [785,786,787]). Graphene may be the ideal conductive additive for hybrid nanostructured electrodes. Other advantages include high surface area (theoretical value of 2630m^2/g) [788] for improved interfacial contact and potential for low manufacturing cost.

High-surface-area graphene sheets have been studied for direct Li-ion storage [789]. In addition, graphene has been used to form composites with SnO_2 for improving capacity and cyclic stability of anodes [790]. Graphene was also used as a conductive additive in self-assembled hybrid nanostructures to enhance high rate performance of electrochemical active materials [791]. See Table 5 for details.

Graphene as hybrid system with VO_5 could be used as cathode to fabricate flexible, thin film Li-ion rechargeable batteries, Fig. 66. Here, graphene can act as the flexible current collector, replacing traditionally used Al, offering additional volumetric capacity, electrochemical stability and mechanical flexibility. In addition, free standing or substrate bound, electrochemically lithiated graphene, can be used as anode.

Graphene may also be used in other energy storage systems as current collector. In this case, free standing or substrate bound graphene films with very high accessible surface area to volume ratio could replace traditional activated carbon materials in the cathode and as current collectors in transparent devices.

Layered TMDs, TMOs and trichalcogenides are promising alternative materials for Li-ion batteries. The weak van der Waals interaction between the layers will allow ions to diffuse without a significant increase in volume expansion. Studies are still at a very preliminary stage and several points such as reversibility, electrochemical stability under high applied voltages (as limited by stability of electrolyte) and high temperature conditions and reactivity with Li upon insertion and removal need to be addressed.

We envisage that many of these issues will be resolvable with the use of hybrid systems, where selectively chosen layered TMDs, TMOs and trichalcogenides can allow for reaction at all contact points between the cathode active material and the electrolyte, rather than at ternary contact points between the cathode active material, the electrolyte, and the electronic conductor (such as carbon black). This will minimizes the need for inactive conductive diluents, which take away from the overall energy density.

D10.2. Graphene supercapacitors

A supercapacitors consists an electrochemical double layer capacitor (EDLC), made of two electrodes and an electrolyte, similar to a traditional battery. The EDLC performance is determined by a combination of a high surface area material and a very small charge separation. In addition the material should have high electrical conductivity, good corrosion resistance, controlled structure, high temperature stability and must be easily processed and incorporated in a composite structure. Graphene is an ideal choice for this [26].There are a number of reports on graphene materials for EDLCs, with the primary objective to demonstrate the capability of graphene as well as develop a low cost material.

The way to optimize performances is by i) maximising the electrode active surface areas; ii) decreasing the electrode thicknesses; iii) increase the operating voltage window; 4) use materials with high conductivity and/or high dielectric constant (the latter especially important for pseudo-capacitor electrodes) [792].

Apart from the mere optimization of the parameters involved in the process, one of the most crucial challenges is the poor mechanical and thermal stability of materials used in current technologies. In fact, the accommodation of ionic species in the charging/discharging process is usually accompanied by enormous volume changes in the host electrodes. The

mechanical strain generated during these continuously repeated processes leads to cracking and crumbling of the electrode materials and loss of capacity over the course of a few cycles.

Graphene, related 2d crystals and hybrids can significantly change electrode and electrolyte properties, and consequently their performance for energy storage and conversion. There are several potential advantages associated with the development of supercapacitors based on these nanomaterials. First, the use of thin layers of conductive TMDs, TMOs and graphene will reduce the electrode thickness and increase the surface area of the active units. Exfoliated TMO (or hybrids graphene-TMOs) will be ultra-thin (capacitance and thickness of the electrodes are inversely proportional), conductive, with high dielectric constants.

The dielectric constant measures the extent to which a material concentrates electric flux. As it increases, the electric flux density increases. This enables objects of a given size, such as sets of metal plates, to hold their electric charge for long periods, and/or to hold large quantities of charge. Intercalation of ions between the assembled 2d flakes and within the thin layers will be also achievable, providing pseudo-capacitance. Moreover, the use of nanostructured thin layers of oxides in supercapacitor electrodes will offer the potential for enhanced volumetric capacitances (up to an order of magnitude higher than with the much less dense carbons currently used).

Table 6*: Summary of graphene-based supercapacitors*

Starting Material	Surface Area (m^2/g)	Specific capacitance and notes	[Ref]
RGO	705	EDLC ultracaps based on CMG-based carbon electrodes. Specific capacitance of 135 and 99 F/g in aqueous KOH and organic electrolyte	[788]
RGO	3100	Specific capacitance of 166 F/g, corresponding volumetric capacitance of 60 F/cm^3	[799]
1) Mesoporous Carbon capsules (MCCs) 2) Microwave exfoliated GO 3) ChemRGO	1500	Specific capacitance MCCs: 134 F/g Microwave exfoliated GO: 41 F/g ChemRGO: 25 F/g (Supercaps with same ionic liquid electrolyte)	[793]
RGO/poly(ionic liquid)	N/A	Specific capacitance~187 F/g	[800]
Electrolyze GO suspensions with lithium perchlorate	N/A	Double layer capacitaor with capacitance/surface area = 240-325 uF/cm^2 10^4 to 1Hz and a phase angle of -84 degrees. Used for AC line filtering	[794]
MnO_2 nanorods electrodeposited onto CNPs	N/A	Specific capacitance: 389 F/gm. Flexible, non-transparent, solid state capacitor.	[801]
RGO	12.7	Specific capacitance 210 F/gm with 0.3A/g discharge rate, or 170f/gm, with 6A/gm discharge current. conductivity of G-PNF is $5.5x10^2$ S/m.	[795]
LPE graphene	N/A	Specific capacitance: 315 F/gm maximum power density~110 kW/kg, energy density~12.5Wh/kg	[796]
RGO	107	Specific capacitance: 31F/gm (24.5F/gm after 1000 cycles) Energy density 30.4 Wh/Kg (GO-MnO2)	[797]
Hybrid electrode graphene/Super-P/TFE	N/A	Specific capacitances 100-250 F/g at a high current density of 1 A/g Energy density 85.6 Wh/kg at 1 A/g at room temperature, 136 Wh/kg at 80 °C	[803]
RGO	320	Specific capacitance of 205 F/g, 170 F/g (~90%) after 120 cycles. Energy density of 28.5 Wh/kg in KOH aqueous electrolyte solution.	[802]

The capacitance at an oxide electrode comprises in fact both double layer and pseudocapacitance (Faradaic) contributions. Both specific surface area of the electrode material, and the potential for charge transfer with possible intercalation/de-intercalation are relevant variables controllable by tailoring the TMOs.

Recent works have shown the possibility to develop graphene-based supercapacitors with high performances [788,798,799,800,801,802], *i.e.* outperforming existing supercapacitors based on activated carbon, see Table 6. Some report graphene-based supercapacitors with energy density comparable with that of Ni metal hydride batteries [803].

A major challenge is to bridge the performance gap between Li-ion batteries, LIBs and EDLCs by developing technologies that can take advantage of both devices. Hybrid supercapacitors, HSC, offer a solution to this problem by combining a capacitive electrode (power source) with a Li battery-like electrode (energy source). The present level of energy/power densities in HSC, as well as their safety, cyclic life and charging performance, are far below the levels required to power demanding systems. The aim is to address these challenges simultaneously by fabricating the next generation HSC based on graphene-core/Metal oxide-shell nanostructured electrodes. The key will be the alignment of graphene sheets to form a hierarchically layered structure on the microscopic level. Two strategies will be followed for the production of highly-aligned graphene sheets. The first will rely on MWCVD, while the second will involve layer by layer solution-based deposition. The vertically aligned graphene sheets would have several distinct advantages over those with random dispersion: 1) much higher electrical and thermal conductivities; 2) larger surface area for interaction with active material, Li ions and electrolytes; 3) better control of volume expansion, etc., all of which give rise to drastically enhanced electrochemical properties and safe operation. The specific tasks include (a) precise synthesis and full characterisation of aligned graphene core/metal oxide shell architectures; (b) establish correlations between the compositional, structural, electrical and ionic properties of core/shell electrodes; (c) develop high energy density, superior power capability and stable lifespan HSCs devices.

The development and implementation of a new generation of supercapacitors based on graphene/2d materials will target: 1) power electronics systems to improve operation efficiency, in particular electrical power delivery and propulsion systems (minimization of energy losses, power quality improvement, DC power transmission, etc.; 2) power electronics systems for efficient renewable energy sources and integration in power grid; 3) power grid equipment to provide efficient operation in power production system and “smart grid”; 4) electric vehicles, in particular electric buses and commercial electric vehicles employing energy efficient electric & hybrid vehicle propulsion systems; 4) remote, GSM based, systems to monitor and control power electronics controlled drives (ASD), etc.; remote control and monitoring systems of distributed industrial objects based on Wide Area Networks (Internet/Extranet) and wireless communication (GSM).

D10.3. *Graphene fuel cells*

A fuel cell is a device that converts the chemical energy from a fuel into electricity through a reaction with oxygen or another oxidizing agent [804]. Hydrogen is the most common fuel [805]. Fuel cells are different from batteries and supercapacitors in that they require a constant source of fuel and oxygen to run, but they can produce electricity for as long as these inputs are supplied. There are many types of fuel cells, but they all consist of an anode (negative side), a cathode (positive side) and an electrolyte that allows charges to move between the two sides of the fuel cell. Electrons are drawn from the anode to the cathode though an external circuit, resulting in a current.

Fuel cells can have numerous applications, in vehicles, power backup systems, mobile phones, smart textiles (embedding digital computing components and electronics), providing a durable supply of electricity. E.g., flexible electronics still suffers from the absence of a continuous source of electricity. However the integration of fuel cells into flexible electronics needs flexible films as electrodes.

Graphene, related 2d crystals and hybrids can also be exploited for the production of clean fuels, such as H_2, as cost effective, renewable energy proces. Photocatalytic splitting of water into H_2 and O_2 using semiconductor-based heterogeneous systems promises to be one of the simplest and most economical methods for H_2 fuel production. A major limitation is the lack of stable semiconductor photocatalysts that can carry out the water splitting in the visible region of the solar spectrum, with high conversion efficiency. Stable efficient and visible light driven photocatalysts can be created by using chemically derived graphene as a support for chalcogenide nanocatalysts. The presence of graphene will serve several purposes. It is expected that its layered structure will not only suppress the semiconductor particle growth, but it will also act as an electron collector and transporter to efficiently lengthen the lifetime of the photo-generated charge carriers.

We plan to use DFT to investigate the structural, electronic and vibrational properties of graphene-based hydrogenated systems, and their dynamics. GNRs sculpted in a fully hydrogenated matrix (graphane) are thermodynamically stable up to ~1000K, and with more regularly saturated edges than their free-standing counterparts. They have tuneable semiconductor properties [806] (Fig. 67a).

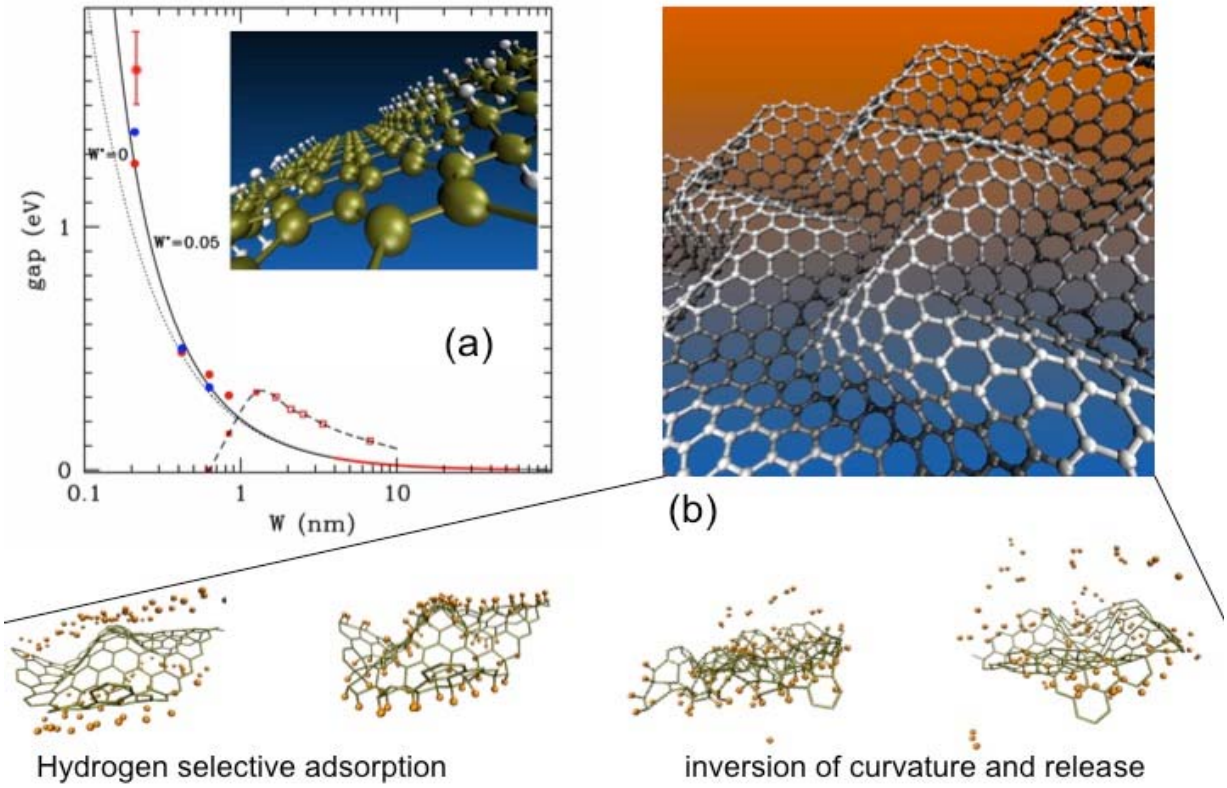

Figure 67*: Graphene-based hydrogenated systems. (a) Electronic properties of graphene-graphane hybrid. Gap value dependence on GNR width in graphane. (b) Corrugated graphene sheet by lateral compression and illustration of controlled hydrogen adsorption and release by curvature inversion [807].*

An extensive study of the properties of a multilayer graphene system corrugated by external compression shows that the hydrogen chemisorption binding energy linearly depends on the local curvature of the graphene sheet [18,807]. MD simulations show that hydrogen

preferentially attaches on concave sites [18,807]. If the local curvature is inverted by *ad-hoc* external fields, hydrogen spontaneously detaches from concave sites. This suggests the possibility of designing a device exploiting the control of corrugation of for efficient hydrogen storage. We thus aim to investigate possible ways for practically achieving corrugation control in graphene, as well as the possibility of using mechanical and vibrational excitation to control adsorption and release of hydrogen.

D10.4. Graphene solar cells

The direct exploitation of solar radiation to generate electricity in PV devices is at the centre of an on-going research effort to utilize the renewable energy. Si is by far the most widely used absorber and currently dominates the PV market [808], with η up to ~25% [809].

Despite significant development over the past decades [810], the high cost of Si-based solar cells is a bottleneck for the implementation of solar electricity on large scale. The development of new materials and concepts for the PV devices is thus fundamental to reduce the overall PV production and to increase efficiency. The latter is crucial in view of applications in mobile devices that have a limited surface area.

Thin film solar cells such as amorphous silicon (a-Si) [811], cadmium telluride (CdTe) [812], copper indium gallium diselenide (CIGS) [813] and thin film crystalline Si are known as second generation PVs. The development of thin film solar cells has been driven by the potential of manufacturing costs reduction. An even cheaper and versatile approach relies in the exploitation of emerging PVs such as organic photovoltaic cells [814] and DSSCs [815]. They can be manufactured economically compared with Si cells, for example by a R2R process [816], even though they have lower energy conversion efficiency. An organic photovoltaic cell relies on polymers for light absorption and charge transport [814]. It consists of a TC, a photoactive layer and the electrode [814]. DSSCs use an electrolyte (liquid or solid) as a charge-transport medium [815]. This type of solar cell consists of a high-porosity nanocrystalline photoanode, comprising TiO_2 and dye molecules, both deposited on a TC [815]. When illuminated, the dye captures the incident photon, generating e–h pairs. The electrons are injected into the TiO_2conduction band and then transported to the counter-electrode [815]. Dye molecules are regenerated by capturing electrons from the electrolyte.

Graphene, thanks to its exceptional mechanical, electronic and optical properties can fulfil multiple functions in PV devices: as TC window, antireflective layer, photoactive material, channel for charge transport, and catalyst [306]. GTCFs can be used as window electrodes in inorganic [817], organic [304] and DSSCs [574], see Fig. 48a,b,c. The best performance achieved to date has η≈ 1.2% using CVD graphene as the TC, with Rs=230Ω/□ and

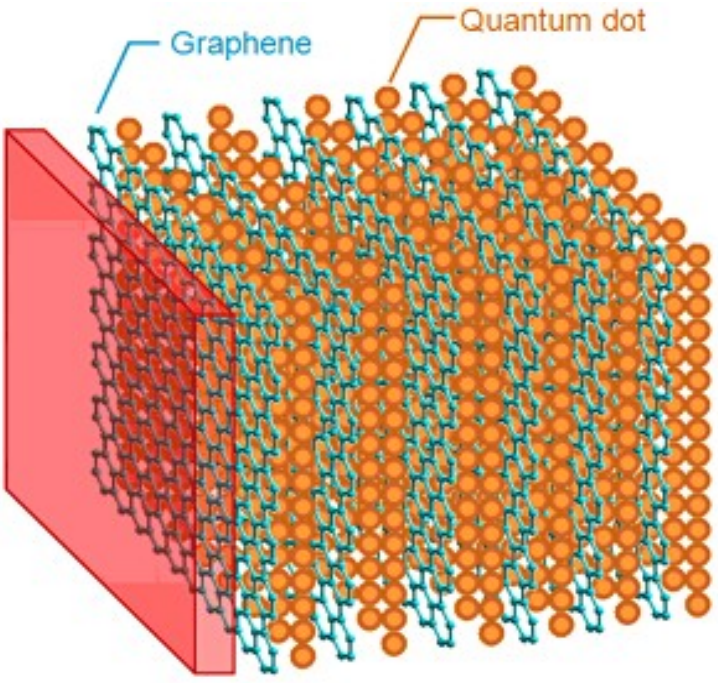

***Figure 68**: Multilayer structure solar cell.*

T=72% [818]. Further optimization is possible, considering that GTCFs with Rs=30Ω/□ and T=90% have been reported [4] and graphene-hybrid structure has shown even better results (Rs 20Ω/□, T=90%) [572].

GO dispersions were also used in bulk heterojunction PV devices, as electron-acceptors, with η~1.4% [819]. η ~12% should be possible with graphene as photoactive material [820].

Graphene can cover an even larger number of functions in DSSCs [306], as for the case of SWNTs, but without the need for sorting strategies [821]. Other than as TC window [574], it can be incorporated into the nanostructured TiO_2 photoanode to enhance the charge transport rate, preventing recombination, thus improving the internal photocurrent efficiency [822]. η~7%, higher than with conventional TiO_2 photoanodes in the same experimental conditions was reported [822]. GQDs with tuneable absorption were designed, and shown to be promising photoactive materials in DSSCs [410]. Further optimization is required for optimum adsorption of these molecules with the TiO_2 nanoparticles by covalently attaching binding groups in order to improve the charge injection.

Another option is to use graphene, with its high specific surface area [28], as substitute for the Pt counter-electrode. A hybrid poly(3,4 ethylenedioxythiophene): poly(styrenesulphonate)PEDOT:PS)/GO composite was used as counter-electrode, getting η~4.5%, comparable to η~6.3% for a Pt counter-electrode tested under the same conditions [823], but now with a cheaper material. More importantly, it was also shown that graphene can be used to replace simultaneously both Pt as catalyst, and the TC electrode [824]. A fundamental step forward towards DSSC cost reduction and large scale integration.

We will target the implementation of graphene in different types of solar cells. This will facilitate their use in a wide range of applications, ranging from mobile devices, printed electronics, building technologies, etc. E.g., in mobile phones, apart the improvement of energy storage devices, with reduced size and weight and with longer and more stable performance, the development of more efficient energy harvesting methods could bring to completely autonomous devices. Graphene maintains its properties even under extreme bending and stretching conditions. This is ideal for its integration in polymeric, rigid and flexible substrates, for the integration in smart windows and other building components. This increases fabrication flexibility, in addition to having economic advantages.

Graphene-plasmonics is also expected to have a role in PV devices, where the efficient electric field concentration of metallic nanoparticles can increase the light-harvesting capacity of graphene by more than an order of magnitude [234].

We propose to a multilayer structure solar cells (see Fig. 68) with graphene and QDs to achieve total light absorption, thus higher efficiency. A multilayer structure heterojunction, based on QDs (MoS_2, WS_2, CdS, PbS, ZnS, etc.) alternating with graphene conductive layers, or coupling a standard DSSC with a Graphene/MoS_2 (or WS_2) tandem solar cells. The aim is to overcome the power conversion efficiency of state of the art solar cells extending the efficiency beyond the Shockley–Queisser limit [825] (~30% for a single junction device) by using multiple sub-cells in a tandem device. Ideally, the sub-cells are connected optically and electrically and stacked in band-gap decreasing order. The cell with the largest band gap is the top absorber. This configuration shifts the absorption onset of the complete device towards longer wavelengths. In addition, high energy photons are converted more efficiently since thermalisation losses of the generated e-h pairs are reduced with the graded band gap structure. e.g., in a series-connected double-junction device, the ideal optical band gaps are~1.6–1.7eV for the top cell and~1.0– 1.1eV for the bottom cell, which extends the efficiency limit to~45% [826].

Our aim is also cost reduction. Fig. 69 reports the estimated cost of DSSCs based on graphene compared with conventional solar cells.

We also propose a hybrid structure graphene/nanodiamond [827] for advanced solar cells

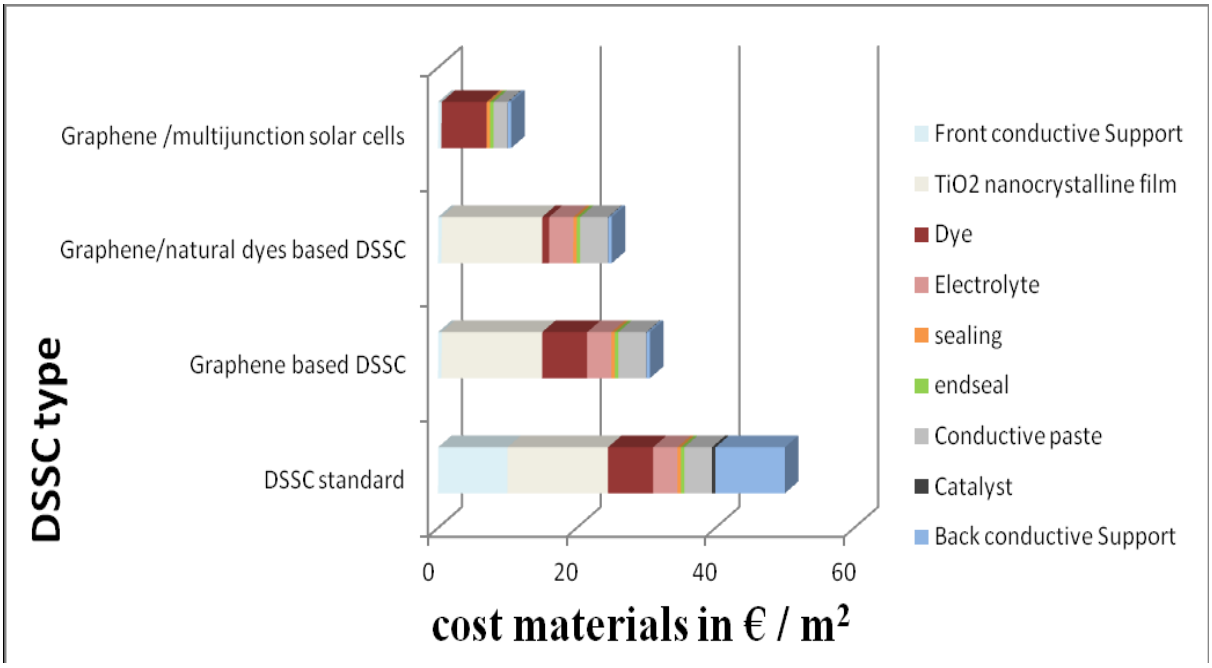

***Figure 69**: Comparison of production costs of different DSSCs. Graphene/multi-junction solar cell has an estimated cost that is roughly 1/5 with respect the standard DSSCs.*

[828], motivated by the extraordinary properties of both materials, and possible interactions between sp^2 and sp^3 carbon materials. The <111> diamond surface could form an ideal interface for heteroepitaxial graphene, with about 2% mismatch. The armchair diamond rings on the<111> surface can be interfaced to 6-membered C rings of graphene. There are several impacting interests in these interfaces. Un-doped nanodiamond could serve as an ideal gate insulator in hybrid diamond-graphene devices. On the other hand, a controllable functionalization of nanodiamond can be used to tune graphene mobility and work functions other than the optical properties. This can be achieved by coupling graphene, using organic chemistry routes via tailored design linkers with functional properties, to nanodiamond. In these solar cells, conductive B-doped nanodiamond serves as anode, while graphene acts as a cathode. If donor-acceptor organic dyes are used for such interfacing, the proposed full carbon structure has advantage in highly effective charge transfer from the HOMO of the organic dye to diamond valence band and in a reversed process on the graphene/ LUMO side.

We will tailor and prepare variously coupled interfaces studying fundamental properties of charge transfer and electrical transport properties: graphene – intrinsic nanodiamond –B-doped nanodiamond heterostructures.

Another approach is the use of chemically synthesized GNRs and/or GQDs sensitizers in solar cells. GQDs have been synthesized with molar extinction coefficients about one order of magnitude larger than inorganic dyes (*i.e.* Ruthenium complexes) [829] and absorption band edge extended beyond 900nm [829]. The next step requires the optimization of the production strategy with the goal of a perfect integration in PV devices.

E. Composite materials, paints and coating

Graphene–based paints can be used for antistatic, EMI (electromagnetic interference) shielding, conductive ink, and gas barrier applications. In principle, the production technology is simple and reasonably developed with most of the graphite mining companies having programs on LPE graphene. In the next few years major developments would be made

in the area of chemical derivatives of graphene in order to control conductivity and optical opacity of the final products.

Graphene, being an extremely inert material can also act as a corrosion barrier. Given that it can be grown directly on the surface of practically any metal under the right conditions, it could form a protective conformal layer, *i.e.* it could be used on rather complex surfaces. However, given that it might be difficult to precisely control the number of layers, the chemical properties of SLG/BLG/TLG would need to be accessed. High growth temperature might become the show-stopper both in technological and economic terms.

While the addition of CNTs to polymer matrices has already been shown to improve mechanical, electrical and thermal properties [830], the challenge is now to exfoliate graphite to SLG in large quantity to be used as an inexpensive and feasible substitute to CNTs. It was demonstrated that incorporation of well-dispersed graphene-sheets into polymers at extraordinarily low filler content results in remarkable impact on the mechanical properties of the polymer [21,22].

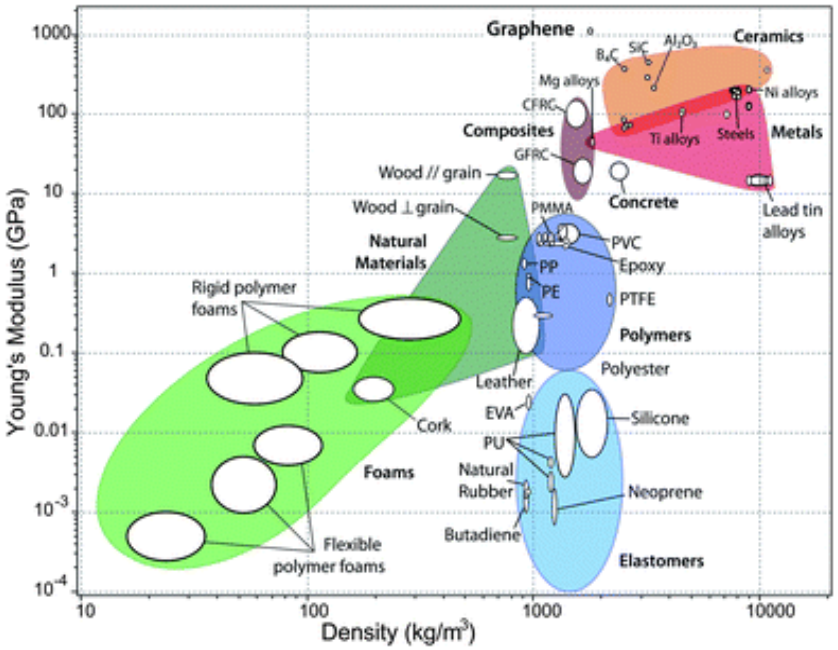

***Figure 70**: Chart of Young's modulus as a function of density comparing graphene properties to more traditional materials. Note the axes are in logarithmic scale. Graphene density was taken as 2200 kg m^{-3} [848].*

The possibility of creating both structural and functional systems is feasible for graphene filled nanocomposites due to the larger specific area and improved interfacial adhesion [298]. The mechanical properties of graphene were measured by nanoindentation using an AFM, obtaining a Young's modulus of 1TPa and fracture strength of 130GPa [9]. Meanwhile, an elastic modulus of 0.25TPa was obtained for CMG monolayers through tip-induced deformation experiments [831]. As a comparison, Fig. 70 compiles the Young's modulus and densities of several materials.

Graphene-based polymer nanocomposites and graphene-nanometals-polymer hybrids will provide improved mechanical properties and engineered electrical and thermal conductivity, fundamental characteristics for avionic/space and homeland security applications.

In real applications, graphene layers composed of different crystalline sheets could be used, even if with worse properties with respect to the ideal, defect-free, SLG. Charge and heat transport are perturbed at inter-sheet domain boundaries, edge defects act as electronic traps, and different sheets easily split apart under mechanical stress, causing device malfunctioning or failure. Furthermore, while record properties can be obtained for isolated graphene, for real world applications graphene will have to be either deposited on or embedded in a third material, which will perturb, often significantly, its properties.

Near-to-medium term applications of graphene composite and inks comprise:

- Fuel tank coatings
- Polymers with EMI or RFI shielding capabilities

- Automotive composites
- Electronic enclosures
- Photonic composites
- Aerospace composite and EMI shielding, etc.
- Heat dissipator in electrical appliances
- Sporting goods
- Coatings and paints
- Etc.

E1. Coatings and placement of graphene inks

Large scale coating and placement of graphene inks can be achieved via vacuum filtration [20], spin coating [413], Langmuir-Blodgett [414], spray coating [415], rod coating [416] and screen printing [417].

Inkjet printing can be directly integrated in processing of electronic and optoelectronic devices [266]. Deposition of fluidic droplets to form patterns directly on substrates offers a mask-less, inexpensive and scalable low-temperature process for large area graphene fabrication. The resolution of inkjet printing can be enhanced by pre-patterning the substrates, so that the functionalized patterns can act as barriers for the deposited droplets [419]. The process is versatile, with a limited number of steps, and a range of components can be printed.

Other possible alternative for large scale (suitable for industrial level) placement of graphene inks are R2R coating, flexographic and gravure printing. For instance, flexographic printing allows higher deposition speed than inkjet printing at the expense of resolution. Traditionally, flexographic inks need to have higher viscosities than inkjet inks [832], however techniques have been developed to partially overcome these limitations and enable flexographic printing of homogenous features using low viscosity inks [832]. This will allow minimization of additives, which tend to be detrimental on the electronic properties.

Our target is to position graphene as the reference material for the production of inks with a large variety of rheological, electrical and optical properties on an industrial scale. The viability of LPE to achieve liquid dispersion of all layered materials means that we can envisage the achievement in less than 5 years of a range of printable inks based on these materials. Different inks could then be mixed or printed to form hybrid heterostructures with novel, on demand, properties.

Printed electronic and optoelectronics based on graphene will likely enter the market before 2020, especially in sectors were high performances devices are not required.

E2. Polymer based graphene composites

In order to exploit on a macroscopic scale some of the unique properties exhibited by graphene, we need to integrate it as nanofiller dispersed in a polymer or inorganic matrix.

Up to date, most efforts have focused on polymer matrices, showing large increases in Young´s modulus, tensile strength, and electrical and thermal conductivity, particularly at low volume fractions (<1%) [21]. Inorganic matrices have received comparatively little attention, but the results so far show that the addition of graphene to ceramic matrices produces large increments in fracture toughness (235% increase at 1.5 vol.%) [833], electrical conductivity (172S/m at 2wt %) [834] and electromagnetic shielding (>99% attenuation for 30 wt %) [835]. However, this field is still in its infancy and several challenges and open questions remain, such as efficient improvement in composite properties at large volume fractions, integration into fibre-reinforced composites, determining scaling behaviour of

mechanical and transport properties in nanocomposites and measuring graphene-matrix interactions on the nanoscale that can be related to bulk composite properties.

The advantages of graphene over traditional fillers and other materials stems from its combination of mechanical and transport properties, as well as chemical and thermal resistance, high surface area and low thermal expansion coefficient. While some of these properties are shared by CNTs, its 2d shape, one-atom thickness and edge atoms provide a clear advantage in several applications, see Table 7. The large surface area of graphene implies that in a composite, the graphene-matrix interface is also very large, thus becoming a powerful engineering parameter to tailor composite properties. In addition, in a graphene composite the combination of size, surface area and thermal conductivity of the nanofiller modifies the matrix properties at the interface by acting as a nucleation point and a heat sink which can stabilise new phases, affect pore structure and overall matrix properties [836,837,838,839,840,841,842,843,844,845, 846,847,848]. These effects deserve further study by modelling and experiment to better understand stress, charge and heat transfer at the graphene-matrix interface, targeting the development of the applications outlined above.

Table 7. *Potential composite improvements with graphene and related applications*

Composite property improvement	Target application
Low CTE and high thermal conductivity in the plane	Heat dissipation in Si-based electronic devices avoiding thermal mismatch
Increased gas and liquid barrier	Lower permeability in fibre-reinforced composites
Integration on flat surfaces	Smart, multifunctional glasses
Enhanced adhesion to matrix through edge atoms and functional groups	Composites for extreme service conditions: high temperature, abrasion, corrosion
Fire retardancy through high thermal conductivity and surface area	Added functionality to ceramics composites
High photocatalytic activity in graphene-inorganic hybrid composites	Self-cleaning surfaces, hydrogen production, DSSC, water purification

An emerging area is the development of hierarchical composites reinforced with traditional macroscopic fibres (e.g. carbon fibre) and graphene, where the nanofiller is present at low volume fractions (where it is more efficient) and imparts added functionality to traditional composites.

This route represents a fast vehicle for the application of graphene in a wide range of industrial applications (aerospace, automotive, etc.), thus deserves further studies by a combination of modelling and experimental work, that take into consideration the whole life-cycle of the materials, addressing issues such as graphene effects on composite processing (e.g. sintering, extrusion), novel properties and new recycling/reusing opportunities.

MD simulations have analysed the interfacial thermal resistance graphene/polymer nanocomposites [849] and compared the heat transfer properties of graphene and CNT polymer nanocomposites [849].

The interfacial mechanical behaviour of the graphene/polymer system was analysed by means of Consistent Valence Force Field (CVFF) to describe the atomistic interactions [850]. However, the literature is still scarce and further studies are required.

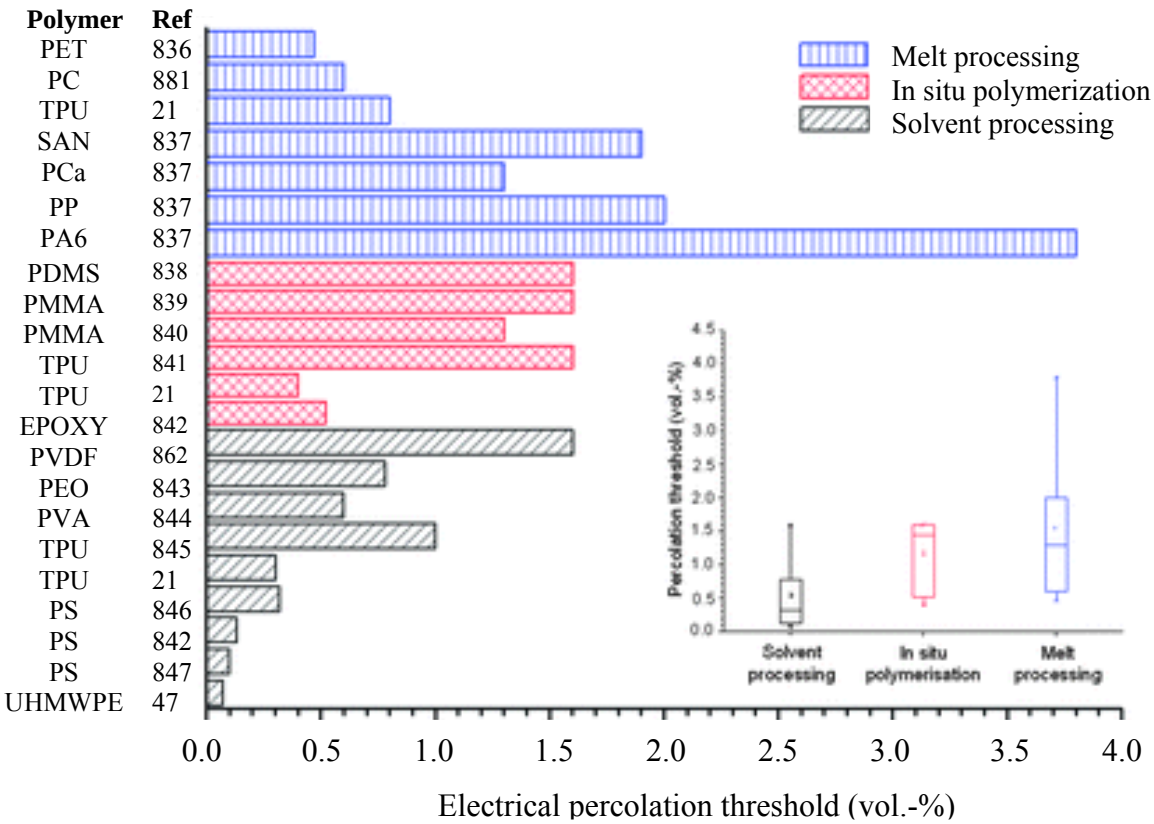

***Figure 71**: Electrical percolation data of graphene/polymer nanocomposites [848].*

A crucial step in graphene nanocomposites will be the dispersion of the carbon nanofillers. A well dispersed state ensures a maximized reinforced surface area, which will affect the neighbouring polymer chains and, consequently, the properties of the whole matrix, see Fig. 71 and table 8. Therefore, large efforts were devoted on achieving a homogeneous and well-dispersed system by developing either covalent or non-covalent functionalisation of the filler surface.

There are also many 2d layered materials that possess exceptional mechanical properties. For example, BN layers have strength and stiffness approaching those of graphene [431], while MoS_2 ones are also relatively strong and stiff [851]. One could imagine preparing composites of such nanosheets embedded in plastics resulting in considerable reinforcement. Initially, we would aim for increasing composite modulus and strength by factors 2-4 with respect to plastic, at low loading level, <1%. Thus, the filler would provide reinforcement without degrading any other filler properties. Later, we could expect to produce higher volume fractions, higher performance composites with mechanical properties exceeding those of structural materials, such as steel at a fraction of the density. In addition, adding layered materials (graphene, BN, MoS_2 etc.) to plastics will reduce gas permeability.

This is very important for the beverage industry. For example, beer manufacturers want to move from glass bottles to PET. However the shelf life of beer in PET is ~2 weeks (cf 30 weeks in glass) [852, 853]. To increase the shelf life, both oxygen and CO_2 permeability need to be cut by a factor of ~5 [853,854]. Diamond-like carbon has been successfully used for this [854]. We can predict that the permeability of a given plastic can be reduced by more than a factor of 10 for <5vol% loading of platelets with aspect ratio>1000 [855]. In addition, combinations of mechanical reinforcement and permeability will be important. For example, beverage manufacturers want to reduce the mass of plastic per bottle, *i.e.* reduce wall

thickness. This will degrade both the structural integrity and gas barrier performance of the bottle. Addition of materials such as exfoliated BN could address both issues simultaneously.

Table 8: *Summary of mechanical properties of graphene/polymer nanocomposites*

Polimer	Reinforcements	Graphene concentration (vol%)	Modulus increase (%)	Tensile strength Increase (%)	Ultimate strain increase (%)	Ref
PVA	GO	2.5	128	70	32	856
PVA	GO	0.49	62	76	-70	857
PMMA	GO	1.7	54	N/A	N/A	858
PCL	GO	2.4	108	36	-90	859
PCL	GO	0.46	50	N/A	N/A	860
Epoxy	TRG	0.05)	31	40	N/A	881
PEN	TRG	2.4	57	N/A	N/A	861
PCA	TRG	1.3	25	N/A	N/A	862
PMMA	TRG	(0.005,0.5)	33,80	N/A	N/A	21
PVDF	TRG	3.1	92	N/A	N/A	863
SAN	TRG	2.3	34	N/A	-58	864
PC	TRG	2.5	52	N/A	-98	
PP	TRG	1.9	43	N/A	-99	
PA6	TRG	2.4	32	N/A	-94	
natural rubber	TRG	1.2	750	N/A	N/A	865
PDMS		2.2	1100	N/A	N/A	865
styrene-butadiene rubber		0.8	390	N/A	N/A	865
TPU	TRG	1.5	43	-23	-15	866
Silicone foam	TRG	0.12	200	N/A	N/A	867
PVA	acid functionalized TRG	0.34	35	N/A	N/A	868
PMMA	amine treated acid functionalized TRG	0.3	70	N/A	N/A	868
TPU	TRG	1.6 1.6 1.5	250 680 210	N/A N/A N/A	N/A N/A N/A	869
	GO	1.6	490-900	N/A	N/A	869
PS	PS-functionalized chemically reduced GO	0.4	57	N/A	N/A	870
TPU	chemically reduced sulfonated-graphene	0.5	120	75	N/A	871
TPU	GO	2.4	900	-19	-60	872
PAN	exfoliation of alkali intercalated graphite	2.1	100	N/A	N/A	873

E3. Graphene-based Epoxy Resins for Advanced Packaging Applications

Epoxy resin is a thermosetting polymer widely used in various industries as coating, adhesive, electrical insulator, and for composite applications [874]. Epoxy has excellent

mechanical and chemical properties, including good dielectrical properties, high dimension stability, hardness, flexibility [875], and excellent chemical resistance [876].

However, epoxy burns easily, so research has been carried out to obtain a fire retardant epoxy [877,878]. One of the most efficient ways to reduce the heat release rate of epoxy is to use carbon materials. Graphene sheets may hold considerable potential as new carbon-based nanofiller and may be preferred over other conventional nanofillers (CNT, carbon nanofiber, etc.) owing to their higher surface area, aspect ratio, tensile strength, thermal conductivity and electrical conductivity [879].

Blended GO with epoxy, an epoxy nanocomposite with excellent thermal conductivities, has been already demonstrated [880]. Nanocomposites with 5 wt% GO shown a 4-fold increment of thermal conductivity compared to pristine epoxy [880]. A comparison on the mechanical reinforcement of thermally exfoliated graphene flakes, single-wall and multi-wall CNTs on the epoxy matrix at a fixed nanofiller content of 0.1 wt% was reported in [881], indicating that graphene flakes significantly out-perform CNTs in terms of Young's modulus, tensile strength and fracture toughness.

We will thus aim to develop smart, light-weight graphene-based packaging systems. This will require new technologies for graphene dispersion and sorting in suitable solvents, for the functionalization and grafting of graphene and nanometals to specific epoxy resins, for new mixing procedures and the application of a complete set of analysis techniques to understand the physical-chemical properties of the composites and hybrids, even at the single nanoparticle level.

E4. Ceramic based graphene composites

Ceramic materials have very valuable properties from the engineering point of view, such as refractoriness, strength and hardness, but they have an important drawback, their low toughness, which often overcomes their potential benefits[882]. The usual approach to increase toughness of ceramics is the inclusion of second phase materials that may act as reinforcing agents by producing extrinsic toughening effects. This is the case of fiber containing composites, or CNT-ceramic composites. Over the past five years, CNT/ceramic composites received great attention, owing to the improved mechanical properties [883]. An extra benefit of CNTs addition is that they render electrically conductive the ceramic composites [884], which makes possible machining by more efficient methods, such as electro-discharge [885]. This benefits from the erosive effect of electrical discharges or sparks. It should be pointed out that usually ceramic materials are costly to machine into complex shapes as consequence of their high hardness and low toughness.

The above advantages may be easily transferred into graphene/ceramic composites. Even though available results are very incipient [880,881,886,887,888], published data already show significant toughening [881] and higher electrical conductivity [886,887]. Graphene ceramic composites also possess further advantages compared to their CNT counterparts, such as the lower cost and commercial availability of graphene (e.g. RGO), and the less stringent processing conditions. The latter aspect is of particular relevance when the high temperatures (usually exceeding 1400°C) required to obtain ceramic materials are considered, which is a disadvantage for CNT composites, as they can be more easily degraded. In this respect, graphene/ceramic composites may even be fabricated using conventional heating methods [888], instead of field assisted sintering techniques, a must for CNT/ ceramic composites [889].

Graphene/ceramic composites may find applications in friction and wear related fields, such as engines components, bearings and cutting tools for metal working operations. Preliminary data already shows extraordinary response of these composites under sliding

contact [890], where exfoliated graphene sheets seem to act as a solid lubricant [890]. As introduced above, the possibility of precise micromachining of hard ceramic composites exploiting the advantage of electrical conduction makes easier the fabrication of MEMS for high temperature uses [891], which springs out as another important field of application.

Significant issues to be resolved include the atomic level characterization of the ceramic/graphene interfaces using HRTEM and focused ion beam methods for micromanipulation and imaging of selected areas. In-situ mechanical testing under mechanical stress, e.g. inside an electron microscope, will help to understand the complex mechanical response of these composites.

E5. 2d organic and inorganic nanocomposites based on chemically modified graphene

The multiple functional groups and unique 2d morphology make CMG an ideal template for the construction of 2d nanocomposites with various organic/inorganic components (see, e.g., Refs. [302,892,893]). Additionally, in case of functionalization with conductive particles the recovered electrical conductivity of CMG may provide a fast-electron- transport channel and can thus promote applications in optoelectronic and electrochemical devices.

CMG can be viewed as a 2d polymer containing extended aromatic frameworks and multiple functional groups. These groups can be used for the covalent attachment of organic and inorganic nanoparticles, including metal and metal oxide nanoparticles and QDs. The assembly of inorganic nanoparticles on the surface of conductive CMGs (see Fig. 72) not only avoids the agglomeration of nanoparticles, but also favours applications when conductivity is a significant concern. To integrate their unique features, fabrication of 2d nanocomposites of CMGs and inorganic nanomaterials has been intensively pursued in the past few years [892,893]. One of the most common strategies is to directly assemble CMGs with pre-prepared inorganic nanoparticles. On the other hand, the in-situ growth of inorganic nanoparticles after adsorption of their precursor salts on the CMGs surface offers an alternative approach. Thereby, various CMGs including GO, RGO, modified GO/RGO and exfoliated graphene have been explored for such purposes [892].

E6. Photonic polymer composites

The demand in optical networking for photonic components that meet performance criteria as well as economic requirements opens the door to novel technologies capable of high-yield, low-cost manufacturing, while delivering high performance and enabling unique functions [894]. An optical communication system requires light sources and detectors, but many additional components make up modern transmission networks. Until the end of the 1980s, these components, including beam splitters, multiplexers and switches, consisted of bulk optics elements, such as lenses and prisms. Bulk optics, however, are inconvenient to handle, highly sensitive to misalignment and prone to instability. All of these problems are avoided in integrated optics systems. These combine miniaturised optical components and waveguides in a highly condensed chip-based device. Their compact, planar layout has clear advantages over bulk optics when deployed in complex systems. Integration permits the reduction of complex multi-function photonic circuits on a planar substrate.

Polymeric materials are the ideal choice for such an integration platform [894,895,896]. They are easily manipulated by methods such as embossing, stamping, sawing, wet or dry etching. They have a low-cost room-temperature fabrication process.

Polymers can be synthesized with customer defined optical characteristics, such as selective transparency bands in different spectral ranges, variable refractive indexes, low birefringence, other than high laser damage threshold and thermal stability. Moreover, the polymers must be easily processable during device fabrication and be economic [897].Polymers traditionally used for optical applications include PMMA [894], polycarbonate [898] and epoxy resins

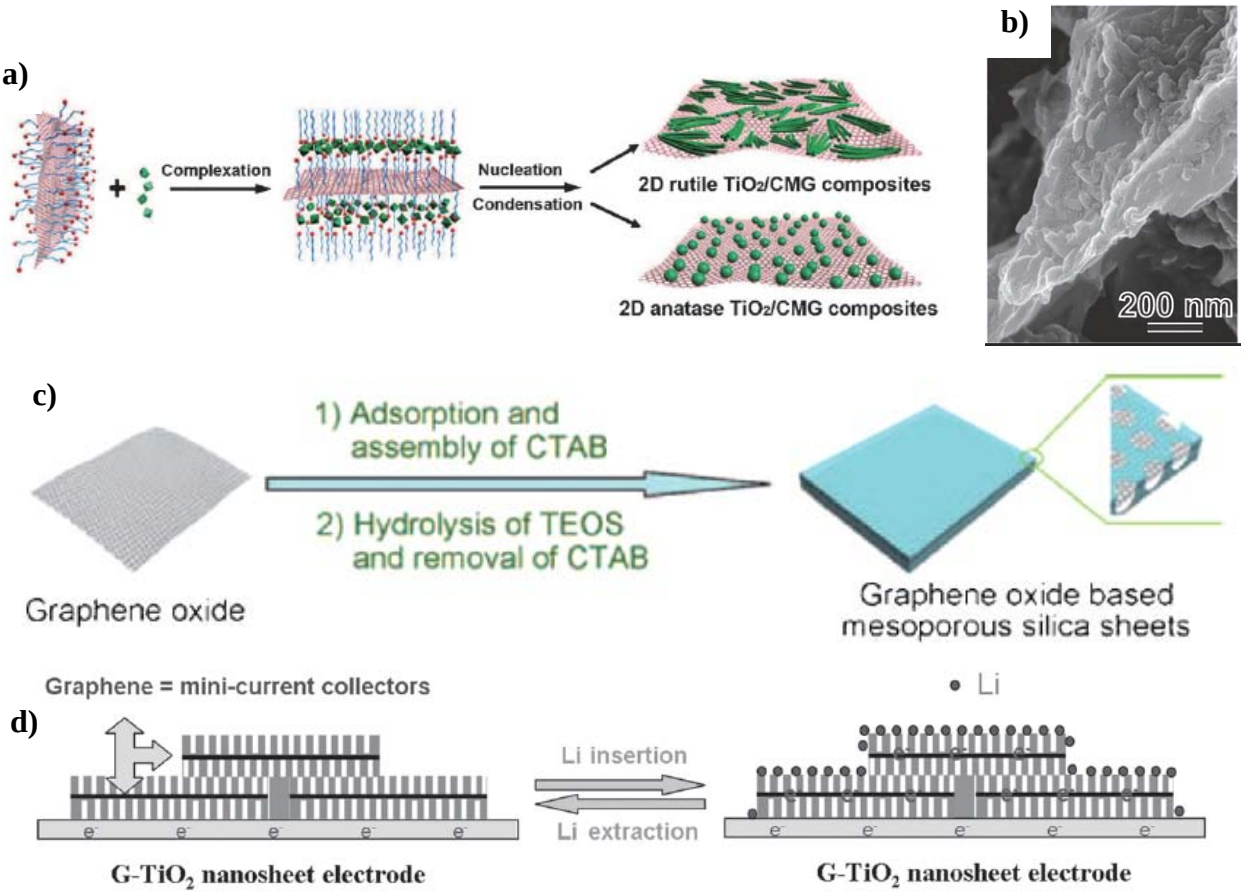

Figure 72*: *Examples of 2d nanocomposites based on CMG [892].

[894]. Deuterated [897] or halogenated polyacrylates [897] and fluorinated polyimides [894] have been developed to address specific issues, such as optical losses [899], heat [897] and environmental stability [897]. Water-soluble polymers, such as PVA [603,898] and cellulose derivatives, such as sodium carboxymethyl cellulose [603], have been widely used both for CNT and graphene-based SAs [603, 900, 901, 902, 903] since stable, high-concentration dispersions can be readily prepared [603]. From the fabrication perspective, PVA is more attractive, because of its mechanical properties [603]. To prepare environmentally stable polymer composites, in particular, against humidity and temperature, graphene can be directly exfoliated in organic solvents [20]. The dispersions are suitable for moisture resistant polymers such as Polycarbonate and PMMA, or copolymers such as SMMA [603]. Siloxane polymers have many attributes that make them viable for polymer waveguides. These can be spin-coated from uncured precursors or polymer solutions and then patterned into the specific waveguide geometries using either reactive ion etch or direct exposure to UV light patterns. Precise control of the refractive index of both core and cladding material can optimise light transmission. Like inorganic materials [904], polymers can be doped to take advantage of optical properties associated with the dopant.

Optical amplifiers are an important component in optical communications [905]. They are needed to enhance the signal, particularly in order to compensate for the intrinsic losses

due to fibre propagation and splitting, switching and multiplexing operations. Amplifiers can be housed in optical fibres or in integrated optics components. EDFAs [904] consist of an active region formed from a length of Er-doped silica fibre. They are often used in telecommunication networks to amplify optical signals in the 1310nm and 1550nm windows. With the emergence of polymer optical fibre, the natural progression from silica-based EDFAs is the doping of rare earths into polymers [906]. There has also been increasing interest in doping rare earths in inorganic and organic waveguide components to make waveguide optical amplifiers. The ease of integrated circuit fabrication provided by polymers, coupled with the expected high-gain performance in rare-earth polymer materials, lead to increased activity in this field [907,908]

Many of the advantages of polymer materials discussed for communications systems also apply to lab-on-a-chip devices. The "lab-on-a-chip" consists in combining a number of biological and chemical analysis processes into one device and miniaturising it [909]. Testing the optical behaviour is an important characterisation step, so integrated optics devices are often required in these new systems. The construction of complex lab-on-a-chip devices can be simplified by taking advantage of the ease of fabrication afforded by various polymer-patterning techniques.

We will develop of a new class of polymer based optoelectronic devices embedding the optical and electronic functionalities of graphene, 2d inorganic layered materials and their hybrid heterostructures. These devices will combine the fabrication advantages of polymer photonics, with the tuneable active and passive optical properties of such materials. Such devices are expected to find a wide range of applications not only in optical communications, but also in bio-medical instruments, chemical analysis, time-resolved spectroscopy, electro-optical sampling, microscopy and surgery.

Novel photonic polymers incorporating graphene, 2d inorganic layered materials and their hybrids will be produced, *i.e.* index matching gels and optical adhesives. These are typically epoxy or silicone-based polymers, having excellent elastic and thermal properties, as well as good chemical stability. Current photonic polymers include acrylates, polyimides, polycarbonates and silicones. However, these give a significant optical loss (>0.5 dB/cm) at the telecom wavelengths, due to C-O, O-H, Si-O and Si-H groups [894]. To achieve optimal 2d layered materials-polymer devices, we will use special formulations of silicone polymers. These will be fluorinated, to reduce the influence of Si-O and Si-H groups on the optical absorption in the telecommunications spectral window [894]. This will allow us to set the optical losses at a very small value, less than 0.5 dB/cm.

E7. Nanoscale, real time, in situ modelling of electrical and mechanical failure in graphene-based composite systems

To have an impact on Society, the properties of an ideal SLG, need to be transferred from the atomic scale to the meso-macroscopic level (continuous layers or bulk materials), and to do this a thorough modelling of graphene-based composites is needed.

Advanced scanning probe, optical and electronic techniques with tailored setups are needed, to observe the behaviour of graphene based composites in situ, in real time, while the material undergoes electrical and/or mechanical stress. By these means, we shall observe and understand the failure mechanism of graphene-based composites for electronic and structural applications, a fundamental step to move graphene from science to technology.

To produce advanced composites, the graphene sheets shall be deposited on/embedded in different, technologically relevant materials such as substrates suitable for microelectronics applications (SiOx, SiC, High-k dielectrics, BN, MoS_2, etc.) and/or organic polymeric materials for structural applications (polyimides, polymetacrylates, epoxies, etc.) [303,910].

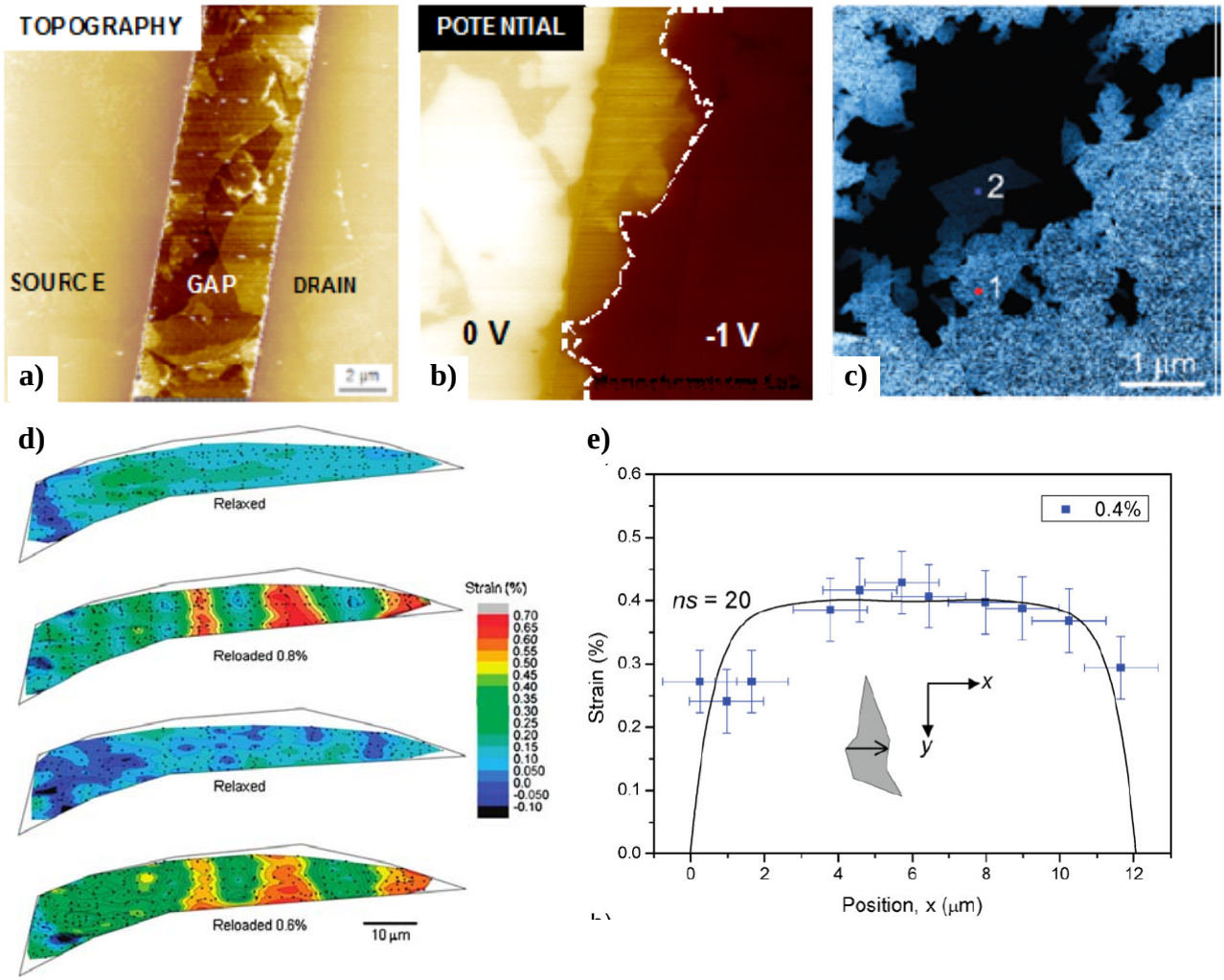

***Figure 73**: Characterization at the micro/nanoscale during electrical (a-c) and mechanical (d,e) stress. a) AFM topography and b) potential image of a FET substrate with partial coverage of single sheets of chemically reduced graphene in the device channel. A 1V bias is applied between source and drain. c) Conductive AFM image of current passing in percolating RGO sheets. d) Contour maps of strain over a SLG embedded in a polymer matrix, in the relaxed states and reloaded to 0.8% and 0.6% strain, as measured by Raman spectroscopy [911]. e) Variation of axial strain with position across a graphene monolayer strained in the x-direction at 0.4% matrix strain [912].*

Advanced scanning probe and electronic techniques with tailored setups (Fig. 72) will be used to visualize, on microscopic scale, the process of electrical/mechanical failure, and to find new ways to improve the materials' properties. Graphene-based materials, thanks to the mesoscopic size of the sheets, their flatness and uniform thickness, are perfect substrates for the use of such advanced microscopic techniques [300,301].

Kelvin Probe Force Microscopy can be used to monitor the charge generation, charge transport and exciton splitting in graphene composites and in graphene-based electronic devices [913,914]. This technique exploits the electrostatic interaction between a scanning probe and the sample to probe the surface electric potential. The lateral resolution attainable is < 50 nm, the potential resolution is <10 mV. The technique is contact-less and does not perturb the surface potential, thus it can be used on working devices (Fig. 73).

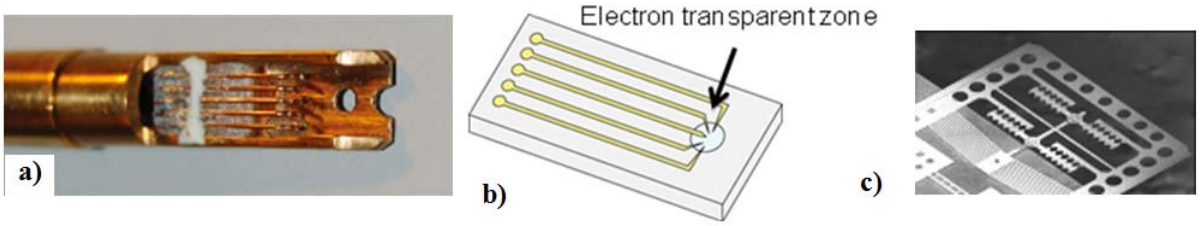

Figure 74 *a) Tip of a TEM specimen holder for in-situ observations with five connections; b) Cartoon of a cartridge matching the five connections of the holder. c) Example of MEMS designed to heat and strain graphene membranes in-situ in a TEM.*

We will also use advanced TEM techniques (e.g. high resolution, interferometric techniques, and electron holography) capable of testing the crystalline quality, as well as probing the functionalization of the surfaces or reconstructing the flakes structure [262,915].

For this purpose dedicated sample holders for TEM observations shall be used (Fig. 74), equipped with a lodging bay on the top for placing different MEMS devices, directly under the electron beam. Electrical connections from outside the TEM will provide electrical inlets and outlets allowing the atomic level characterization of the structural, chemical and electronic properties of individual nanostructures under external stimuli. The final aim is a full integration of in-situ and ex-situ measurements to correlate nanoscale and mesoscale properties with device operation characteristics.

Targeted theoretical and computational modelling of the interaction of the sheets will be fundamental to understand and improve the material properties. Given the mesoscopic scale on which charge transport and mechanical failure take place, the modelling using ab initio or molecular mechanics will have to be complemented with more coarse-grained models [915], able to simulate inter-sheet interactions on the 10-1000 nm length scale (Fig.75).

In parallel to nanoscale characterization and modelling, the mechanical/electrical properties of the different graphene-based materials should also be characterized at the macro-scale by conventional procedures.

E8. Industrial value chain for graphene composites

Modelling and control of graphene inter-sheet interactions, as well as the interaction of graphene with different materials, is a though challenge. This will be addressed with a strong attention to the most promising technological end-uses of the materials developed in such a way, to achieve a significant and clear impact. To move from scientific results to technological impact, any credible developmental effort will have to be driven by the actors covering the entire value chain of the potential products addressed.

Collaboration with industries form different sectors (from high-performance electronics to low-cost consumer products) will be fundamental to address basic research, as well as to establish quantitative requirements for the materials to be technologically useful.

Any new technology, no matter how revolutionary it is, has to face major economic issues to move from R&D stage to large scale commercialization (the so-called “valley of death”). Usually, innovative, un-optimized technologies cannot rival well-established, optimized technologies already commercial. To overcome this issue, we will first focus on development of graphene-based materials for applications in sectors where, due to the high end value and the small production scale, cost is a relevant but not a dramatic issue, and new technologies can rapidly become competitive for small scale production (high performance mechanics, aerospace, biomedical, specialized electronics, etc.).

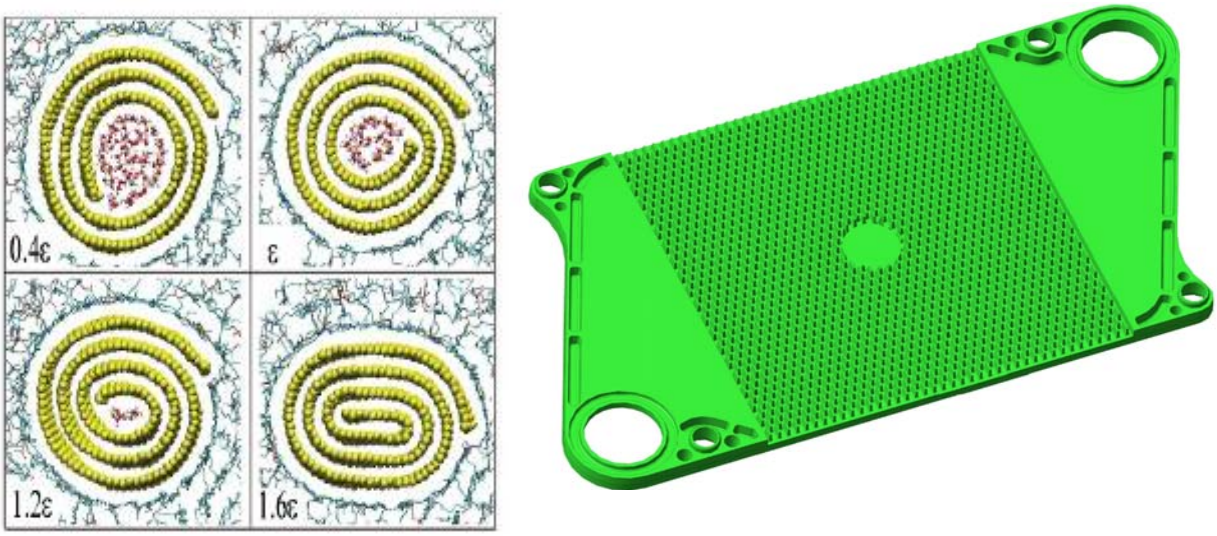

***Figure 75**: Modelling and design of graphene based products: a) Graphene nanoscrolls. b) Design of a polymer heat-exchanger plate based on graphene composites.*

As an example, we will target applications for aerospace or biomedical sensing, where performance is more important than mere cost, and where production scale is on the thousands rather than on the millions items scale. Next generation aerospace, see Fig. 76 [916] vehicles will rely heavily on nanotechnology and materials science to develop large lightweight structures with designed properties based on high performance materials, innovative manufacturing and assembly processes with the objective of mass, cost and schedule reduction.

The main challenge is to use materials with stronger and tailor-able properties associated with lightness, and design components in a way that reduces the global failure rates and life-cycle cost. This can be achieved by development of "smart" materials which, while being lighter and stronger than the previous ones, shall allow easy, possibly real-time sensing and monitoring for mechanical failure or leakage.

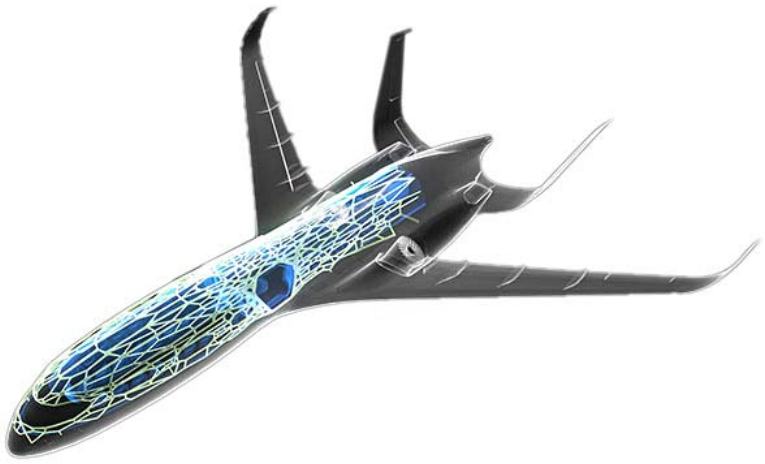

***Figure 76**: Intelligent concept for Airbus 2050 [916].*

Graphene-based composites with low charge percolation threshold, high mechanical strength and excellent gas permeation barrier can be ideal candidates for aerospace applications. The technology developed for high-performance materials used for airlocks, space station modules, launchers and lunar shelters could successively be implemented in technological/commercial applications quite rapidly, to be extended in a second stage to larger scale applications such as packaging, automotive and aeronautic technology.

We also plan to use graphene-organic composites for the development of heat exchangers combining the properties of polymers (mouldable into compact high-exchange area designs, resistant to corrosive environment, and light) with the exceptionally high thermal conductivity of graphene. The idea is to use nano-filled polymers based on a combination of a few weight per-cent units of CNTs and FLGs, with high temperature resistant polymer carriers [917], for the development [918] of high-surface-area heat exchanger prototypes for

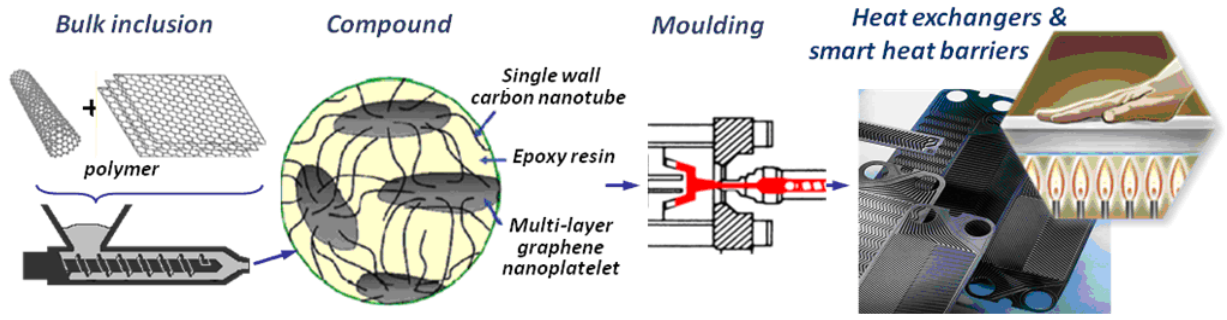

Figure 77: *Schematic of development from atomic to full scale of nanofilled polymer heat exchangers based on combination of CNTs and FLG in a polymer matrix.*

aggressive environments like those encountered in marine appliances (intercoolers of naval diesel engines) or in the chemical industry (Fig. 77).

The distinctive properties of thermally-conductive polymers will also be tested for applications in the recovery of low temperature heat in automotive applications, such as the recovery of heat from exhaust gases and in many electro-domestic appliances (e.g. refrigerators, washing machines, dishwashers, ovens, etc.) [919].

F. Impact on health and environment

Nanosafety research cannot be dissociated from the development of new nanotechnologies. Graphene is not devoid of possible risks on human health or the environment and cannot be excluded from this type of investigation, in view of its responsible industrial use. It is of fundamental importance to explore which is the level of toxicity that graphene might reach and the degree of safety [920,921].

Graphene is part of a bigger family that has been identified as the Graphene-Family Nanomaterials (GFNs) [920]. Clarifying the existence of multiple graphene forms allows to better understanding the differences between the components of the family and eventually correlating their toxicity with the physico-chemical characteristics of each member. GFNs comprise FLGs, GO, RGO, graphene nanosheets, and ultrafine graphite (more than 10 sheets but below 100 nm in thickness). Several studies have been devoted to assess the in vitro and in vivo toxicity effects of GFNs. Some clearly showed no particular risks, while others suggested that graphene might become a health hazard.

Inhalation, for example, is one of the key routes of human exposure. Some GFNs have aerodynamic size that may lead to inhalation and deposition into the respiratory tract with possible implication on the formation of granulomas and lung fibrosis. However, the biological responses certainly vary depending on the number of layers, lateral size, stiffness, hydrophobicity, surface functionalization, dose administered and purity of the material. Not much is known about potential differences in biological behaviour between large and small sheets of graphene, or even FLG versus multi-layer graphene. This is a potentially interesting topic which certainly deserves deep study. The major results are hereafter discussed and critically presented in view of the further studies that still need be performed. Current studies are not exhaustive, nor do they cover all aspects associated to the impact of graphene on health and environment (Table 9). In the latter case, there is a clear lack of information.

F1. In vitro impact of graphene

A comparative study reported that graphene induces stronger metabolic activity than SWNTs (Table 9) [922]. High level of lactate dehydrogenase, sign of cell membrane damage associated to necrosis, was measured. Reactive oxygen species (ROS) were generated in a concentration and time dependent manner, indicating an oxidative stress mechanism. Caspase 3 activation, indicative of apoptosis, was also significant and time dependent.

***TABLE 9**: Impact of graphene on health and environment*

Material	*In vitro* model	*In vivo* model	Effects	Ref
CVD graphene	Neuronal PC12 cells	–	Increase of activation of caspase 3; Release of lactate dehydrogenase; Generation of ROS	922
GO	Human fibroblasts (HDF)	–	Toxicity at dose > 50 µg/ml Decrease of cell adhesion Cell apoptosis	925
GO	–	mice	Chronic toxicity; Death Lung granulomas	925
Carboxylated GO	Monkey renal cells (Vero)	–	Cell uptake; No lactate dehydrogenase leakage No cell death or apoptosis up to 300 µg/ml	924
GO and RGO	A549 cells	–	Slight decrease on cell proliferation; No apoptosis or cell death up to 85 µg/ml	926
RGO	A549 cells	–	Remarkable reduction of cell viability	926
GO	A549 cells	–	No cell uptake; Size dependent cytotoxicity Dose dependent oxidative stress	927
PEG coated GO	RAJI; HCP-116; OVCAR-3; U87MG; MDA-MB-435; MCF-7	–	No cytotoxicity up to 100 µg/ml	307, 928
RGO	Blood platelets	–	Strong aggregatory response Extensive pulmonary thromboembolism	932
RGO	–	mice	Less effective in platelet aggregation	932
RGO	Human hepatoma HepG2 cells	–	Moderate variation on protein levels	924
GO	–	mice/rats	Dose dependent pulmonary toxicity; Granoulomatous lesions; Pulmonary aedema fibrosis; Inflammatory cell infiltration	933
GO and graphene	Alveolar macrophages Alveolar epithelial cells	–	Generation of ROS, Inflammation, Apoptosis Increased rate of mitochondrial respiration	934
GO and graphene	–	mice	Pulmonary toxicity inflammation	934
Graphene dispersed in 0.5% BSA	THP-1 celles	–	Inflammation cytokine release (IL1B)	938
Graphene dispersed in 0.5% BSA	–	rat	Acute pulmonary inflammatory response	938
CVD graphene	Neuronal PC12 cells	–	Increase of activation of caspase 3; Release of lactate dehydrogenase; Generation of ROS	922
GO	Human fibroblasts (HDF)	–	Toxicity at dose > 50 µg/ml Decrease of cell adhesion Cell apoptosis	925

This indicates that the shape of the material plays a primary role. In another work, GO and carboxylated GO were tested on monkey renal cells (Vero cells) [923]. After treating Vero cells with 25 μg/ml of both materials, it was found that GO accumulated mainly at the cell membrane provoking significant destabilization of F-actin alignment. More hydrophilic carboxylated GO was instead internalized by the cells accumulating in the perinuclear region, without affecting cytoskeletal morphology. Cell viability was studied by Alamar Blue assay.

GO significantly affected the cell viability at 50 μg/ml, while hydrophilic GO was not toxic up to 300 μg/ml. No lactate dehydrogenase leakage was measured suggesting that there is no physical damage of cell membrane (leading to necrosis) by both nanomaterials, but that likely another mechanism of cell death, involving intracellular stress triggering programmed cell death is contributing. Indeed, oxidative stress was measured in a dose dependent manner. Alternative tests consisted in the analysis of the possible changes on protein profile [924]. RGO and SWNTs were compared by measuring the expression of a high number of proteins involved in the metabolic pathway, redox regulation, cytoskeleton formation and cell growth. While SWNTs severely interfered with the expression of a series of these proteins, only moderate variation of protein levels was observed on human hepatoma HepG2 cells treated with RGO. GO was also used to analyse the effects on human fibroblasts [925]. Dose dependent toxicity on cells was observed. In particular, the cells underwent apoptosis at concentration>50 μg/ml. An opposite result was reported by Ref. [926], with only a slight decrease on proliferation of the A549 cell line without signs of apostosis or cell death up to 85μg/ml. The same material treated with hydrazine to generate RGO resulted instead highly cytotoxic, remarkably lowering the viability of the same type of cells. Non toxicity of GO on A549 cells was also confirmed by another independent study [927]. A dose-dependent oxidative stress induction was evidenced, while a slight loss of cell viability was observed at the highest concentration (200μg/ml). As the material is not internalized by the cells, it has been found instead that cell culture nutrients are adsorbed by GO and this depletion seems responsible of the oxidative stress.

Alternatively to the reduction with hydrazine, other chemical approaches can be used to modify GO. Pegylation modulates the cytotoxic effect on a series of cell lines, including Raji, MCF-7, U87MG and others, without affecting cell viability up to 100 μg/ml [307,928]. PEG-GO less than 50nm in side, was found to be stable in physiological conditions. No evident toxicity (*i.e.* cell death or apoptosis) was measured at various concentrations on HCT-116 cells [929]. This functionalized GO penetrates cells following an endocytosis mechanism.

The current results can be considered as important initial data. However, it is necessary not to generalize, but take into consideration the great variability of the material. It is essential to compare the different types of GFNs and correlate their impact on cells to their physico-chemical characteristics and, in case, to the chemical modifications introduced. This will avoid generalizing and describing all types of graphene as eventually dangerous for human health if some of them are not.

F1.1. Use of graphene for regenerative medicine

The evaluation of the cytotoxic effects of graphene has important implication on its use as support for tissue regeneration, cell growth, cell differentiation, etc. Indeed, graphene has been explored as substrate for neuronal interfacing [930]. Mouse hyppocampal cells were cultured on a graphene substrate to analyse if the neural functions were affected during the development and maturation. The results revealed high biocompatibility, low toxicity, no morphological changes, while neurite numbers and length, sprout and outgrowth increased. The potential use of graphene as a material for neuronal interfacing represents a promising approach in future biomedical applications. Similarly, different surfaces covered by graphene

were also demonstrated to induce cell differentiation [931]. In particular, graphene allowed to control and accelerate the proliferation of human mesenchymal stem cells [931]. Cell viability was maintained and no change in cell morphology was observed during the differentiation process, which was enhanced in the case of cells in direct contact with graphene in comparison to other types of surfaces, like glass or Si wafers [931]. This case study represents an interesting example how bone regeneration can be achieved without growth factors often required for this purpose. It also proves the safety use of graphene that remains intact after cell growth. This opens the possibility of actively integrating such nanomaterial into regenerated or repaired tissues.

F2. In vivo impact of graphene

In-vivo toxicity was also investigated in parallel to the impact at cellular level. GO and RGO were used to analyse the effect on blood platelets, the cells responsible for the maintenance of homeostasis and thrombus formation [932]. GO elicited strong aggregatory response in platelets [932], while intravenous administration in mice induced extensive pulmonary thromboembolism [932]. This behaviour was associated to the charge distribution on the GO surface, as the aggregation properties were significantly lowered, when the material was chemically treated to generate RGO [932]. *In vivo* toxicity of GO labelled with the radiotracer ^{188}Re was evaluated in mice and rats following intravenous administration [933]. Using a dose of 10 mg/kg, significant pathological changes including inflammatory cell infiltration, pulmonary aedema and formation of granulomas were found. On the other hand, GO showed good biocompatibility with red blood cells at low dose, while haemolysis was induced at 80μg/ml of material tested. These results were confirmed by another study in which GO was injected in mice, evidencing formation of granulomas in lungs, spleen and liver without any appearance of kidney clearance. Pulmonary toxicity is a major concern in case of the industrial production of nanomaterials, as their respirability might cause damages and eventually long term diseases on people in contact with these materials. It was reported that GO provokes severe and persistent injury in lungs following direct injection into the organs of mice [934]. But the toxicity effects were clearly reduced in the case of pristine LPE graphene dispersed in Pluronic surfactant [935]. The use of alveolar macrophages and epithelial cells evidenced an increase of the rate of mitochondrial respiration, generation of ROS and apoptosis [936,937]. These results apparently highlight how the oxidation of graphene contributes to pulmonary toxicity. In a recent study, the risk to the respiratory system was also suggested for pristine graphene dispersed in bovine serum albumin [938]. FLGs were found to deposit beyond the ciliated airways following inhalation. Acute inflammatory responses in mice and inflammation by cytokine release in THP-1 cells and frustrated macrophage phagocytosis were evidenced. The inflammogenicity *in vitro* and *in vivo* was attributed to the respirable aerodynamic diameter [939], the index that determines the respirability of a particle and the side of deposition. It is very difficult to understand the differences in these two studies, suggesting opposite behaviour of pristine graphene. Likely the morphology of the tested materials, the number of layers, the surface area, and the dispersion procedures are amongst the parameters that can give rise to the different toxicity properties. The modulation of toxicity *in vivo* can be achieved through chemical functionalization [575, 576]. GO pegylation reduces the toxic effect following intravenous administration in mice (see Secton F4).

As for the impact *in vitro*, many parameters need to be taken into consideration when GFNs are tested for toxicity. Indeed, the variability of the samples is extremely high. It is fundamental to consider and to describe the morphological and physico-chemical characteristics of each type of samples, without making any generalization, which can risk

introducing bias when statements on “toxicity” or “non-toxicity” of graphene are presented or emphasized. Toxicity of graphene is closely associated to its surface functionalization. Size is the second important parameter that needs to be carefully considered.

F3. Bacterial toxicity

Concerning the toxicity effects of graphene-based materials on microorganisms, there is a series of recent studies on different types of bacteria [926,929,938,940,946]. The apparent antibacterial activity might find interesting applications in antimicrobial products (Table 10).

TABLE 10: *Applications of graphene derivatives in antimicrobial products.*

Material	*In vitro* model	*In vivo* model	Effects	Ref
GO RGO	*E.coli* *S. aureus*	–	Bacterial inactivation	940
GO RGO	*E.coli*	–	Bacterial inactivation Reduction of metabolic activity Bacterial membrane damage	926
Graphite Graphite oxide GO RGO	*E.coli*	–	Bacterial inactivation Bacterial membrane damage Oxidative stress	929
GO	*E.coli*	–	Fast bacterial growth	941
GO	*Shewanella*	–	Increased bacterial growth	946

GO and RGO were tested against gram-negative *E. coli* and gram-positive *S. Aureus* [940]. Both showed antimicrobial activity, RGO being more efficient in inactivating both types of pathogens. Gram-negative were however more resistant. Similar results were found by Ref. [926] on *E. Coli*, this time with GO more bactericidal. Effects on the metabolic activity at different concentrations were complemented by the damage of the microorganism cell membrane, as assessed by TEM. To expand further these studies, the antimicrobial mechanism was analysed using different materials, such as graphite, graphite oxide, GO and RGO [929]. Again, higher antibacterial activity was found for GO, which had the smallest average size among the different types of graphene derivatives. Direct contact of bacteria with graphene sheets induced a loss of membrane integrity. No reactive oxygen species generated by superoxide anions were detected. But oxidation of glutathione, a redox state mediator in bacteria, was instead observed. These results suggest that the GO antimicrobial action contributes to both membrane disruption and oxidative stress. The physico-chemical characteristics of graphene materials seem to play an important role in the efficiency of

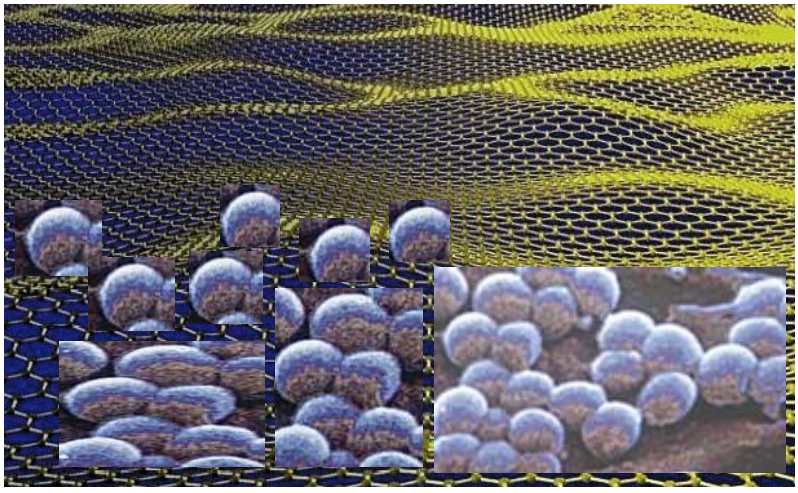

Figure 78: *Representation of bacteria in contact with a graphene surface.*

bacterial killing, therefore can be tailored to reduce the adverse impact on health and environment. These results were questioned by a recent study [941], where GO was added to *e.coli* and bacteria grew faster by forming dense biofilms around the suspended nanomaterial. Only the combination with Ag nanoparticles showed cell death. In view of these findings, the exploration of the GO bacteriostatic properties certainly needs further studies (Fig. 78). Comparison between the available data is difficult as the conditions of cell cultures and type of starting materials differ in the reported experiments. On the other hand, these conflicting data can stimulate the research towards the assessment of the antimicrobial role of graphene, as a function of its physico-chemical properties.

F4. Biodistibution and pharmacokinetics

The study of the bio-distribution, accumulation and elimination of graphene nanomaterials is a fundamental step to understand the risks associated to their uses. Few studies using functionalized GO have been reported [942,943]. Bio-distribution studies have shown that GO accumulates predominantly in the lungs, while low uptake by reticuloendothelial system was measured. GO exhibited long circulation time in comparison to other carbon forms. No pathological modifications in different organs were evidenced after injection of 1 mg/kg body weight along 14 days [933]. However, significant changes were observed in lung at a dose of 10 mg/kg. PEG-GO instead accumulates mainly in the tumour of tumour-bearing animals, with lower uptake by reticuloendothelial system (RES), without exerting significant toxic effects [942]. The same material was intravenously injected, after being radio-labelled, to assess the organ bio-distribution and the excretion routes. Following an initial accumulation in RES, a gradual elimination was observed between 3 and 15 days [942]. After three months the graphene sheets were completely eliminated without toxic effects. The body weight of the animals was not affected at all concentrations used. No signs of abnormality were observed in major organs including kidney, liver, spleen, heart and lung [942]. This type of modified graphene was also studied to evaluate more thoroughly the pharmacokinetics, the long-term bio-distribution and the toxicity effects [943]. These parameters were analysed by radio-labelling the GO with ^{125}I. Following again the intravenous administration, the graphene sheets accumulated into the RES including spleen and liver. They were gradually cleared by both renal and fecal elimination as assessed by detecting the radioactivity into the urine and feces samples [943]. The tested dose of 20 mg/kg did not provoke evident toxicity in a period of 3 months as proved by measuring the biochemical parameters in blood, and the haematological markers (white blood cells, red blood cells, haemoglobin, platelets, etc.). All parameters appeared normal on the treated animals. Histological examination of the different organs did not evidence damage or lesions excepting an increase of colour of spleen and liver due to accumulation of brown graphene. However, the identification of the exact clearance mechanism is still lacking.

These data are extremely interesting, although they can be considered only preliminary. It is indeed necessary to compare the behaviour of different graphene nanomaterials, other animal models, higher doses, and different route of administrations. These studies will allow understanding the effects of graphene materials once administered on purpose, or by accidental exposure, in order to push further their implementation in different fields.

F5. Biodegradation

The assessment of the bio-persistance, bioaccumulation and biodegradation of novel nanomaterials is fundamental for their safe implementation. Indeed, the study of biodegradability of carbon-based materials is of paramount importance to translate their use

into biomedical devices or therapeutic tools, and in parallel to anticipate the possible risks when integrated into novel electronic composites. A careful characterization of the material will allow elucidating and clarifying the role of surface modification and its biological impact. This will allow to eventually proposing solutions on the treatment and use of graphene. It will allow improving the knowledge on toxicology of this carbon form, and it will prospect to translate such type of nanomaterials into clinical applications including therapy, diagnostics and imaging. As recently demonstrated for CNTs [944], GO undergoes an enzymatic degradation by horseradish peroxidase in the presence of hydrogen peroxide (Fig. 79) [945].

The same behaviour was not found for RGO, which seems to be more resistant to the enzyme. This has important implications on the design of safer graphene derivatives to minimize the risks for human health and environment. Alternatively, it is possible to modify GO using microorganisms. The family of bacteria called *Shewanella*, which consists of dissimilatory metal-reducing bacteria, was able to affect the GO [946]. Opposite to the results obtained on *E. coli* and *S. aureus* that are inactivated by GO (see Section G3), these pathogens are not inhibited, but they were able to reduce GO by microbial respiration, providing a unique nontoxic approach to the synthesis and modification of graphene flakes. The mechanism of reduction involved both direct extracellular electron transfer and electron mediators at the interface between cells and flakes. This work can be extended to other species of microorganisms not only to modify but eventually degrade graphene (Section F6).

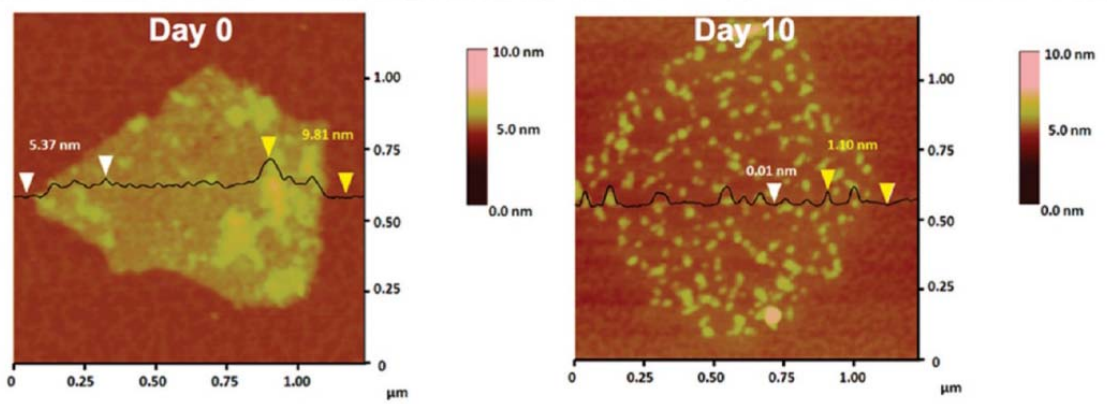

Figure 79: *GO biodegradation by horseradish peroxidase in the presence of H_2O_2 ([945])*

F6. Environmental impact

To date, there are no available studies which focus on the ecotoxicology and environmental impact of graphene and its family members. Amongst the other carbon allotropes, the majority of works concerns fullerenes [947]. The studies highlight the effect of fullerene ingestion and its associated toxicity in several model organisms: fresh water crustaceans [947], marine copepods [947] and fish [947]. Several data are also currently available on the eco-toxicological effects of CNTs in various organisms [948]. Few reports are available for microorganisms and plants. Most of studies on the CNT eco-toxicity were conducted on representative species of the aquatic environment and, to a lesser extent, on terrestrial organisms [949]. Based on the experience acquired with these types of carbons, it is important to explore the impact of graphene, GO, RGO and any other related structure on the environment. With the development of graphene production, the multiplication of its uses, and arrival in the marketplace, it is essential to assess exposure in real conditions and fully understand the life-cycle of this material.

F7. 2d crystals and hybrids

To our knowledge, there are no studies on health and environment impact of other 2d crystals and their hybrids with graphene or other materials. This is probably due to the lack of efficient methods of preparation to afford sufficient amounts of materials to assess their toxic or ecotoxic effects. For BN layers we can benefit from studies already available on the BN nanotubes or cubic-BN. Cubic-BN is a component of surgical cutting tools. It remains in small amount on implants as a result of the manufacturing process. However, this material does not affect cell survival even at high concentration (40μg/ml) [950]. BN nanotubes coated with polylysine were recently tested on a model of muscle cells (C_2C1_2). The tubes are able to penetrate these cells without affecting their viability, nor interfering with the formation of myotubes, during cell differentiation [951,952]. Alternatively, BN nanotubes were functionalized with dendritic structures bearing carbohydrate ligands to their periphery by non covalent adsorption. The generated complexes interacted with proteins and cells without modifying cell proliferation and viability [953]. Ref. [954] reported that morphological alterations in different cell populations exposed to BN nanotubes are cell-type dependent. These results are extremely useful and will inspire new investigations on the different structures of 2d crystals and hybrids developed in parallel to graphene.

F8. Perspectives

Future research is necessary to thorough explore the biological responses and the toxicity of GFNs and 2d crystals by taking into consideration their different physico-chemical properties. There are several key factors associated to the toxicity of new nanomaterials. The generation of oxygen reactive species, the indirect toxicity because of GFN adsorption of important biomolecules, and physical toxicity associated to the interaction with the lipids constituting cell membranes, tissues and organs need to be carefully studied and analysed. In addition, study of the uptake as a function of the dimensions is necessary. Side dimensions of graphene might affect the population of the receptors involved in the mechanisms of penetration dependent on energy (i.e. endocytosis/phagocytosis active mechanisms). If passive mechanisms, like in the case of CNTs [955], are taking place, it is interesting to understand how the flat form of the material affects the membrane organization (*i.e.* membrane disruption or sliding between the lipid bilayers) [956]. These studies will guide the safe design, production and manufacturing of GFNs and 2d crystals, minimizing risks for health and environment.

G. Biomedical applications

The application of nanotechnology for treatment, diagnosis, monitoring and control of biological systems is called “nanomedicine” [957]. Various nanoparticles offer unique properties as drug delivery systems and image agents. Several varieties are available, ranging from polymeric and metallic particles, to liposomes, dendrimers, microcapsules, etc. All of these systems are currently under development [958].

Amongst carbon-based materials, graphene is one of the most promising. A common approach for covalent functionalization of graphene employs GO, which offers a new class of solution-dispersible polyaromatic platform for performing chemistry.

The presence of the functional groups makes GO strongly hydrophilic [298,299], allowing water dispersion. Moreover, the functional groups allow GO to interact with a wide range of inorganic and organic species in non-covalent, covalent and ionic manner, so that

functional hybrids can be synthesized [959]. Furthermore, in contrast to pure graphene, GO is fluorescent over a broad range of wavelengths [960]. The use of tunable fluorescence has already been demonstrated in biological applications for sensing [961,962] and drug delivery [307]. Additional chemical processing and modification should continue towards this end.

Research on graphene for biomedical applications is progressing very quickly due to the previous know-how gained in the long and exhaustive research on CNTs. The surface chemistry is adaptable from one system to the other. Both materials show similar behaviour, with graphene having the advantage over CNT of its unique 2d shape.

Current challenges include the controlled chemical functionalization of graphene with functional units to achieve both good processability in various media, and fine tuning of various physico-chemical properties. One aim of the controlled surface oxidation is the production of anchoring points for additional surface groups such as:

-Attachment of biomolecules (peptides, DNA, growth factors…) via carboxyl groups: KOH/NaOH activation to induce carboxylic acid functional groups

-PEG coatings to get prolonged blood circulation half-life and avoid agglomeration.

-Sulfonation

-Halogenation. For instance, fluorination changes the surface hydrophobicity, while surface bromination provides a starting point for subsequent conversion into other functional groups, such as amines, anilines, alcohols, or thiols.

GO provides a robust framework in which two or more components can be incorporated to give multifunctional capabilities [963]. For instance, the conjugation of multiple components such as fluorescent molecules, tumour-targeting moieties, anticancer drugs or siRNA to GO represents a viable strategy not only to target human cancer, but also for imaging from inside the body by magnetic resonance or fluorescent imaging. The ability to simultaneously image and treat tumours with nanocarriers may prove advantages over conventional chemotherapies with the added value of reducing secondary effects. Nanocarriers are considered as molecular transporters to shuttle various types of biological molecules, including drugs, proteins, DNA, RNA, into cells by the endocytosis mechanism.

Requirements:

All materials intended to be used in nanomedicine, should be tested and investigate their effect on cells, animals and environment. Also, biosafety evaluation should be performed.

The small size of graphene flakes compared to microparticles allows them to interact more efficiently with cells, be safely injected and diffuse further into tissues and into and through individual cells. Thus, in this respect, particle size is a key parameter. Indeed, size and shape will control particle flow. Graphene sheets should flow along capillaries, lymphatics or tumour vessels without obstructions. Flow will also be dependent on surface functionalization, and aggregation of graphene flakes should be avoided at any time.

For imaging agents it is essential to have a rapid clearance from blood to obtain low background signals and high quality images. The surface charge and hydrodynamic diameter of the nanoparticles in the presence of plasma proteins are important for their bio-distribution, excretion and rapid clearance from blood.

Size control and/or size separation of various scales is necessary and note easily achieved to suitable interface with biological systems *in vitro* or *in vivo*. Ultracentrifugation and filtering is the common way to control size. Particles should be tracked inside the body by fluorescent agents, for example.

G1. Image and diagnose

Luminescent QDs are widely used for bio-labelling and bio-imaging. However, their toxicity and potential environmental hazard limit widespread use and *in-vivo* applications. Fluorescent bio-compatible carbon-based nanomaterials might be a more suitable alternative. Fluorescent species in the IR and NIR are useful for biological applications, because cells and tissues show little auto-fluorescence in this region [964]. The optical properties could be exploited in biological and medical research, such as imaging, and, consequently, diagnose.

Luminescent graphene based materials can now be routinely produced covering IR, visible and blue spectral ranges [166,305,307,960, 965]. Ref. [307] exploited photoluminescent GO for live cell imaging in the NIR with little background.

We will target the exploitation of graphene-based materials for imaging and diagnosis. The development of graphene in this field is parallel to the investigation of toxicity effects of GFNs. Another issue to be addressed is tracking the graphene-based materials inside cells.

G2. Hyperthermia: photo thermal ablation of tumours

Long and branched PEG coated CNTs and graphene exhibit prolonged blood circulation half-life [966]. This allows them to repeatedly pass through tumour vascularisation, benefiting tumour uptake via the enhanced permeability and retention effect (EPR) of cancerous tumours. LPE graphene, due to its 2d nature and the achievable 10-50nm dimensions [106], shows a better performance and distinctive behaviour with respect to CNTs, such as RES accumulation [942] and improved EPR [967], promoting high tumour passive targeting. This therapy is based on the energy transfer process occurring during the irradiation of a material generating heat sufficient for cell destruction at temperatures higher than 40ºC [968]. Both CNT and graphene are promising photothermal agents for *in vivo* tumour destruction. This therapy, prior developed for CNTs, was extended in the last few years also to graphene [969].

Hyperthermia treatment has the advantage of being less risky to the body, due to fewer side effects and the possibility of repeating treatment, as compared to surgery, chemotherapy and radiation therapy. Nano-hyperthermia is considered a promising alternative to conventional thermal ablation [970]. A variety of nanoparticles with specific properties such as electrical, optical, thermal etc., have been tested to induce various enhanced hypetermia with the aim to improve significantly the treatment efficiency of conventional heating [970].

Recently, it was reported that encapsulated iron oxide nanoparticles in a graphene matrix improve the properties connected to hyperthermia applications. Also, graphene decorated with V/Au or Pt nanoparticles improve the catalytic properties of the nanoparticles. Hydroxiapatite nanoparticles have been grown on graphene [971] and show excellent results as scaffolding according to “in vivo” experiments.

Biological systems mostly lack chromophores that absorb in the NIR region. Preliminary *in-vitro* and *in-vivo* experiments have already been carried out [970,972]. We aim to further pursue this promising line of research.

G3. Targeted drug delivery

Delivering medicines, see Fig. 80, to a patient in a controlled manner is one of the main research areas in nanomedicine. The nanodevices should deliver a certain amount of a therapeutic agent for a prolonged and controlled period of time to a targeted diseased area within the body.

Graphene's water soluble derivatives have potential application in drug delivery [307,928,973] and enzyme immobilization [974].

PEG-GO was applied as a nanocarrier to load anticancer drugs via non-covalent physisorption, and its cellular uptake was studied with satisfactory results [307]. The loading and release of doxorubicin hydrochloride, for example, was investigated as anticancer drug [975]. The loading ratio (weight ratio of loaded drug to carriers) of GO reached 200% more than others nanocarriers, such as nanoparticles that usually have a loading ratio lower than 100%. [976]. It was also reported that GO functionalized with sulfonic acid followed by covalent binding of folic acid molecules allows to specifically target human breast cancer cells [972]. Controlled loading of two cancer drugs as doxorubicin [973] and camptonectin [977] via π-π stacking and hydrophobic interactions was investigated.

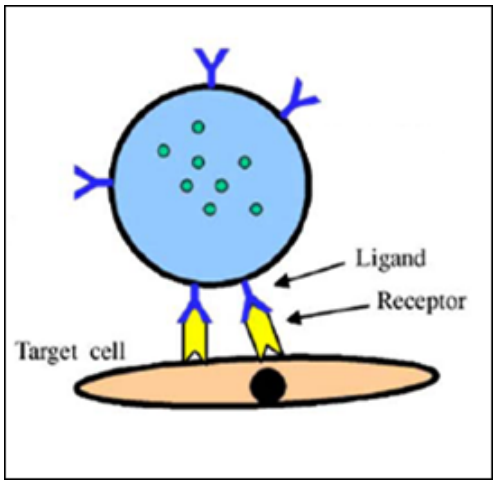

***Fig. 80**: Scheme of drug delivery*

These preliminary results pave the way for the engineering of graphene-based drug delivery. Our aim is to position graphene-based materials as the new platform of choice for drug delivery system.

G4. Bioelectronics and biosensors

The integration of electronics with biological components is one of the current challenges on the path towards bioelectronics, which holds great promise for developing prostheses for ill or injured organs as well as leading to a fundamental understanding of the brain.

Biology and electronics interface at three levels: molecular, cellular and skeletal. For any implanted bio-electronic material, the initial interactions at the bio-molecular level will determine long term performance. While bio-electronic is frequently associated with skeletal level enhancements (*i.e.* artificial muscles), electronic communication with living cells is of interest with a view to improving the results of tissue engineering or the performance of implants such as bionic eyes or ears.

In the quest towards bioelectronics, different materials were proposed and investigated. The operation in physiological media demands special material properties, such as electrochemical stability, biocompatibility, and electronic and chemical functionality. Among other materials, such as metals and semiconductors like Si and GaAs, carbon-based materials are expected to provide considerable advantages. Graphene offers a unique combination of physical, chemical

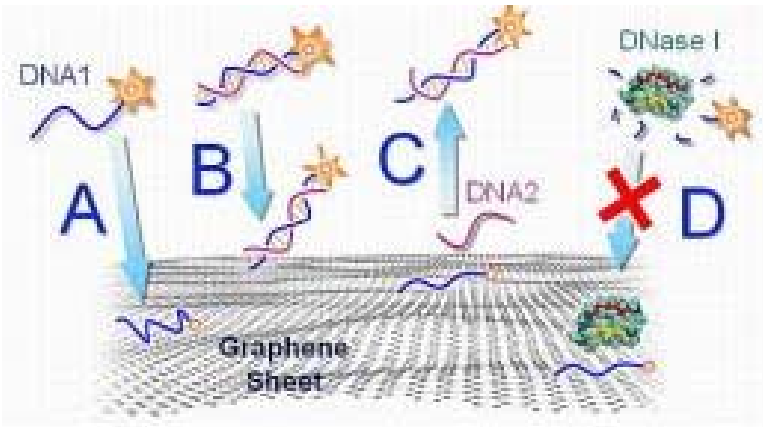

Figure 81: *Illustration of how fluorescent-tagged DNA interacts with functionalized graphene. Both ss-DNA (A) and ds-DNA (B) adsorb on the surface, but the interaction is stronger with ssDNA, causing the fluorescence on the ssDNA to darken more. C) A complimentary DNA nears the ssDNA and causes the adsorbed ssDNA to detach from the surface. D) DNA adsorbed onto graphene is protected from being broken down by enzymes [983].*

and electronic properties, which makes it a material of choice to surpass the state-of-the-art for bioelectronics and biosensor applications [752,978,979,980,981]. Indeed, graphene is impervious to the harsh ionic solutions found in the human body [982]. Moreover, graphene's ability to conduct electrical signals means it can interface with neurons and other cells that communicate by nerve impulse, or action potential [982]. These features make graphene very promising for next-generation bionic technology [979,982].

Current research in nano-biosensors is experiencing a fast growth due to the wide range of novel applications for human care.

A biosensor is a device for the detection of an analyte that combines a biological component with a physicochemical detector component. Immunosensors are used as analytical techniques for sensitive and selective detection of proteins, with wide applications in clinical diagnosis, biomedical research, food quality control and environmental monitoring, for example for the detection of cancer biomarkers (See Fig. 81) [983].

Since Si biocompatibility is low, the possible use of Si transistors in the human body, requires their coating with metal oxide (*i.e.* Ir oxide [984]) to boost their stability in solution [982]. Thus, other semiconductor technologies are also explored such as GaN [985], SiC [986] and diamond [987,988]. There is however an ever increasing interest in flexible biosensors [989]. Transparency is also important [988]. Another objective is to increase the device intelligence by integrating computation and decision power.

The use of graphene in biosensors should allow the development of flexible and transparent sensors. It also supposes an improvement of impedance and biocompatibility, with a high added value. It could also be used to implement grids of switches to control multi-arrays biosensors or integrate computing/decision power. The main applications are health, medical, pharmaceutical, impedance sensors, DNA chips, bio-lab on chip, bio-monitoring, and biomedical calibration.

This field requires transferable SLG or FLGs. Graphene on SiC could be also used. Good electrical properties, such as high carrier mobility, are not compulsory.

The main challenges are the functionalization for optimal sensing, contacts optimization, passivation optimization, switches arrays development.

The challenges for the development of ultra-sensitive graphene sensors on flexible substrates are many, but the impact of such technology would be even greater. Part of the technology challenges are similar to those shared by other applications of graphene. Amongst others, they include the preparation of high quality graphene films, novel concepts for surface nanostructuring using top-down semiconductor technology as well as nanopatterning with biomolecules based on (bottom-up) chemistry, etc.

One of the future targets is the stimulation of neurons with electric signals, studying how the live network reacts and modifies itself. One goal of such research could be neural prostheses that augment or restore damaged or lost functions of the nervous system. The development of brain implants on flexible substrates, which can record with high sensitivity the electrical and chemical activity of neurons, is fundamental

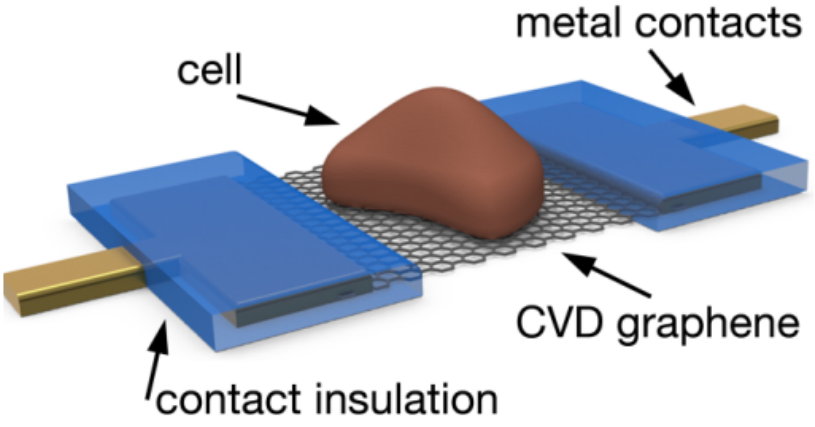

***Figure 82**: Schematic GFET with a cell on the gate area [979]*

for future applications. This is one of the limitations that graphene can solve. Indeed, in the current technology, most of the implants are based on metal electrodes [979]. However, in addition to some issues with biocompatibility and stability under the harsh environment conditions of in vivo implants, metal electrodes have a limited electronic functionality [979]. In that respect, the use of GFET would enable additional electronic functionality, due to the inherent amplification function of these devices. The sensing mechanism of these devices is simple: variations of the electrical and chemical environment in the vicinity of the FET gate region will be converted into a variation of the transistor current. Graphene can be employed to fabricate arrays of transistors [979] to detect the electrical activity of electrogenic cells (*i.e.* electrically active cells, see Fig. 82), overcoming the limitation of the Si technology, such as the relatively high electric noise and the integration with flexible substrates. Moreover, Si-based materials are not stable under physiological conditions [990,991].

Other important challenges for bioelectronics and biosensor applications are fabrication and *in electrolyte* characterization of graphene-based nanoelectrode arrays, *in vitro* studies of graphene biocompatibility, extensive electrophysiology characterization of the electrical and chemical graphene/cell synapse, etc.

Future challenges are the development of graphene-based bioelectronics and biosensor devices on flexible substrates such as parylene and kapton, already used for in vivo implants [979]. Such graphene-based flexible devices will be exploited for the development of brain implants. Moreover, studies will be conducted towards the realization of artificial retina based on flexible graphene FET array, see Fig. 83.

Indeed, degenerative retinal diseases like retinitis pigmentosa and age-related macular degeneration are amongst the most common origins of blindness [992,993]. Electronic visual prostheses represent a prospective therapeutic option of increasing importance in otherwise incurably impaired patients [993]. Several devices have been extensively tested on animal experiments, and according to the placement of the electrodes, possible stimulation sites are located subretinally, epiretinally, along the optic nerve or cortically [993]. The idea is to implant electrode arrays in the retina to inject current underlying, still-functional neural cells. Electrical patterns corresponding to visual images thereby can be created, and the brain can interpret them as vision [992,993]. However, anatomical, physiological and pathophysiological aspects must be considered for application [992,993]. The optimal integration of the prosthesis into the highly complex system of the visual pathway is fundamental to provide an appropriate retinal substitute. In this context, a major challenge needs to be overcome: how to build implants which adapt to the eye's curvature [994]. This is necessary to prevent unwanted cell growth beneath the implant other than being critical for good focus. Also, curved implants provide larger areas which can in turn capture larger images [995]. Because graphene is so thin, it could improve the interface between retinal implants and eye tissues.

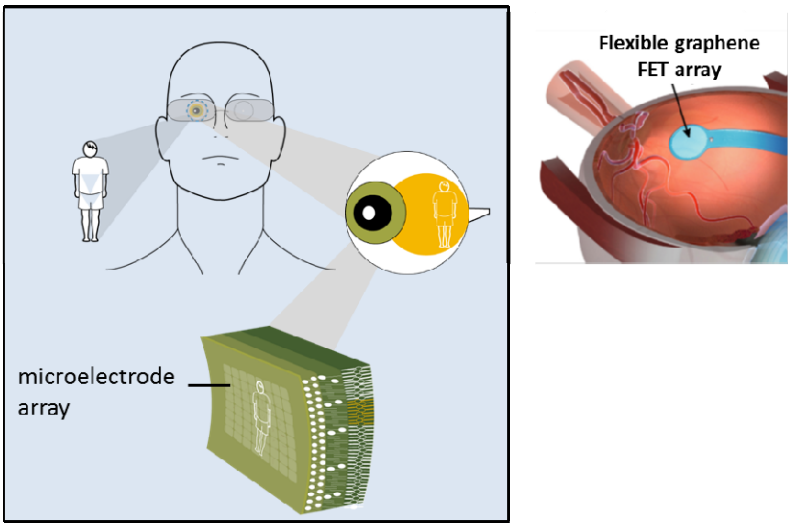

***Figure 83**: Concept for artificial retina based on flexible graphene FET array.*

Graphene can also be an ideal platform to tackle many other technical challenges. Indeed, more efficient wireless data and energy supply, combined with decreasing space requirement, longer durability and increased safety of the device are required [993]. Moreover, for high resolution, extremely small and densely mounted electrodes are needed. From today's perspective it is unclear in which approach graphene will lead to the best functional long-term results. However, it may be assumed that there will not be one single universal solution and the specific adjustment of a method to a particular disease will be fundamental [993]. In this context, the exceptional properties of graphene will play a crucial role, whether graphene layers are biocompatible with cultures of retinal neuron cells.

G5. Single-molecule genomic screening devices

Nanopores-nanosized holes that can transport ions and molecules are very promising devices for genomic screening, in particular DNA sequencing. The idea of using nanopores for DNA sequencing was proposed already more than 20 years ago [996]. The first experimental proof of translocation of DNA molecules was reported in 1996 using the biological protein pore α-hemolysin [997], albeit without sequence information. It has taken significantly more time to establish that single nucleotides can be discriminated within the traversing DNA, most prominently because the speed of translocating DNA has been too fast (on the order of a microsecond per base) to identify individual bases [998]. Sequencing DNA with nanopores offers exciting potential advantages over other sequencing technologies, but thus far the reading of the bases from a DNA molecule in a nanopore has been hampered by the fast translocation speed of DNA, together with the fact that several nucleotides contribute o the recorded signal. In theory, the basic idea of nanopores sequencing is straightforward: pass a DNA molecule from head to tail through a nanoscale pore in a membrane, and read off each base when it is located at the narrowest constriction of the pore, using the ion current passing through the pore to probe the identity of the base.

Several strategies have been tried to address the fast translocation speeds. Ss-DNA molecules were statically captured in the α-hemolysin nanopore using a DNA hairpin or a protein attached to the DNA end, either of which are too large to enter the pore. This allowed the detection of single-nucleotide mutations in the immobilized DNA [999,1000,1001]. In other work, α-hemolysin was modified to include a cyclodextrin ring that binds free mononucleotides, which therefore reside in the pore for long enough (up to 10 ms) to be distinguished by different ionic current levels for each of the four bases [1002].

More recently, the use of DNA polymerases that drive a DNA template through a nanopore in single-nucleotide steps as DNA is synthesized was advanced [1003]. Ref. [1003] found that a DNA polymerase from the phage phi29 was potentially suitable to this approach because it remained bound to DNA, even against the force of an applied voltage needed to insert the DNA into the pore. The polymerase, which processes DNA at a rate of about one nucleotide every ten milliseconds or slower, lowered the translocation speed of DNA by four orders of magnitude compared with freely translocating DNA [1003].

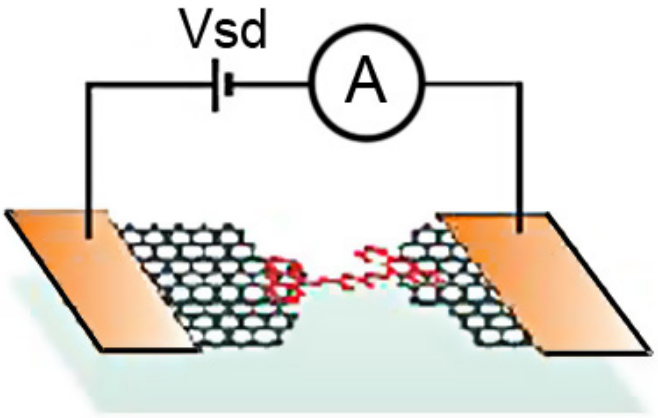

Figure 84: *Single-molecule transistor with graphene electrodes [1006].*

However, currently state of the art solid-state nanopores suffer the drawback that the channel constituting the pore is long, ~100 times the distance between two bases in a DNA molecule (0.5 nm for single-stranded DNA). Refs. [1004,1005] demonstrated that ultrathin nanopores fabricated in SLG can be exploited to realize single-molecule DNA translocation. The pores are obtained by placing a graphene flake over a microsize hole in a SiN_3 membrane and drilling a nanosize hole in the graphene using an e-beam [1004]. As individual DNA molecules translocate through the pore (DNA blocking the path for ionic current through the pore), characteristic temporary conductance changes are observed in the ionic current through the nanopore, setting the stage for future single-molecule genomic screening devices [1004].

Recently, 12nm gaps were formed between two graphene electrodes, which act as electrical contacts for molecules that bridge the gap, see Fig. 84 [1006]. The devices are stable at room temperature. This technique could be used to contact a variety of objects (molecules, particles), as well as to explore functionalization of the contacts. The graphene electrodes in turn can be contacted by a variety of metals, including ferromagnets, superconductors, etc. Building on the early experiments on DNA translocation [1004,1005], sensitivity will be pushed with the ultimate goal of resolving individual bases in ssDNA. As an alternative to measuring ionic currents, devices will be developed where tunnelling between two sheets of graphene is modified by the passage of a DNA molecule.

G6. Gene transfection

Genetic material (such as supercoiled plasmid DNA or siRNA), or even proteins such as antibodies, may be transfected [1007,1008,1009]. This consists in intentionally introducing nucleic acids or other biological active molecules into the cells [1010]. Gene therapy to cure diseases which are difficult for traditional clinical methods has been actively pursued for decades in both the academic world and in industry. The major obstacle in this area, however, is to develop non-viral based safe and efficient gene delivery vehicles, in which nanomaterials are usually involved [1011,1012,1013,1014]. Even though much progress has been reported concerning the use of cationic polymers and various inorganic nanomaterials such as CNTs, silica nanoparticles and nanodiamonds, as gene delivery vehicles [1011,1012,1013,1014,1015,1016], a lot more effort is still demanded to develop non-toxic nano-vectors with high gene transfection efficiency for potential gene therapy.

Graphene-based materials have already been demonstrated to benon-toxic nano-vehicles for efficient gene transfection [1017], by using GO bound with cationic polymers, polyethyleneimine (PEI) [1017]. Cellular toxicity tests revealed that GO-PEI complex exhibits significantly reduced toxicity to the treated cells compared to the bare PEI polymer [1017]. Moreover, the positively charged GO-PEI complexes are able to further bind with plasmid DNA (pDNA) for intracellular transfection of the enhanced green fluorescence protein (EGFP) gene in HeLa cells [1017]. While EGFP transfection with PEI appears to be ineffective, high EGFP expression is observed using the corresponding GO-PEI as the transfection agent [1017]. On the other hand, GO-PEI shows similar EGFP transfection effectiveness but lower toxicity compared with PEI [1017]. The first results [1017] suggest graphene to be a novel gene delivery nano-vector with low cytotoxicity and high transfection efficiency, promising for future applications in non-viral based gene therapy.

Whether and how the structure of graphene (e.g. size, thickness) would affect the gene transfection efficiency, however, remains an important question that requires further investigation within the graphene flagship consortium. Moreover, driven by thepreliminary results that highlight the promise of graphene as a novel nano-carrier for safe and efficient gene transfection, small interfering RNA (siRNA) with therapeutic functions may also be delivered by graphene complexes into cancer cells for potential gene therapy. This could be

further combined with graphene based chemotherapy and photothermal therapy as demonstrated earlier [307,942,973,976,1018], for future multimodal therapies of cancer.

G7. Thin Films, Joint prostheses (physical synthesis)

Some medical applications require hydrophobic materials with a non-cell adhesive surface, such as devices in contact with human blood (e.g., artificial heart valves) or joint prostheses in the friction area, while others need a cell-adhesive surface to assure complete tissue integration of the implanted material in the human body. Graphene may be another possibility as biocompatible coating if it performs better than the other carbon layers, as nano-diamond coatings [1019] or diamond-like carbon [854, 1020]. For this purpose, graphene-inks deposition techniques, as well as epitaxial growth, should adapt to have a competitive cost and be able to cover large and complexes surfaces. Moreover, graphene-based materials could be useful as coating of medical tools. However, this research area is still at the beginning of development with huge room for improvement [1021,1022].

Graphene can also be used as reinforcement for polymeric and ceramic prostheses. Indeed, small percentages of graphene or GO, improve polymer elongation at break leading to a tougher material performance and tribological behaviours. This was already tested in GO based nanocomposites and it is the starting point towards the exploitation of graphene based materials for the realization of prostheses [1023].

H. Science and Techology Roadmap for Graphene, related 2d crystals and hybrids

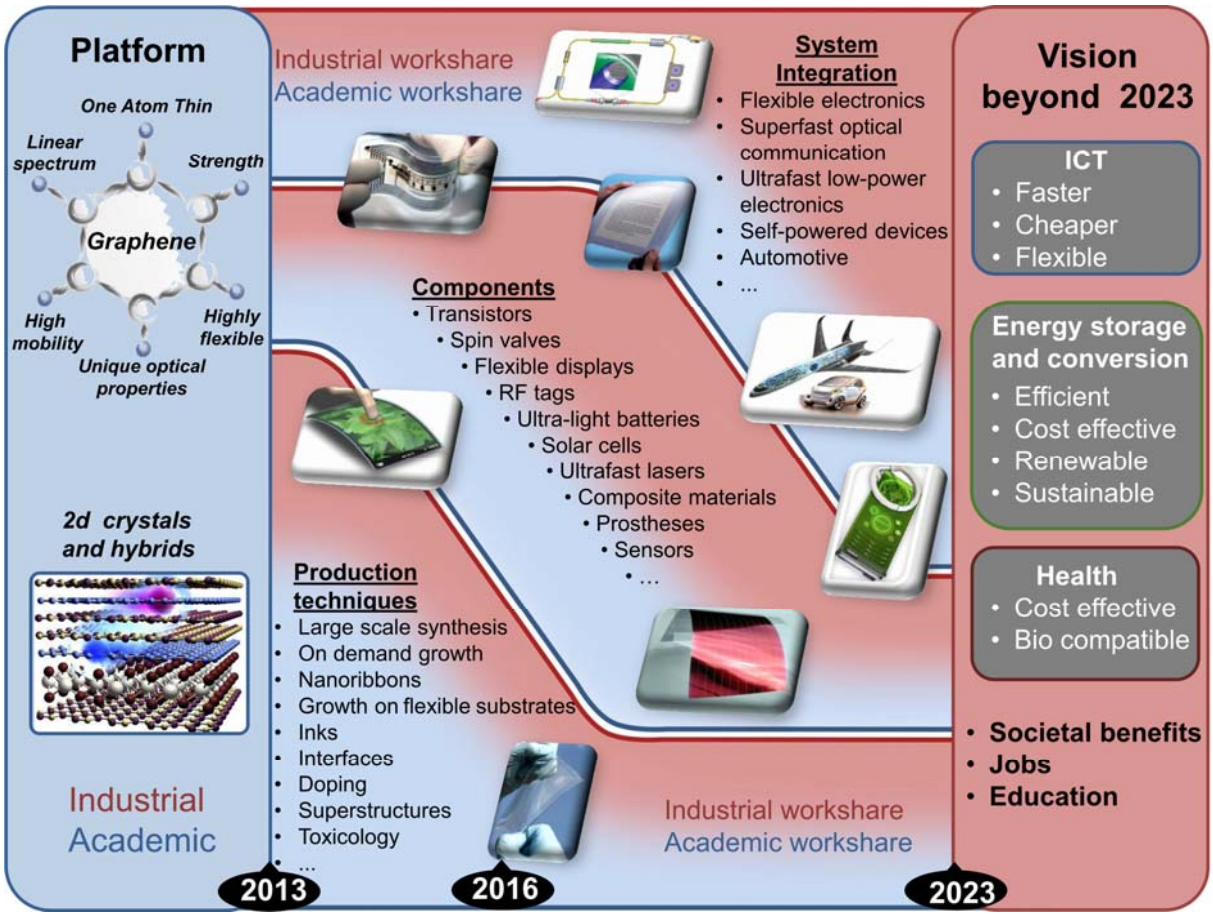

***Figure 85**: Strategic S&T roadmap for graphene, 2d crystals and hybrids.*

The S&T roadmap follows a hierarchical structure where the strategic level reported in Fig. 85 is connected to more detailed roadmap shown in Fig. 86 and analyses in different areas of science and technology. These general roadmaps are the condensed form of the topical roadmaps presented in the document and give the key technological targets that must be met in order for some key applications to become commercially competitive and the forecasts for when the targets are predicted to be met.

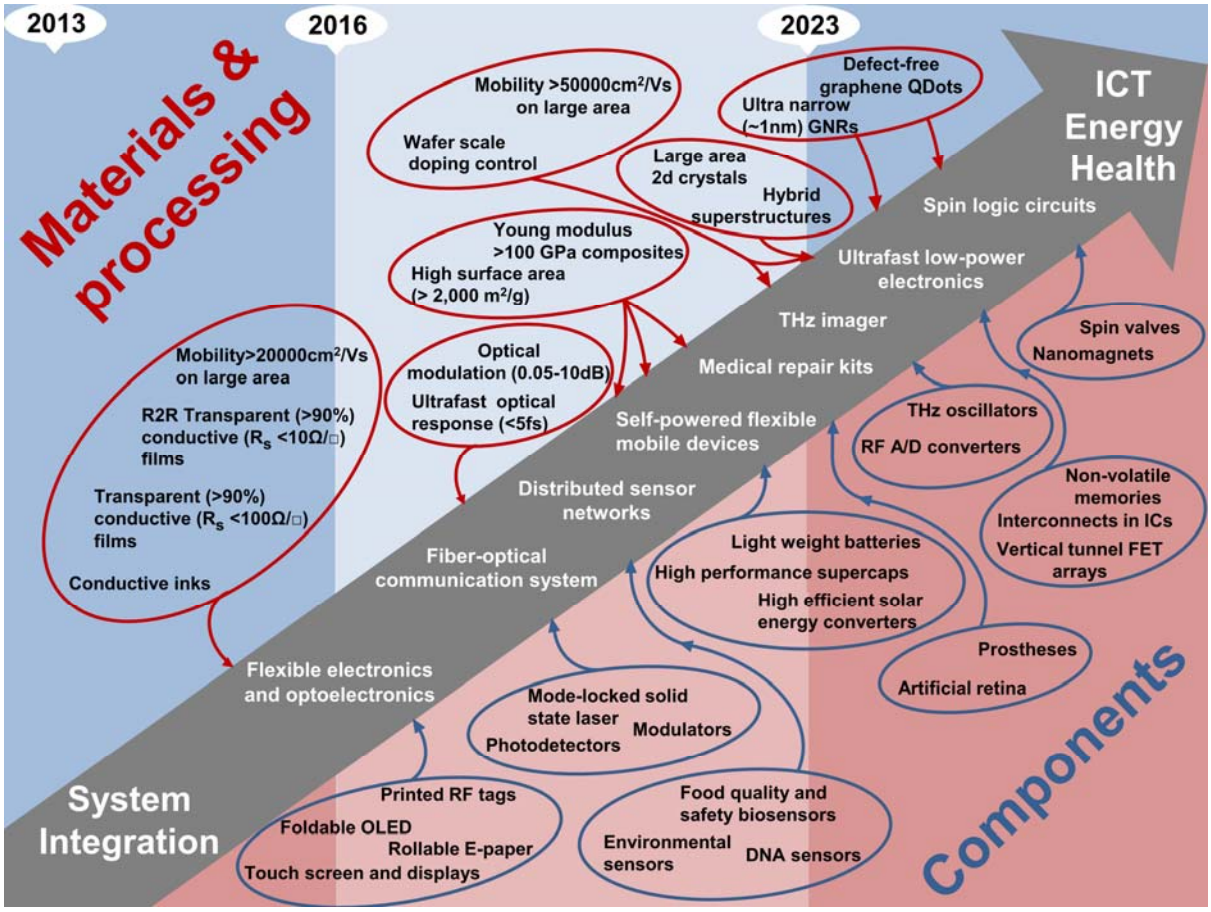

***Figure 86**: Detailed S&T roadmap for graphene, 2d crystals and hybrids.*

References

[1] H. Kroemer, *Rev. Mod. Phys.,***73,** 783 (2001)
[2] K. S. Novoselov, *et al, Science,* **306**, 666 (2004)
[3] K. Novoselov, *et al, PNAS***, 02**, 10451 (2005)
[4] S. Bae, *et al, Nature Nanotech.,* **5**, 1 (2010)
[5]http://ec.europa.eu/research/horizon2020/pdf/workshops/secure_clean_and_efficient_energy_challenge/summary_report_workshop_on_14_july_2011.pdf#view=fit&pagemode=none
[6] http://research.nokia.com/morph
[7] Y-M Lin, *et al, Science,* **332**, 1294 (2011)
[8] ITRS roadmap 2009, www.itrs.net (2011)
[9] C. Lee, *et al.*, *Science,* **321**, 385 (2008)

[10] D. E. Nikonov, G. I. Bourianoff, P. A. Gargini, *Journal of superconductivity and novel magnetism* **19**, 497 (2006)
[11] M. N. Baibich*, et al, Phys. Rev. Lett*., **61**, 2472 (1988)
[12] A. Fert, *Reviews of Modern Physics,* **80,** 1517 (2008)
[13] W. Y. Kim, K. S. Kim, *Nature Nanotech*., **3**, 408 (2008)
[14] W. Y. Kim, Y. C. Cheol, K. S. Kim, *J. Mater. Chem*. **18**, 4510 (2008)
[15] L. Brey, H. A. Fertig, *Phys. Rev. B*, **76**, 205435 (2007)
[16] A. Rycerz, *et al, Nature Phys.,* **3**, 172 (2007)
[17] R. Nandkishore, L. S. Levitov and A. V. Chubukov, *Nature Phys*. **8**, 158 (2012)
[18] D. Elias, *et al, Science,* **323**, 610 (2009)
[19] R. Nair, *et al, Small,* **6**, 2877 (2010)
[20] Y. Hernandez, *et al, Nature Nanotech.,* **3**, 563 (2008)
[21] T. Ramanathan, *et al, Nature Nanotech.,* **3**, 327 (2008)
[22] D. A. Dikin, *et al, Nature,* **448**, 457 (2007)
[23] J. Coleman, *et al, Science,* **331**, 568 (2011)
[24] A. S. Mayorov, *et al, Nano Lett.,* **11**, 2396 (2011)
[25] S. V. Morozov, *et al*, *Phys. Rev. Lett.,* **100**, 016602 (2008)
[26] F. Liu, P. M. Ming, and J. Li, *Phys. Rev. B,* **76**, 064120 (2007)
[27] J. S. Bunch, *et al.*, *Nano Lett.,* **8**, 2458 (2008)
[28] A. A. Balandin, *et al, Nano Lett*., **8**, 902 (2008)
[29] A. K. Geim, *Reviews of Modern Physics,* **83**, 851 (2011)
[30] J. Moser, A. Barreiro, and A. Bachtold, *Appl. Phys. Lett.,* **91**, 163513 (2007)
[31] K. S. Novoselov, *Reviews of Modern Physics,* **83**, 837 (2011)
[32] L. Britnell, *et al, Science***,** **35**, 947 (2012)
[33] A. K. Geim, *Science,* **324**, 1530 (2009)
[34] E. McCann and V. Fal'ko, *Phys. Rev. Lett*., **96**, 086805 (2006)
[35] J. Oostinga, *et al, Nature Mater.,* **7**, 151 (2007)
[36] Y. Zhang, *et al, Nature,* **459**, 820 (2009)
[37] M. G. Mohiuddin, *et al. Phys. Rev. B***,** **79**, 205433 (2009)
[38] V.I. Fal'ko, *Nature Phys.,* **3**, 161 (2007)
[39] A. C. Ferrari, *et al*., *Phys. Rev.Lett.,* **97**, 187401 (2006)
[40] A. C. Ferrari, *Solid State Comm*., **143**, 47 (2007)
[41] Y.-J. Yu, *et al. Nano Lett*., **9**, 3430 (2009)
[42] J. Martin, *et al.Nature Phys.,* **4**, 144 (2008)
[43] V. Cheianov, V. Fal'ko, *Phys. Rev. B,* **74**, 041403 (2006)
[44] M. Katsnelson, K. Novoselov, A. Geim, *Nature Phys.,* **2**, 620 (2006)
[45] V. Cheianov, V. Fal'ko, B. Altshuler, *Science,* **3,** 1252 (2007)
[46] K. Bolotin, *et al, Solid State Comm*., **146**, 351 (2008)
[47] X. Du, *et al, Nature Nanotech.,* **3**, 491 (2008)
[48] K. Novoselov,*et al, Nature,* **438**, 197 (2005)
[49] Y. Zhang, *et al, Phys. Rev. Lett*., **94**, 176803 (2005)
[50] Y. Zhang, *et al, Nature,* **438**, 201 (2005)
[51] K. Novoselov, *et al., Nature Phys.,* **2**, 177 (2006)
[52] K. von Klitzing, G. Dorda, M. Pepper, *Phys. Rev. Lett*., **45**, 494 (1980)
[53] X. Du, *et al.*, *Nature,* **462**, 192 (2009)
[54] A. Tzalenchuk, *et al, Nature Nanotech.,* **5**, 186 (2010)
[55] T.-J. Janssen, *et al, Phys. Rev. B,* **83**, 233402 (2011)
[56] K. Iwamoto, *et al, Appl. Phys. Lett*. **92**, 132907 (2008)
[57] I. Meric *et al. Nature Nanotech*., **3,** 654 (2008)
[58] S. Lara-Avila, *et al, Advanced Mater.,* **23**, 878 (2011)
[59] T. Maeda, H. Otsuka, A. Takahara, *Progress in Polymer Science,* **34**, 581 (2009)
[60] H. H. Hererscheֿ, *et al. Nature,* **446**, 56 (2007)
[61] W. K. Chong, C. H. Heng, *J. Appl. Phys*. **84**, 2977 (1998)
[62] J. A. Robinson, *et al*, *Appl. Phys. Lett.* **98**, 053103 (2011)

[63] P. Blake, *et al, Appl. Phys. Lett.,* **91**, 063124 (2007).
[64] D. Abergel, A. Russell, V. Fal'ko, *Appl. Phys. Lett.,* **91**, 063125 (2007)
[65] C. Casiraghi, *Nano Lett.,* **7,** 2711 (2007)
[66] F. Tuinstra, and J. L. Koenig, *J. Chem. Phys*., **53**, 1126 (1970)
[67] A. C. Ferrari and J. Robertson, *Philos. Trans. R. Soc. Ser. A,* **362**, 2477 (2004)
[68] J. Yan, *et al, Phys. Rev. Lett*., **98**, 166802 (2007)
[69] T.Ando,*J. Phys. Soc. Jpn.,* **76**, 024712 (2007)
[70] M. O. Goerbig, *et al, Phys. Rev. Lett.,* **99**, 087402 (2007)
[71] D. M.Basko, *et al, Phys. Rev. B,* **80**, 165413 (2009)
[72] A. Das, *et al, Nature Nanotech*., **3**, 210 (2008)
[73] L. M. Malard, *et al, Phys. Rev. B,* **76**, 201401 (2007)
[74] S. Pisana, *et al, Nature Mater*., **6**, 198 (2007)
[75] J.Yan, *et al, Phys. Rev. Lett.***105**, 227401 (2010)
[76] C. Faugeras, *et al., Phys. Rev. Lett*., **107**, 036807(2011)
[77] N. Ferralis, R. Maboudian, and C. Carraro, *Phys. Rev. Lett.,* **101**, 156801 (2008)
[78] A. Das, *et al, Nature Nanotech*., **3**, 210 (2008)
[79] C. Casiraghi, *et al., Appl. Phys. Lett.,* **91***,* 233108 (2007*)*
[80] C. Casiraghi, *et al, Nano Lett*., **9**, 1433 (2009)
[81] A. C.Ferrari, *et al, Phys. Rev. B,* **64**, 075414 (2001)
[82] A. Bostwick *et al, Nature Phys.,* **3**, 36 (2007)
[83] M. Mucha-Kruczynski, *et al, Phys. Rev. B,* **77**, 195403 (2008)
[84] M. Goerbig, *et al., Phys. Rev. Lett*., **99**, 087402 (2007)
[85] C. Faugeras, *et al, Phys. Rev. Lett*., **103**, 186803 (2009)
[86] D. Abergel, V. Fal'ko - *Phys. Rev. B,* **75**, 155430 (2007)
[87] A. Kuzmenko, *et al, Phys. Rev. B,* **80**, 165406 (2009)
[88] T. A. Land, *et al.,Surf. Sci*. , **264**, 261 (1992)
[89] A. K. Geim, K. S. Novoselov, *Nature Mater.,* **6**, 183 (2007)
[90] N. Tombros, *et al, Nature,* **448**, 571 (2007)
[91] E. Hill, *et al, IEEE Trans. Magn*., **42**, 2694 (2006)
[92] C. Jozsa, *et al. Phys Rev Lett*., **100**, 236603 (2008)
[93] A. Fert, *et al. Spin transport in graphene,* Graphene 2011
[94] J. W. McClure, *Phys. Rev.,* **104**, 666 (1956)
[95] A. Ney, *et al, Appl. Phys. Lett*., **99**,102504 (2011)
[96] P. Esquinazi, *et al, Phys. Rev. Lett*. **91**, 227201 (2003)
[97] R. R. Nair, *et al., Nature Phys*., **8**, 199 (2012)
[98] P. Y. Huang, *et al.Nature*, **469**, 389 (2011)
[99] L. Tapasztò, *et al, Appl. Phys. Lett*. **100**, 053114 (2012)
[100] K. S. Kim, *et al. Nature,* **457**, 706 (2009)
[101] A. Bagri, *et al, Nano Lett*. **11**, 3917 (2011)
[102] H-Y. Cao, H. Xiang, X. G. Gong, arXiv:1110.3483v1 (2011)
[103] O. V. Yagzev, *et al.Nature Mater.*, **9**, 806 (2010)
[104] J. Lahiri, *et al*. *Nature Nanotech.,* **5**, 326 (2010)
[105] D. Gunlycke, *et al.Phys. Rev. Lett.,* **106**, 136806 (2011)
[106] O. M. Maragó, *et al, ACS Nano,* **4**, 7515 (2010)
[107] Q. Yu, *et al. Nature Mater*., **10**, 443 (2011)
[108] W. Cai, *et al. Nano Lett*., **10**, 1645 (2010)
[109] S. Chen*, et al. ACS Nano,* **5**, 321 (2011)
[110] K. K. Gomes, *et al, Nature,* **483**, 306 (2012)
[111] A. Singha, *et al, Science,* **332** 1176 (2011)
[112] L. Tarruell, *et al, Nature,* **483**, 302 (2012)
[113] M. Gibertini, et al, *Phys. Rev. B,* **79**, 241406(R) (2009)
[114] G. Roati, *et al., Nature,* **453**, 895 (2008)

[115] H. Hwang, *et al, Phys. Rev. Lett.,* **99**, 226801 (2007)
[116] M. Polini, *et al, Phys. Rev. B,* **77**, 081411(R) (2008)
[117] C. F. Hirjibehedin, *Phys. Rev. B,* **65**, 161309(R) (2002)
[118] E. H. Hwang and S. Das Sarma, *Phys. Rev. B,* **75**, 205418 (2007)
[119] A. Principi, M. Polini, and G. Vignale, Phys. Rev. B, **80**, 075418 (2009)
[120] C. Albrecht, *et al, Phys. Rev. Lett*., **86**, 147 (2001)
[121] E. Räsänen, *et al*, arXiv:1201.1734
[122] S.-L. Zhu, S.-L., B. Wang and L.-M. Duan, *Phys. Rev. Lett*., **98**, 260402 (2007)
[123] D. Clément,*et al*, *Phys. Rev. Lett*., **102**, 155301 (2009)
[124] P. Soltan-Panahi, *et al., Nature Phys*., **7**, 434 (2011).
[125] C.L. Kane, E.J. Mele, *Phys. Rev. Lett*., **95**, 226801 (2005)
[126] C.R. Moon, C.P. Lutz, and H.C. Manoharan, *Nature Phys*., **4**, 454 (2008)
[127] K. Nakada, *et al., Phys. Rev. B,* **54**, 17954 (1996)
[128] K. Wakabayashi and T. Aoki, *Int. J.of Mod. Phys. B,* **16**, 4897 (2002)
[129] S. Lakshmi, *et al. Phys. Rev. B,* **80**, 193404 (2009)
[130] J. M. Poumirol, *et al. Phys. Rev. B,* **82** (2010)
[131] S. Roche, *Nature Nanotech*., **6**, 8 (2011)
[132] V. H. Nguyen, *et al. J. App. Phys*., **106** (2009)
[133] V. H. Nguyen, *et al*. *Appl. Phys. Lett*. **99,** 042105 (2011)
[134] M. Y. Han, *et al., Phys. Rev. Lett.,* **98,** 206805 (2007)
[135] P. Avouris, *Nano Lett.,* **10**, 4285 (2010)
[136] C. Stampfer, *et al, Phys. Rev. Lett.,* **102,** 056403(2009)
[137] S. Droscher, *et al*, *Phys. Rev*. B, **84** (2011)
[138] J. F. Dayen, *et al, Small,* **4**, 716 (2008)
[139] M. C. Lemme, *et al, ACSNano,* **3**, 2674 (2009)
[140] F. Molitor, *et al. Semicond. Sci. Tech.,* **25**, 034002 (2010)
[141] M. Y. Han, *et al. Phys. Rev. Lett.,* **104**,056801(2010)
[142] X. L. Li, *et a,. Science,* **319**, 1229 (2008)
[143] D. V. Kosynkin, *et al, Nature,* **458**, 872 (2009)
[144] L. Y. Jiao, *et al, Nature,* **458**, 877 (2009)
[145] A. J. M. Giesbers, *et al, Sol. Stat. Comm.,* **147**, 366 (2008)
[146] L. Tapaszto, *et al, Nature Nanotech.,* **3**, 397 (2008)
[147] S. S. Datta, *et al,Nano Lett.,* **8**, 1912 (2008)
[148] L. J. Ci, *et al, Adv. Mater*., **2**, 4487 (2009)
[149] L. C. Campos, *et al, Nano Lett.,* **9**, 2600 (2009)
[150] M-W. Lin *et al, Nanotechnology* **22** 265201 (2011)
[151] X. R. Wang, *et al, Phys. Rev. Lett.,* **100** (2008)
[152] J. M. Poumirol, *et al, Phys. Rev* B, **82,** 121401(R) (2010)
[153] C. O. Girit, *et al, Science,* **323**, 1705 (2009)
[154] X. T. Jia, *et al, Science,* **323**, 1701 (2009)
[155] B. Song, *et al, Nano Lett.,* **11**, 2247 (2011)
[156] J. M. Englert, *et al. Angewandte Chemie-International Edition,* **50**, A17 (2011)
[157] G. Franc, *et al, Phys. Chem. Chem. Phys*., **13**, 14283 (2011)
[158] J. Cai, *et al, Nature,* **466**, 470 (2010)
[159] G. Dobrick, *et al, physica status solidi (b)* **247***,* 896 (2010)
[160] L. Scipioni, *et al*, *Adv. Mater. Proc.* **166**, 27 (2008)
[161] D. C. Bell, *et al, Nanotechnology,* **20**, 455301 (2009)
[162] T. G. Pedersen, *et al, Phys. Rev. Lett.,* **100**, 136804 (2008)
[163] Y-W. Son, M. L. Cohen, S. G. Louie, Nature, **444**, 347 (2006)
[164] A. Cresti and S. Roche, *New Journal of Physics,* **11**, 095004 (2009)
[165] B. Krauss, *et al,Nano Lett.,* **10**, 4544 (2010)
[166] J. Lu, *et al, ACS Nano,* **3**, 2367 (2009)
[167] L. A. Ponomarenko, *et al, Science*, **320**, 356 (2008)
[168] Z. Chen *et al, Physica E,* **40**, 228 (2007)

[169] M. Kim *et al, Nano Lett.*, **10**, 1125 (2010)
[170] A. Sinitskii, and J. M. Tour, *IEEE Spectrum,* **47**, 28 (2010)
[171] N. Tombros, *et al, Nature Phys.,* **7**, 697 (2011)
[172] F. Prins, *et al, Nano Lett.,* **11**, 4607 (2011)
[173] X. Wang, *et al, Nature Nanotech*., **6**, 563 (2011)
[174] L. Dössel *et al, Angewandte Chemie,* **50**, 2540 (2011)
[175] J. Bai, *et al, Nature Nanotech*.**,5**, 190 (2010)
[176] C. Joachim, *et a., Adv. Mater.,* **24**, 312 (2012)
[177] F. Molitor, *et al, Appl. Phys. Lett.,* **94**, 222107 (2009)
[178] X. L. Liu, D. Hug, L. Vandersypen, *Nano Lett.,* **10**,1623 (2010)
[179] A. Allen, A. Martin, A. Yacoby, arXiv:1202.0820
[180] H. Zhang, *et al, Phys. Rev. Lett*. **108**, 056802 (2012)
[181] H. B. Heersche, *et al, Nature,* **446**, 56 (2007)
[182] A. Shailos, *et al, Europhys. Lett.,* **79**, 57008 (2007)
[183] X. Du, I. Skachko, and E. Y. Andrei, *Phys. Rev. B,* **77**, 184507 (2008)
[184] T. Dirks, *et al, Nature Phys*., **7**, 386 (2011)
[185] C. Beenakker, *Phys. Rev. Lett.,* **97**, 067007 (2006)
[186] M. Feigel'man, M. Skvortsov, K. Tikhonov, *JEPT Lett.,* **88**, 747 (2008)
[187] B. Kessler, *et al, Phys. Rev. Lett.,* **104**, 047001 (2010)
[188] P. Rickhaus, *et al, Nano Lett.*, **12**, 1942 (2012)
[189] C. H. Park, *et al, Nature Phys.,* **4,** 213 (2008)
[190] M. Barbier, *et al, Phys. Rev. B,* **77**, 115446 (2008)
[191] A. Isacsson, *et al, Phys. Rev. B,* **77**, 035423 (2008)
[192] R. Balog, *et al, Nature Mater*., **9**, 315 (2010)
[193] L. Brey and H. A. Fertig, *Phys. Rev. Lett.,* **103**, 046809 (2009)
[194] E. Marseglia, *Int. Rev. Phys. Chem.,* **3**, 177 (1983)
[195] J. Wilson, A. Yoffe, *Adv. Phys.,***18**, 193 (1969)
[196] T. Pillo, *et al, Phys. Rev. Lett.,* **83**, 3494 (1999)
[197] T. Pillo, *et al, Phys. Rev. B,* **64**, 245105 (2001)
[198] P. Aebi, *et al, J. Electron Spectrosc. Relat. Phenom.,* **117**, 433 (2001)
[199] K. Horiba, *et al, Phys. Rev. B,* **66**, 073106 (2002)
[200] L. Perfetti, *et al, Phys. Rev. Lett*., **90**, 166401 (2003)
[201] L. Perfetti, *et al, Phys. Rev. B,* **71**, 153101 (2005)
[202] M. Bovet, *et al, Phys. Rev. B,* **67**, 125105 (2003)
[203] M. Bovet, *et al, Phys. Rev. B,* **69**, 125117 (2004)
[204] F. Clerc F, *et al, J. Phys.: Condens. Matter,* **16**, 3271 (2004)
[205] S. Colonna, *et al, Phys. Rev. Lett*., **94**, 036405 (2005)
[206] T. Yokoya, *et al, Science***, 94**, 2518 (2001)
[207] F. Clerc, *et al, J. Phys. Condens. Matter.,* **19**, 355002 (2007)
[208] D. Moncton, J. Axe, F. Disalvo, *Phys. Rev. B,* **16**, 801 (1977)
[209] F. Gamble, B. Silbernagel, *J. Chem. Phys*., **63**, 2544 (1975)
[210] M. Hasan and C Kane, *Rev. Mod. Phys.,* **82**, 3045 (2010)
[211] Z. Ren, *et al, Phys Rev B,* **82**, 241306 (2010)
[212] Gmelin Handbook of Inorganic and Organometallic Chemistry, 8th ed.; Springer-Verlag: Berlin, 1995; Vol. B7
[213] A. Splendiani, *et al, Nano Lett.,* **10**, 1271 (2010)
[214] A. Radisavljevic, *et al, Nature Nanotech.,* **6**, 147 (2011)
[215] G. L. Frey, *et al, J. Am. Chem. Soc.,* **125**, 5998 (2003)
[216] A. Kudo, *J. Am. Chem. Soc.,* **121***,* 11459(1999)
[217] K. Chang, and W. X. Chen, *Journal of Materials Chemistry,* **21**, 17175 (2011)
[218] R. J. Smith, *et al, Adv. Mater.,* **23**, 3944 (2011)
[219] Y. Hu, *et al*, *Journal of Alloys and Compounds,* **509**, 10234 (2011)
[220] J. T. Zhang, *et al*, *J. Phys. Chem. C,* **115**, 6448 (2011)
[221] S. V. Prasad, J. S. Zabinski, *Nature,* **387**, 761 (1997)

[222] M. Osada and T. Sasaki, *J. Mater. Chem.*, **19**, 2503 (2009)
[223] P. Poizot, *et al., Nature,* **407**, 496 (2000)
[224] V. Subramanian, *et al, Journal of Power Sources*, **159**, 361 (2006)
[225] J. M. Soon and K. P. Loh, *Electrochemical and solid state letters*, **10**, A250 (2007)
[226] S. Bertolazzi, J. Brivio, A. Kis, *ACS Nano,* **5**, 9703 (2011)
[227] C. Li, *et al, Nanotechnology,* **20**, 6 (2009)
[228] Y. Yoon, K. Ganapathi and S. Salahuddin, *Nano Lett*., **11**, 3768 (2011)
[229] L. Esaki, *Phys. Rev.,* 109, 603 (1958)
[230] F. Jerome, S*cience,* **264**, 553 (1994)
[231] H. Min, *et al, Phys. Rev. B,* **78**, 121401 (2008)
[232] E. Vdovin, *et al*, *Science,* **290**, 122 (2000)
[233] M. Heiblum, *et al*, *Phys. Rev. Lett.,* **55**, 2200 (1985)
[234] T.J. Echtermeyer, *et al, Nature Comm.,* **2,** 458 (2011)
[235] E. A. Carter, *Science,* **321**, 800 (2008)
[236] D. Foerster, P. Koval, and D. Sánchez-Portal, *J. Chem. Phys.* **135**, 074105 (2011)
[237] H. Bethe, E. Salpeter, *Physical Review* **84**, 1232 (1951)
[238] P. H. Tan, *et al, Phys. Rev. Lett*., **99**, 137402 (2007)
[239] P. H. Tan, *et al, Physica E*, **40**, 2352 (2008)
[240] W. Kohn and L. J. Sham, *Phys. Rev. A*, **140**, 1133 (1965)
[241] http://www.prace-ri.eu/PRACE-offers-access-to-Europe-s
[242] F. Guinea, *Physics,* **3**, 1 (2010)
[243] T. Moldt, *et al*, *ACS Nano,* **5**, 7700 (2011)
[244] A. Balan, *et al, J. Phys. D: Appl. Phys.,* **43** 374013 (2010)
[245] K. B. Albaugh, *J. Electrochem. Soc.* **138** 3089 (1991)
[246] B. N. Chickov, *et al*, *Appl. Phys. A,* **63**, 115 (1996)
[247] F. Bonaccorso, et al, submitted (2012)
[248] S. Dhar, *et al*, *AIP Advances,* **1**, 022109 (2011)
[249] D. A. Sokolov, *et al.*, *J. Phys. Chem. Lett.,* **1**, 2633 (2010)
[250] M. Lotya, *et al, J. Am. Chem. Soc.,* **131**, 3611 (2009)
[251] T. Hasan, *et al, Phys. Status Solidi B,* **247**, 2953 (2010)
[252] T. Svedberg, K. O. Pedersen, The Ultracentrifuge, Oxford Univ.Press, London **1940**
[253] M. Behrens, Z.Hoppe-Seyler's*, physiol. Chem*., **258**, 27 (1939)
[254] U. Khan, *et al, Small,* **6**, 864 (2010)
[255] V. Alzari, *et al, J. Mater. Chem.,* **21**, 8727 (2011)
[256] J. W. Williams, *et al, Chem. Rev.*, **58**, 715 (1958)
[257] J. J. Crochet, *et al, J. Am. Chem. Soc.,* **129**, 8058(2007)
[258] M. S. Arnold, *et al, Nature Nanotech*., **1**, 60 (2006)
[259] F. Bonaccorso, *et al, J. Phys. Chem. C,* **114**, 17267 (2010)
[260] A. A. Green, M. C. Hersam, *Nano Lett.,* **9**, 4031 (2009)
[261] J. H. Lee, *et al, Adv. Mater.,* **21**, 4383 (2009)
[262] C. Valles, *et al, J. Am. Chem. Soc.,* **130**, 15802 (2008)
[263] D. Li, *et al*, *Natute Nanotech.,* **3**, 101 (2008)
[264] D. Nuvoli, *et al, J. Mater. Chem.,* **21**, 3428 (2011)
[265] X. An, *et al, Nano Lett.,* **10**, 4295 (2010)
[266] F. Torrisi, *et al, ACS Nano,* **6**, 2992 (2012)
[267] O. M. Maragó, *et al, Nano Lett*., **8**, 3211 (2008)
[268] O. M. Maragó, *et al, Physica E*., **8**, 2347 (2008)
[269] P. Jones, *et al, ACS Nano*, **3**, 3077 (2009)
[270] P. Schaffautl, *Journal fur praktische Chemie* **21**, 155 (1841)
[271] B. C. Brodie, *Ann. Chim. Phys*. **59**, 466 (1860)
[272] L. V. Staudenmaier, *Ber. Deut. Chem. Ges.* **31**,1481 (1898)
[273] A. Hérold, *Bull. Soc. Chim. Fr*., **187**, 999 (1955)
[274] L. B. Ebert, *Annu. Rev. Mater. Sci.,* **6**, 181(1976)
[275] R. C. Croft, *Quarterly Reviews, Chemical Society*, **14,** 1 (1960)

[276] A. Lerf, *et al, J. Phys. Chem. B,* **102**, 4477 (1998)
[277] P. K. Ang, *et al, ACS Nano*, **3**, 3587 (2009)
[278] F. L. Vogel, *et al, Materials Science and Engineering,* **31**, 261 (1977)
[279] G. M. T. Foley, *et al, Solid State Commun*., **24**, 371 (1977)
[280] J. Shioya, *et al, Synth.Met*., **14**, 113 (1986)
[281] W. Zhao, *et al, J. Am. Chem. Soc.,* **133**, 5941 (2011)
[282] J. Kwon, *et al, Small,* **7**, 864 (2011)
[283] N. B. Hannay, *et al, Phys. Rev. Lett*., **14**, 225 (1965)
[284] M. Winter, *et al., Adv. Mater.* **10**, 725 (1998)
[285] T. Weller, *et al, Nature Phys*., **1**, 39 (2005)
[286] N. Emery, *et al, Phys. Rev. Lett.,* **95**, 087003 (2005)
[287] N. Emery, *Adv. Mater*., **9**, 044102 (2008)
[288] R. Yazami, *Electrochim. Acta,* **45**, 87 (1999)
[289] R. Yazamiand and P. J.Touzain, *Power Sources,* **9**, 365 (1983)
[290] P. Arora, R.E. White and M. Doyle, *J. Electrochem. Soc.*, **145** 3647 (1998)
[291] G. Pistoia, *et al, Electrochim. Acta*, **41** 2683 (1996)
[292] G. Amatucci, *et al, J. Power Sources*, **69** 11 (1997)
[293] A. Catheline, *et al, Chem. Comm.,* **47**, 5470 (2011)
[294] C. Schafhaeutl, *Phil. Mag.,* **16**, 570 **(**1840)
[295] W. S. Hummers, R. E. Offeman, *J. Am. Chem. Soc.,* **80**, 1339 (1958)
[296] S. Stankovich, *et al, Carbon,* **45**, 1558 (2007)
[297] J. I. Paredes, *et al, Langmuir,* **24**,10560 (2008)
[298] S. Stankovich, *et al, Nature,* **442**, 282 (2006)
[299] C. Mattevi, *et al, Adv. Funct.Mater.,* **19**, 2577 (2009)
[300] J. M. Mativetsky *et al,J. Am. Chem. Soc.,* **132**, 14130 (2010)
[301] J. M. Mativetsky *et al, J. Am. Chem. Soc.,* **133**, 14320 (2011)
[302] M. Melucci, *et al, J. Mater. Chem.,* **20**, 9052 (2010)
[303] E. Treossi, *et al, J. Am. Chem. Soc.,***131**, 15576 (2009)
[304] X. Wang, *et al, Angew. Chem.,* **47**, 2990 (2008)
[305] T. Gokus, *et al, ACS Nano,* **3,** 3963 (2009)
[306] F. Bonaccorso, *et al, Nature Photon.,* **4**, 611 (2010)
[307] X. Sun, *et al, Nano Res.,* **1,** 203 (2008)
[308] S. Talapatra, *et al, Phys. Rev. Lett.* **95,** 097201 (2005)
[309] P. O. Lehtinen, *Phys. Rev. Lett*., **93,** 187202 (2004)
[310] O. V. Yazyev, L.Helm, *Phys Rev B*, **75**,125408 (2007)
[311] J. Hong, *et al, Small,* **9,** 1175 (2011)
[312] P. Coletti, *et al, Phys. Rev. B,* **81** (2010)
[313] W. Chen, *et al, J. Am. Chem. Soc.,* **129**, 10418 (2007)
[314] Y-L. Wang, *et al, Phys. Rev. B,* **82**, 245420 (2010)
[315] H. Huang, *et al, ACS Nano,* **3**, 3431 (2009)
[316] J. Mao, *et al, J. Am. Chem. Soc*., **131**, 14136 (2009)
[317] M. Roos, *et al, Beilstein J. Nanotechnol*., **2**, 365 (2011)
[318] V. Bellini, *et al, Phys. Rev. Lett.,* **106**, 227205 (2011)
[319] E. G. Acheson, Manufacture of Graphite. U.S. Patent 615648 (1896)
[320] C. Berger, *et al*, *J. Phys. Chem. B,* **108**, 19912 (2004)
[321] K. V. Emtsev, *et al, Nature Mater.,* **8**, 203 (2009)
[322] I. Forbeaux, *et al, Appl. Surf. Sci.,* **162**, 406 (2000)
[323] A. Charrier, *et al, J. Appl. Phys.,* **92**, 2479 (2002)
[324] A. Van Bommel, *et al, Surf. Science,* **48**, 463 (1975)
[325] K. V. Emtsev, *et al, Phys. Rev. B,* **77**, 155303 (2008)
[326] J. Hass, *et al, Phys. Rev. Lett.,* **100,** 125504 (2008)
[327] C. Riedl, *et al, Phys. Rev. Lett.***103**, 1 (2009)
[328] W. De Heer, *et al,Proc. Nat. Acc. of Science,* **108**, 16900 (2011)
[329] W. De Heer, arXiv:1012.1644v1.

[330] J. Hass*, et al, Appl. Phys. Lett*., **89**, 143106 (2006)
[331] J. Hass, *et al ,Phys Rev B,* **78**, 205424 (2008)
[332] G. M. Rutter, *et al, Science,* **317**, 219 (2007)
[333] R. Tromp, J.Hannon, *Phys Rev Lett.,* **102**, 106104 (2009)
[334] G. R. Fonda, *Phys, Rev*., **21**, 343 (1923)
[335] V. Sorkin, Y. W. Zhang, *Phys. Rev. B,* **81**, 085435 (2010)
[336] M. Sprinkle, *et al.,Nature Nanotech*., **5**, 727 (2010)
[337] J. Kedzierski, *et al, Electron Devices, IEEE Transactions,* **55**, 2078 (2008)
[338] H. Lipson, and A. R. Stokes, *Proc. R. Soc. Lond. A,* **181,** 101 (1942)
[339] J. Biscoe, and B. E. Warren, *J. Appl. Phys.,* **13,** 364 (1942)
[340] V. J. Kehrer, H. Leidheiser, *J. Phys. Chem.,* **58**, 550 (1954)
[341] L. C. Isett, J. M. Blakely, *Surf. Sci.,* **58**, 397 (1976)
[342] F. J. Himpsel, *et al, Surf. Sci*., **115**, L159 (1982)
[343] A. T. N'Diaye, *et al, Phys. Rev. Lett.,* **97**, 215501 (2006)
[344] J. C. Hamilton, J. M. Blakely, *Surf. Sci.,* **91**, 199 (1980)
[345] C. Oshima *et al, Japan. J. Appl. Phys.,* **16** 965 (1977)
[346] Y.Gamo, *et al*, *Surf. Sci.,* **374**, 61 (1997)
[347] A. Reina, *et al, Nano Lett.,* **9**, 30 (2009)
[348] A. Reina, *et al, Nano Research,* **2,** 509 (2009)
[349] Q. Yu, *et al, Appl. Phys. Lett*., **93,** 113103 (2008)
[350] M. E. Ramon, *et al, Acs Nano,* **5,** 7198 (2011)
[351] G. Bertoni, *et al, Phys. Rev. B,* **71**, 075402 (2004)
[352] J. Coraux, *et al, Nano Lett.,* **8**, 565 (2008)
[353] J. Vaari, *et al, Catal. Lett.,* **44**, 43 (1997**)**
[354] C. Busse, *et al, Phys. Rev. Lett.*, **107**, 036101 (2011)
[355] P. W. Sutter, J.-I. Flege, E. A. Sutter, *Nature Mater.,* **7**, 406 (2008)
[356] D. E. Jiang, *et al, J. Chem. Phys.,* **130**, 074705 (2009)
[357] H. Zhang, *et al, J. Phys. Chem. C,* **113**, 8296 (2009)
[358] M. M. Ugeda, *et al, Phys. Rev. Lett.,* **104**, 096804 (2010)
[359] A. T. N'Diaye, *et al, New J. Phys.,* **11**, 113056 (2009)
[360] C. Oshima, A. Nagashima, *Condens. Matter,* **9**, 1 (1997)
[361] A. N. Obraztsov, *et al, Carbon,* **45**, 2017 (2007)
[362] X. Li *et al*, *Science,* **324**, 1312 (2009)
[363] A. E. Karu, M. Beer, *J. Appl. Phys.,* **37**, 2179 (1966)
[364] X. Li, *et al, Nano Lett.,* **10,** 4328 (2010)
[365] Q. Yu, *et al, Nature Mater.,* **10**,443 (2011)
[366] P. Nemes-Incze, *et al, Appl. Phys. Lett.*, **99**, 023104 (2011)
[367] O. V. Yagzev, *et al, Nature Mater*., **9**, 806 (2010)
[368] J. Lahiri, *et al, Nature Nanotech.,* **5**, 326 (2010)
[369] D. Gunlycke, *et a,.Phys. Rev. Lett.,* **106**, 136806 (2011)
[370] Z. Li, *et al, ACS Nano,* **5**, 3385 (2011)
[371] P. Y. Huang, *et al, Nature,* **469**, 389 (2011)
[372] D. Kondo, *et al, Appl. Phys. Exp.,* **3**, 025102 (2010)
[373] M. H. Rummeli, *et al,ACS Nano,* **4**, 4206 (2010)
[374] B. L. French, *et al*, *J. Appl. Phys.,* **97**, 114317(2005)
[375] J. Wang, *et al, Carbon,* **42**, 2867 (2004)
[376] B. L. French, *et al, Thin Solid Film,* **494**,105 (2006)
[377] K. Kobayashi, *et al, J. Appl. Phys*., **101**, 094306 (2007)
[378] A. T. Chuang, *et al,Appl. Phys. Lett.,* **90**, 123107 (2007)
[379] A. T. H. Chuang, *et al, Diamond & Related Materials,* **15**, 1103 (2006)
[380] S. Mori, *et al, Diamond & Related Materials,* **20**, 1129 (2011)
[381] A. Dato, *et al*, *Nano Lett.,* **8**, 2012 (2008)
[382] J. Kim, *et al, Appl. Phys. Lett.* **98**, 091502 (2011)

[383] A. Guermonue, *et al, Carbon,* **49**, 4204 (2011)
[384] R. John, *et al*, *Nanotechnology,* **22**, 165701 (2011)
[385] http://www.electronicsweekly.com/Articles/20/01/2011/50309/first-silicon-carbide-mosfet-from-cree.htm
[386] S. Aisenberg, R. Chabot, *J. Appl. Phys*., **42**, 2953 (1971)
[387] J. Hwang, *et al, J. Crystal Growth,* **312***,* 3219 (2010)
[388] A. Michon, *et al, Appl. Phys. Lett.,* **97***,*171909 (2010)
[389] W. Strupinski, *et al, Nano Lett.,* **11***,*1786 (2011)
[390] M. A. Fanton, *et al, ACS Nano,* **5***,* 8062 (2011)
[391] J. Sun, *et al , Appl. Phys. Lett*., **98**, 252107 (2011)
[392] A. Scott, *et al, Appl. Phys. Lett.,* **9**,073110 (2011)
[393] X. Ding, *et al, Carbon,* **49**, 2522 (2011)
[394] C. R. Dean, *et al, Nature Nanotech*., **5**, 722 (2010)
[395] Y. Kubota, *et al, Science,* **317**, 932 (2007)
[396] Y-M. Lin, *et al, Science,* **327**, 662 (2010)
[397] A. Y. Cho, J. R. Arthur *Prog. Solid State Chem.***10**, 157 (1975)
[398] V. Umanski, *et al*, *J. Cryst. Growth*, **311**, 1658 (2009)
[399] C. K. Ko, *et al*, *Electronic Letters,* **32**, 2099 (1996)
[400] J. Hackley, *et al, Appl. Phys. Lett., **95**,* 133114 (2009)
[401] O. Seifarth, *et al,* DOI: 10.1109/SCD.2011.6068742
[402] A. Barreiro, *et al*, arXiv:1201.3131v1
[403] B. Westenfelder, *et al, Nano Lett*., **11**, 5123 (2011)
[404] J. J. Schneider, *Chem Cat Chem,* **3**, 1119 (2011)
[405] A.Turchanin, *et al, ACS Nano,* **5**, 3896 (2011)
[406] J. Wu, W. Pisula, K. Müllen, *Chem. Rev.* **107**, 718 (2007).
[407] Q. H. Wang, M. C. Hersam, *Nature Chemistry* **1**, 206 (2009).
[408] C.-A. Palma, P. Samorì, *Nature Chem*., **3**, 431(2011)
[409] A. Candini, *et al, Nano Lett.,* **11,** 2634 (2011)
[410] X. Yan, *et al. Nano Lett.***, 10**, 1869 (2010)
[411] L. Zhi, K. A. Müllen, *J. Mater.Chem.,* **18**, 1472 (2008)
[412] A. Luican, *et al*, *Phys. Rev. Lett*., **106**, 126802 (2011)
[413] G. Eda, G. Fanchini, M. Chhowalla *Nature Nanotech.,* **3**, 270 (2008)
[414] X. Li, *et al, Nature Nanotech*, **3**, 538 (2008)
[415] P. Blake, *et al, Nano Lett.,* **8**, 1704 (2008).
[416] T.Hasan, *et al,*submitted 2012
[417] M. Qian, *et al, Nanotechnology,* **20,** 425702 (2009)
[418] A. Vijayaraghavan, *et al, ACS Nano,* **3,** 1729 (2009)
[419] Y. Noh, *et al, Nature Nanotech.,* **2**, 784 (2007)
[420] S. Nedev, *et al, Nano Lett.,* **11**, 5066 (2011)
[421] N. Alem, *et al, Phys. Rev. B,* **80** 15 (2009)
[422] C. Lee, *et al, ACS Nano,* **4**, 2695 (2010)
[423] K. F. Mak, *et al, Phys. Rev. Lett.,* **105**, 4 (2010)
[424] H. Li, *et al.,Small* DOI: 10.1002/smll.201101016 (2011)
[425] A. Ayari, *et al, J. Appl. Phys.,* **101***,* 1 (2007)
[426] B. Radisavljevic, M. B. Whitwick, A. Kis, *ACS Nano,* **5**, 9934 (2011)
[427] W. Q. Han, *et al,Appl. Phys. Lett*., **93** 22 (2008)
[428] Y. Lin, T. V. Williams, J. W. Connell, *J. Phys. Chem. Lett.,* **1**, 277 (2010)
[429] Y. Lin, *et al*, *J. Phys. Chem. C,* **115**, 2679 (2011)
[430] J. H. Warner, *et al,ACS Nano,* **4**, 1299 (2010)
[431] C. Y. Zhi, *et al, Adv. Mater*., 21, 2889 (2009)
[432] K. G. Zhou, *et al*, *Angewandte Chemie-International Edition,* **50**, 10839 (2011)
[433] G. Cunningham, *et al*, *ACS Nano* 2012**,** *in press*.
[434] M. S. Strano, *et al, J. Nanoscience and Nanotechnology,* **3**, 81 (2003)
[435] V. Buck, *Thin Solid Films,* **198**, 157 (1991)

[436] A. K. Rai, *et al, Surf. Coat. Technol*., **92**, 120 (1997)
[437] A. Matthäus, *et al, J. Electrochem. Soc*., **144**, 1013(1996)
[438] M. Genut, *et al, Thin Solid Films,* **217**, 91(1992)
[439] M. Hirano, S. Miyake, *Appl. Phys. Lett.,* **47**, 683 (1985)
[440] K.Ellmer, in: Low Temperature Plasmas edited by R. Hippler, H. Kersten, M. Schmidt, and K. H. Schoenbach (Wiley-VCH, Berlin, 2008), p. 675.
[441] J. Szczyrbowski, *et al, Thin Solid Films,* **351**, 254 (1999)
[442]A. Nagashima, *et al*, *Phys. Rev. B,* **51**, 4606 (1995)
[443] Y.Zhang, *et al,* ArXiv.1111.5072
[444] Q. Li, *et al, Nano Lett.,* **4**, 277 (2004)
[445] H. Zheng, *et al,Nano Lett.,***10**, 5049 (2010)
[446] B. Li, *et al, ACS Nano,* **5**, 5957 (2011)
[447] L. A. Ponomarenko,*et al,Phys. Rev. Lett*., **102**, 206603 (2009)
[448] D. Li, *et al*, *Naure Nanotech.,* **3**, 101 (2008)
[449] T. Tanaka, *et al*, *Surface Review and Letters,* **10**, 721 (2003)
[450] L. Ponomarenko, *et al*, *Nature Phys.,* **7**, 958 (2011)
[451] V. M. Pereira, and A. H. C. Neto, *Phys. Rev. Lett*., **103**, 046801 (2009)
[452] M. Mucha-Kruczynski, I. Aleiner, V. Fal'ko, *Phys. Rev. B,* **84**, 041404 (2011)
[453] A. Mayorov, *et al, Science,* **333**, 860 (2011)
[454] Z. Liu, *et al, Nano Lett.,* **11**, 2032 (2011)
[455] P. Vogt, *al, Phys, Rev. Lett*.DOI: 10.1103/PhysRevLett.108.155501 (2012)
[456] G. G. Guzman-Verri and L.C. Lew Yan Voon, *Phys. Rev. B***76**, 75132 (2007)
[457] M. Houssa, *et al, J. Electrochem.Soc.,* **158**, H107 (2011)
[458] P. De Padova, *et al, Appl. Phys. Lett*., **96**, 261905 (2010)
[459] C-C. Liu, *et al, Phys. Rev. Lett*., **107**, 076802 (2011)
[460] X-L. Qi and S-C. Zhang, *Rev. Mod. Phys*., **83**, 1057 (2011)
[461] B. H. Hong, *"Synthesis and applications of graphene for flexible electronics" Graphene 2011 at Imagine nano2011*
[462] S. Y. Zhou, *et al, Nature Mater*., **6**, 770 (2007)
[463] T. Kawasaki, *et al, Surf. Rev. Lett.,* **9**, 1459 (2002)
[464] P. Shemella and S. K. Nayak, *Appl. Phys. Lett*., **94**, 032101 (2009)
[465] X. Peng and R. Ahuja, *Nano Lett*., **8** 4464 (2008)
[466] D. Wei, *et al, Nano Lett.,* **9**, 1752 (2009)
[467] L. Ci, *et al, Nature Mater.,* **9**, 430 (2010)
[468] T. O. Wehling, *et al, Nano Lett.,* **8**, 173 (2008)
[469] E. McCann, *Phys. Rev. B,* **74,** 161403 (2006)
[470] E. V. Castro, *et al, Phys. Rev. Lett.,* **99**, 216802 (2007)
[471] T. Ohta, *et al, Science*, **313**, 951 (2006)
[472] F. Schwierz, *Nature Nanotech.,* **5**, 487 (2010)
[473] F. Cervantes-Sodi, *et al, Phys. Rev. B*, **77**, 165427 (2008)
[474] G. E. Moore, in *Tech. Dig. ISSCC* 20–23 (IEEE, 2003)
[475] F. Schwierz, H. Wong, J. J. Liou, *Nanometer CMOS* (Pan Stanford, 2010)
[476] J. D. Meindl, Q. Chen, and J. A. Davis, *Science*, **293**, 2044 (2001)
[477] M. C.Lemme, *et al, IEEE Electron Dev. Lett.,* **28**, 282 (2007)
[478] Y-M. Lin, *et al, Nano Lett.,* **9,** 422 (2009)
[479] L. Liao, *et al, Proc. Natl Acad. Sci. USA,* **107,** 6711 (2010)
[480] D. B. Farmer, *et al, Nano Lett.,* **9,** 4474 (2009)
[481] I. Meric, *et al,* in *Tech. Dig. IEDM 2008*, paper 21.2 (IEEE, 2008)
[482] J. Kedzierski, *et al, IEEE Trans. Electron. Dev.,* **55,** 2078 (2008)
[483] J. S. Moon, *et al, IEEE Electron Dev. Lett.,* **30,** 650 (2009)
[484] J. Kedzierski, *et al, IEEE Electron Dev. Lett.,* **30,** 745(2009)
[485] L. Liao*, et al, Nanotechnology,* **21,** 015705 (2010)
[486] A. Konar, T. Fang, and D. Jena, *Phys. Rev. B*, **82**, 115452 (2010)
[487] A. K. Geim, MRS 2009 keynote lecture

[488] S.-L. Li, *et al, Nano Lett*., 10, 2357 (2010)
[489] S.-L. Li, *et al, ACS Nano,* **5**, 500 (2011)
[490] W. Kim, *et al, Nano Lett.,* **3**, 193 (2003)
[491] D. Estrada, *et al, Nanotechnology*, **21**, 085702 (2010)
[492] E. U. Stützel, *et al,Small,* **6**, 2822 (2010)
[493] A. Sagar, *et al, Appl. Phys. Lett.,* **99**, 043307 (2011)
[494] S.-J. Han, *et al, Nano Lett*., **11**, 3690 (2011)
[495] E. Guerriero, *et al, Small,* **8**, 357 (2012)
[496] L. G. Rizzi, *et al*, submitted (2012)
[497] B. N. Szafranek, *et al, Nano Lett*., **12**, 1324 (2012)
[498] L. Liao, *et al, Nano Lett.,* **10**, 1917 (2010)
[499] X. Wang, *et al, Phys. Rev. Lett.,* **100,** 206803 (2008)
[500] F. Xia, *et al, Nano Lett.,* **10,** 715 (2010)
[501] A. Naeemi and J. Meindl, *IEEE Electron Device Lett.*, **28**, 428 (2007)
[502] S. K. Banerjee, *et al*, *IEEE Electron Device Lett.*, **28**, 428 (2007)
[503] S. M. Sze, *Physics of Semiconductor Devices* (Wiley-Interscience, New York, 1981).
[504] R. Sordan, F. Traversi, and V. Russo, *Appl. Phys. Lett*., **94**, 073305 (2009)
[505] F. Traversi, V. Russo, and R. Sordan, *Appl. Phys. Lett*., **94**, 223312 (2009)
[506] H. Wang, *et al, IEEE Electron Device Lett.,* **30**, 547 (2009)
[507] N. Harada, *et al,*, *Appl. Phys. Lett*., **96**, 012102 (2010)
[508] X. Yang, *et al, ACS Nano,* **4**, 5532 (2010)
[509] X. Yang, *et al,IEEE Electron Device Lett*., **32**, 1328 (2011)
[510] V. Barone, O. Hod, and G. E. Scuseria, *Nano Lett*., **6**, 2748 (2006)
[511] Y.-W. Son, M. L. Cohen, and S. G. Louie, *Phys. Rev. Lett*., **97**, 216803 (2006)
[512] J. E. Ayers, *Digital Integrated Circuits: Analysis and Design* (CRC Press, Boca Raton, 2009)
[513] H. Schmidt, *et al, Appl. Phys. Lett.,* **93**, 172108 (2008)
[514] A. Sagar, *et al, Nano Lett*. **9**, 3124 (2009)
[515] D. B. Farmer, *et al*, Nano Lett.**9**, 388 (2009)
[516] T. Lohmann, K. von Klitzing, and J. H. Smet, *Nano Lett*., **9**, 1973 (2009)
[517] A. Gutin, *et al, IEEE T. Circuits Syst.,* **58**, 2201 (2011)
[518] H. Knapp, *et al, IEEE Bipolar/BiCMOS Circuits and Technology Meeting (BCTM)* (2010) pp. 29–32.
[519] A. Konczykowska, *et al, 18th International Conference on Microwave Radar and Wireless Communications (MIKON)* (2010) pp. 1–4.
[520] N. Joram, *et al,Semiconductor Conference Dresden (SCD)* (2011) pp. 1–4
[521] N. Joram, *et al,IEEE MTT-S International Microwave Symposium Digest* (MTT) (2011) pp 1–4
[522] K.-T. Park , *et al,IEEE J. Solid-State Circ.,* **43**, 919 (2008)
[523] Y. Shin, in VLSI Circuits, 2005. Digest of Technical Papers (2005) pp. 156–159
[524] D. Nobunaga, *et al,* in *Solid-State Circuits Conference, 2008.ISSCC 2008. Digest of Technical Papers. IEEE International* (2008) pp. 426–625
[525] S. K. Hong, *et al, IEEE Electron Device Lett*., **31**, 1005 (2010)
[526] A. J. Hong, *et al, ACS Nano,* **5**, 7812 (2011)
[527] J. K. Park, *et al, Nano Lett.,* **11**, 5383 (2011)
[528] N. Zhan, *et al, Appl. Phys. Lett.,* **99**, 113112 (2011)
[529] C. Wu, *et al, Appl. Phys. Lett.***100**, 042105 (2012)
[530] A. Hsu, H. Wang, J. Wu, J. Kong, and T. Palacios, *IEEE Electron Device Lett.*, **31**, 906 (2010)
[531] T. Palacios, *Nature Nanotech.*, **6**, 464 (2011)
[532] G. Liu, *et al, Appl. Phys. Lett.,* **95**, 033103 (2009)
[533] Q. Shao, *et al, IEEE Electron Device Lett*., **30**, 288 (2009)
[534] S. Rumyantsev,*et al, Journal of Physics: Condensed Matter,* **22**, 395302 (2010)
[535] A. A. Balandin, *Nature Mater*., **10**, 569 (2011)
[536] Y. Wu, *et al, Nature,* **472**, 74 (2011)
[537] L. Liao, *et al, Nano Lett*. , DOI:10.1021/nl201922c (2011)
[538] J. L. Hood, *Audio Electronics* (Newnes, Oxford, 1999)

[539] A. D. Liao, *et al,Phys. Rev. Lett.,* **106**, 256801 (2011)
[540] K.-J. Lee, A. Chandrakasan, and J. Kong, *IEEE Electron Device Lett*., **32**, 557 (2011)
[541] M. C. Beard, G. M. Turner, C. A. Schmuttenmaer, *J. Phys. Chem. B*, **106**, 7146 (2002)
[542] F. Schwierz and J. J. Liou *Modern Microwave Transistors – Theory, Design, and Performance* (Wiley, 2003).
[543] X. Duan, *et al, Nature,* **467**, 305 (2010)
[544] C. A. Moritz, P. Narayanan, C. O. Chui, *Nanoscale application specific integrated circuits. Nanoelectronic Circuit Design*. 1st ed. Niraj K. Jha and Deming Chen, New York: Springer, 2011. 215-76
[545] S. Datta and B. Das, *Appl. Phys. Lett.,* **56**, 665 (1990)
[546] Y. Zheng,*et al, Phys. Rev. Lett*., **105,** 166602 (2010)
[547] H. Young Jeong, *et al, Nano Lett.,* **10,** 4381 (2010)
[548] M. I. Katsnelson, *Mater. Today*, **10**, 20 (2007)
[549] T. Yokoyama, *Phys. Rev. B*, **77**, 073413 (2008)
[550] W. Han and R.K. Kawakami, *Phys. Rev. Lett.,* **107,** 047207 (2011)
[551] T. Maassen, *et al, Phys. Rev. B,* **83**,115410 (2011)
[552] W. Han, *et al, Phys. Rev. Lett*. **105**, 167202 (2010)
[553] W. H. Wang, , *et al, Appl. Phys. Lett.* **93**, 183107 (2008)
[554] A. Ghirri, *et al, Adv. Funct. Mat.,* **20**, 1552 (2010)
[555] M. Lopes, *et al, ACS Nano,* **4**, 7531 (2010)
[556] B. Dieny, *et al, J. Appl. Phys*., **69**, 4774 (1991)
[557] D. A. Abanin, *et al, Science,* **332**, 328 (2011)
[558] D. Loss, D. Di Vincenzo, *Phys. Rev. A,* **57**, 120 (1998)
[559] B. Trauzettel, *et al, Nature Phys.,* **3**, 192 (2007)
[560] R. J. Gordon, *MRS Bulletin,* **8**, 53 (2000)
[561] I. Hamberg, C. G. Granqvist, *J. Appl. Phys.,* **60**, R123 (1986)
[562] L. Holland, G. Siddall, *Vacuum,* **3**, 375 (1953)
[563] T. Minami, *Semicond. Sci. Technol.,* **20**, S35 (2005)
[564] C. G. Granqvist, *Sol. Energy Mater. Sol. Cells,* **91**, 1529 (2007)
[565] C. D. Sheraw, *et al, Appl. Phys. Lett.,* **80**, 1088 (2002)
[566] J. Y. Lee, *et al, Nano Lett.,* **8**, 689 (2008)
[567] S. De, *et al, ACS Nano,* **3**, 1767 (2009)
[568] H. Z. Geng, *et al, J. Am. Chem. Soc.,* **129**, 7758 (2007)
[569] Z. Wu, *et al*, *Science,* **305**, 1273 (2004)
[570] S. De, J. N.Coleman, *ACS nano,* **4**, 2713 (2010)
[571] D. R. Sahu, S. Y. Lin, J. L. Huang, *Appl. Surf. Sci.,* **252**, 7509 (2006)
[572] Y. Zhu, *et al*, *ACS Nano*, **5**, 6472 (2011)
[573] S. Gilje, *et al.,Nano Lett.***7**, 3394 (2007)
[574] X. Wang, L. Zhi, K. Mullen, *Nano Lett.,* **8**, 323 (2007)
[575] H. A. Becerril, *et al, ACS Nano,* **2**, 463 (2008)
[576] J. Wu, *et al, ACS Nano,* **4**, 43 (2009)
[577] T. Hasan, *et al,* Graphene Technology: Production, Assembly and Applications 15–16 July 2011, University of Cambridge, Cambridge, (UK)
[578] P. J. King,*et al, ACS Nano***4**, 4238 (2010)
[579] P. Matyba,*et al*,*ACS Nano* **4**, 637 (2010)
[580] C. Thiele and R. Das, *IDTechEx* www.IDTechEx.com
[581] G. Giovannetti, *et al, Phys. Rev. Lett.,* **101,** 026803 (2008)
[582] K. F. Mak, *et al, Phys. Rev. Lett*., 105, 136805 (2010)
[583] T. Korn, *et al, Appl. Phys. Lett*. 99, 102109 (2011)
[584] G. Eda, *et al, Nano Lett.*, **11**, 5111 (2011)
[585] T. Maeda, *Display* **5**, 82 (1999)
[586] M.Silfverberg, *5th International Symposium, Mobile HCI 2003*, Udine, Italy, 2003.
[587] E. Mallinckrodt, A. L. Hughes, W. Sleator, *Science*, **118**, 277 (1953)
[588] R. M. Strong, D. E., Troxel, *IEEE Transactions*, **11**, 72 (1970)

[589] A. Nathan, *et al*, Proceeding of IEEE Doi: 10.1109/JPROC.2012.2190168
[590] H. G. Craighead, J. Cheng, S. Hackwood, *Appl. Phys. Lett.,* **40**, 22 (1982)
[591] C. D. Sheraw, *et al. Appl. Phys. Lett.,* **80**, 1088 (2002)
[592] F. H. L. Koppens, D. E. Chang, F. J. García de Abajo, *Nano Lett.,* **11**, 3370 (2011)
[593] M. Liu, *et al, Nature*, **474**, 64 (2011)
[594] A. Urich, K. Unterrainer, and T. Mueller, *Nano Lett.*, **11**, 2804 (2011)
[595] L. Prechtel, *et al, Nature Comm*.**3**, 646 DOI: 10.1038/ncomms1656
[596] K. Kneipp, *et al*, *Chem. Rev.***99**, 2957 (1999)
[597] U. Keller, *Nature,* **424**, 831 (2003)
[598] O. Okhotnikov, A. Grudinin, M. Pessa, *New J. Phys.,* **6**, 177 (2004)
[599] M. Breusing, C. Ropers, T. Elsaesser, *Phys. Rev. Lett*., **102**, 086809 (2009)
[600] D. Sun, *et al, Phys. Rev. Lett.,* **101**, 157402, (2008)
[601] R. R. Nair, *et al, Science,* **320,** 1308 (2008)
[602] Z. Sun, *et al. ACS nano,* **4**, 803 (2010)
[603] T.Hasan,*et al, Adv. Mat.* **21**, 3874 (2009)
[604] Z. Sun, *et al,* The Conference on Lasers and Electro-Optics (Baltimore, US, 2011), JWA79
[605] D. Popa, *et al, Appl. Phys. Lett.,***97**, 203106 (2010)
[606] Z. Sun, *et al, Nano Res.,* **3**, 653 (2010)
[607] D. Popa, *et al, Appl. Phys. Lett.,* **98**, 073106 (2011)
[608] Y. M. Chang, *et al, Appl. Phys. Lett.,* **97**, 211102 (2010)
[609] A. Martinez, K. Fuse, S. Yamashita, *Appl. Phys. Lett.,* **99**, 121107 (2011)
[610] H. Zhang, *et al, Opt. Commun.,* **283**, 3334 (2010)
[611] H. Zhang, *et al, Laser Phys. Lett.,* **7**, 591 (2010)
[612] H. Yu, *et al, ACS Nano,* **4**, 7582 (2010)
[613] Y. M. Chang, *et al, Appl. Phys. Lett.,* **97**, 211102 (2010)
[614] F. Wang, *et al.* Submitted
[615] M. J. F. Digonnet, *Rare-Earth-Doped Fiber Lasers and Amplifiers* (Marcel Dekker, 2001)
[616] A. Martinez, *et al, Opt. Express,* **18**, 23054 (2010)
[617] Y.-W. Song, *et al, Appl. Phys. Lett.,* **96**, 051122 (2010)
[618] W. Koechner, *Solid-State Laser Engineering* (Springer, New York, 2006)
[619] W. D. Tan, *et al, Appl. Phys. Lett.,* **96**, 031106 (2010)
[620] W. B. Cho, *et al, Opt. Lett.*, In press (2011)
[621] C.-C. Lee, *et al, J. Nonlinear Opt. Phys. Mater.* **19**, 767 (2010)
[622] M. Bass, G.Li, E. V. Stryland, Handbook of Optics IV (McGraw-Hill, 2001)
[623] J. Wang, *et al, Adv. Mater.,* **21,** 2430 (2009)
[624] Y. Xu, *et al, Adv. Mater.,* **21,**1275 (2009)
[625] S. A. Mikhailov, *Europhys.Lett.,* **79,** 27002 (2007)
[626] J. J. Dean, H. M van Driel, *Appl. Phys. Lett.,* **95,** 261910 (2009)
[627] E. Hendry, *Phys. Rev. Lett.,* **105**, 097401 (2010)
[628] C. Lecaplain, *et al, Optics Letters*, **35**, 3156 (2010)
[629] M. J. Weber, Handbook of Laser Wavelengths., CRC, 1999.
[630] S. Rausch, *et al, Optics Express*, **16**, 9739 (2008)
[631] W. B. Cho, *et al,* Opt. Lett. 36 4089 (2011)
[632] M. E. Fermann,A. Galvanauskas and G. Sucha, Ultrafast Lasers Technology and Applications., Marcel Dekker, Inc., 2003.
[633] D. Lorenser, *et al, IEEE Journal of quantum electronics* **42**, 838 (2006)
[634] L. Krainer, *et al, IEEE Journal of quantum electronics* 38, 1331 (2002)
[635] C. Rulliere, Femtosecond laser pulses, Springer, 2005
[636] T. K. Kim, *et al, Optics Letters*, **36**, 4443 (2011)
[637] B. E. A. Saleh, M. C. Teich, *Fundamentals of Photonics* Ch. 18, 784–803 (Wiley, 2007)
[638] J. M. Dawlaty, *et al, Appl. Phys. Lett.,* **93,** 131905 (2008)
[639] A. R. Wright, J. C. Cao, C. Zhang, *Phys. Rev. Lett.,* **103,**207401 (2009)
[640] T. Mueller, F. Xia, P. Avouris, *Nature Photon.,* **4,** 297 (2010)
[641] F. T. Vasko, V. Ryzhii, *Phys. Rev. B,* **77,** 195433 (2008)

[642] J. Park, Y. H. Ahn, C. Ruiz-Vargas, *Nano Lett.,* **9,** 1742 (2009)
[643] F. Xia, *et al, Nano Lett.,* **9,** 1039 (2009)
[644] F. Xia, *et al, Nature Nanotech.,* **4,** 839–843 (2009)
[645] P. Blake, *et al, SolidState Commun.,* **149,** 1068 (2009)
[646] Y. M. Kang, *et al, Nature Photon.,* **3,** 59 (2009)
[647] A. B. Kuzmenko, *et al*, *Phys. Rev. Lett.,* **100,** 117401 (2008)
[648] E. J. H. Lee, *et al, Nature Nanotech.,* **3,** 486 (2008)
[649] V. G. Kravets, *et al, Phys. Rev. Lett.,* **105,** 246806 (2010)
[650] V. G. Kravets, F. Schedin, A. N. Grigorenko, *Phys. Rev. Lett.,* **101,** 087403 (2008)
[651] X. D. Xu, *et al, Nano Lett.,* **10,** 562 (2010)
[652] P. Weinberger, *Philosophical Magazine Letters* **88**, 897 (2008)
[653] W. Franz, *Z. Naturforschung* **13a** 484 (1958)
[654] L. V. Keldysh, J. Exptl. Theoret. Phys. (USSR) **33**, 994 (1957)
[655] G. Konstantatos, *et al, Nature*, **442**, 180 (2006)
[656] G. Konstantatos, E. H. Sargent, *Nature Nanotech.,* **5**, 391 (2010)
[657] J. S. Lee, *et al, Nature Nanotech.,* **6**,348 (2011)
[658] G. Kostantatos, et al, arXiv:1112.4730v1 (2011)
[659] C. M. Drain, B. Christensen and D. Mauzerall, *Proceedings of the National Academy of Science USA*. **86**, 6959 (1989)
[660] J.A. Schuller, *et al, Nature Mater.,* **9**, 193 (2010)
[661] S. Lal, S. Link, N. J. Halas, *Nature Photon.,* **1**, 641 (2007)
[662] S. Savasta, *et al, ACS Nano,* **4**, 6369 (2010)
[663] W. Zhang, *et al, Phys. Rev. Lett.,* **97**, 146804 (2006)
[664] R. D. Artuso and G. W. Bryant, *Nano Lett.,* **8**, 2106 (2008)
[665] A. O. Govorov, *et al, Nano Lett.,* **6**, 984 (2006)
[666] M. A. Noginov, *et al, Nature,* **460**, 1110 (2009)
[667] F. Schedin, *et al, ACS Nano,* **4**, 5617 (2010)
[668] A. Ridolfo, *et al*, *Phys. Rev. Lett.,* **105**, 263601*(*2010)
[669] T. Gokus, *et al, ACS Nano,* **3**, 3963(2009)
[670] L. M. Vatsia, *Research and Development Technical Report ECOM*-7023, (1972)
[671] M. Ettenberg, *Advanced Imaging*, **20**, 29 (2005)
[672] X. Gao, *et al, Nature Biotech*., **22**, 969 (2004)
[673] Y. T. Lim, *et al, Molecular Imaging*, **2**, 50 (2003)
[674] S. Kim, *et al, Nature Biotech.*, **22**, 93, (2004)
[675] R. Schödel, *et al, Nature*, 419, 694 (2002)
[676] W. Herrmann, *et al, Economic Geology*, **96**, 939 (2001)
[677] M. Golic, K. Walsh, P. Lawson, Appl. Spectroscopy, **57**, 64A (2003)
[678] J. Kang, *et al, IEEE International Conference on Image Processing*, 2757, (2006)
[679] V. Amendola, M. Meneghetti, *Adv. Funct. Mater.,* **22**, 353 (2012)
[680] H. DeVoe, *J. Chem. Phys*. **41**, 393 (1964)
[681] K. Yee, *IEEE Transactions on Antennas and Propagation* **14**, 302 (1966)
[682] P. K. Jain, *et al, Accounts of chemical research*, **41**, 1578 (2008)
[683] V. Amendola, M. Meneghetti, *Phys. Chem. Chem. Phys.,* **11**, 3805 (2009)
[684] L. Vicarelli, *et al, arXiv*:1203.3232v1 (2012)
[685] J. Chen, *et al, arxiv*:1202.4996 (2012)
[686] B. Ren, G. Picardi and B. Pettinger, *Rev. Sci. Instrum*. **75**, 4 (2004)
[687] F. Bonaccorso, *et al, Rev. Sci. Instrum*. **78**, 103702 (2007)
[688] P. G. Gucciardi, *et al, Thin Solid Film*, **516**, 8064 (2008)
[689] L.Novotny and B. Hecht, Principles of nano-optics (Cambridge University Press 2006)
[690] N. Ocelic, A. Huber, R. Hillenbrand, *Appl. Phys. Lett.,* **89**, 101124 (2006)
[691] A. Vakil, N. Engheta, *Science*, **332**,1291 (2011)
[692] F. Varchon, *et al*, *Phys. Rev. Lett*., **99**, 126805 (2007)
[693] D. Bohm and D. Pines, *Phys. Rev*. **82**, 625 (1951)

[694] D. Pines and D. Bohm, *Phys. Rev*. **85**, 338 (1952)
[695] D. Bohm and D. Pines, *Phys. Rev*. **92**, 609 (1953)
[696] S. H. Abedinpour, *et al, Phys. Rev. B*, **84**, 045429 (2011)
[697] M. S. Kushwaha, *Surface Science Reports,* **41**, 1, (2001)
[698] W. Cai, V. Shalaev, *Optical Metamaterials: Fundamentals and Applications, Springer science+business Media LLC* 2010
[699] S. L. Cunningh, A. A. Maradudi and R. F. Wallis, *Phys. Rev. B*, **10**, 3342 (1974)
[700] S. I. Bozhevolnyi, *et al. Nature*, **440**, 508 (2004)
[701] I. Llatser, *et al*, Prospects of Graphene-enabled Wireless Communications
Graphene 2012
[702] S. R. Best abd J. D. Morrow, *IEEE antennas and wireless propagation letters,* **1**, 112 (2002)
[703] V. Ryzhii, *et al. J. Appl. Phys.* **106** 084507 (2009)
[704] V. Ryzhii, *Jpn. J. Appl. Phys*. **45**, L923 (2006)
[705] C. C. Serra, *et al, IEEE antennas and wireless propagation letters,* **10**, 776 (2011)
[706] S. Coe, et al, *Nature,* **420**, 800 (2002)
[707] J. Lee, *et al*, *Adv. Mater.,* **12**, 1102 (2000)
[708] L. Carbone, *et al*, *Nano Lett.,* **7** , 2942 (2007)
[709] B. O. Dabbousi, *et al*, *J. Phys. Chem. B*, **101**, 9463 (1997)
[710] D. V. Talapin, *et al*, *Nano Lett.,* **1**, 207 (2001)
[711] S. A. Maier and H. A. Atwater, *J. Appl. Phys.* **98**, 011101 (2005)
[712] C. A. Spindt, *J. Appl. Phys.***47**, 5248 (1976)
[713] I. Brodie and C. A. Spindt, *Advances in electronics and electron physics*, **83**, 1 (1992)
[714] W. I. Milne, *et al, E nano newsletter* (Sep 2008)
[715] http://www.digitimes.com/news/a20100121PD207.html
[716] R. V. Latham, *High-Voltage Vacuum Insulation: Basic Concepts and Technological Practice*. ed (1995) Academic, London.
[717] S. A. Gavrilov, *et al, Tech. Phys. Lett*. **30**, 609 (2004)
[718] N. Xu, S. Huq, *Materials Science and Engineering: R: Reports,* **48**, 47 (2005)
[719] W. I. Milne, *et al, Diam. Relat. Mater.,* **10**, 260 (2001)
[720] A. Ilie, *et al, J. Appl. Phys.,* **90,** 2024 (2001)
[721] L. A. .Chernozatonskii, *et al, Chem. Phys. Lett.,* **233**, 63 (1995)
[722] A. G. Rinzler, *et al, Science,* **269**, 1550 (1995)
[723] W. A. de Heer, A. Chatelain, D. Ugarte, *Science,* **270**, 1179 (1995)
[724] N. De Jonge and J-M. Bonard. *Philosophical Transactions of the Royal Society A: Mathematical, Physical and Engineering Sciences,* **362**, 2239 (2004)
[725] Y. Wu, *et al, J. Mater. Chem.,* **14***,* 469 (2004)
[726] G. Eda, *et al,Appl. Phys. Lett.,* **93**, 233502 (2008)
[727] Z-S.Wu, *et al, Adv. Mater*., **21**, 1756 (2009)
[728] Z. Xiao, *et al, ACS Nano,* **4**, 6332 (2010)
[729] H. M. Huang, *et al, Appl. Phys. Lett.,* **96**, 023106 (2010)
[730] T. Paulmier, *et al,Appl. Surf. Sci*., **180**, 227 (2001)
[731] K. Nakada, *et al,Phys. Rev. B: Condens. Matter Mater. Phys.,* **54**, 17954 (1996)
[732] O. V. Yazyev, *Rep. Prog. Phys.*, **73** , 056501 (2010)
[733] P. J. Mohr, B. N. Taylor, D. B. Newell, *Rev. Mod. Phys.,* **80**, 633 (2008)
[734] A. S. Biris, *et al, J. Biomed. Opt*. **14**, 021007 (2009)
[735] K. R. Ratinac, *et al, Environ. Sci. Technol.,* **44,** 1167 (2010)
[736] S. Pisana, *et al, IEEE Transactions on Magnetics,* **46**, 1910 (2010)
[737] T. D. Boone, *et al, IEEE Transactions on Magnetics,* **42**, 3270 (2006)
[738] Y.G.Semenov, J.M. Zavada, K.W. Kim, *et al, Appl. Phys. Lett.,* **97**, 3 (2010)
[739] C.H. Chen, *et al*, DOI: 10.1109/TRANSDUCERS.2011.5969794 (2011)
[740] E.W. Hill, A. Vijayaragahvan, K. Novoselov, *Sensors Journal, IEEE* **11**, 3161 (2011)
[741] B.Bahreyni, Chapter 10: Survey of Applications, in Fabrication and Design of Resonant Microdevices. 2008, Elsevier
[742] S. Y. Kim, H.S. Park, *Nanotechnology,* **21**, 10 (2010)

[743] A. Sakhaee-Pour, M. T. Ahmadian, A. Vafai, *Solid State Communications,* **145**, 168 (2008)
[744] C. L. Wong, *et al, Journal of Micromechanics and Microengineering,* **20**, 11 (2010)
[745] A. K. Naik, *et al, Nature Nanotech.,* **4**, 445 (2009)
[746] B. Lassagne, *et al, Nano Lett.,* **8**, 3735 (2008)
[747] H.-Y. Chiu, *et al, Nano Lett.,* **8**, 4342 (2008)
[748] K. Jensen, K. Kim, A. Zettl, *Nature Nanotech.,* **3**, 533(2008)
[749] C. Chen, *et al, Nature Nanotech.,* **4**, 861 (2009)
[750] A. M. van der Zande, *et al, Nano Lett*., **10**, 4869 (2010)
[751] Y. Dan, *et al, Nano Lett.,* **9**, 1472 (2009)
[752] F. Schedin, *et al, Nature Mater.,* **6**, 652 (2007)
[753] M. Remskar, *et al, Appl. Phys. Lett*. **69,** 351 (1996)
[754] M. Chhowalla and G. A. J. Amaratunga, *Nature* **407**, 164 (2000)
[755] M. Field, *et al, Phys. Rev. Lett.,* **70**, 1311 (1993)
[756] S. Gustaffson, *et al, Phys. Rev. Lett.,* **96**, 076605 (2006)
[757] J. R. Sootsman, *et al, Angew. Chem. Int. Ed*., **48**, 8616(2009)
[758] F. J. Di Salvo, *Science*, **285**, 703 (1999)
[759] B. Poudel, *et al,Science,* **320**, 634 (2008)
[760] D. Ragone, SAE Technical Paper 680453, (1968), doi:10.4271/680453
[761] M. Winter, R. J.Brodd, *Chem Rev*., **104**, 4245 (2004)
[762] P. G. Bruce, B. Scrosati, J. M. Tarascon, *Angew Chem Int Ed.,* **47**, 2930 (2008)
[763] J. Maier, *Nature Mater.,* **4**, 805 (2005)
[764] J. M. Tarascon, M. Armand, *Nature,* **414**, 359 (2001)
[765] A. M. Wilson, B. M. Way, J. R. J. Dahn, *Appl. Phys*., **77**, 363 (1995)
[766] Y. Yua, *et al*, *Electrochim. Acta*, **54**, 7227 (2009)
[767] M. Walkihara, *Mater Sci Eng R,* **33**, 109 (2001)
[768] M. S. Whittingham,*Chem Rev*., **104**, 4271 (2004)
[769] A. S. Arico, *et al, Nature Mater.,* **4**, 366 (2005)
[770] J. S. Sakamoto, B. Dunn, *J. Mater. Chem.,* **12**, 2859 (2002)
[771] Y. Zhu, *et al,ACS Nano,* **5**, 3333 (2011)
[772] X. Zhu, *et al*, *J. Power Sources*, **196**, 6473 (2011)
[773] C. Zhang, *et al*, *Carbon*, In press (2012)
[774] L. Ji, *et al*, *Energy and environmental science,* **4**, 3611 (2011)
[775] K. Zhang, *et al*, *Appl. Mater. Interfaces,* **4***, 658* (2012)
[776] Z.-S Wu, *et al*, *ACS Nano,* **5**, 5463 (2011)
[777] J. Xiao, *et al*, *Nano Lett*., **11**, 5071 (2011)
[778] Z-S. Wu, *et al*, *ACS Nano,* **4**, 3187 (2010)
[779] A. M. L. Reddy, *et al*, *ACS Nano,* **4**, 6337 (2010)
[780] B. Z. Jang, *et al*, *Nano Lett.,* **11**, 3785 (2011)
[781] A. V. Muruganet, *et al*, *Chem. Mater.,* **21**, 5004 (2009)
[782] D. Pan, *et al*, *Chem. Mater.,* **21**, 3136 (2009)
[783] C. Wang, *et al*, *Chem. Mater*., **21**, 2604 (2009)
[784] G. Wang, *et al*, *Carbon,* **47**, 2049 (2009)
[785] Z. H. Chen, J. R. Dahn, *J. Electrochem. Soc.*, **149**, A1184 (2002)
[786] P. P. Prosini, D. Zane, M. Pasquali, *Electrochim. Acta*, **46**,3517 (2001)
[787] R.Dominko, *et al, J. Electrochem. Soc.,***152**, A607(2005)
[788] M. D. Stoller, *et al, Nano Lett.,* **8**, 3498 (2008)
[789] E. Yoo, *et al,Nano Lett.,* **8**, 2277 (2008)
[790] S.-M. Paek, E. Yoo, I. Honma, *Nano Lett.,* **9**, 72 (2009)
[791] D. Wang, *et al, ACS Nano,* **3**, 907 (2009)
[792] P. Simon, *Nature Mater.,* **7**, 845 (2008)
[793] S. Murali, *et al*, *Phys. Chem. Chem. Phys*., **13**, 2652 (2011)
[794] K. Sheng, *et al*, *Scientific Reports*, **2**, 247 (2012)
[795] Q. Wu, *et al*, *ACS Nano,* **4**, 1963 (2010)
[796] G. Yu, *et al*, *Nano Lett.,***11**, 2905 (2011)

[797] Z-S. Wu, *et al, ACS Nano*, **4**, 5835 (2010)
[798] M. D. Stoller, *et al*, *Energy Environ. Sci.* in press (2011)
[799] Y. Zhu, *et al*, *Science*, **332**, 1537 (2011)
[800] T. Y. Kim, *et al*, *ACS nano,* **5**, 436 (2011)
[801] L. Yuan, *et al, ACS Nano,* **6**, 656, (2012)
[802] Y. Wang, *et al*, *J. Phys. Chem. C*, **11**3, 13103 (2009)
[803] C. Liu, *et al, Nano Lett.,* **10**, 4863 (2010)
[804] W. R. Grove, Phil. Mag. Ser. **3**,127 (1839)
[805] A. C. Dillon, et al, Nature, **386**, 377 (1997)
[806] V. Tozzini and V. Pellegrini, *Phys. Rev. B,* **81**,113404 (2010)
[807] V. Tozzini and V. Pellegrini, *J. Phys. Chem. C*, **115**, 25523 (2011)
[808] D. M. Chapin, C. S. Fuller, and G. L. Pearson, *J. Appl. Phys*., **25**, 676 (1954)
[809] M. A. Green, *et al, Prog. Photovolt. Res. Appl*., **7**, 321 (1999)
[810] L. M. Peter, *Phil. Trans. R. Soc. A,* **369**, 1840 (2011)
[811] D. Carlsson, C. Wonski, *Appl. Phys Lett.,* **28**, 671 (1976)
[812] J. Lebrun *Proceedings of the international conference on the physics and chemistry of semiconductor heterojunctions and layer structures* 163 (1970)
[813] L. Kazmerski, F. R. White, G. K. Morgan, *Appl. Phys Lett.,* **29,** 268 (1976)
[814] H. Hoppe, N. S. Sariciftci, *MRS Bulletin,* **19**, 1924 (2004)
[815] B. O'Regan, M. Gratzel, *Nature*, **353**, 737 (1991)
[816] F. C. Krebs, *Org. Electron.,* **10**, 761 (2009)
[817] X. Li, *et al,Adv. Mater*., **22**, 2743 (2010)
[818] L. G. De Arco, *et al*, *ACS Nano,* **4**, 2865 (2010)
[819] Z. Liu, *et al, Adv. Mater.,* **20**, 3924 (2008)
[820] V. Yong, J. M. Tour, *Small,* **6**, 313 (2009)
[821] F. Bonaccorso, *International Journal of Photoenergy* **2010**, Article ID 727134 (2010)
[822] N. Yang, *et al, ACS Nano,* **4**, 887 (2010)
[823] W. Hong, *et al, Electrochem.Commun.,* **10**, 1555 (2008)
[824] F. Bonaccorso, *et al*, Graphene-based Natural Dye-Sensitized Solar Cells" Graphene 2011, Imaginenano, Bilbao, (Spain).
[825] W. Shockley and H. J. Queisser, *J. Appl. Phys.,* **32**, 510 (1961)
[826] S. P. Bremner, M. Y. Levy and C. B. Honsberg, *Prog. Photovoltaics*, **16**, 225 (2008)
[827] Y. Wang, *et al, ACS Nano,* **6**, 1018 (2012)
[828] K. K. Manga, *et al, Adv. Mater*. DOI: 10.1002/adma.201104399 (2012)
[829] X. Yan, *et al, Nano Lett*., **10**, 1869 (2010)
[830] J. Coleman, *et al, Adv. Mater*., **18**, 689 (2006)
[831] C. Gómez-Navarro, M. Burghard and K. Kern, *Nano Lett.*, **8**, 2045 (2008)
[832] N. Graddage, *et al, Roll to Roll Printing of Aqueous Pristine Graphene Dispersions*, Graphene 2012
[833] L. S. Walker, *et al, ACS Nano,* **5**, 3182 (2011)
[834] K. Wang, *et al, MRS Bulletin,* **46**, 315 (2011)
[835] A. P. Singh, *et al, Nanotechnology,* **22**, 465701 (2011)
[836] M. Kujawski, J. D. Pearse and E. Smela, *Carbon*, **48**, 2409 (2010)
[837] S. R. Wang, *et al.*, *Macromolecules*, **42**, 5251 (2009)
[838] N. Liu, *et al*, *Adv. Funct. Mater.*, **18**, 1518 (2008)
[839] H. J. Salavagione, G. Martinez and M. A. Gomez, *J. Mater. Chem.*, **19**, 5027 (2009)
[840] P. M. Ajayan and J. M. Tour, *Nature*, **447**, 1066 (2007)
[841] H. Pang, T. Chen, G. Zhang, B. Zeng and Z.-M. Li, *Mater. Lett.*, **64**, 2226 (2010)
[842] M. Moniruzzaman and K. I. Winey, *Macromolecules*, **39**, 5194 (2006)
[843] H. B. Lee, *et al*, *J. Macromol. Sci., Part B: Phys.*, **49**, 802 (2010)
[844] X. Xiao, T. Xie and Y. T. Cheng, *J. Mater. Chem.*, **20**, 3508 (2010)
[845] H. C. Schniepp, *et al, J. Phys. Chem. B*,**110**, 8535 (2006)
[846] D. R. Dreyer, *et al, Chem. Soc. Rev.*, 2010, **39**, 228
[847] D. Tasis, *et al,Chem. Rev.*, **106**, 1105 (2006)

[848] R. Verdejo, *et al, J. Mater. Chem.*, **21**, 3301 (2011)
[849] L. Hu, T. Desai, and P. Keblinski, *J.Appl. Phys.,* **110**, 033517 (2011)
[850] A. P. Awasthi, D. C. Lagoudas, D. C. Hammerand, *Modelling and Simulation in Materials Science and Engineering,* **17**, 015002 (2009)
[851] M. C. Simmonds, *et al, Surface and Coatings Technology,* **126**, 15 (2000)
[852] C. W. Bamforth and J. M. Krochta,*Food Packaging and Shelf Life A Practical Guide*
Edited by Gordon L Robertson CRC Press 2009 Pages 215–229
[853] N. Boutroy, *et al, Diamond & Related Materials,* **15,** 921 (2006)
[854] C. Casiraghi, J. Robertson, and A. C. Ferrari, *Mater. Today,* **10**, 44 (2007)
[855] G. Choudalakis, A. D. Gotsis *European Polymer Journal,* **45**, 967 (2009)
[856] Y. Xu, *et al, Carbon,* **47**, 3538 (2009)
[857] J. Liang, *et al, Adv. Funct. Mater*., **19**, 2297 (2009)
[858] J. Y. Jang, *et al, Compos. Sci. Technol.,* **69**, 186 (2009)
[859] W. Kai, *et al, J. Appl. Polym. Sci*., **107**, 1395(2008)
[860] D. Cai, M. Song, *Nanotechnology*, **20**, 315708 (2009)
[861] H. Kim, C. W. Macosko, *Macromolecules,* **41**, 3317 (2008)
[862] H. Kim, C. W. Macosko, *Polymer*, **50**, 3797(2009)
[863] S. Ansari and E. P. Giannelis, *J. Polym. Sci., Part B: Polym. Phys.,* **47**, 888 (2009)
[864] P. Steurer, *et al, Macromol.Rapid Commun.,* **30**, 316 (2009)
[865] R. K. Prud'homme, *et al,* W.O. Patent 2008045778 A1, 2008.
[866] D. A. Nguyen, *et al,Polym. Int.*, **58**, 412 (2009)
[867] R. Verdejo, *et al, J. Mater. Chem.,* **18**, 2221 (2008)
[868] B. Das, *et al, Nanotechnology,* **20**, 125705 (2009)
[869] H. Kim, Y. Miura, C. W. Macosko, *Chem. Mater.,* **22**, 3441 (2010)
[870] M. Fang, *et al, J. Mater. Chem.,* **19**, 7098 (2009)
[871] J. Liang, *et al, J. Phys. Chem. C,* **113**, 9921 (2009)
[872] D. Cai, K. Yusoh, M. Song, *Nanotechnology,* **20**, 085712 (2009)
[873] J. J. Mack, *et al, Adv. Mater.,* **17**, 77 (2005)
[874] P. B. Messersmith and E. P. Giannelis,*Chem. Mater*., **6**, 1719 (1994)
[875] S. A. Kumar, *et al, Prog. Org. Coat*., **55**, 207(2006)
[876] G. Das, *et al, Prog. Org. Coat.,* **69**, 495 (2010)
[877] C. S. Wu, *et al, Polymer,* **43**, 4277 (2002)
[878] P. M. Hergenrother, *et al, Polymer*, **46**, 5012 (2005)
[879] G. Wang, *et al, J. Phys. Chem. C*., **112**, 8192 (2008)
[880] S. R. Wang, *et al, Macromolecules,* **42**, 5251 (2009)
[881] M. A. Rafiee, *et al, ACS Nano,* **3**, 3884 (2009)
[882] G. D. Zhan, *et al, Nature Mater*., **2**, 38 (2003)
[883] P. M. Ajayan, *et al, Nature,* **375**, 564 (1995)
[884] G. D. Zhan, *et al, Appl. Phys. Lett*., **83**, 1228 (2003)
[885] O. Malek, *et al, Mater. Today,* **14**, 496 (2011)
[886] Y. Fan, *et al,Carbon,* **48**,1743 (2010)
[887] C. Ramírez, *et al, Carbon,* **49**, 3873 (2011)
[888] O. Tapasztó, *et al,Chem. Phys. Lett.,* **511**, 340 (2011)
[889] G. D. Zhan, *et al, Appl. Phys. Lett*., **83**, 1228 (2003)
[890] J. Gonzalez-Julian, *et al, J. Amer. Ceram. Soc.,* **94**, 2542 (2011)
[891] L. A. Liew, *et al, Sensors and Actuators* A, **89**, 64 (2001)
[892] D. Wu, *et al, Chemistry - A European Journal***17**, 10804 (2011)
[893] M. Quintana ,*et al*,*Chem. Commun.***47**, 9330 (2011)
[894] H. Ma, A. K. Y. Jen, L. R. Dalton, *Adv. Mater.,* **14**, 1339, (2002)
[895] L. Eldada, Photonics West (2002)
[896] L. Eldada, SPIE magazine, **26**, may (2002)
[897] S. H. Kang, *et al*, *Macromolecules*, **36** , 4355 (2003)
[898] V. Scardaci, *et al*, *Adv. Mater*., **20**, 4040 (2008)
[899] T. Matsuura, *et al*, *Appl. Opt*., **38** , 966 (1999)

[900] Z. Sun, *et al*, *Appl. Phys. Lett*., **93**, 061114 (2008)
[901] Z. Sun, *et al*, *Appl. Phys. Lett*., **95**, 253102, (2009)
[902] F. Wang, *et al*, *Nature Nanotech*., **3**, 738 (2008)
[903] F. Bonaccorso, *et al*, Microoptics Conference (MOC) paper **E3** (2011)
[904] R. J. Mears, *et al*, *IEEE Electr.Lett.,* **23**, 1026 (1987)
[905] S. Shimada, H. Ishio (editors), *Optical amplifiers and their applications*, Wiley, 1992
[906] H. Liang, *et al*, *Optics Lett.,* **29**, 477 (2004)
[907] C. Koeppen, *et al*, *J. Opt. Soc Am. B*, **14**, 155 (1997)
[908] L. H. Slooff, *et al, J. Appl. Phys.,* **91**, 3955 (2002)
[909] M. A. Burns, *et al*, *Science,* **282**, 484 (1998)
[910] A. Liscio, *et al, J. Mater. Chem*., **21**, 2924 (2011)
[911] R. J. Young, *et al, ACS Nano,* **5**, 3079 (2011)
[912] L. Gong, *et al, Adv. Mater*., **22**, 2694 (2010)
[913] V. Palermo, *Adv. Mater*., **18**, 145 (2006)
[914] A. Liscio, V. Palermo, and P. Samori, *Acc. Chem. Res*., **43**, 541 (2010)
[915] X. Shi, *et al, Appl. Phys. Lett*., **96**, 053115 (2010)
[916] http://www.guardian.co.uk/business/2011/june/14/airbus-air-transport-2050-vision#/?picture=375733267&index=1
[917] Z. Han, A. Fina, *Prog. Polym. Sci*., **36**, 914 (2011)
[918] E. Chiavazzo and P. Asinari, *Nanoscal. Res. Lett.*, **6**, 249 2011
[919] M. Marting-Galleco, *et al*, *Polymer,* **52**, 4664 (2011)
[920] V. C. Sanchez, *et al*, *Chem. Res. Toxicol.,* **25**, 15 (2012)
[921] Z. Liu, *et al*, *Nanomedicine Lond.,* **6**, 317 (2011)
[922] Y. Zhang, *et al*, *ACS Nano,* **4**, 3181 (2010)
[923] A. Sasidharan, *et al*, *Nanoscale,* **3**, 2461 (2011)
[924] J. Yuan, *et al*, *Toxicol Lett.,* (2011)
[925] K. Wang, *et al, Nanoscale Res. Lett.,* **6,** 8 (2011)
[926] W. Hu, *et al*, *ACS Nano,* **4**, 4317 (2010)
[927] Y. Chang, *et al*, *Toxicol. Lett.,* **200**, 201 (2011)
[928] Z. Liu, *et al*, *J. Am. Chem. Soc.,* **130**, 10876 (2008)
[929] S. Liu, *et al*, *ACS Nano,* **5**, 6971 (2011)
[930] N. Li, *et al*, *Biomaterials,* **32**, 9374 (2011)
[931] T. R. Nayak, *et al*, *ACS Nano,* **5**, 4670, (2011)
[932] S. K. Singh, *et al*, *ACS Nano,* **5**, 4987 (2011)
[933] X. Zhang, *et al*, *Carbon,* **49**, 986 (2011)
[934] M. C. Duch, *et al,Nano Lett.,***11**, 5201 (2011)
[935] J-W. T. Seo, *et al, J. Phys. Chem. Lett*., **2**, 1004 (2011)
[936] A. Müller,*et al, EMBO J.,***18**, 339 (1999)
[937] C. Stefanelli, *et al, Biochem. J.,* **347***,* 875 (2000)
[938] A. Schinwald, *et al, ACS Nano,* **6**, 736 (2012)
[939] J. M. Samet, *et al, New England Journalof Medicine*, **343**,1742 (2000)
[940] O. Akhavan, *et al*, *ACS Nano,* **4**, 5731 (2010)
[941] O. N. Ruiz, *et al*, *ACS Nano,* **5**, 8100 (2011)
[942] K. Yang, *et al*, *Nano Lett.,* **10**, 3318 (2010)
[943] K. Yang, *et al*, ACS *Nano,* **5**, 516 (2011)
[944] J. Russier, *et al*, *Nanoscale,* **3**, 893 (2011)
[945] G. P. Kotchey, *et al*, *ACS Nano,* **5**, 2098 (2011)
[946] G. Wang, *et al*, *Nano Res.,* **4**, 563 (2011)
[947] E. Oberdörster, *et al*, *Carbon*, **44**, 1112 (2006)
[948] S. Perez, *et al*, *TrAC, Trends Anal. Chem.,* **28**, 820 (2009)
[949] E. J. Petersen and T. B. Henry, *Environ. Toxicol. Chem.,* **31**, 60 (2012)
[950] K. Koga, *et al, Toxicol. in vitro,* **20**, 1370 (2006)
[951] G. Ciofani, *et al, Int. J. Nanomed*., **5**, 285 (2010)
[952] G. Ciofani, *et al, BBRC,* **394**, 405 (2010)

[953] X. Chen, *et al, J. Amer. Chem. Soc*., **131**, 890 (2009)
[954] L. Horváth, *et al, ACS Nano,* **5**, 3800 (2011)
[955] L. Lacerda, *et al*, *Biomaterials,* **33**, 3334 (2012)
[956] A. V. Titov, *et al, ACS Nano,* **4**, 229 (2010)
[957] R. A. Freitas Jr. *Nanomedicine, Volume I: Basic Capabilities,* 1999, ISBN 157059645X
[958] V. P. Torchilin. *Nanoparticulates as drug carriers*. Imperial College Press, 2006
[959] K. P. Loh, *et al. Nature Chem.,* **2**, 1015(2010)
[960] G. Eda, *et al, Adv. Mater*., **22**, 505 (2009)
[961] M. Dankerl, *et al*, *Adv. Func. Mater.,* **20**, 3117 (2010)
[962] P. K. Ang, *et al*, *J. Am. Chem. Soc.,* **30**, 14392 (2008)
[963] M. Liong, *et al, ACS Nano*, **2**, 889 (2008)
[964] J. V. Frangioni, *Curr.Opin. Chem. Biol*., **7**, 626 (2003)
[965] Z. Luo, *et al, Appl. Phys. Lett.,* **94**, 111909 (2009)
[966] Z. Liu, *et al, Nano Res*., **1**, 85 (2009)
[967] H. Shen, *et al*, *Theranostics,* **2**, 283 (2012)
[968] Z. M. Markovic, *et al, Biomaterials,* **32**, 1121 (2011)
[969]X. Liu, *et al, Biomaterials,* **32**, 144 (2011)
[970] Q. Wang and J. Liu, Intracellular delivery. Fundamental Biomedical Technology 2011, vol. 5, part 3, 567-598
[971] A. R. Biris, *et al,* J. *Phys. Chem. C*, **115**, 18967 (2011)
[972] P. Huang, *et al, Theranostic,* **1**, 240 (2011)
[973] L. Zhang, *et al, Small,* **6**, 537 (2010)
[974] F. Zhang, *et al, J. Phys. Chem. C,* **114**, 8469 (2010)
[975] X. Xu, *et al, European Journal of Pharmaceutics and Biopharmaceutics*, **70**, 165 (2008)
[976] X. Yang, *et al. J. Phys. Chem. C,* **112**, 17554 (2008)
[977] H. Bao, *et al, Small* **7**, 1569 (2011)
[978] T. Cohen-Karni, *et al*, *Nano Lett.,***10**, 1098 (2010)
[979] L. H Hess, *et al*, *Adv. Mater.,***23**, 5045 (2011)
[980] L. H. Hess, *et al*, *Appl. Phys. Lett.,* **99**, 033503 (2011)
[981] Z. Chenet, *et al*, *Nano Lett.,***10**, 1864 (2010)
[982] C. Schmidt, *Nature,* **483**, S37 (2012)
[983] Y. Lin, *et al, Small,* **6**, 1205 (2010)
[984] S. Cogan, *Annual Review of Biomedical Engineering*, **10**, 275 (2008)
[985] S. A. Jewett, *et al, Acta Biomaterialia,* **8**, 728 (2012)
[986] S. Santavirta,*et al,Arch Orthop Trauma Surg.,* **118**, 89 (1998)
[987] L. Tang, *et al,Biomaterials,* **16**, 483 (1995)
[988] A. Härtl, *et al, Nature Mater.,* **3**, 736 (2004)
[989] C. Li, J. Han, C. H. Ahn, *Biosensors and Bioelectronics,* **22**, 1988 (2007)
[990] S.-J. Xiao, M. Textor, N. D. Spencer, *Langmuir,* **14**, 5507 (1998)
[991] E. S. Gawalt, *et al, Langmuir*, **19**, 200 (2003)
[992] L. B. Merabet, *et al, Nature Review Neuroscience,***6**, 71 (2005)
[993] M. Matthaei, *et al, Ophthalmologica,* **225**, 187 (2011)
[994] R. Dinyari, *et al, Appl. Phys. Lett.*, **92**, 091114 (2008)
[995] R. Dinyari, *et al,* electron Devices Meeting (IEDM), 2009 IEEE International
[996] D. W. Deamer and M. Akeson, *Trends in Biotechnology,* **18**, 147 (2000)
[997] J. J. Kasianowicz, *et al, Proc. Natl. Acad. Sci. USA,***93**, 13770 (1996)
[998] D. Branton, *et al, Nature Biotech.,* **26**, 1146 (2008)
[999] N. Ashkenasy, *et al, Angewandte Chemie-International Edition,* **44**, 1401 (2005)
[1000] D. Stoddart, *et al, Proc. Natl. Acad. Sci. USA,***106**, 7702 (2009)
[1001] W. Vercoutere, *et al, Nature Biotechnology,* **19**, 248 (2001)
[1002] J. Clarke, *et al,Nature Nanotechnology,* **4**, 265 (2009)
[1003] K. R. Lieberman, *et al, J. Am. Chem. Soc.,* **132**, 17961 (2010)
[1004] G. F. Schneider, *et al*, *Nano Lett.,* **10**, 3163 (2010)
[1005] C. A. Merchant, *et al,Nano Lett.*, **10**, 2915 (2010)

[1006] F. Prins, *et al*, *Nano Lett.,***11**, 4607 (2011)
[1007] S. Menuel, *et al*, *Bioconjugate Chem.,***19**, 2357 (2008)
[1008] S. Bacchetti, F. Graham, *Proc. Natl. Acad. Sci. USA,* **74**, 1590 (1977)
[1009] M. Tsukakoshi, *et al,Applied Physics B-Photophysics and Laser Chemistry,* **35**, 135 (1984)
[1010] G. Zhang, *et al, Hum. Gene Ther.*, **8**, 1763 (1997)
[1011] Z. Liu, *et al, Angew. Chem., Int. Ed.*, **46**, 2023 (2007)
[1012] C. Hom, *et al, Small*, **6**, 1185 (2010)
[1013] T. A. Xia, *et al, ACS Nano*, **3**, 3273(2009)
[1014] X. Q. Zhang, *et al, ACS Nano*, **3**, 2609 (2009)
[1015] B. Chertok, A. E. David and V. C. Yang, *Biomaterials*, **31**, 6317 (2010)
[1016] S. Son, K. Singha and W. J. Kim, *Biomaterials*, **31**, 6344 (2010)
[1017] L. Feng, S. Zhang, Z. Liu, *et al, Nanoscale,* **3**, 1252 (2011)
[1018] F. Liu, J. Y. Choi and T. S. Seo, *Biosens. Bioelectron*., **25**, 2361 (2010)
[1019] L. Yang , B. W. Sheldon, T. J. Webster. *J Biomed Mater Res A.,* **91**, 548 (2009)
[1020] A. Grill, *Diamond and Related Materials*, **12**, 166 (2003)
[1021] H. Lexe, *Nanotechnology,* **20**, 325701 (2009)
[1022] R. Hauert, *Tribol.Internat*., **37**, 991 (2004)
[1023] G. Gonçalves, *et al. J. Mater Chem.*, (2010)